Investigating JMJD5 loss of function models to identify and characterise lethal interactions in cancer

Sonia Piasecka

A thesis submitted to the University of Birmingham for the degree of **DOCTOR OF PHILOSOPHY**

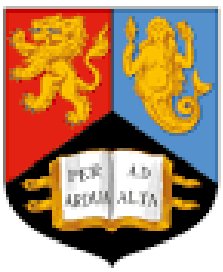

UNIVERSITY OF BIRMINGHAM

Institute of Cancer and Genomic Sciences
College of Medical and Dental Sciences
University of Birmingham

September 2024

Abstract

2-Oxoglutarate (2-OG) Oxygenases are biologically important enzymes involved in both the hydroxylation and demethylation of nucleic acids and proteins. These enigmatic enzymes play important roles in several human diseases, including cancer. JMJD5 is an essential gene that belongs to the 'JmjC-only' sub-family of 2-OG oxygenases. It was originally identified as a histone demethylase, but more recent evidence supports its assignment as a protein hydroxylase with complex roles in cancer. JMJD5 has been implicated in a plethora of biological processes, with emerging evidence supporting a role in DNA damage repair (DDR). In this thesis, I have begun to investigate the effect of JMJD5 mutations and loss of function in cancer. We show that cancer variants impair JMJD5 expression, activity and function in GS. We subsequently demonstrate that JMJD5 knockdown causes replication stress in tumour cell lines and that this phenotype is dependent on its enzymatic activity. Importantly, we demonstrate that loss of JMJD5 can sensitise cancer cells to various DNA-damaging agents including PARP, ATM and ATR inhibitors, highlighting its potential as a therapeutic target. Finally, we evaluated the effect of first-in-class inhibitors of JMJD5 on cancer cell lines. We showed that these novel JMJD5 inhibitors decreased cancer cell viability, increased replication stress, and caused cell cycle perturbations. We also evaluated their ability to sensitise cells to DDR inhibitors and obtained promising results. Overall, our work supports the role of JMJD5 as a promising target for anticancer therapies, particularly in combination with other agents.

Acknowledgements

First and foremost, I would like to thank Mat for all the guidance and support during those 4 years of this PhD. I know that this projects was challenging in many ways with a lot of experiments not working as expected.

Secondly, I would like to thank Sally for all the training, help and guidance through this project as well as during the writing of this thesis.

I also would like to thank all past and present members of the Coleman lab including Regina, Eline, Christian, Tristan, Uncaar and Arashpreet. Special thanks to Arashpreet for all the moral support. I also wish to give special thanks to Uncaar for being super helpful.

Most importantly, I would like to thank my partner, and now fiancé Pete, for all the support you gave me through those difficult years. Thanks to you, I made it to the end.

Many thanks to all of my family and friends for believing in me. Special thanks my dear friend Nicole who is the only friend that can understand the PhD struggles. Thank you for listening to me and being super supportive.

Lastly, I would like to express gratitude to Cancer Research UK for funding this PhD project.

Declaration

I declare that this thesis is entirely my own work, with the exception of the following:

Original pEF6-HA-JMJD5 and pIHZ 3XFLAG-JMJD5 (WT and H321A) were generated by others including Professor Mathew Coleman, Doctor Sally Flatcher and Mr Uncaar Boora.

Figure 2.4 was generated by Dr Sally Fletcher

Primer design for primers used in qPCR experiments in Figures 3.13, 3.15B and 3.16B was done by Dr Sally Fletcher

The chemical structures of JMJD5 inhibitors in Figures 4.1 and 4.2 were generated by Dr Lennart Brewitz

The IC50 values for the JMJD5 inhibitors in Figures 4.1 and 4.2 were generated by Dr Lennart Brewitz

Experimental data shown in Figure 4.13 was generated by Dr Sally Fletcher.

Table of Contents

List of Figures

List of Tables

List of Abbreviations

2HG 2-hydroxyglutarate

2OG 2-oxoglutarate

7-AAD 7-Amino-Actinomycin

2,4-PDCA Pyridine-2,4-dicarboxylic acid

DAPI 4’,6-diamidino-2-phenylindole

ATM Ataxia Telangiectasia mutated kinase

ATR ATM-Rad3-related kinase

BER Base excision repair

CC50 Half-maximum cytotoxicity concentration

CHK1 Checkpoint kinase 1

CHK2 Checkpoint kinase 2

DMOG Dimethyloxalglycine

DDR DNA damage response

DSBH Double-stranded β helix

RS DNA replication stress

DSB Double strand break

eRF1 Eukaryotic release factor 1

EV Empty vector

FIH Factor inhibiting HIF

GI Genome instability

GS Genome stability

GFP Green fluorescent protein

HR Homologous recombination

HIF Hypoxia inducible factor

HREs Hypoxia response elements

IP Immunoprecipitation

IC50 Half-maximum inhibitory concentration

IPTG Isopropyl ß-D-1-thiogalactopyranoside

IDH Isocitrate dehydrogenases

JMJD Jumonji domain containing protein

JMJD5 Jumonji domain containing protein 5

JmjC Jumonji-C domain

KDM Lysine demethylase

MINA53 Myc induced nuclear antigen 53kDa

MMS methyl methanesulfonate

NO66 Nucleolar protein 66 kDa xi

NLS Nuclear localisation signal

NHEJ Non-homologous end joining

PARP Poly ADP-ribose polymerase

PI propidium iodide

PCR Polymerase chain reaction

PTM Post-translational modification

PKM2 pyruvate kinase muscle isozyme

PHD Prolyl-hydroxylase domain

PHDs prolyl hydroxylases

RCCD1 Regulator of Chromosome Condensation Domain containing protein 1

RPS6 Ribosome protein S6

siRNA Small interfering RNA

shRNA Short hairpin RNA

ssDNA Single stranded DNA

SSBs Single strand breaks

WT Wild-type

VHL E3- ubiquitin ligase von Hippel–Lindau

qPCR Quantitative PCR

Chapter 1: Introduction

1.1 Hydroxylation, a post-translational modification catalysed by 2-oxoglutarate oxygenases

1.1.2 Protein hydroxylation is a post-translational modification

Post-translational protein modifications (PTMs) play a key role in a plethora of biological processes by modifying the chemical composition of proteins. They are involved in the regulation of mechanisms such as gene expression, cell cycle control, and DNA damage repair (DDR) and their dysregulation is implicated in many diseases (Ramazi and Zahiri, 2021). There are over 400 known PTMs with the most prevalent ones being phosphorylation, methylation, acetylation and ubiquitylation. Protein hydroxylation is a poorly characterised PTM that involves the generation of a hydroxyl group through the transfer of a single oxygen atom onto a target substrate (Loenarz et al., 2008). In addition to the hydroxylation of proteins, other macromolecules including DNA, RNA and lipids can also be hydroxylated, highlighting the significance of this PTM in a wide range of cellular processes (Loenarz et al., 2008). The first indication of the importance of this type of modification in mammalian cells came from studies of collagen biosynthesis which demonstrated hydroxylation of prolyl and lysyl residues. It also became apparent that dysregulation of this process can lead to diseases such as scurvy where ascorbate deficiency (co-factor dependencies are described in Section 1.1.3) leads to reduced collagen hydroxylase activity (Ploumakis and Coleman, 2013). The discovery that protein hydroxylases control hypoxia signalling (Kaelin and Ratcliffe, 2008) led to an increase in interest and research in this area.

1.1.3 Overview of the functionally diverse roles of 2OG oxygenases

Hydroxylation is mainly carried out by proteins that belong to a family of enzymes called 2-oxoglutarate (2OG) Oxygenases. The enzymatic activity of 2OG oxygenases relies on the availability of nutrients such as the Kreb's cycle intermediate 2OG, oxygen, Fe (II), and, in

some cases, reducing agents like ascorbate (Loenarz and Schofield, 2011). Members of the 2OG family play key roles in a variety of fundamental cellular processes such as biosynthesis, hypoxic sensing, fatty acid metabolism as well as regulation of gene expression (McDonough et al., 2010). Therefore, their dysregulation has been implicated in a variety of diseases including cancer (Fletcher and Coleman, 2020).

The 2OG oxygenase family can be divided into subgroups based on their biochemical activity (demethylases and hydroxylases) or their target (proteins, lipids or nucleic acid). Over 60 members of the 2OG oxygenase family have been identified and their classification is presented in Figure 1.1.

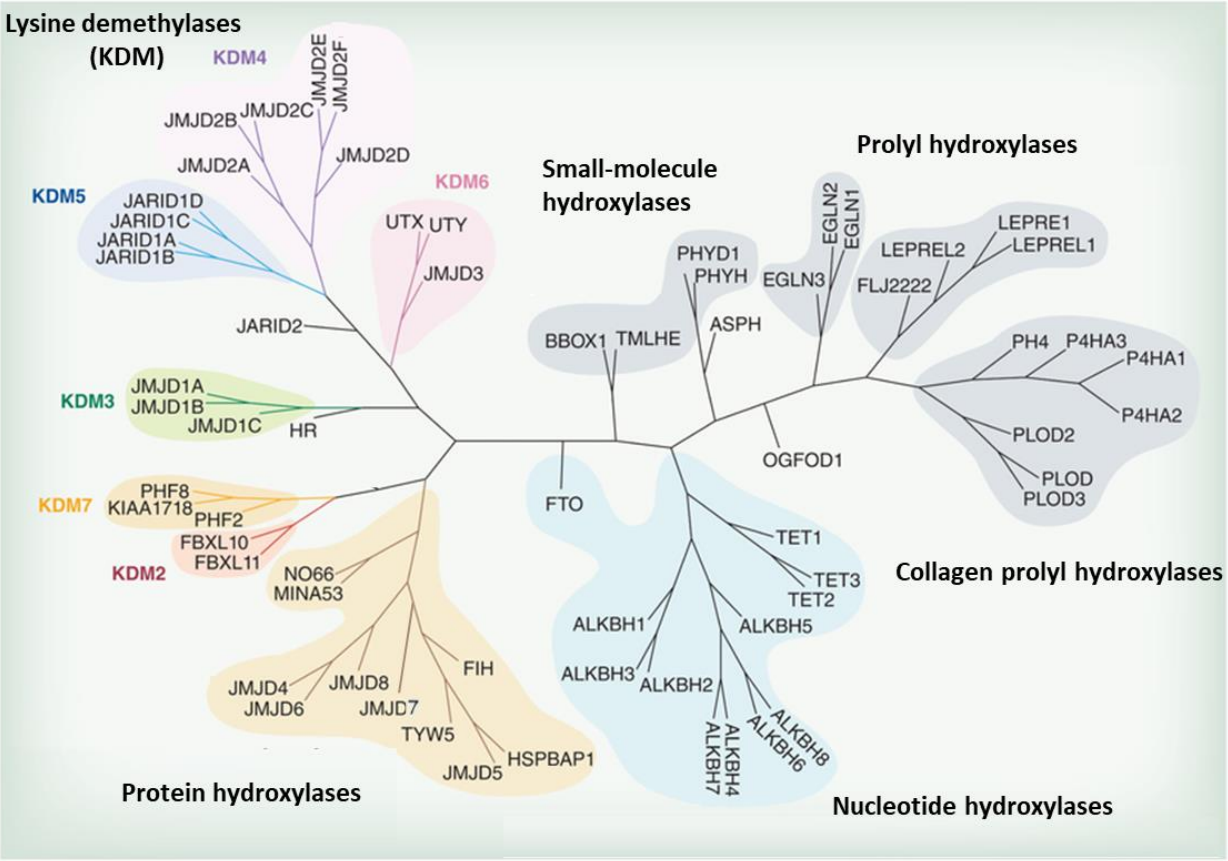

Figure 1. 1 Phylogenetic tree of 2OG dependent oxygenases.

Enzymes are clustered based on sequence homology. Sub-families of enzymes with shared substrate specificity including lysine demethylases (KDM), protein, nucleotide, prolyl, collagen, and small-molecule hydroxylases are highlighted in different colours. Proteins labelled in black

represent those that are not classified into any specific subfamilies. Figure adapted from Johansson et al. 2014.

The catalytic domain of 2OG oxygenases has a double-stranded β helix (DSBH) fold consisting of eight antiparallel β strands that form a barrel-like structure which contains binding sites for the co-factors (McDonough et al., 2010). Initiation of catalysis requires binding of 2OG, which promotes binding of the substrate and subsequently oxygen (Figure 1.2.). A reactive intermediate is formed through oxidative decarboxylation of 2OG, which oxidises the primary substrate with the generation of by-products CO_2 and succinate (Fletcher and Coleman, 2020). Some members of the 2OG oxygenase family such as lysine demethylases (KDMs) can catalyse demethylation through hydroxylation of Nε-methyl groups of histone lysine residues, to produce a hemiaminal intermediate that is broken down into formaldehyde and the demethylated product (Figure 1.2A) (Loenarz et al., 2008).

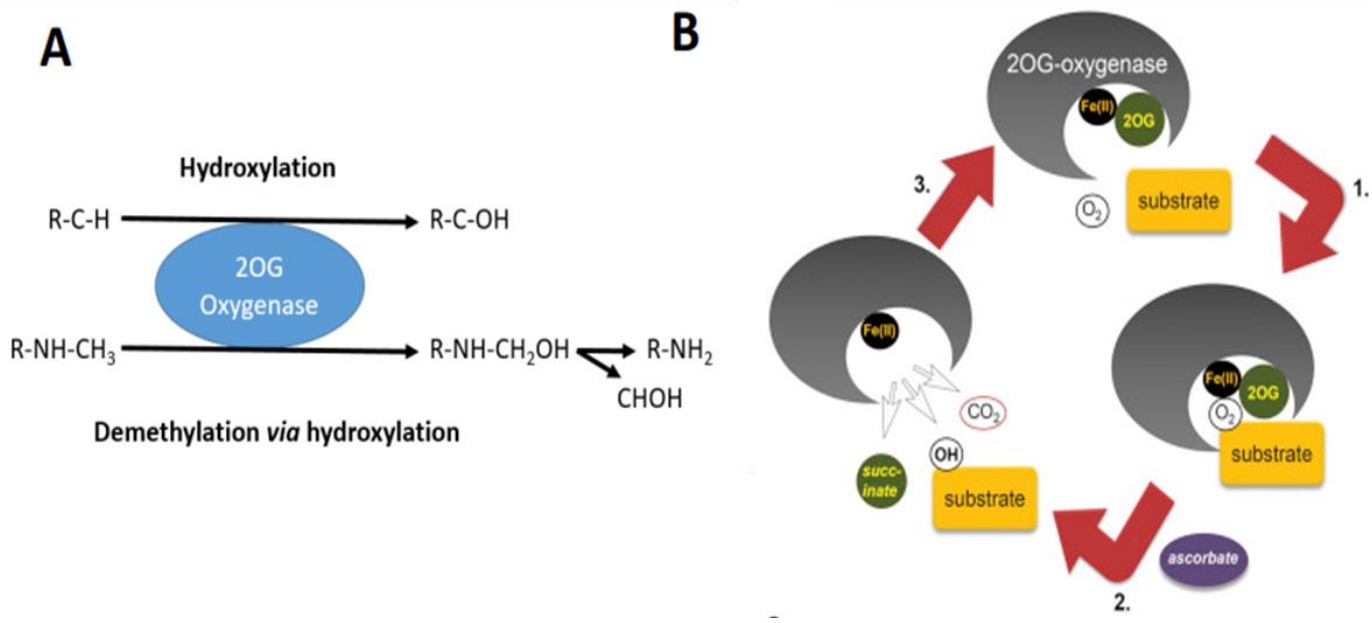

Figure 1. 2 2OG oxygenase family catalyse hydroxylation reaction.
A. 2OG-oxygenases can catalyse hydroxylation or demethylation via hydroxylation. B. Simplified graphical representation of the catalytic cycle. Figure taken from Ploumakis and Coleman, 2015.

1.1.4 2OG-oxygenases as cellular sensors

2OG oxygenases have the potential to act as cellular sensors due to their dependence on nutrient availability. Their activity can be altered by changes in cellular environment and metabolism such as hypoxia or the presence of oncometabolites (Loenarz et al., 2008).

1.1.5 Oxygen sensing-Regulation of HIF1α

The most well-known example of oxygen sensing is the regulation of Hypoxia-Inducible Factor (HIF) by prolyl hydroxylases (PHDs). HIF is composed of two subunits: HIFα and HIFβ. The alpha subunit has three isoforms: HIF1α, HIF2α and HIF3α. The expression and activity of HIF1α is tightly regulated by oxygen levels whereas HIF3α has no transactivation domain and HIF2α is only expressed at particular developmental stages in selected tissues (Patel et al., 2010; Gu et al., 1998). In normoxic conditions, HIF1α is rapidly degraded. Oxygen is needed for the hydroxylation of prolyl residues of HIF1α by PHD1-3 (Masson et al., 2001). Hydroxylated HIF1α is recognised by the E3- ubiquitin ligase von Hippel–Lindau (VHL) protein and undergoes rapid proteasomal degradation (Jaakkola et al., 2001). During hypoxic conditions, the hydroxylation of HIF1α by PHDs is blocked due to lack of oxygen which prevents HIF1α from being degraded. Additionally, the HIFβ subunit is constitutively expressed, allowing both subunits to form a heterodimer and initiate the gene expression via the activation of hypoxia response elements (HREs) (Strowitzki, Cummins and Taylor, 2018). Another enzyme that negatively regulates HIF-1α in normoxic conditions is Factor inhibiting HIF (FIH). FIH is a protein hydroxylase that belongs to a class of enzymes called JmjC-only 2OG oxygenase (discussed in more detail below) that catalyses the hydroxylation of asparagine 803 residue on HIF-1α which blocks its association with the p300/CBP co-activator (Strowitzki, Cummins and Taylor, 2018).

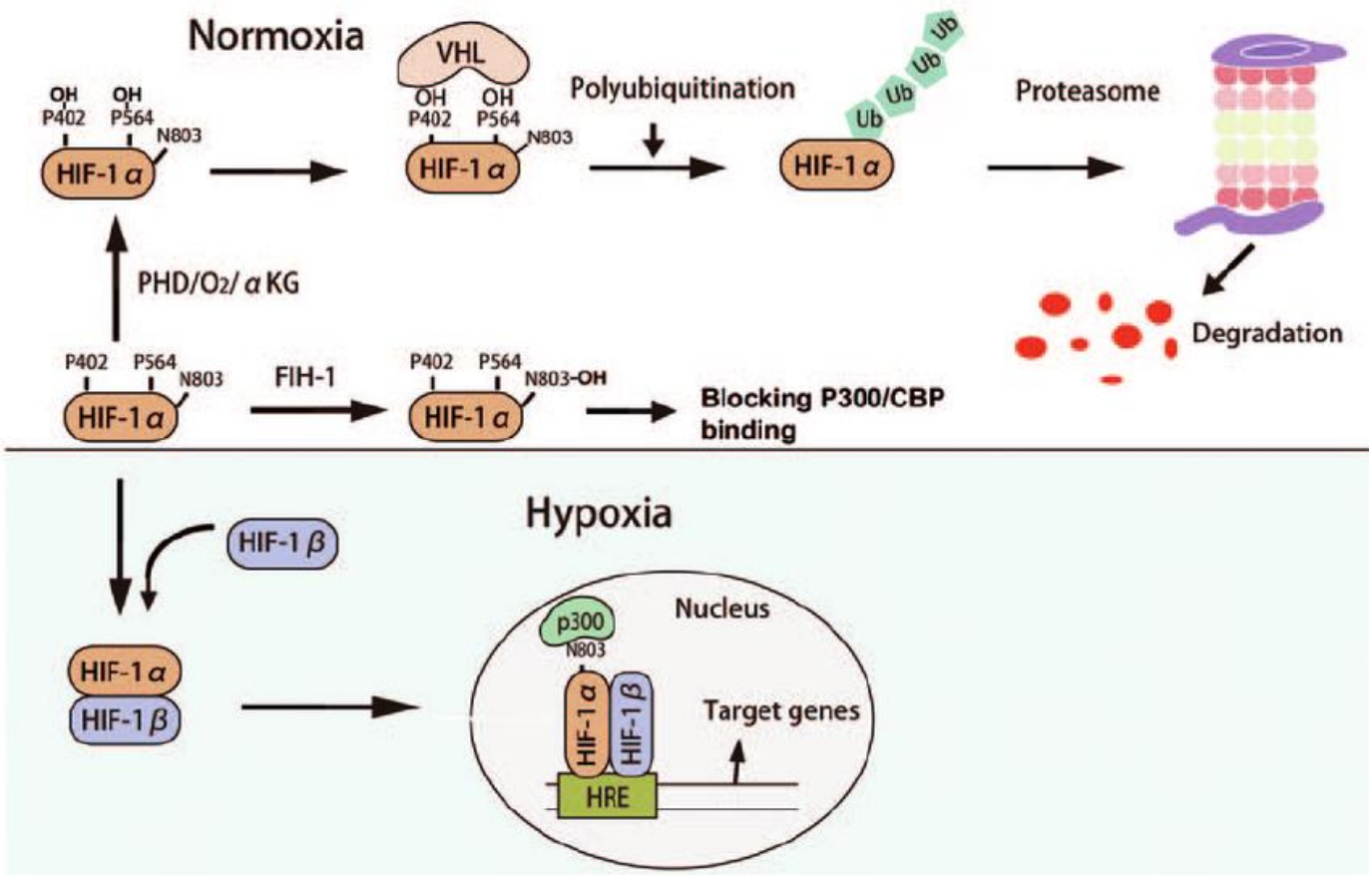

Figure 1. 3 Regulation of HIF by 2OG oxygenases.

In normoxia, HIF-1α is hydroxylated by prolyl hydroxylase domain (PHD) protein and factor-inhibiting HIF (FIH). Prolyl hydroxylation enables recognition of HIF-1α by von Hippel-Lindau E3 ubiquitin ligase (VHL) which leads to its proteasomal degradation. The hydroxylation of asparagine residue of HIF-1α by FIH blocks the association with transcriptional activators P300 or CREB-binding protein (CBP). Under hypoxic conditions HIF-1α a becomes stable and forms dimer with HIF-1β that associates with p300/CBP and binds the hypoxia response element (HRE) to start transcription of target genes. Figure taken from Lin et al., 2014.

Not all 2OG oxygenases are likely to be sensitive to physiological changes in oxygen levels. There is currently an incomplete understanding of the different oxygen sensitivities of enzymes within the family, which warrants further research (Loenarz et al., 2008).

1.1.6 Oncometabolites

2OG oxygenases activity can also be altered by the presence of oncometabolites (Loenarz et al., 2008). Examples of oncometabolites include 2-hydroxyglutarate (2-HG), fumarate or

succinate, which can accumulate as a result of mutations in isocitrate dehydrogenases (IDH), fumarate hydratase, and succinate dehydrogenase, respectively. Due to their structural similarity to 2OG, these oncometabolites can result in competitive inhibition of a variety of 2OG oxygenases. Indeed, several studies have demonstrated competitive inhibition of members of the 2OG family including KDM7A by oncometabolites *in vitro* (Xu et al., 2019). Such inhibition of 2OG-oxygenases by the presence of oncometabolites was shown to promote tumorigenesis due to dysregulation in DNA repair pathways (Inoue et al.,2016; Sulkowski et al., 2020). For example, mutations in IDH1 are linked to increased formation of double-strand breaks (DSBs) due to inhibition of KDM4A/B (Sulkowski et al., 2017). Moreover, inhibition of KDM4A/B by elevated levels of fumarate and succinate was shown to inhibit homologous recombination in hereditary leiomyomatosis and renal cell cancer (Sulkowski et al., 2018). In addition, increased H3K9 methylation as a result of 2HG accumulation has been linked to downregulation of ataxia telangiectasia mutated (ATM) kinase- a central mediator of DDR, in IDH1-mutated acute myeloid leukaemia (Inoue et al.,2016).

Another important mechanism by which oncometabolites can contribute to tumorigenesis is pseudohypoxia. Pseudohypoxia is a result of PHDs inhibition which leads to HIF stabilisation and activation of hypoxia response genes under normoxic conditions. This drives tumorigenesis via increased angiogenesis, increased cell survival and proliferation as well as metabolic reprogramming (Hayashi et al., 2019).

Collectively, the data indicates that the generation of oncometabolites within a tumour environment may further contribute to tumorigenesis by dysregulation of DDR pathways and pseudohypoxia, possibly due to inhibition of 2OG oxygenases.

1.1.7 JmjC domain-containing proteins

Jumonji C domain-containing (JmjC) proteins are a novel class of 2OG oxygenases that play an important role in various biological processes due to their role as demethylase or

hydroxylases targeting histones and non-histone proteins (Huang et al., 2013). The JmjC catalytic domain is a type of DSBH fold conserved across the 2OG family originally identified as the protein product of the jumonji gene (Klose et al., 2006). There are over 30 members of the family that are characterised by a cupin-type domain composed of around 150 amino acids known as the JmjC domain which confers hydroxylation or demethylation via hydroxylation activity (Saran et al., 2018). Many members of the family are aberrantly expressed or mutated in different diseases like neurological disorders and tumours and are shown to play a role in cancer cell proliferation (Ishimura et al., 2015).

KDMs are epigenetic regulators of gene expression due to their histone demethylase activity. In addition to the JmjC domain they also have other structural domains essential for their interaction with chromatin (Klose et al., 2006). This family comprise around 20 proteins (Figure 1.1) where different members possess various selectivity for particular histone residues as well as the methylation status of that residue (McDonough et al., 2010). They have been associated with diseases including cancer due to their role in epigenetic regulation (Johansson et al., 2014).

1.1.8 JmjC-only proteins

Some of the members of the JmjC domain family are a phylogenetically distinct class from KDMs and are classified as JmjC-only subfamily. Their members possess a protein hydroxylase activity and differ from KDMs due to their lack of DNA or chromatin-binding domains (hence the reference to 'only') (Klose et al., 2006), (Youn et al., 2012). Protein hydroxylases can catalyse the hydroxylation of prolyl, lysyl, asparaginyl, arginyl, aspartyl or histidyl residues of target proteins. The family includes 10 proteins: MINA, NO66, JMJD4, JMJD5, JMJD6, JMJD7, JMJD8, FIH, TYW5 and HSPBAP1 (Youn et al., 2012). Most of the members are thought to catalyse protein hydroxylation instead of demethylation which leads to challenges and controversies associated with biochemical misassignments (Flecher and Coleman, 2020). For example, various studies have reported histone demethylase and histone clipping activity

to JMJD5 (Liu et al., 2017; Shen et al., 2017; Hsia et al., 2010). However, detailed structural and biochemical studies support its function as protein hydroxylase (Wang et al., 2013; Wilkins et al., 2018) (discussed in more detail below). Moreover, studies involving JMJD6 failed to confirm reported histone demethylase activity (Islam et al., 2019). The tendency of misassignment of histone demethylation activity to proteins in the JmjC-only family extends to more members such as MINA, NO66, JMJD4 or JMJD7 (Flecher and Coleman, 2020). Moreover, the controversy in this field also extends to biological targets of JmjC-only family members (Flecher and Coleman, 2020).

MINA and NO66 are two ribosomal oxygenases with reported roles in ribosomal hydroxylation where MINA targets Ribosomal protein 27A (RPL27a) and NO66 has specificity towards Ribosomal protein L8 (RPL8) (Ge et al., 2012). Interestingly, both MINA and NO66 have been implicated in cancer with NO66 reported to act as an oncogene in glioblastoma (Wang et al., 2019) or colorectal cancer (Nishizawa et al., 2017). Nonetheless, the role of MINA in tumorigenesis is more complex with studies reporting its role as either oncogene or tumour suppressor gene depending on cancer type. Elevated MINA expression levels have been observed in several cancer types, including oesophageal (Tsuneoka et al., 2004), colorectal (Teye et al. 2004) or breast cancer (Thakur et al., 2014). Apart from MINA and NO66, TYW5 is also reported to function in translation, targeting RNA rather than protein (Ploumakis and Coleman, 2015).

Another member of the family that is also upregulated in cancer is JMJD4, which hydroxylates eukaryotic release factor 1 (eRF1) for optimal translation termination (Ploumakis and Coleman, 2015; Feng et al., 2014). In addition to JMJD4, JMJD6 which was recently reported to catalyse lysine hydroxylation of 48 proteins (Cockman et al., 2022), is shown to be overexpressed in various cancer types including breast (Lee et al., 2012) or lung cancer (Zhang et al., 2006).

JMJD7 has been found to target the Developmentally Regulated GTPase 1 and 2 (DRG1 and DRG2) for hydroxylation. The impact of this modification is not yet fully understood, but DRGs are known RNA interactors. JMJD7 is implicated in cancer where it has been identified as both an oncogene and a tumour suppressor gene (Liu et al., 2017; Zhu et al., 2016).

The catalytic potential of JMJD8 is uncertain due to a substitution in a key iron-coordinating residue (Yeo et al., 2016). Nevertheless, studies based on mutations in FIH suggest that two histidines may be sufficient to bind iron and have catalytic activity (Hewitson et al., 2008), which indicates that JMJD8 could have a hydroxylation activity. JMJD8 is primarily found in the cytoplasm and endoplasmic reticulum but can move to the nucleus where it may act as a transcriptional co-repressor of TET1 (Khoueiry et al., 2017). JMJD8 is also involved in processes such as cellular metabolism and NFκB signaling, (Yeo et al., 2016) and has also been linked to cancer (Ding et al., 2013).

FIH not only regulates HIFs but also hydroxylates asparagine residues within ankyrin repeat domains (ARDs) of various proteins, as highlighted by Cockman et al. (2006). ARDs, which consist of 30-34 residue repeats, each formed by two α-helices connected by a β-hairpin, are crucial for protein-protein interactions (Li et al., 2006). Hydroxylation by FIH occurs in numerous proteins, such as NF-κB (Cockman et al., 2006), myosin phosphatase target subunit 1 (MYPT1) (Webb et al., 2009) or Notch receptors (Coleman et al., 2007). Additionally, FIH's enzymatic activity also targets aspartate (Yang et al., 2011b) and histidine (Yang et al., 2011a) residues within ARDs. Despite this extensive list of FIH substrates, the specific functional outcomes of ARD hydroxylation are yet to be understood.

Heat shock protein beta-1 associated protein 1 (HSPBAP1) was initially discovered as interacting with heat shock protein 27 (Liu et al., 2000). However, a substrate has not been identified yet. It has been linked to cancer development (Yang et al., 2015). Another member

of the family for which substrate assignment remains controversial is JMJD5 (Fletcher and Coleman, 2020).

1.2 JMJD5

JMJD5 belongs to the JmjC-only sub-family of 2OG oxygenases. There was a lot of controversy regarding the classification of JMJD5 and its biochemical role with some publications reporting its role as a histone demethylase (Ishimura et al., 2015), (Hsia et al., 2010), (Amendola et al., 2017) and other publications presenting its role as protein hydroxylase (Del Rizzo et al., 2012; Wang et al., 2013; Wilkins et al., 2018).

Originally, JMJD5 was characterised as histone H3K36m2 demethylase regulating gene expression and therefore, was named KDM8 (Hsia et al., 2010). Another report suggested that JMJD5 is an endopeptidase that clips methylated arginine residues on histone tails (Liu et al., 2017; Shen et al., 2017). However, a number of independent studies failed to detect reported histone demethylase activity both *in vitro* and *in vivo* (Youn et al., 2012; Del Rizzo et al., 2012; Shen et al.,2017; Wilkins et al., 2018; Oh and Janknecht, 2012). Indeed, the structural comparison of JMJD5 with other members of the JmjC family indicates greater structural and sequence homology with the asparaginyl and histidyl hydroxylase FIH, the lysyl hydroxylase JMJD6 and the RNA hydroxylase TYW5 than with JmjC lysine demethylases (KDMs) (Liu et al., 2017; Shen et al.,2017).

The most recent evidence supports the protein hydroxylase classification of JMJD5. JMJD5 was shown to catalyse C-3 hydroxylation of arginine residues on a synthetic peptide derived from the Regulator of Chromosome condensation domain-containing protein 1 (RCCD1) and the 40S ribosomal protein (RPS6) (Wilkins et al., 2018). This study also presented the crystal structure of the JMJD5 catalytic domain in a complex with 2OG. Similarly to other JmjC hydroxylases, the JMJD5 catalytic domain features eight β-strands, seven α-helices, five additional β-strands as well as three 3_{10} helices. Also, as for other 2OG oxygenases, the catalytic

activity of JMJD5 depends on the presence of an iron cofactor, which is coordinated by a conserved HXD/E...H motif that is composed of histidine (H321), aspartate (D323), and another histidine (H400) residues (Wilkins et al., 2018). Moreover, the direct interaction with 2OG is facilitated by four residues: Y272, K336, S318, and N327 whereas residues W310, L329, and V402 for the hydrophobic pocket to stabilise 2OG binding (Wilkins et al., 2018). Notably, unlike other JmjC-only hydroxylases, JMJD5 has a more compact catalytic pocket for 2OG binding (Islam et al., 2022). In addition to that, JMJD5 was shown to lack the active site region responsible for the binding of Nε -methylated lysine residues present in KDMs (Wilkins et al., 2018). However, apart from the evidence presented, the precise cellular substrates and biochemical function of JMJD5 remain unclear.

The JMJD5 structure contains a C-terminal JmjC domain which occupies over 30% of the protein sequence and a poorly characterised N-terminal region (Huang et al. 2013). Figure 4.1 shows the schematic diagram of JMJD protein structure.

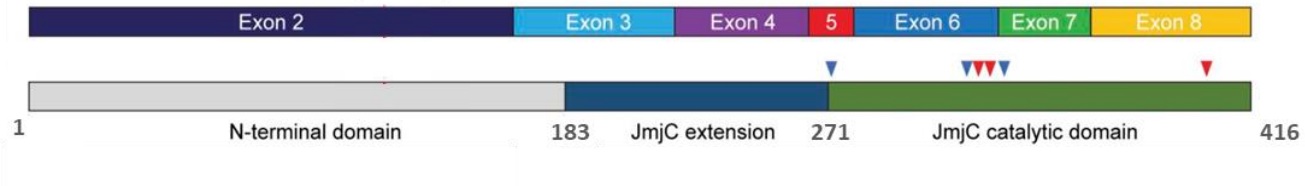

Figure 1.4 Schematic diagram of JMJD5 gene and protein structure.

The exons are aligned with their respective protein domains, Fe(II)- and 2OG-binding residues are marked by red and blue arrowheads, respectively.

Hueng et al. reported that the N-terminus is essential for the subcellular localisation of JMJD5 as it contains both a nuclear localization signal (NLS) and a chromosome region maintenance 1 (CRM1)-dependent nuclear export signal (NES) region (Huang et al. 2013). Interestingly, one reported and confirmed role of the JMJD5 N-terminus is to aid the interaction with the RCCD1 (Marcon et al., 2014; Wu et al., 2017). Marcon et al. reported that the interaction with RCCD1

is essential for proper chromosomal segregation as the loss of JMJD5 and RCCD1 leads to an increase in the number of multipolar spindles (described in more detail below).

1.2.1 Biological roles of JMJD5

The *KDM8* gene is located on chromosome 16 at position 12.1 and is conserved from worms to humans (Del Rizzo et al., 2012). JMJD5 is a metazoan JmjC protein that has been implicated in a plethora of essential cellular processes including embryonic development, cell cycle regulation, and regulation of mitosis (described in greater detail below). In addition, there are a number of other reported functions of JMJD5 including osteoclastogenesis, tumour metabolism, circadian rhythm regulation and a role in the DNA damage response (DDR).

JMJD5 was shown to be crucial in embryonic development as homozygous deletion of JMJD5 leads to embryonic lethality in mice due to an increase in p53 expression (Oh and Janknecht, 2012). Although JMJD5 was reported to downregulate p53 activity by interacting with its DNA-binding domain (Ishimura et al., 2012), the relevance of this potential interaction and its role in the JMJD5 knockout mouse phenotype, remains unclear. Moreover, several independent reports implicate JMJD5 in positively regulating cell cycle progression and proliferation via regulating cyclin-dependent kinase inhibitor 1 (CDKN1A) (Ishimura et al., 2012), (Zhu, Hu and Baker, 2014), (Huang et al., 2015).

In addition, two reports suggest that JMJD5 may contribute to the regulation of mitosis via cytoplasm accumulation and stabilisation of spindle microtubules (He et al., 2016), (Marcon et al., 2014). Due to its interaction with RCCD1, JMJD5 is reported to regulate chromosome segregation. Knockdown of either JMJD5 or RCCD1 has been shown to result in spindle assembly defects and disturbed mitosis leading to chromosome instability, one of the key characteristics of various cancer types (Marcon et al., 2014). JMJD5 depletion was also shown to sensitise cancer cells to microtubule targeting agents such as vincristine, which the authors

suggest raises the possibility that JMJD5 could work as a biomarker to predict patient response to this type of chemotherapeutic drug (He et al., 2016), (Wu et al., 2016).

JMJD5 has also been implicated in other processes such as osteoclastogenesis or tumour metabolism regulation. JMJD5 was reported to contribute to osteoclastogenesis by negative regulation of osteoclast differentiation through degradation of nuclear factor of activated T-cells calcineurin-dependent 1 (NFATc1) (Youn et al., 2012). Additionally, JMJD5 has also been implicated in tumour metabolism regulation by its interaction with pyruvate kinase muscle isozyme (PKM2) (Wang et al., 2014). This leads to nuclear translocation of PKM2 and activation of HIF-1α to initiate transcription of target genes involved in glucose metabolism. Since altered metabolism is one of the hallmarks of cancer, these observations have contributed to the suggestion that JMJD5 could be a novel oncogene.

Moreover, in *Arabidopsis*, JMJD5 is also thought to play a role in circadian rhythm regulation by acting in partnership with the timing of Cab1 expression (TOC1) and upregulates the expression of clock genes expressed at dawn (Jones et al., 2010; Jones and Harmer, 2011). However, these reports were generally studied in the context of JMJD5's controversial histone demethylase activity, raising questions about how JMJD5 protein hydroxylase activity is involved.

1.2.2 JMJD5 in replication stress and DNA repair

There are several lines of evidence suggesting that JMJD5 may play a role in the DDR. JMJD5 was identified in a genome-wide RNA interference screen as essential in protecting genome stability (GS) in somatic cells (Pothof et al., 2003). More recently, JMJD5 was reported to regulate homologous recombination (HR) in response to DNA damage. In a study in *C.elegans*, Amendola et al. found that JMJD5 is required for the repair of DSBs through HR and that loss of JMJD5 activity causes ionizing radiation sensitivity and aberrant retention of RAD-51 at sites of DSBs (Amendola et al., 2017). In addition, a separate study identified JMJD5 as one of

the genes whose loss causes sensitivity or resistance to DNA-damaging agents in CRISPR screens (Olivieri et al., 2020). Moreover, Shen et al. suggest that there is a potential induction of JMJD5 in response to certain types of DNA damage (Shen et al., 2017). They reported that treatment with DNA-damaging agents such as Camptothecin, Etoposide, and UV light-induced JMJD5 expression in A549 lung cancer cells (Shen et al., 2017).

1.2.3 JMJD5 in disease

A recent study by Fletcher et al. (2023) explored the role of JMJD5 in a newly identified developmental disorder marked by intellectual disability, severe failure to thrive, and relative macrocephaly. This disorder was notably associated with elevated 'replication stress' (RS) (further detailed in Chapter 3), which was dependent on the catalytic function of JMJD5. The disorder affected two patients who both carried biallelic mutations in the *JMJD5* gene: a missense mutation causing a C123Y substitution inherited from the mother and mutation that results in intronic deletion in intron 7-8 was inherited from the father (Flecher et al. 2023). Interestingly, the mother that carried a C123Y variant of JMJD5 had an early onset breast cancer at the age of 42 (Dr Sally Fletcher, personal communication) indicating the possible role of JMJD5 in cancer.

1.2.4 Roles of JMJD5 in cancer

JmjC domain-containing proteins have recently gained increasing interest due to their contribution to malignant tumour development (Yao et al., 2019). JMJD5 has been associated with anti-oncogenic and pro-oncogenic activity indicating its context-dependent role in cancer.

JMJD5 was shown to have oncogenic activity in breast and colorectal cancers in which its overexpression is correlated to lower patient survival (Hsia et al., 2010), (Zhang et al., 2015), (Zhao et al., 2015). Increased expression of JMJD5 is also reported to be required for MCF-7 breast cancer cell proliferation, induction of epithelial to mesenchymal transition, and metastasis (Zhao et al., 2015). JMJD5 was also shown to regulate the cell cycle of breast cancer

cells by inducing cyclin A1 transcription regulating G2/M transition (Hsia et al., 2010), (Zhang et al., 2015). JMJD5 has also been shown to play a potential role in colorectal carcinoma pathophysiology as its inhibition results in a reduction of proliferation, migration and invasion of the colon cancer cell line Caco-2 (Zhao et al., 2015). Similar results were found in oral squamous cell carcinoma, where JMJD5 knockdown inhibited proliferation, invasion and migration as well as induced apoptosis of HSC-3 and SCC-25 cells. Interestingly, in the same study, JMJD5 suppression reduced tumour growth in the mouse xenograft model (Yao et al., 2019). Moreover, JMJD5 have the potential as a prognostic indicator in non-small cell lung cancer patients that receive platinum-based chemotherapy: JMJD5 was found to be overexpressed in ~30% of cases and its high expression was significantly correlated with poor overall survival and poor progression-free survival time in those patients (Xiang et al., 2019). JMJD5 was also shown to have a pro-tumorigenic role in prostate cancer, where its overexpression correlated with the development of therapy resistance. JMJD5 was found to be overexpressed in both prostate tumour samples as well as prostate cancer cell lines and its knockdown reduced the proliferation of prostate cancer cells when compared to non-malignant cells (Wang et al., 2019). Furthermore, overexpression of JMJD5 was shown to promote therapeutic resistance through interaction with PKM2 and activation of androgen receptors leading to androgen-independence. Therefore, JMJD5 may have potential as a therapeutic target for therapy-resistant prostate cancer. Additionally, JMJD5 is also reported to be an oncogenic driver in glioblastoma as JMJD5 knockdown increases PKM2 enzymatic activity and suppresses glycolysis and proliferation in glioblastoma cells (Song et al., 2022).

In contrast, in hepatocellular carcinoma (HCC) JMJD5 may have tumour suppressor activity, with decreased expression correlating with shorter patient survival. JMJD5 was reported to inhibit the proliferation of HCC cells by activating the expression of CDKN1A (Wu et al., 2016). Interestingly, JMJD5 was originally identified in a tumour suppressor gene screen in

mouse models in which reduced JMJD5 expression increased mutational rates (Suzuki et al., 2006). Additionally, a multi-cohort retrospective study of transcriptional profiles in 25 types of cancer identified a gene signature including JMJD5, KDM6B, P4HTM, ALKBH4 and ALKBH7 that is associated with favourable cancer prognosis (Chang et al., 2017). This study reported that JMJD5 was downregulated in liver and pancreatic tumour samples when compared to healthy tissue and that low expression was correlated with higher risk of death in this cohort. JMJD5 expression was also found to be inversely correlated with the level of hypoxia, i.e. tumours with low JMJD5 expression were more hypoxic and the associated patients had reduced survival (Chang et al., 2017). In addition to that, another study looked at the association between JMJD5 and pancreatic cancer and reported that decreased JMJD5 expression promoted cell proliferation and glycolytic metabolism in pancreatic cancer cells by negatively regulating c-Myc expression (Wang et al., 2022). JMJD5 is also suggested to be a tumour suppressor gene in the context of lung cancer as it was recently reported that JMJD5 knockdown promotes the non-small cell lung cancer cell proliferation *in vitro* and xenograft tumour growth *in vivo* (Liu et al., 2023).

Overall, the complex assignment of JMJD5 to have both pro and anti-tumorigenic activity indicates that its role in cancer may be highly context-dependent.

1.3 2OG oxygenases as drug targets

As 2OG oxygenases are crucial enzymes involved in a range of disease-associated cellular processes, they are attractive targets for drug development. Interestingly, it has already been demonstrated that it is possible to successfully target this class of enzymes as competitive inhibitors of the PHD enzymes have been developed and are currently being evaluated in clinical trials (Yeh et al., 2017) (further discussed in Chapter 4). Notably, inhibitors targeting members of the 2OG oxygenase family have shown promise in preclinical cancer studies, with compounds like GSK-J1 (Chu et al., 2020), and TACH101 (Chandhasin et al., 2023)

demonstrating anticancer effects. Recently, inhibitors of MINA53 (Nowak et al., 2021), JMJD6 (Ran et al., 2019; Xiao et al., 2022; Zheng et al., 2022) and JMJD7 (Liu et al., 2017) were developed and also show anticancer potential in various studies. Nonetheless, whether other members of the JmjC-only family can be successfully targeted is not yet known.

1.4 Aims of this study

The overall aim of this project was to enhance our understanding of the role of JMJD5 in cancer by focusing on evaluating the effects of JMJD5 loss in the context of RS and DDR.

1) JMJD5 is mutated in cancer, which is consistent with its potential tumour-suppressor activity. Whether these mutations are damaging is not fully defined, as such, functional studies are required to investigate this. We hypothesise that mutations in JMJD5 impair its function and affect RS in cancer cells. Therefore, the aims of this project was to evaluate the impact of JMJD5 mutations on its function and RS response.

2) Proteins involved in RS and DDR are often targeted in cancer. However, whether JMJD5 could be a therapeutic target in the same way is not yet known. We hypothesise that loss of JMJD5 may sensitise cancer cells to DDR inhibitors. Therefore, we aimed to evaluate the effect of JMJD5 loss in combination with other DDR inhibitors and anticancer agents on cancer cell survival, RS and DDR.

3) JMJD5 is emerging as a promising new oncology target. Research into the development of JMJD5 inhibitors is therefore needed to assess their potential as promising anti-cancer agents. We hypothesise that targeting JMJD5 with specific inhibitors may induce RS and DNA damage in cancer cells, making them more susceptible to cell death. Therefore, the last aim of this study was to characterise the effect of first-in-class JMJD5 inhibitors on cancer cells and evaluate their potential as anticancer agents.

Chapter 2: Functional characterisation of selected JMJD5 cancer mutations

2.1 Introduction

As discussed in Chapter 1, JMJD5 has been reported to regulate various biological processes essential for normal development. Interestingly, JMJD5 also has a complex role in cancer with conflicting evidence supporting its role as a tumour suppressor or oncogene depending on the cancer type, which suggests a context-dependent role in tumorigenesis. Recently, inherited mutations in the *KDM8* gene which impair JMJD5 enzymatic activity were shown to contribute to novel developmental disorder that is characterised by intellectual disability, severe failure to thrive and relative macrocephaly (Fletcher et al., 2023). Interestingly, this phenotype was linked to an increase in basal RS. Moreover, unresolved and persistent RS leads to increased genomic instability (GI) which is an important driver of tumourigenesis and has been recognised as one of the hallmarks of cancer (Hanahan and Weinberg, 2011). Therefore, in this chapter, I have aimed to investigate whether JMJD5 is functionally inactivated by mutations in cancer. We provide a brief overview of RS before presenting the findings.

2.1.1 DNA replication

DNA replication is crucial for maintaining genomic integrity, as errors in this process can lead to mutations, GI and cancer. Faithful DNA replication is essential for organism survival, as it preserves genetic information across generations and supports normal development and cellular function. It entails the synthesis of a complementary DNA strand based on an original template, a process crucial for ensuring the fidelity of genome copies in daughter cells (Bell and Dutta, 2002).

Before the DNA unwinds during replication, several crucial preparatory steps occur to ensure the process is accurate and efficient. First, specific proteins recognise and bind to the origins of

replication, designated sequences where replication will commence (Bell and Dutta, 2002). Subsequently, these proteins recruit additional factors, including cell division cycle 6 (CDC6), CDC10 dependent transcript 1 (CDT1), and the MCM2-7 helicase complex, to form the pre-replication complex (pre-RC) (Riera, Fernandez-Cid and Speck, 2013; Mizushima et al., 2000). This assembly licenses the origin, ensuring each DNA segment is replicated only once per cell cycle. Activation of the helicase is then achieved through phosphorylation by cyclin-dependent kinases (CDKs) and Dbf4-dependent kinase (DDK) (Li, Dao and Zhai, 2023). Subsequently, the DNA helicase unwinds the DNA double helix, forming a replication fork with two single-stranded templates (Figure 2.1) (Leman and Noguchi, 2013). One strand termed the "leading" strand, is synthesised continuously by DNA polymerase ε, while the other, known as the "lagging" strand, is synthesised discontinuously using RNA primers and DNA polymerase δ, resulting in Okazaki fragments. These fragments are subsequently joined by DNA ligase (Leman and Noguchi, 2013). DNA replication occurs bidirectionally from sites termed origins of replication.

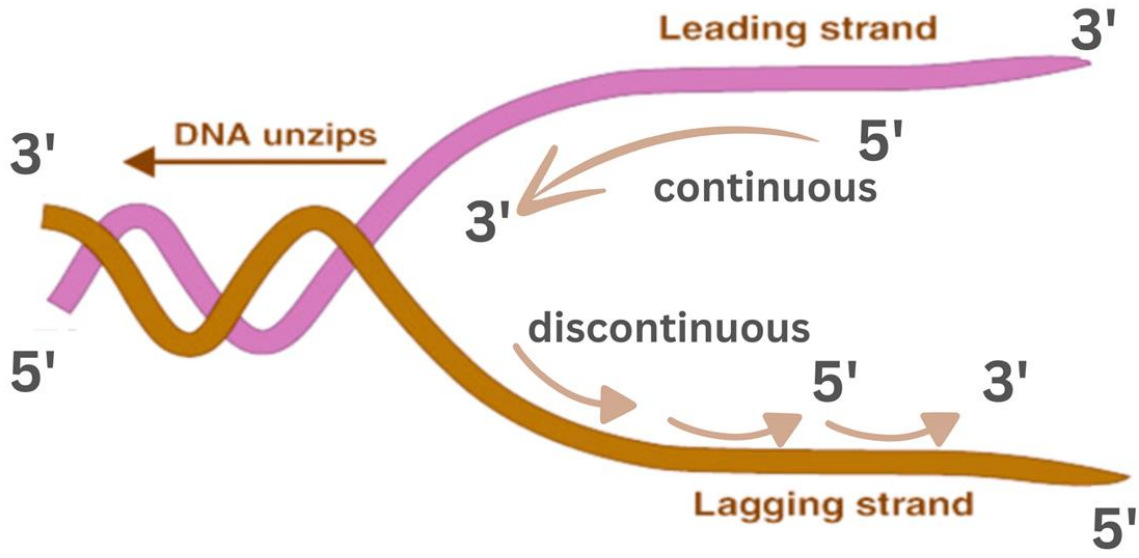

Figure 2.1 DNA replication fork progression.
On the leading strand, the DNA replication process of adding nucleotide bases by DNA polymerase is continuous whereas synthesis of the lagging strand is discontinuous where small DNA fragments named Okazaki fragments are synthesised and joined together via ligation.

2.1.2 DNA replication stress

During DNA replication, the replication machinery may encounter many obstacles or blockages causing the replication fork to slow or stall, resulting in RS (Zeman and Cimprich, 2014). This inhibition of DNA replication during prolonged RS can lead to under-replicated DNA or DNA damage. Therefore, RS response pathways are essential for genome stability. Below, we outline the causes of RS, the response pathways and its importance in human disease.

2.1.3 Causes of RS

There are various causes of RS that can be broadly categorised as endogenous or exogenous factors. Endogenous sources include physical obstacles such as sites of DNA damage or secondary DNA structures (Zeman and Cimprich, 2014, Thys and Wang, 2015); common fragile sites (CFS) such as telomeres and repetitive sequences (Krasilnikova and Mirkin, 2004). In addition, supercoiling of DNA, formation of R-loops (RNA hybridisation to DNA) during DNA transcription or collisions between transcription machinery and replisome can cause RS (Figure 2.2) (Kemiha et al. 2021; Helmrich et al. 2011). RS can also be the consequence of improper origin firing or lack of essential factors like nucleotides or histones (Figure 2.2) (Toledo et al., 2013, Anglana et al., 2003, Mejlvang et al., 2014).

Exogenous sources of RS include chemotherapeutic agents such as cisplatin, ionising radiation, ultraviolet light or other agents such as hydroxyurea or aphidicolin (Figure 2.2) (Vesela et al., 2017). Cisplatin induces RS through the formation of DNA interstrand crosslinks, which obstruct the progression of replication machinery (Vesela et al., 2017). In addition, hydroxyurea can cause RS via inhibition of the enzyme ribonucleotide reductase therefore limiting the deoxyribonucleotides available for DNA replication and leading to the accumulation of single-stranded DNA (ssDNA) (Vesela et al., 2017). Aphidicolin inhibits DNA polymerases preventing elongation of DNA chains during replication (Figure 2.2) (Vesela et al., 2017).

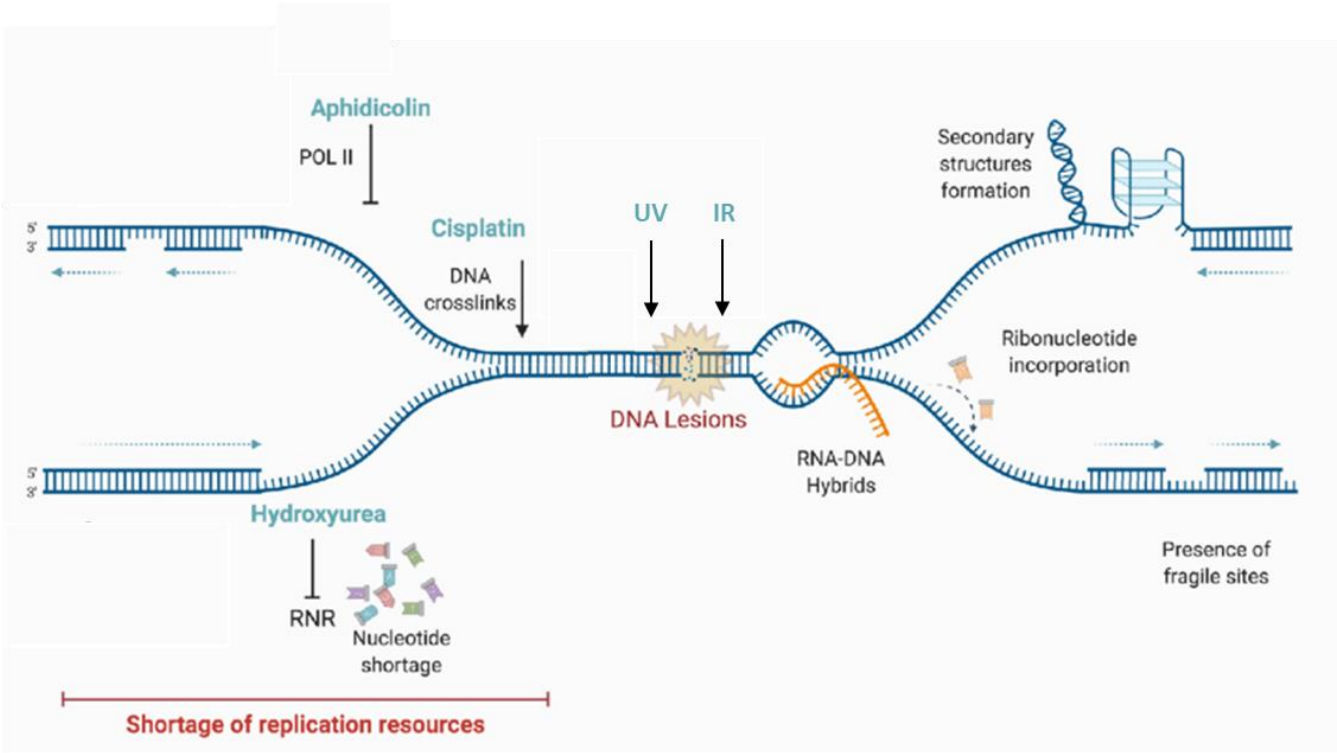

Figure 2.2 Causes of Replication Stress.

Endogenous causes of RS include DNA lesions, RNA-DNA hybrids, fragile sites or DNA secondary structures. Exogenous sources include chemicals such as hydroxyurea or aphidicolin, chemotherapeutic agents including cisplatin, or ionizing radiation (IR) and ultraviolet (UV). Figure taken and modified from Willaume et al., 2021

One of the consequences of RS is the separation of the DNA helicase from the replisome (Byun et al., 2005). Separation can occur when the replisome encounters an obstruction but the helicase keeps moving and unwinding the DNA. This leads to the formation of single stranded DNA (ssDNA) which is a hallmark of RS (Gelot et al., 2015). The response to RS aims to restore fork progression enabling replication fidelity and avoiding genomic instability.

2.1.4 RS response pathways

The first step in the RS response is the binding of Replication Protein A (RPA) to ssDNA in order to prevent nuclease degradation and activate the downstream response pathway (Fanning et al., 2006). This leads to the recruitment of 'ATM-Rad3-related' (ATR) kinase by ATR-interacting protein (ATRIP) to RPA sites (Figure 2.3) (Ball et al., 2007, Zou and Elledge, 2003, (Cimprich and Cortez, 2008). Additionally, the RAD9-RAD1-HUS1 complex is loaded onto

the primer-template junction on 5' ssDNA, recruiting TopBP1 to activate ATR via RAD9 interaction (Figure 2.3) (Majka et al., 2006, Lee et al., 2007, Mordes et al., 2008). ATR activation leads to phosphorylation of the histone variant H2AX (Ward and Chen, 2001) as well as further amplification of the RS response. The signal amplification is achieved by phosphorylation of checkpoint kinase 1 (chk1) (Lopez-Girona et al., 2001) which, once activated, phosphorylates further cellular substrates and results in cell cycle arrest (Figure 2.3) (Smits et al., 2006). The purpose of cell cycle arrest is to give time for successful DNA repair and replication fork restart and to prevent replication fork collapse which would result in the formation of toxic single-ended DSBs (Cortez, 2015).

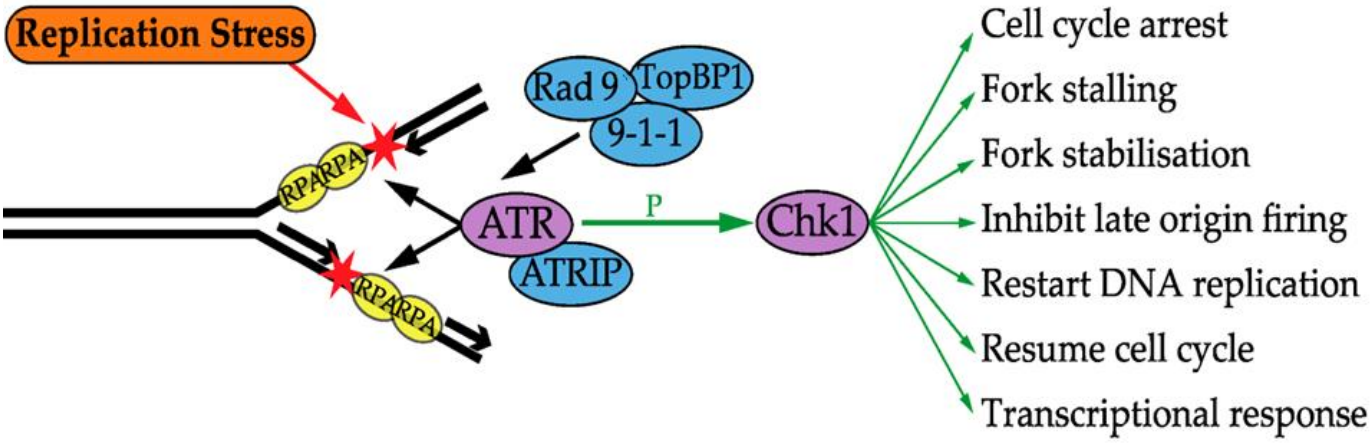

Figure 2.3 The cellular response to RS.

The separation of the helicase unwinding the parental DNA from the DNA polymerase that synthesizes new DNA can result in stretches of single-stranded DNA (ssDNA). This ssDNA is bound by RPA, which stimulates ATR recruitment by ATRIP protein. In addition, the RAD9-RAD1-HUS1 complex (9-1-1) recruits TopBP1 to activate ATR via RAD9 interaction. Activated ATR phosphorylates chk1 which further phosphorylates downstream targets to amplify the signal. Figure taken from Herlihy and de Bruin, 2017.

Another process that assists with correct DNA replication is dormant origin activation, which is particularly important when two converging forks stall. During origin licensing, there is an excess of MCM complexes loaded on DNA and while most of them are dormant during an unperturbed S phase, they can be activated during RS to ensure complete DNA replication around a stalled fork (Das et al., 2014, Ge et al., 2007, Woodward et al. 2006). Activation of

these dormant origins is orchestrated by the ATR-chk1 pathway through MCM2 phosphorylation (Ge and Blow, 2010; Cortez et al., 2004).

Cells must repair damage and complete DNA replication to maintain genomic stability. If not achieved during the S phase, cells can attempt to do so in the G2 phase and early mitosis, primarily through mitotic DNA synthesis (MiDAS). MiDAS aims to prevent under-replicated DNA and chromosome separation defects by completing replication before mitosis (Minocherhomji et al., 2015). Remaining lesions that persist into mitosis can lead to ultrafine DNA anaphase bridges (UBs), often associated with CFS, which can be repaired by MiDAS (Garribba et al., 2018).

In summary, while DNA replication is essential for preserving genomic integrity, challenges such as RS can impede this process, requiring the activation of response pathways to protect genomic stability and mitigate the risk of mutagenesis and cancer formation.

2.1.5 Consequences of RS: Developmental disease and cancer

Mutations in several genes encoding proteins crucial for DNA replication and the response to RS are associated with genetic disorders impacting development. They are broadly categorised as Primordial Dwarfism (PD) (Harley et al., 2016, Bicknell et al., 2011b, Reynolds et al., 2017). The affected individuals are characterised by pre- and post-natal growth retardation. For example, ATR mutations are present in a PD disorder called ‘Seckel syndrome’ and manifest through impaired RS response associated with clinical growth retardation phenotypes (O'Driscoll et al., 2003). Recently, biallelic mutations in the gene encoding *DONSON* (involved in the stabilisation and progression of replication forks) have been found as a novel cause of Meier- Gorlin syndrome which is associated with disturbances in the early stages of DNA replication (Knapp et al., 2020). Interestingly, JMJD5 mutations have also been implicated in novel developmental disorder associated with RS which may indicate its role in replication fidelity (Flecher et al., 2023).

Mutations in genes crucial for DNA replication and the response to RS not only impact developmental disorders like PD but also play a pivotal role in cancer. Interestingly, JMJD5, which has been associated with developmental disorders related to RS, also exhibits context-dependent roles in cancer. Therefore, we aimed to investigate the effect of JMJD5 cancer mutations in the context of GS.

2.1.6 JMJD5 is mutated in cancer

Since the Coleman group has an interest in exploring the role of protein hydroxylases in cancer, they have investigated if KDM8 mutations are observed in tumours. They mined online databases COSMIC and cBioportal and generated a list of all the reported KDM8 mutations across different cancer types. Based on this, a mutation profile mapped onto the JMJD5 protein was generated, which shows multiple mutational 'hot-spots' and recurrent mutations (Figure 1.4). Whether these mutations are damaging is not fully defined, as such, functional studies are required to investigate this. Therefore, one of the aims of this project was to evaluate the impact of selected KDM8 mutations on its function and RS response.

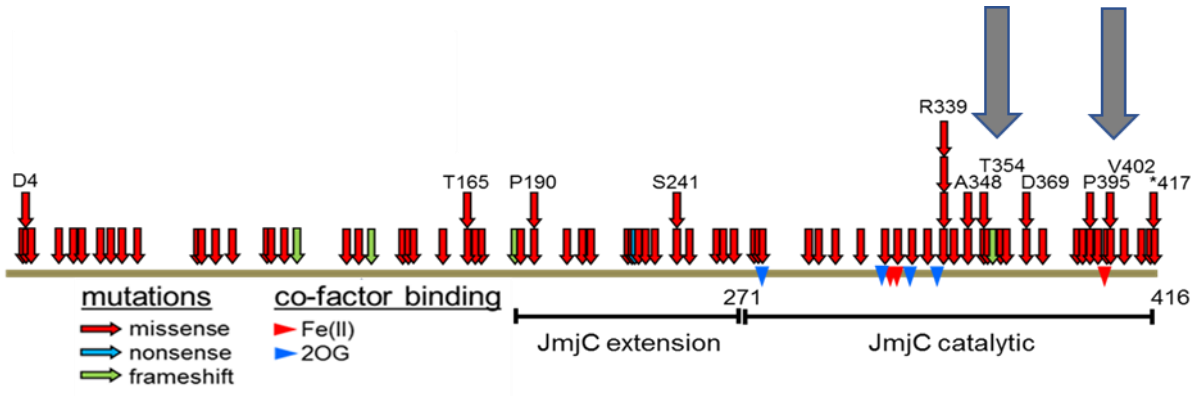

Figure 2.4 Mutation profile of KDM8 gene which shows multiple mutational 'hot-spots' and recurrent mutations.

The KDM8 structure with known mutation hotspots compiled from cBioportal and COSMIC. Work and figure was done by Dr Sally Fletcher. Grey arrows indicate the selected P395Q and T354M mutations further characterised below in the results section.

2.2 Results

2.2.1 Characterisation of selected *KDM8* mutations

In order to investigate the potential phenotypic consequences of these mutations I have focused on variants located within the catalytic domain and within a mutation hotspot. Based on those criteria, I selected two variants: P395Q and T354M. The P395Q missense mutation was reported in lung squamous cell carcinoma. This mutation is located within the JmjC catalytic domain and is within a mutation hotspot. T354M was present in carcinoma of the large intestine and is also located in the catalytic domain and in a mutation hotspot.

Firstly, we wanted to bioinformatically predict the potential consequences of these mutations on JMJD5 structure and function. To do so we used two online tools: Polyphen-2 and SIFT, which generate a score to predict whether an amino acid change is likely to be tolerated based on a few different factors such as sequence conservation, structural information, functional annotations and sequence homology (Adzhubei et al., 2010, Sim et al., 2012). The SIFT score represents the probability that the mutation can be tolerated, therefore low score indicates that the mutation is likely to be deleterious. In contrast, PolyPhen-2 scores the probability that the substitution of amino acid is damaging. This means that the high score represents deleterious mutation. Notably, both missense mutations are predicted by Polyphen-2 and SIFT to be highly damaging- scores of 0 (for P395Q) and 0.03 (for T354M) for SIFT, and a score of 1 (for both mutations) for Polyphen-2 probability (Table 2.1).

Table 2.1 Selected KDM8 variants and their Polyphen-2 and SIFT scores.

The SIFT low score indicates that mutation is likely to be deleterious whereas, for Polyphen-2 the higher the score the more confident the prediction that the mutation will be deleterious.

AA change	Codon change	Cancer Type	Mutation type	Polyphen-2 score	SIFT score
P395Q	c.1184 C>A	Lung Squamous Cell Carcinoma	Substitution - missense	1	0
T354M	c.1061 C>T	Carcinoma of Large Intestine	Substitution - missense	1	0.03

2.2.2 KDM8 mutations affect protein expression

Firstly, we started by assessing the impact of these mutations on JMJD5 protein levels and predicted potential structural consequences. To investigate the effect of the mutations on protein expression we transfected HEK293T cells with a pEF6 expression vector containing HA-tagged JMJD5. We have used pEF6 FLAG-JMJD7 as a transfection control and actin as a loading control. Interestingly, Western blot evaluation demonstrated reduced expression of P395Q when compared to wild type (WT) (Figure 2). The level of expression of T354M was also reduced when compared to WT, but more modestly than P395Q (Figure 2.5).

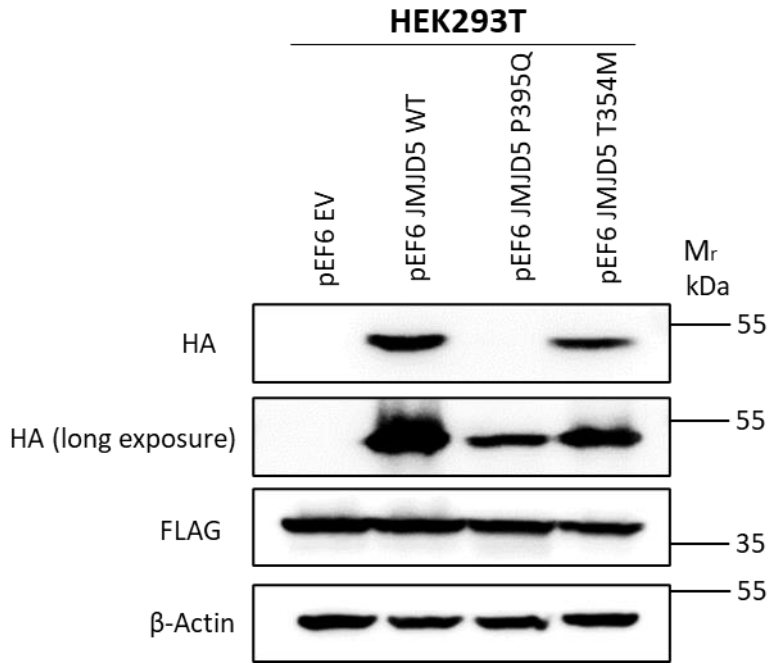

Figure 2.5 KDM8 mutations affect protein expression.

The effect of P395Q and T354M mutations on the JMJD5 expression in HEK293T cells. Cells were transfected for 72 hours with a pEF6 expression vector expressing empty vector (EV) or HA-tagged JMJD5, harvested and immunoblotted for HA (JMJD5), Flag as transfection control and Actin as loading control. N=3

To explore potential reasons behind the differential effects of the P395Q and T354M on JMJD5 protein expression we used the rotamer tool in Chimera software to model the substitutions. The results suggest that the substitution of proline to glutamine at position 395 may cause several clashes with the backbones of Glycine 203 and Arginine 204, which could explain why the protein is less stable (Figure 2.6). On the other hand, the rotamer tool suggests that the substitution of threonine to methionine at position 354 in T354M is unlikely to result in any structural clashes with other residues (Figure 2.6).

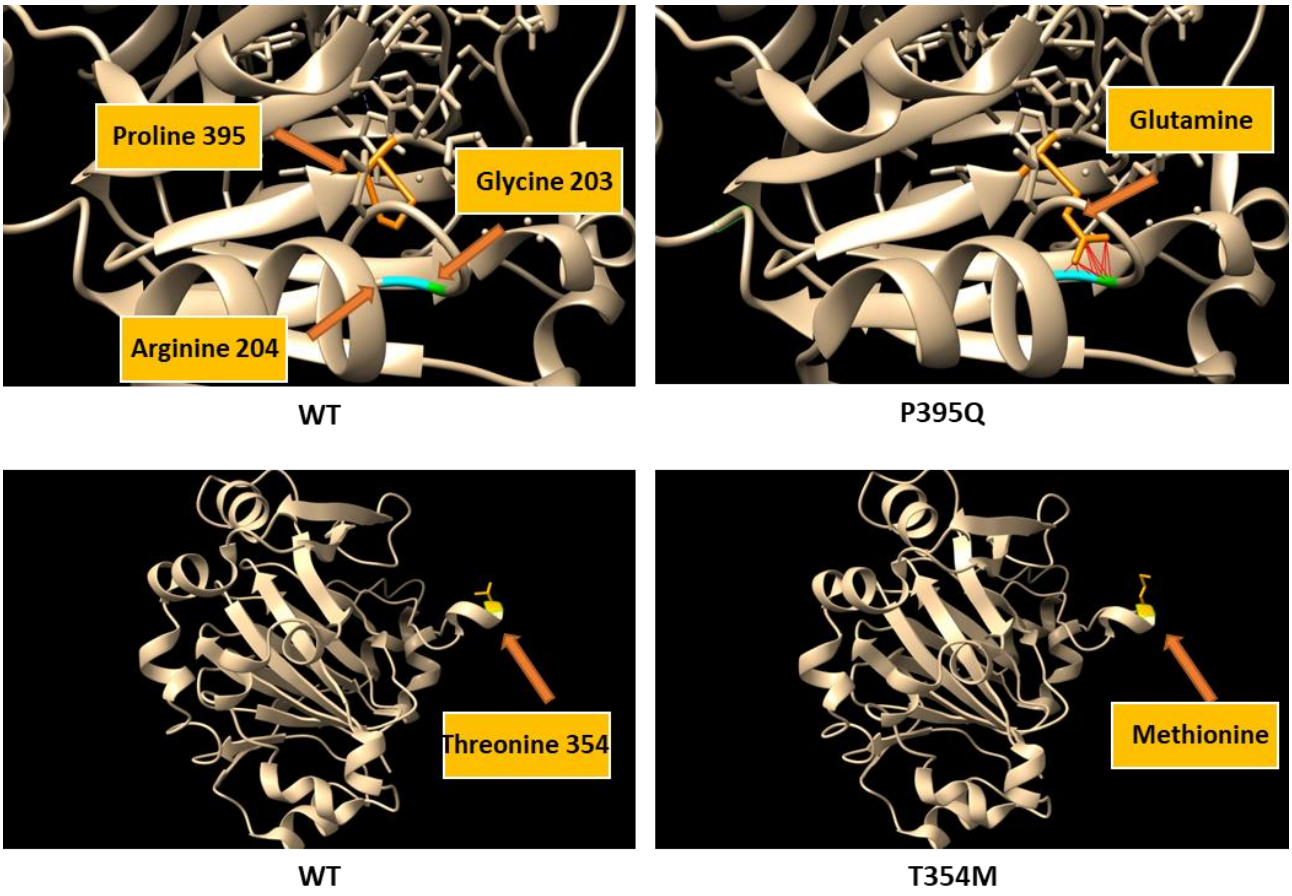

Figure 2.6 KDM8 mutations affect protein stability.
Structural analysis of the WT JMJD5 structure and mutations. The right upper panel shows the catalytic domain with P395Q mutation where proline 395 is substituted to glutamine which structurally interferes with arginine 204 and glycine 203 residues (marked as red lines on the figure). The right lower panel shows a catalytic domain with substitution of threonine to methionine in T354M which is unlikely to result in any structural clashes with other residues.

2.2.3 Selected *JMJD5* mutations affect enzymatic activity *in vitro*

We have shown that selected *KDM8* gene mutations can affect JMJD5 protein expression. Since JMJD5 is an enzyme, we were interested in investigating whether these mutations also impact its activity. To do so, we carried out *in vitro* hydroxylation assays using recombinant human GST-tagged JMJD5 purified from bacteria. In this assay, we incubated equal amounts of recombinant GST-tagged WT or mutant JMJD5 with cofactors Fe (II), ascorbate, 2-OG and with a substrate. As the physiological substrate of JMJD5 has not yet been identified, we used a synthetic peptide consisting of residues 129-144 from the RPS6 as an *in vitro* substrate for

JMJD5. This RPS6 peptide has previously been identified in an MS-based assay to be an *in vitro* hydroxylation substrate for JMJD5 (Wilkins et al., 2018). We used the Succinate-Glo hydroxylation assay (Promega) to indirectly monitor hydroxylase activity. This assay is based on the principle that succinate formed during the hydroxylation reaction is converted to ATP through a series of enzymatic reactions involving succinate dehydrogenase and other components in the assay system, which then supports luciferase activity (Figure 2.7A). We used a JMJD5 variant with a mutation in a critical iron-binding residue (H321A) as a loss of activity control and WT JMJD5 as a positive control. As 2-OG can be converted to succinate in the absence of substrate ('uncoupled turnover'), the raw values were converted into a fold change based on 'coupled' activity- resulting from a hydroxylation event.

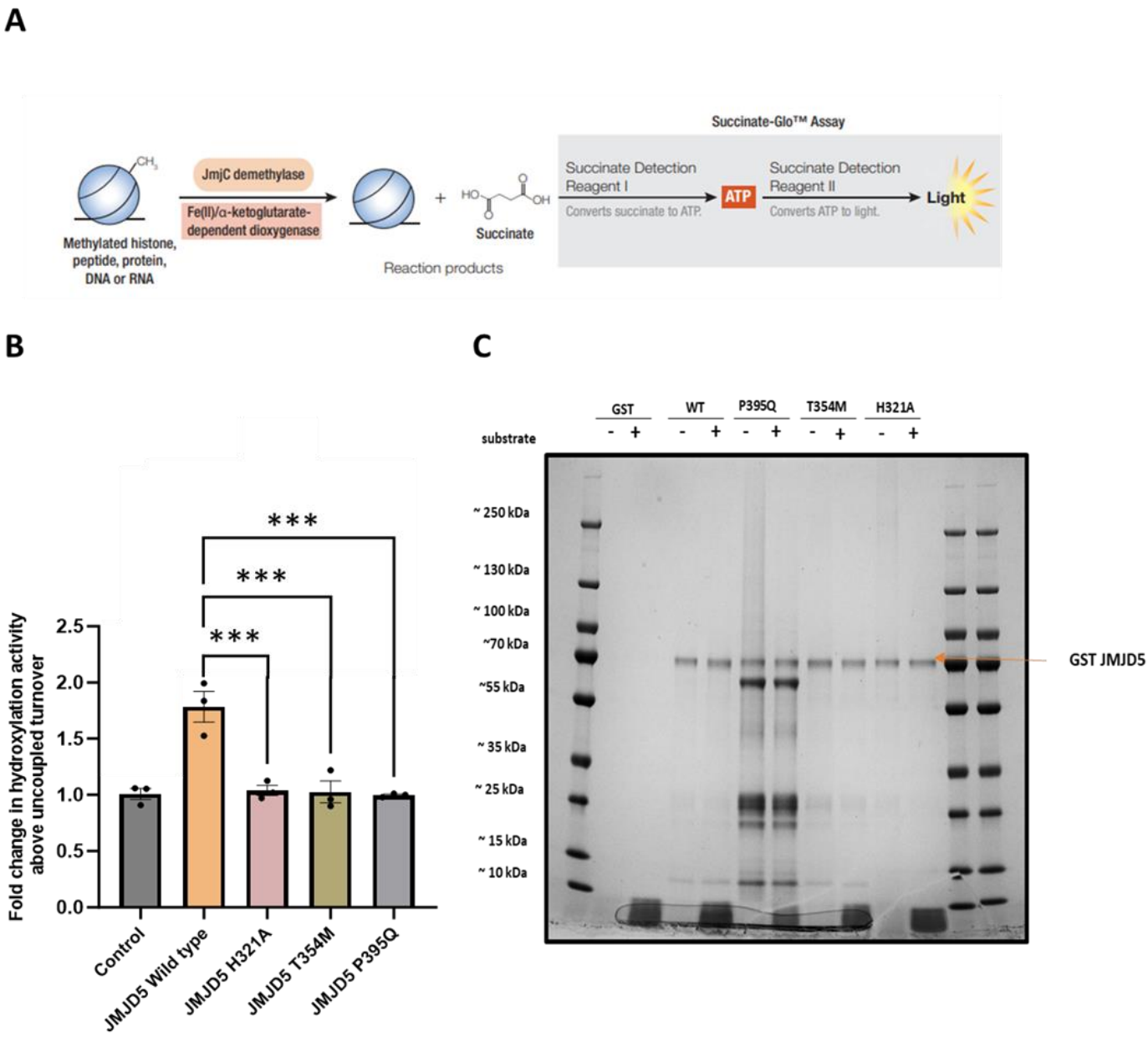

Figure 2.7 Selected KDM8 mutations affect the in vitro hydroxylation activity.

A. Schematic representation of the assay used to detect in vitro hydroxylation. Taken from Succinate Glo assay protocol from Promega. B. 20 µg recombinant JMJD5 proteins were incubated with Fe(II), 2-OG, ascorbate and RPS6 peptide for 1 hour at 37°C. The activity was then monitored using the succinateGlo assay. Data represent mean ± SEM from three independent experiments. Statistical analyses used one-way ANOVA with Bonferroni's post hoc test [with p-value ≤ 0.001 (***)]. C. 2 µL reaction loaded on the gel and stained with Coomassie to visualise JMJD5 protein. The orange arrow indicates GST JMJD5.

We found that the hydroxylation activity of P395Q and T354M mutants was significantly reduced when compared to the WT JMJD5, at the levels close to inactive H321A mutant (Figure

2.7B). Figure 2.7C shows the Coomassie-stained SDS-PAGE gel of the reaction products demonstrating equal loading of each JMJD5 variant. We note the presence of major additional species in the P395Q samples that likely represent cleavage products, which may be consistent with the lower overall yield for this mutant (data not shown). These observations could be due to the intrinsic structural instability predicted above, and consistent with the lower expression observed in cells. Overall, our biochemical and structural analyses indicate that these two cancer mutants are likely to have significantly reduced activity and function in cells.

2.2.4 Investigating if JMJD5 loss causes replication stress and if it is dependent on its enzymatic activity

Recently, Fletcher et al. showed that germline JMJD5 pathogenic variants present in two affected patients resulted in a human developmental disorder associated with increased RS phenotype. Moreover, these phenotypes could be rescued by reconstitution of a WT JMJD5 but not catalytically inactive JMJD5 (H321A), which highlights the importance of JMJD5 *activity* in genome stability. Interestingly, the mother of two affected patients who carried a C123Y variant of JMJD5 had an early onset breast cancer at the age of 42 years that could not be explained by a large gene panel of known breast cancer-associated mutations (Sally Fletcher, personal communication), consistent with a role for JMJD5 activity in RS and cancer.

Next, we wanted to investigate the consequences of loss of JMJD5 activity in tumour cells. Therefore, we wanted to develop a JMJD5 loss of function and reconstitution model to investigate the role of JMJD5 activity in regulating RS in cancer cells. We first set out to establish a JMJD5 knockdown model in a tumour cell line.

2.2.4.1 JMJD5 knockdown increases replication stress markers in A549 cells

The Coleman group have observed that JMJD5 may be important in replication stress response in U2OS osteosarcoma cells and HeLa cervical cancer cells (unpublished data). Therefore, I wanted to expand on this work by evaluating the effect of JMJD5 inhibition in other tumour cell lines. Preliminary work by Dr Sally Fletcher suggested that A549 would present a useful model to study the effect of JMJD5 mutations on RS. Additionally, the P395Q mutation was reported in lung adenocarcinoma. Interestingly, the role of JMJD5 in lung cancer is complex with reports supporting both its anti-oncogenic (Li et al., 2021; Liu et al., 2023; Shen et al., 2023) and pro-oncogenic activity (Xiang et al., 2019). Due to those reasons, we wanted to investigate whether JMJD5 knockdown has an impact on RS in A549 cells.

To evaluate the effect of JMJD5 knockdown on RS we assessed the formation of commonly used markers, micronuclei and 53BP1 bodies. Micronuclei are extra-nuclear bodies containing fragments of damaged chromosomes and/or whole chromosomes that were not reincorporated into the nucleus during mitosis (Luzhna, Kathiria and Kovalchuk, 2013). Micronuclei can form as a result of many cellular events such as problems in mitosis, in addition to RS, and can be visualised by staining with DAPI (Fenech et al., 2011). 53BP1 (P53 binding protein 1) is an important component of the DDR and plays a key role in orchestrating the choice of DSB repair pathway (Mirza-Aghazadeh-Attari et al., 2019). Accumulation of nuclear 53BP1 bodies in the G1 phase indicates RS in the previous S-phase. In order to identify cells in the G1 phase, co-staining with CENPF can be used, as CENPF only accumulates in cells that are in the G2/M phase and it is not expressed in G1 cells (Liao et al., 1995). Therefore, to assess the formation of 53BP1 bodies only CENPF-negative cells are counted.

We knocked down JMJD5 using a previously validated siRNA and performed immunofluorescent (IF) staining to evaluate the number of micronuclei and 53BP1 bodies

(Figure 2.8). We found that JMJD5 depletion in A549 cells leads to an increase in both micronuclei (Figure 2.8C) and 53BP1 bodies (Figure 2.8D) suggesting increased RS when compared to the control. The knockdown efficiency of JMJD5 was evaluated via Western blot (Figure 2.8E). Next, we were interested in whether this phenotype is dependent on JMJD5 enzymatic activity.

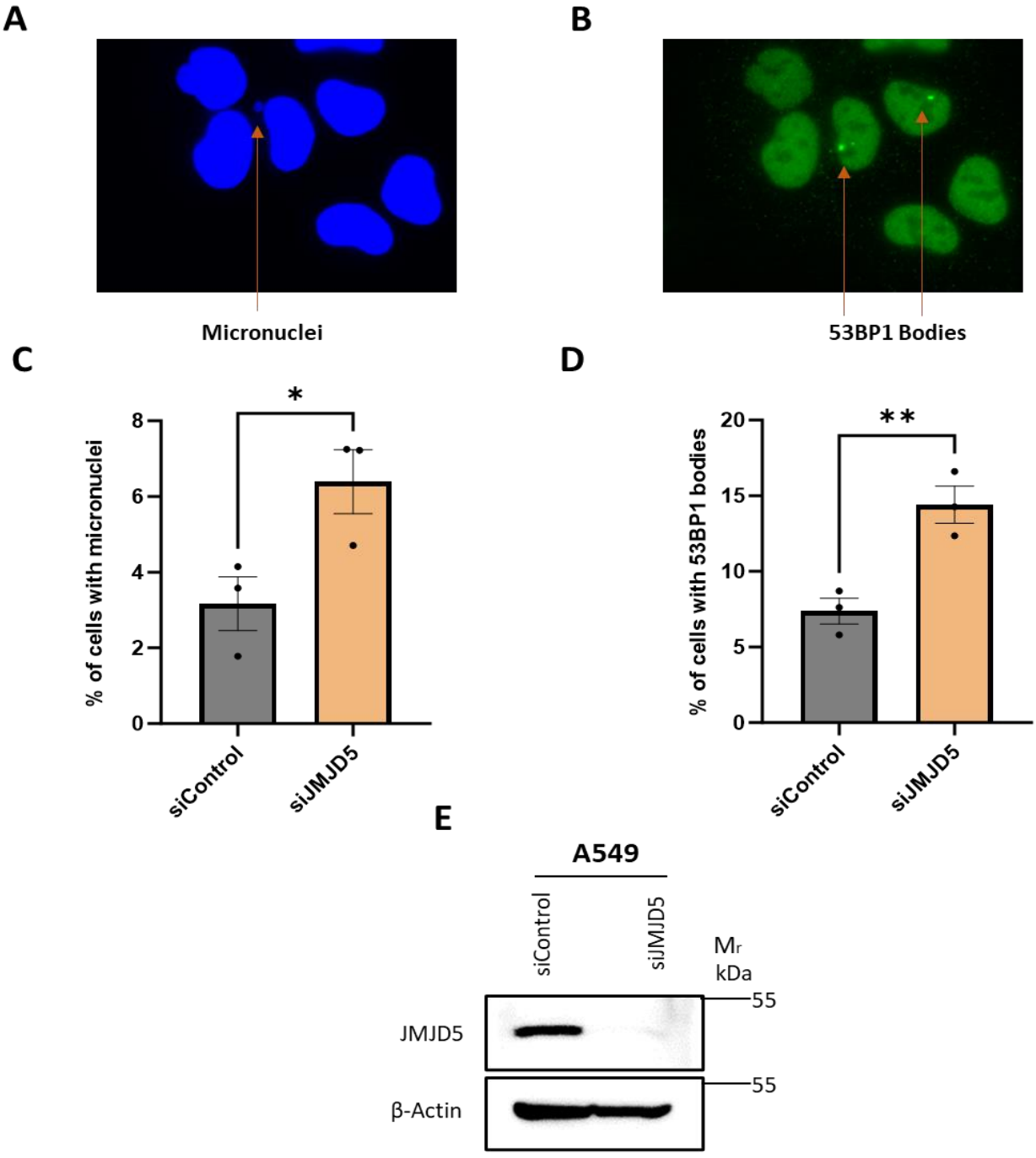

Figure 2.8 JMJD5 knockdown increases replication stress markers in A549 cells.
Cells were transfected with siRNA for 72 hours and stained with DAPI (blue) and 53BP1(green) A. and B. Example IF with observed micronuclei (A.) and 53BP1 bodies (B.) C. *Percentage of cells that contained any micronuclei and D. Percentage of G1 cells that contained any 53BP1 bodies. Data represent mean ± SEM from three independent experiments. To measure the percentage of micronuclei 500 cells were counted whereas for 53BP1 bodies 250 cells were counted. Statistical analyses used unpaired t-test [with p-value ≤ 0.05(*), ≤0.01 (**)]. E. Representative Western blot (N=3) evaluating the efficiency of JMJD5 depletion.*

2.2.4.2 Generation and characterisation of stable doxycycline-inducible 3xFLAG-JMJD5 A549 cell line

Recently, Fletcher et al. showed that the RS phenotype associated with a novel human developmental disorder was dependent on JMJD5 hydroxylase activity. To do so the authors compared patient cells reconstituted with either WT or catalytically inactive JMJD5. Therefore, we wanted to take a similar approach and reconstitute JMJD5 knockdown A549 cells with either WT, P395Q, or T354M JMJD5. Since the siRNA sequence used for JMJD5 knockdown is 3'UTR targeting, the JMJD5 cDNA could be considered 'siRNA-resistant' allowing us to examine the effect of exogenously introduced JMJD5.

WT and mutant JMJD5 cDNAs were PCR cloned into the lentiviral vector pTIPZ and lentivirus particles were generated using HEK293T cells for transduction of A549 cells. We generated A549 stable cell lines expressing doxycycline-inducible FLAG-tagged JMJD5 wild-type, or P395Q, T354M, or H321A variants, or an empty vector (EV) control. Successfully transduced cells were selected due to constitutive expression of a puromycin resistance gene. The pTIPZ vector contains a tetracycline-inducible promoter that allows the expression of the gene of interest upon the addition of doxycycline. After successful antibiotic selection of transduced cells, a doxycycline dose titration was performed to compare expression levels between WT JMJD5 and the variants. This allowed a comparison of endogenous and exogenous JMJD5 protein levels, with the aim of identifying a doxycycline concentration sufficient for the close to physiological expression of exogenous JMJD5. Because of concerns about the instability of the cancer mutants (see above), we tested a range of doxycycline concentrations (0, 25, 100 and 1000 ng/mL) for 72 hours (Figure 5A). For WT JMJD5 and H321A, we used 25 ng/mL doxycycline (based on previous results within the Coleman group). Although T354M was successfully expressed with 25 ng/mL of doxycycline, P395Q expression was minimal. However, at the highest dose used (1000 ng/mL), the P395Q variant was expressed at similar levels to endogenous JMJD5 (Figure 2.9). We note the presence of weak exogenous expression

in the WT, H321A and T354M samples not treated with doxycycline, which is probably a result of 'leaky' expression from the pTIPZ vector. There are a few potential explanations for this, one being the presence of fetal bovine serum (FBS) in the cell culture media that can contain residual tetracycline levels. Another possibility is the affinity of transcriptional activators to the tet operator which can result in low activation in the absence of tetracycline/doxycycline.

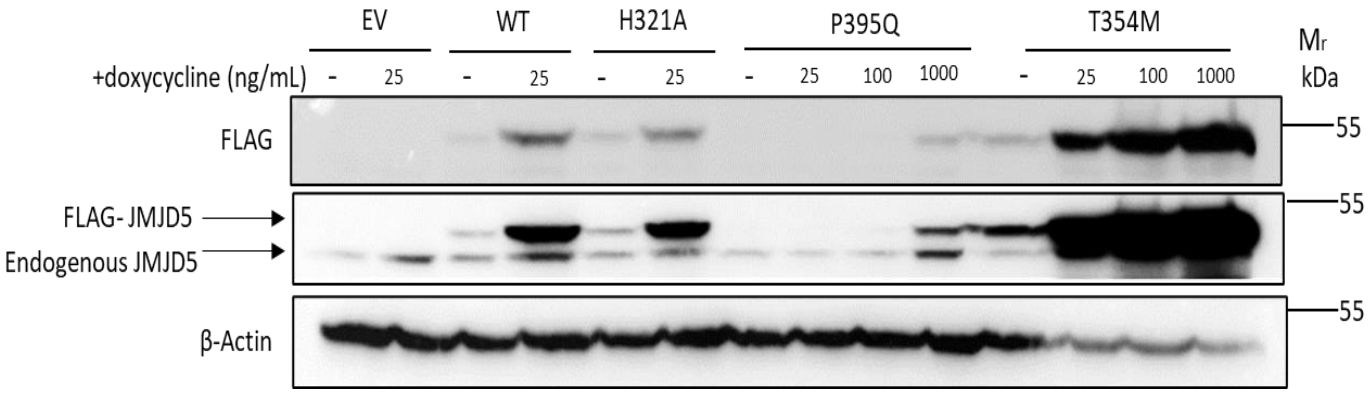

Figure 2.9 Characterisation of stable A549 cell line expressing doxycycline-inducible FLAG-tagged JMJD5.

*A549 cells were treated with doxycycline at the indicated concentrations for 72 hours, lysed and blotted for FLAG, JMJD5 and Actin.*upper band - exogenous JMJD5, lower band – endogenous JMJD5.N=3*

We also wanted to evaluate the potential heterogeneity of the exogenous JMJD5 expression in our stable cell lines. Therefore, we carried out IF staining for FLAG-tagged JMJD5. The cells were treated with the indicated doses of doxycycline for 72 hours to induce the expression of WT or mutant JMJD5. EV cells were used to identify any background staining. We observed low levels of FLAG-JMJD5 in WT, H321A, and T354M cells in the absence of doxycycline, consistent with the Western blot results (Figure 2.10). There was no FLAG-JMJD5 P395Q expression detected at 25 ng/mL doxycycline, while the highest dose resulted in weak expression.

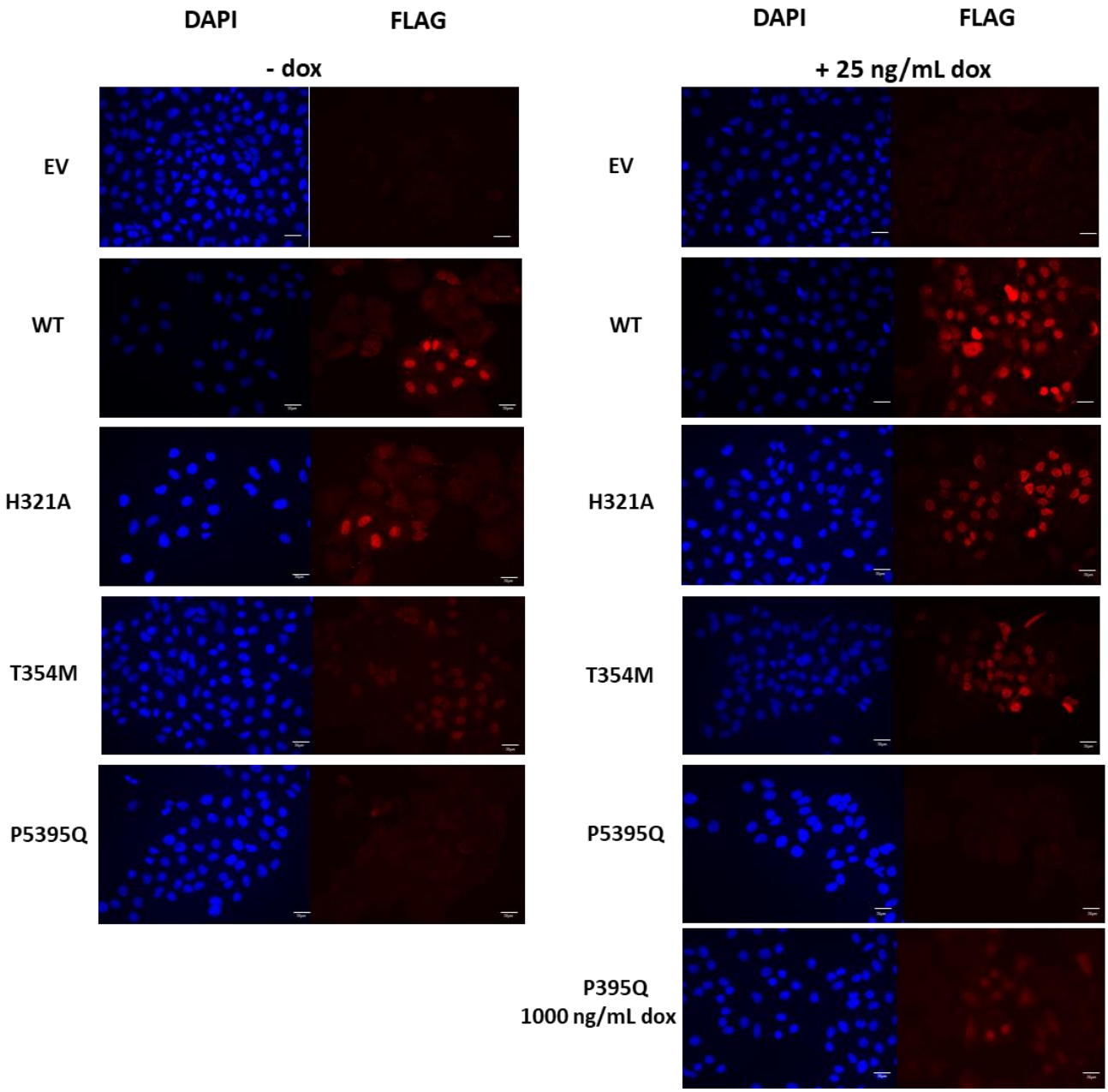

Figure 2.10 Representative immunofluorescence images of stable A549 cells.
The cells were treated with an indicated dose of doxycycline together with no doxycycline controls for 72 hours, fixed and stained with DAPI and FLAG. Scale bars = 20μm

2.2.4.3 JMJD5 knockdown-induced replication stress cannot be rescued by JMJD5 cancer mutants

Once the doxycycline-inducible pTIPZ system was established we tested whether exogenously expressed JMJD5 can rescue the RS phenotype induced by endogenous JMJD5 knockdown. The expression of JMJD5 variants was induced for 7 days followed by the siRNA knockdown

of endogenous JMJD5. The effect of JMJD5 WT and mutants on the RS profile was evaluated by measuring micronuclei and 53BP1 using IF staining. Successful endogenous JMJD5 knockdown was confirmed by Western blotting (Figure 2.11A). As expected, the analyses indicated that WT JMJD5 is able to rescue the formation of both micronuclei (Figure 2.11B) and 53BP1 bodies (Figure 2.11C) induced by endogenous JMJD5 knockdown demonstrated by the significant decrease in the percentage of cells with micronuclei or 53BP1 bodies when compared to EV. Importantly, H321A failed to rescue the RS phenotype, consistent with prior observations that the potential role of JMJD5 in replication fidelity is activity-dependent. Notably, and consistent with the lack of hydroxylase activity of P395Q and T354M described above, the re-expression of neither P395Q nor T354M variants could rescue the RS phenotype. Collectively, the data suggests that JMJD5 activity is important for maintaining replication fidelity and that this function can be compromised by mutations identified in tumours.

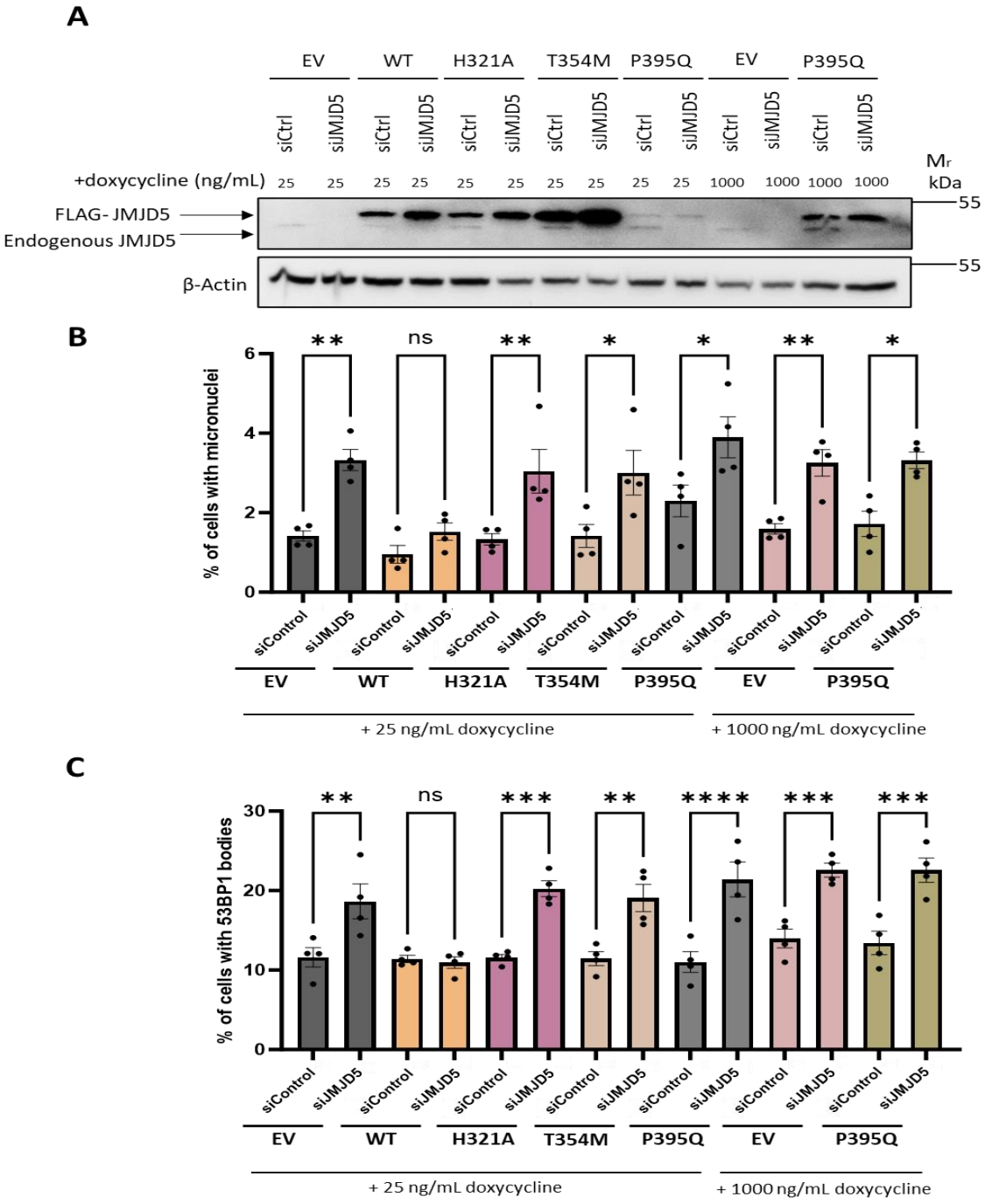

Figure 2.11 JMJD5 knockdown-induced replication stress can be rescued by exogenously expressed JMJD5 but not the characterised mutants.

pTIPZ EV, WT JMJD5, or JMJD5 mutant cells were transfected with the indicated siRNA for 72 hours before the cells were harvested and stained A. Western blot evaluation of JMJD5 expression (N=3). Actin as a loading control. B. and C. Cells expressing WT JMJD5, but not the JMJD5 mutants, were able to rescue (B) micronuclei and (C) 53BP1 bodies. For micronuclei above 500 cells were counted and for 53BP1 bodies above 250 cells in the G1 phase were counted. Data represent mean ± SEM from four independent biological experiments. Statistical analyses used one-way ANOVA with Bonferroni's post hoc test [with p-value ≤ 0.05(*), ≤0.01 (**), ≤0.001 (***) and ≥0.05 (ns))].

2.2.5 Generation of JMJD5 reconstitution system in HCA-7 cell line

The research presented above focused on investigating selected JMJD5 cancer mutations by re-expressing them in JMJD5 WT tumour cells following knockdown. To take an orthogonal approach, we were motivated to study tumour cell lines with endogenous JMJD5 mutations. The HCA-7 colon adenocarcinoma cell line was identified as carrying a heterozygous T354M JMJD5 missense mutation following analysis of the CBioPortal database by the Coleman group (Dr Sally Fletcher, personal communication).

Before undertaking extensive RS analysis in the HCA-7 cells we wanted to validate the presence of the T354M missense mutation. Therefore, genomic DNA was purified and gene regions surrounding the T354M mutation were amplified via PCR and analysed using Sanger sequencing. The presence of the T354M point mutation was identified on the sequencing chromatograms by the overlap of a red peak corresponding to thymine, with a blue peak corresponding to cytosine at the 1032-1035 position (Figure 2.12). Two overlapping peaks indicate heterozygosity of the alleles. Moreover, the peaks have similar intensities which may indicate that two alleles are present in equal amounts. Therefore, our analysis indicated that there is at least one copy of the JMJD5 gene that is mutated however, we did not know how many copies of WT *JMJD5* gene are present as the chromatogram did not show an exact 1:1 ratio of thymine to cytosine.

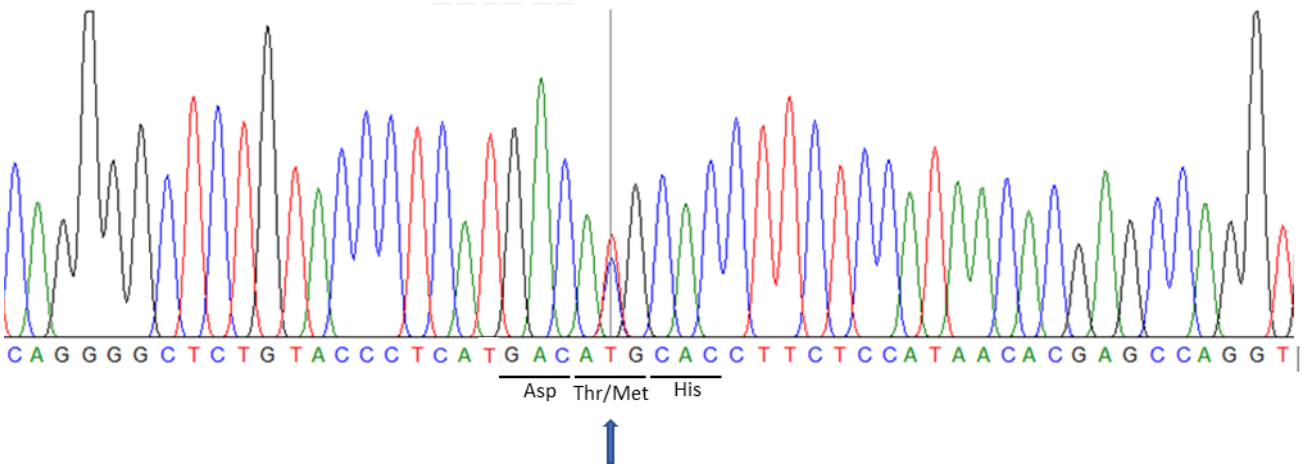

Figure 2.12 Generation of JMJD5 reconstitution system in HCA-7 cell line.

Genomic DNA was isolated and analysed by sequencing at position 1032-1035 in HCA-7 cells. The blue peak corresponds to cytosine and the red peak represents thymine.

Earlier, we demonstrated that the T354M variant was significantly less active than WT JMJD5. Moreover, we have also observed that exogenous re-expression of the T354M variant was not able to rescue the RS phenotype induced by endogenous JMJD5 loss. To achieve this, we hypothesised that re-expressing WT JMJD5 may be able to reduce basal RS levels in these cells. Therefore, I generated a reconstitution system in HCA-7 cells with the same doxycycline-inducible pTIPZ vectors (EV or WT JMJD5). To evaluate the levels of JMJD5 expression the cells were treated with various doses of doxycycline (Figure 2.13). We concluded that 10 ng/mL of doxycycline was able to induce the expression of WT JMJD5 above the endogenous levels and we decided to use that dose for our reconstitution experiments together with no doxycycline controls, which also provided 'leaky' expression to physiological levels.

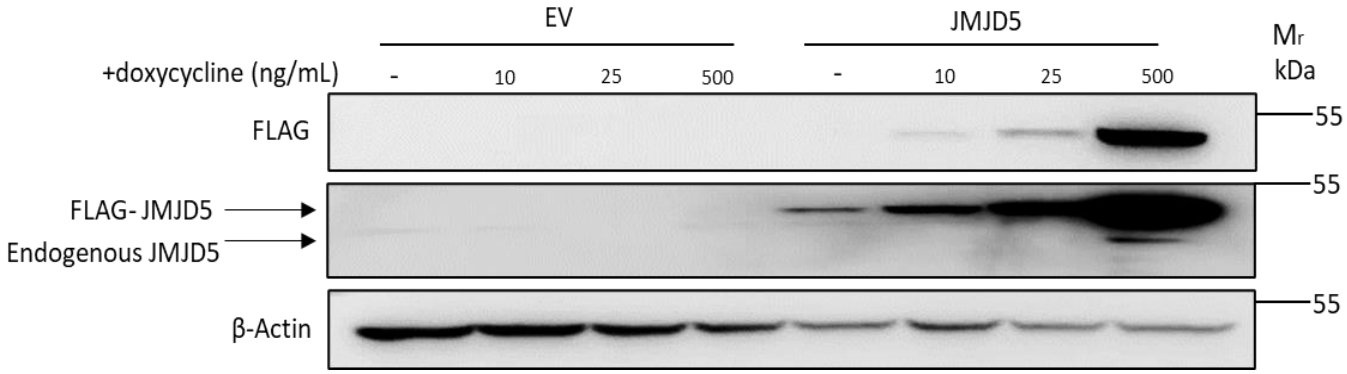

Figure 2.13 Western blot evaluation of JMJD5 expression in HCA-7 cells.
pTIPZ EV or WT JMJD5 cells were transfected with the indicated siRNA for 72 hours before the cells were harvested and blotted for JMJD5 and Actin. N=3

2.2.6 The effect of exogenous expression of wild type JMJD5 on basal replication stress in HCA-7 cells

After validation of the HCA-7 reconstitution system, we used it to explore if the exogenous expression of WT JMJD5 would affect basal RS in HCA-7 cells. Our results indicate that exogenous expression of WT JMJD5 does not significantly impact the amount of RS markers such as micronuclei (Figure 2.14A) and 53BP1 bodies (Figure 2.14B). Although there was a trend towards a modest JMJD5-dependent reduction in RS markers, this was not statistically significant. Therefore, we did not pursue this model further.

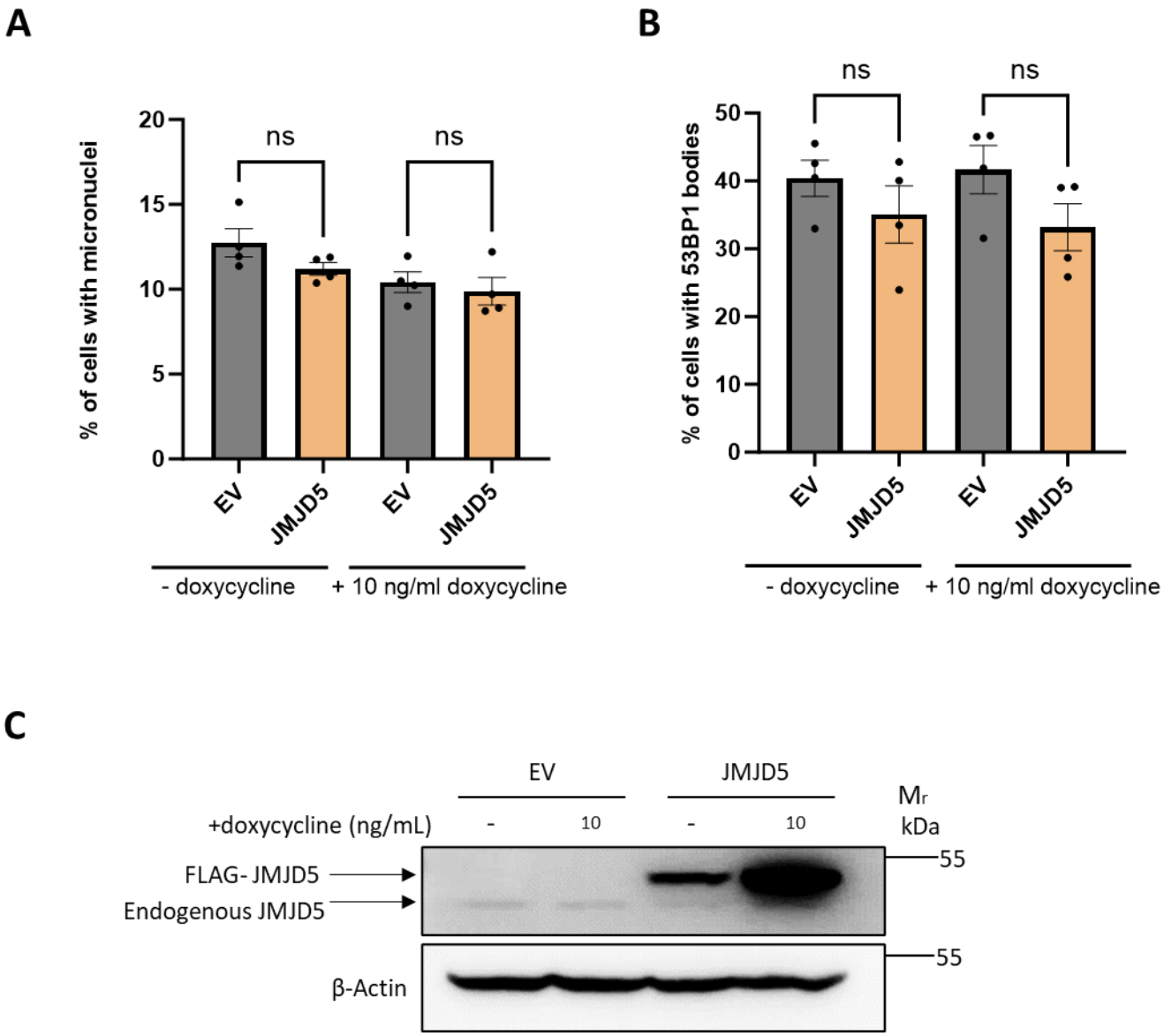

Figure 2.14 The effect of exogenous expression of WT JMJD5 on basal replication stress in HCA-7 cells.

A. and B. HCA-7 cells expressing exogenous WT JMJD5 did not have significantly different levels of (A) micronuclei and (B) 53BP1 bodies than cells transfected with EV control. Data represent mean ± SEM from four independent biological replicates. For micronuclei above 500 cells were counted and for 53BP1 bodies above 250 cells in the G1 phase were counted. Statistical analyses used one-way ANOVA with Bonferroni's post hoc test [≥0.05 (ns))]. C. Representative Western blot of HCA-7 pTIPZ JMJD5 rescue system with Actin loading control. N=3

2.3 Discussion

In this chapter, we have characterised selected JMJD5 cancer mutations for structural and expression analysis as well as the effect on *in vitro* hydroxylation activity. We have shown that cancer variants impair JMJD5 expression, activity and function in GS.

2.3.1 Are JMJD5 mutations damaging?

Our structural analysis indicated that the T354M substitution might not significantly affect the structure of the catalytic domain, whereas P395Q is predicted to cause a high number of clashes with the backbones of other amino acids (Figure 2.6). However, it is important to note that these are predictions based on probability and modelling, and not a resolved structure which warranted functional characterisation of these mutations in cellular models.

Our cell-based experiments indicated that there was reduced expression of P395Q (Figure 2.5), perhaps consistent with the structural analysis. Interestingly, there was a poor yield of the P395Q JMJD5 recombinant protein from bacteria when compared to WT JMJD5. Moreover, we noted the presence of probable cleavage products in the P395Q JMJD5 lanes of the Coomassie-stained gel (Figure 2.7). Together, these observations are consistent with the P395Q mutation affecting folding and stability. We also evaluated protein hydroxylation activity and discovered that the P395Q mutant lacks activity (Figure 2.7), which could be due to effects on folding because proline at position 395 is possibly a key structural residue, and its substitution with glutamine introduced clashes with surrounding residues, disrupting overall conformation and stability of the protein. Another possibility is that the P395Q mutation could block JMJD5 enzymatic activity without causing major effects on overall folding or stability by interfering with cofactor binding or the active site configuration.

Although the T354M variant impaired hydroxylation activity *in vitro*, and function in cells, it seems unlikely this was due to the kind of folding/stability issues proposed for P395Q as the T354M mutant did not exhibit significant differences in overall protein stability compared to

the WT. This suggests that T354M might influence enzyme function through mechanisms like altered cofactor binding. The substitution of threonine with methionine could affect electrostatic properties that influence the binding or positioning of essential cofactors like Fe(II) or 2OG, disrupting effective cofactor interaction and leading to reduced enzymatic activity. Moreover, T354 might be involved in maintaining the correct conformation of the region necessary for substrate binding. As such, the substitution could cause changes in the local protein structure or dynamics, affecting the alignment or accessibility of the active site. Therefore, a full-length structure could help identify if the mutation affects inter-domain interactions or overall protein architecture.

Although these results are potentially interesting, there are a few limitations that should be considered. Firstly, we do not know whether these mutations impact JMJD5 hydroxylase activity in cells. However, this line of investigation is currently not possible as a physiologically relevant JMJD5 substrate has not yet been identified (discussed in more detail in Chapter 4). Our evaluation of the effect of cancer mutations on JMJD5 hydroxylase activity is therefore currently limited to an *in vitro* hydroxylation assay with a short synthetic substrate peptide. Overall, our data indicate that JMJD5 mutations might have functional consequences in cells, contributing to cancer, therefore it prompts further investigation of other JMJD5 mutations.

Collectively, our current data suggests that the selected JMJD5 cancer mutations studied here are loss of function mutations, which may support the importance of JMJD5 as a tumour suppressor rather than an oncogene. Further investigations into the downstream effects of JMJD5 mutations on cellular pathways and tumour phenotypes are warranted to uncover potential therapeutic targets for cancer treatment.

2.3.2 JMJD5 is essential for maintaining genome stability and is inactivated in cancer

Fletcher et al. (2023) showed that JMJD5 mutations present in affected patients result in a human developmental disorder that is associated with increased RS. Moreover, the Coleman group has unpublished evidence that JMJD5 may be important in replication fidelity in U2OS osteosarcoma cells and HeLa cervical cancer cells (Sally Fletcher – personal communication). As part of this project, we wanted to expand on this work by choosing an additional model. We have presented that JMJD5 knockdown leads to increased RS in A549 cells as indicated by the increase in micronuclei and 53BP1 bodies (Figure 2.8). Our work presented in this thesis helps to demonstrate that the potential role of JMJD5 in replication fidelity is not restricted to a single cell type or disease.

We used the A549 model to evaluate whether the role of JMJD5 in GS is functionally inactivated by cancer variants. Our data suggests that the re-expression of WT JMJD5 is able to fully rescue the RS phenotype induced by endogenous JMJD5 knockdown (Figure 2.11). In contrast, the re-expression of P395Q and T354M cancer mutants did not result in the rescue of either micronuclei or 53BP1 body formation. This data indicates that cancer variants inactivate the function of JMJD5 in genome stability and possibly replication fidelity.

One interesting line for further research would be to explore the importance of JMJD5 in other cancer types. This could support the identification of specific cancer types that might be particularly sensitive to JMJD5 targeted therapy. Similar to strategies targeting replication factors (Gu et al., 2023), targeting JMJD5 could potentially sensitise selected types of cancers to DNA-damaging agents. This approach could selectively target tumour cells over normal cells, which typically exhibit lower levels of RS, and lead to the development of novel combination therapies that involve JMJD5 inhibitors (discussed further in Chapter 4).

One limitation of our RS analysis is that we have only measured in-direct markers (micronuclei and 53BP1 bodies). A more direct method of measuring RS is the DNA fibre analysis, which allows the progression of DNA replication to be monitored. This assay is based on incorporation of halogenated thymidine nucleotide analogues into replicating DNA in cells that can be further visualised using immunofluorescence. It allows the identification of different fibre structures and quantification of stalled forks as well as fork asymmetry which are both key markers of RS. It will be interesting to investigate the role of JMJD5 in tumour cell replication using such assays in the future. During the course of this project, DNA fibre analysis was initiated using A549 cells, and representative images of the fibre structures are presented in Figure 2.15. However, due to time constraints, it was not possible to obtain a sufficient amount of data to draw definitive conclusions. This aspect of the study will be pursued further in future.

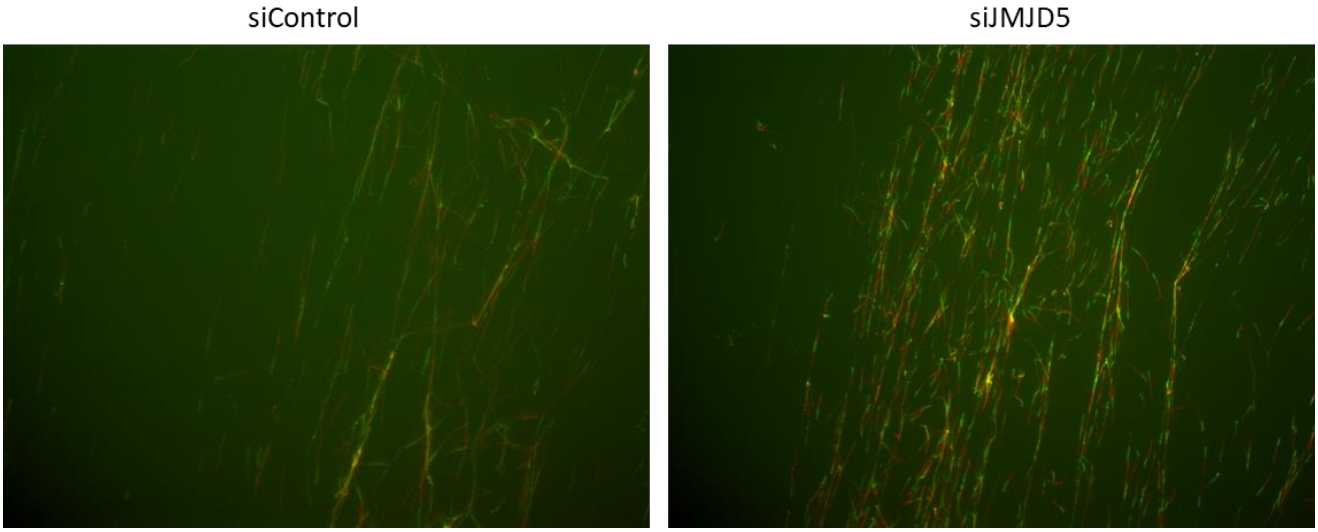

Figure 2.15 The representative images of DNA fibres in control and JMJD5 knockdown A549 cells.

Another techniques that assess the RS should be used such as quantification of RPA foci or bromodeoxyuridine (BrdU) incorporation for foci and/or cell cycle FACS analysis. As mentioned in the introduction, RPA is a ssDNA-binding protein that stabilizes ssDNA at replication forks (Fanning et al., 2006). Increased or persistent RPA foci indicate an accumulation of ssDNA suggesting unresolved RS (Saxena and Zou, 2022). The exposure of ssDNA can also be detected by BrdU staining (Saxena and Zou, 2022). BrdU is a synthetic

thymidine analog that is incorporated into DNA in place of thymidine during DNA replication (Yu, Wang and Wang, 2022). The presence of BrdU foci indicates the locations of active DNA replication. As such, a reduction or abnormal distribution of foci indicates RS, as replication forks may stall or collapse. In FACS analysis, BrdU incorporation identifies S-phase cells (Yu, Wang and Wang, 2022). Combined with DNA content staining with propidium iodide (PI), it reveals whether replication is slowed, stalled, or blocked in response to stress.

2.3.3 Model to study endogenous JMJD5 cancer mutations

We identified HCA-7 cells as a cancer cell line that harbours a JMJD5 mutation (T354M) that we had previously shown was enzymatically and functionally inactivating. To validate the relevance of using this cell line for studying the effects of JMJD5 mutations in cancer, we first carried out genomic DNA sequencing to confirm the presence of the T354M mutation (Figure 2.12). The presence of both WT and mutant alleles raises questions about JMJD5 function in such contexts. If the mutation is heterozygous, it is possible that the WT allele can compensate for the mutant allele, mitigating the impact of the JMJD5 T354M mutation. This might be one potential explanation for why we did not observe a significant impact of re-expressing WT JMJD5 on basal RS markers in these cells (Figure 2.14). An alternative explanation could be that multiple other mutations in different genes could be contributing to basal RS in these cells. Interestingly, HCA-7 cells are reported to have a frameshift mutation in the p53 gene (Liu and Bodmer, 2006) which may result in the loss of p53 function and influence the cellular responses including RS to WT JMJD5.

Another approach to model endogenous JMJD5 cancer mutations could be via CRISPR-based techniques in JMJD5 WT cells. Employing a CRISPR-based approach would provide a ‘cleaner’ genetic context in which to study the effects of JMJD5 mutations. This technique would allow for the controlled introduction of specific mutations and enable us to specifically test the importance of heterozygosity.

2.3.4 Chapter conclusions

In conclusion, the data described in this chapter suggest that JMJD5 mutations found in cancer could have a functional effect on RS and genome stability in tumour cells. Other factors involved in related biology are attracting attention as novel drug targets in cancer, including in combination with DNA-damaging agents or DDR inhibitors. In the next chapter, we explore the consequences of JMJD5 loss in the context of such treatments.

Chapter 3: JMJD5 loss of function sensitises tumour cells to DNA damage response inhibitors

3.1 Introduction

In chapter 2 we showed that JMJD5 enzymatic activity is essential for genomic stability and possibly replication fidelity in cancer cell lines. Interestingly, this phenotype was not limited to a single cell line but extended to different cell lines derived from various tumour types. This opens the possibility that targeting JMJD5 could potentially sensitise a variety of tumour types to DNA-damaging anticancer agents by potentiating the RS phenotype, resulting in DNA damage and cell death. Here in this chapter, I investigate this possibility in more detail. First, I provide an overview of DNA damage response pathways and the anticancer agents that target them.

3.1.2 DNA damage responses (DDR)

DNA repair is essential for genome stability because it corrects errors and damage in the DNA, preventing mutations that can lead to cancer and other diseases. There are different types of DNA damage and mechanisms that have evolved to repair them. Single-strand breaks (SSBs) occur in one of two DNA strands and are usually repaired by base excision repair (BER)/SSBR (Tasaki et al., 2018). In addition, there are other types of DNA damage such as base modifications, pyrimidine dimers, DNA crosslinks or bulky adducts. DSBs involve both DNA strands and are extremely cytotoxic. Failure to repair them is a major factor contributing to genome instability. DSBs are repaired either via HR or non-homologous end joining (NHEJ) (Tasaki et al., 2018). Although HR is the primary choice of repair for DSBs, it is only active in the S and G2 phases of the cell cycle. It uses a homologous DNA template to ensure accurate

repair (Wright et al., 2018). In contrast, NHEJ provides faster DNA repair during every stage of the cell cycle but is more error-prone (Pannunzio et al., 2018).

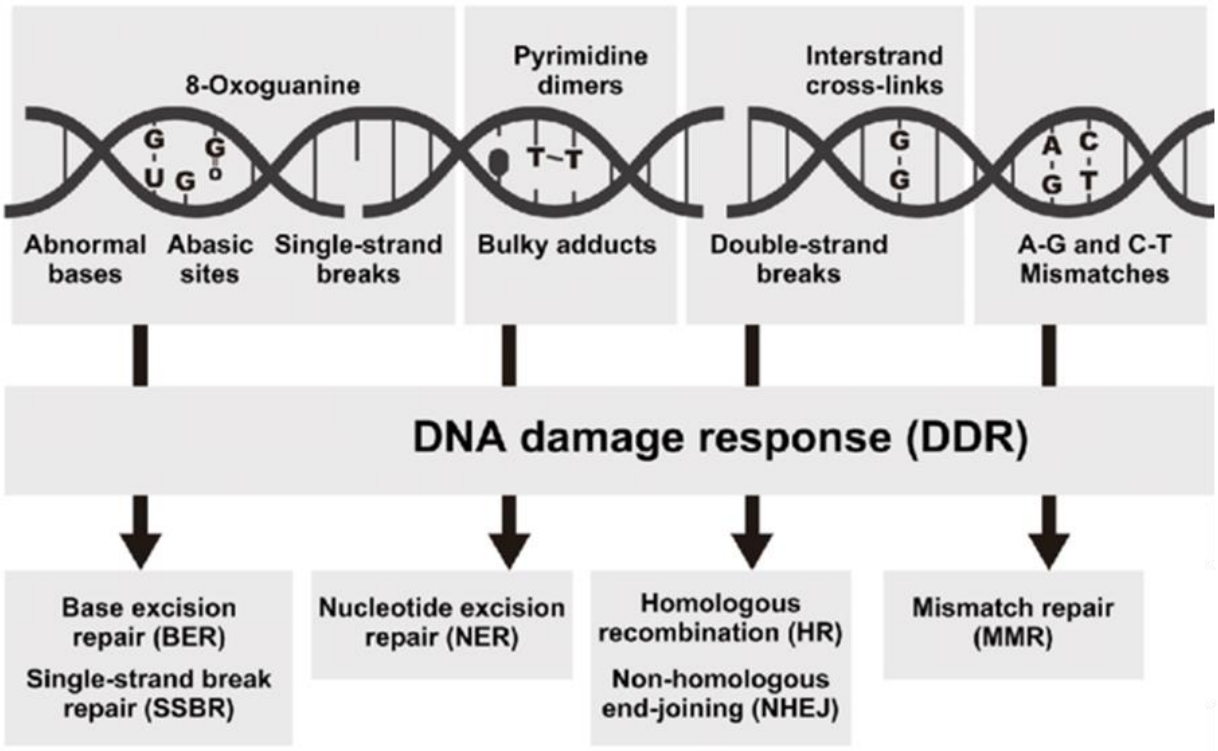

Figure 3.1 DNA repair mechanisms.

Base excision repair (BER) is a DNA repair mechanism responsible for removing and replacing damaged bases. Nucleotide excision repair (NER) addresses bulky adducts and cross-linking lesions caused by UV radiation or chemical exposure. The mismatch repair (MMR) pathway corrects base mismatches and insertion-deletion loops that occur during replication. Single-strand breaks are primarily repaired by BER/SSBR. Double-strand breaks (DSBs) in DNA are repaired through two main pathways: HR and NHEJ. Figure adapted from Tasaki et al., 2018.

Among the various factors involved in DNA repair, the ATM gene is particularly important in the DDR. It encodes for a serine/threonine kinase that plays an essential role in the DNA damage response. Specifically, ATM responds to DNA DSBs by activating cellular pathways leading to cell cycle arrest and DNA repair (Choi, Kipps and Kurzrock, 2016). Mutations in *ATM* result in a rare, childhood autosomal recessive disorder mainly characterised by cerebellar impairment, weakened immune system, presence of telangiectasia, radiosensitivity and increased risk of cancer (McKinnon, 2004). Germline mutations in *ATM* are present in around

1% of the population and correlate with increased cancer predisposition, particularly breast, pancreatic, lung, thyroid, and prostate cancers (Choi, Kipps and Kurzrock, 2016). ATM mutations are present in a variety of tumours with the highest prevalence of around 40% in mantle cell lymphoma, ~ 18% in colorectal cancers and ~10% in lung and prostate cancers (Choi, Kipps and Kurzrock, 2016).

In the event of DNA damage, ATM is recruited to DSBs by the MRN complex (consisting of MRE11-NBS1-RAD50), resulting in ATM autophosphorylation and phosphorylation-mediated activation of a range of downstream targets including p53, checkpoint kinase 2 (Chk2), BRCA1, KAP1, RAD50, SMC1, MDC1, and H2AX (Riches et al., 2020). This leads to cell cycle arrest and DNA repair or apoptosis. An overview of the mechanism of action of ATM is presented in Figure 3.2.

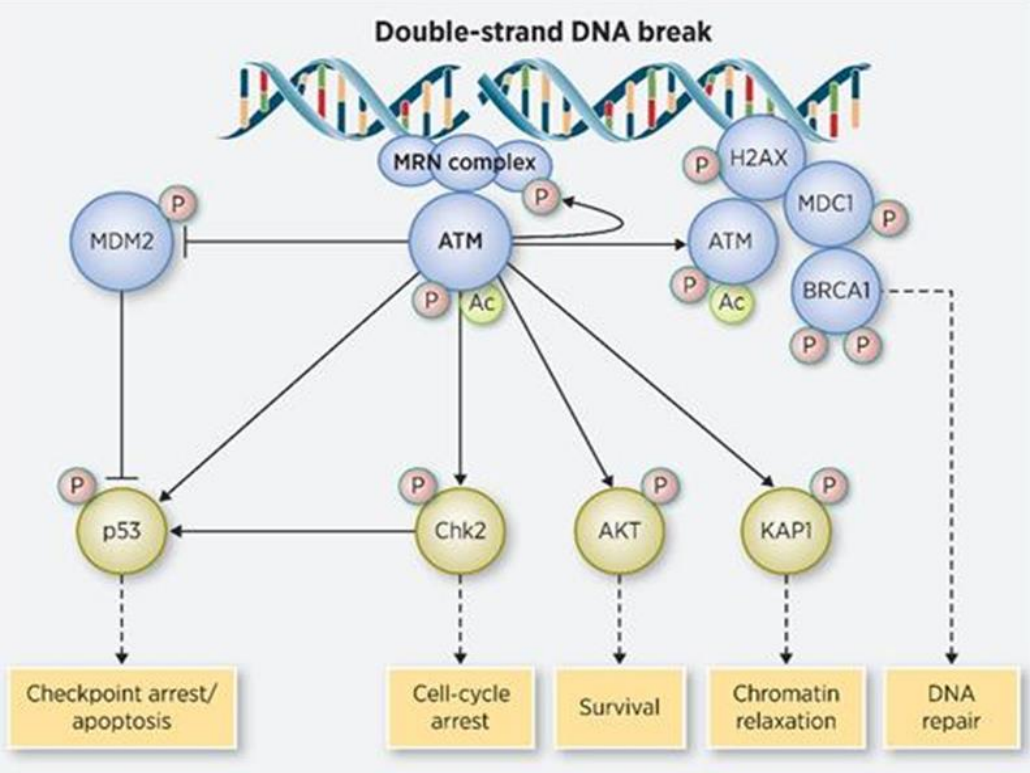

Figure 3.2 The mechanism by which ATM contributes to the HR pathway.
ATM contributes to the homologous recombination (HR) pathway by being recruited to sites of DNA double-strand breaks (DSBs) detected by the MRE11–RAD50–NBS1 (MRN) complex. Upon recruitment, ATM is activated through autophosphorylation and subsequently

phosphorylates and activates several key proteins, including MDC1, histone H2AX (γH2AX), BRCA1/2, checkpoint kinase 2 (Chk2), p53, and KRAB-associated protein 1 (KAP1). This activation cascade leads to cell cycle arrest, chromatin relaxation, and DNA repair. If the damage is irreparable, it results in prolonged cell cycle arrest and apoptosis. Taken from Choi, Kipps and Kurzrock 2016.

In addition to the *ATM*, the ATR also plays a critical role in DDR. The ATR serine/threonine kinase is a member of the phosphatidylinositol-3-kinase-like kinase family (PIKKs) and is the main kinase that responds to single-stranded DNA associated with stalled replication forks (Saldivar, Cortez and Cimprich, 2017). ATR activation leads to the phosphorylation of the effector kinase checkpoint kinase 1 (Chk1), which results in G2/M checkpoint arrest, stabilization of replication forks for successful DNA replication, and DNA repair. ATR also plays a role in DSB repair by working together with ATM to coordinate the detection and signalling processes, as well as facilitating HR and checkpoint activation. The cross-talk between these two pathways ensures efficient and robust DNA repair (Marechal and Zou, 2013). ATR is essential for cell survival and its deletion results in embryonic lethality in mice. As such, complete loss of ATR function is very rare in cancer (Marechal and Zou, 2013).

3.1.3 Synthetic lethality in DDR biology

The DDR is an essential process in maintaining genomic stability and preventing carcinogenesis. As such, dysregulation of this process is one of the hallmarks of cancer. Due to existing mutations in the cancer cells, they often rely on certain DDR pathways that compromise alternative repair mechanisms creating a vulnerability that can be exploited therapeutically. Therefore, targeting DDR pathways aims to exacerbate genomic instability in tumour cells, pushing them towards unsustainable levels of damage and eventually death. The discovery that BRCA1/2-deficient cancer cells are sensitive to poly-ADP ribose polymerase (PARP) inhibition was a major advance in this area (Bryant et al., 2005). Such an interaction, where mutation/inhibition of one gene is compatible with cell survival, but simultaneous

inhibition of other complementary pathways is lethal, has been named 'synthetic lethality' (Topatana et al., 2020).

PARP inhibitors are clinically approved for tumours with HR deficiency which includes breast, ovarian and prostate cancers. The list of approved PARP inhibitors for cancer therapy is outlined in Table 3.1. In the event of DNA damage, PARP is involved in the repair of SSBs whereas BRCA1/2 plays a key role in promoting the repair of DSBs by HR.

Table 3.1 List of clinically approved PARP inhibitors and their indications.
Adapted from Zheng et al., 2020.

PARP inhibitor	Indications	Cancer Type	Year of approval
Olaparib	HER2-negative, BRCA-mutated Maintenance for recurrent ovarian Advanced ovarian after 3+ lines chemo mCRPC in patients with HRR (homologous recombination repair) gene mutations	Breast, Ovarian, Prostate, Pancreatic	2014 (Ovarian), 2018 (Breast), 2019 (Pancreatic), 2020 (Prostate), 2023 (mCRPC)
Rucaparib	Treatment and maintenance BRCA-mutated ovarian cancer Metastatic castration-resistant prostate cancer	Ovarian, Prostate	2016 (Ovarian), 2020 (Prostate)
Niraparib	Maintenance of recurrent ovarian Under investigation for BRCA-mutated breast cancer	Ovarian	2017 (Ovarian)
Talazoparib	HER2-negative, germline BRCA-mutated cancer locally advanced/metastatic	Breast	2018 (Breast) Metastatic castration-resistant prostate cancer (mCRPC) (2023)

There are a few suggested mechanisms of action of PARP inhibitors. Originally it was proposed that in the context of PARP inhibition, unrepaired SSBs are converted to DSBs during DNA

replication, which are normally repaired in the process of HR in BRCA1/2 proficient cells. However, in cells with BRCA deficiency, DNA damage cannot be repaired efficiently, which leads to cell death (Livraghi et al., 2015). More recent evidence suggests that the mechanism of action of PARP inhibitors is based on PARP trapping where PARP is trapped on the DNA due to the inability to auto-PARylate, which leads to replication fork collapse and the introduction of DSBs (Rose et al., 2020). Different PARP inhibitors exhibit varying efficacies in PARP trapping which influences their therapeutic outcomes. Talazoparib for example has strong PARP trapping capabilities, making it highly effective in inducing synthetic lethality in BRCA-mutated cells. In contrast, Olaparib exhibits moderate trapping efficiency (Hopkins et al., 2019). These differences are attributed to variations in the molecular structure of the inhibitors, which affect their binding affinity and ability to stabilize the PARP-DNA complex (Hopkins et al., 2019).

The development of therapies based on the concept of synthetic lethality opened up a new era of targeted cancer therapies as they are one of the most effective anti-cancer treatments approved in the last decade. Indeed, it was soon discovered that synthetically lethal interactions are not limited to BRCA and PARP inhibitors, but further extend to other proteins playing a significant role in the DDR, such as ATM and ATR kinases.

Deficiency in ATM function leads to genomic instability due to loss of DSB repair, rendering the cell dependent on other repair pathways. Since persistent unrepaired SSBs can be converted to DSBs, which cannot be repaired effectively in ATM-deficient cells, targeting SSB repair has been evaluated in ATM-deficient tumours. A number of *in vitro* studies have shown that ATM deficiency sensitises cells to PARP inhibitors in mantle cell lymphoma (Williamson et al., 2010) and pancreatic (Perkrofer et al., 2017), colorectal (Wang et al., 2017) and lung tumour cells (Jette et al., 2019). Furthermore, sensitivity to PARP inhibitors is enhanced when there is also loss or mutation in TP53 in ATM-deficient mantle cell lymphoma (Williamson et al., 2012) and

gastric cancer (Kubota et al., 2014). In the last few years, ATR inhibitors were also developed as a potential therapy for ATM-deficient cancers, due to the role of ATR in RS (Choi, Kipps and Kurzrock, 2016; Min et al., 2017).

In ATM-deficient cancer cells, pharmacological inhibition of ATR was shown to induce synthetic lethality *in vitro* as well as *in vivo* in mouse xenograft models (Vendetti et al., 2015; Wallez et al., 2018). Moreover, ATR inhibition also synergised with PARP inhibitors and resulted in a superior effect on ATM-deficient cancer cells in preclinical studies (Rafiei et al., 2020; Lloyd et al., 2020). Four ATR inhibitors: AZD6738- Ceralasertib, M6620 (VX-970), BAY1895344 and M4344 (VX-803) have progressed into phase I clinical trials and demonstrated promising responses in various solid tumours with phase II trials still ongoing.

3.1.4 JMJD5 as a potential target

In the previous chapter, we presented data supporting a critical role for JMJD5 in maintaining GS. Overall, the existing research suggests that JMJD5 may have a role in replication fidelity and/or the DDR, which might suggest that JMJD5 is a potential target for anticancer treatment.

Interestingly, a recently published genome-wide CRISPR dropout screen using three different cancer cell models identified a synthetic lethal interaction between JMJD5 and Olaparib, a PARP inhibitor (Zimmermann et al., 2018). Interestingly, this is the first time such a functional interaction has been described for 2OG-oxygenases. Furthermore, in subsequent CRISPR screens, JMJD5 was identified as a possible lethal interaction with ATM inhibition (Dr Nicholas Davies and Professor Tanja Stankovic, personal communication). Therefore, in this chapter, we have aimed to investigate the synergistic interactions of JMJD5 loss of function models with DDR proteins in terms of RS phenotype, cell cycle and cell viability. This research aimed to study how JMJD5 loss influences cellular responses to DNA-damaging agents and other chemotherapeutics, and whether these interactions could be exploited to target tumour cells.

3.2 Results

3.2.1 JMJD5 knockdown sensitises A549 cells to ATM, ATR and PARP inhibitors

As JMJD5 is overexpressed in a variety of cancers and is often associated with poor prognosis, we were interested in investigating if JMJD5 may be a useful clinical target. As mentioned above, JMJD5 was identified in a CRISPR screen to have a possible lethal interaction with ATM inhibition. Therefore, we were interested to see if the downregulation of JMJD5 affects the sensitivity of cells to ATM inhibitors. To do that we have selected the ATM inhibitor AZD0156, which is a potent and selective bioavailable ATM inhibitor currently being evaluated in phase I trial (NCT02588105) for advanced solid tumours.

We chose to perform a colony survival assay, which is a gold standard for evaluating the effect of ionizing radiation on cancer cells *in vitro* and can also be used for measuring the effect of cytotoxic agents *in vitro*. Therefore, A549 cells were transfected with siControl or JMJD5 targeting siRNA and after 72 hours were treated with ATM inhibitor at different concentrations for 24 hours. After 24 hours the media was changed, and cells were left to form colonies for 8 days. The surviving fraction was calculated based on the plating efficiency of the treated cells compared to the plating efficiency of the control cells (either siControl or siJMJD5 cells). Importantly, JMJD5 knockdown sensitised A549 cells to ATM inhibition (Figure 3.3A).

We therefore hypothesised that a similar synergistic effect might be observed with ATR inhibitors, as both ATM and ATR are key regulators of the DDR, albeit with distinct roles. We chose Ceralaserib, which is a selective ATR inhibitor that is currently being tested in various phase I and II trials alone or in combination with other therapies for solid cancers (Dillon et al. 2024). Interestingly, colony formation assay indicated that JMJD5 knockdown also sensitises cells to ATR inhibitor treatment (Figure 3.3B).

As mentioned above, Zimmermann et al. published the results of a genome-wide CRISPR dropout screen which identified a synthetic lethal interaction between JMJD5 and Olaparib, a

PARP inhibitor (Zimmermann et al., 2018). Based on the synthetic lethal interaction identified we hypothesize that the knockdown of JMJD5, in combination with PARP inhibition, will also result in enhanced cytotoxicity in cancer cells. To explore this, we have used Talazoparib, which is a more potent PARP inhibitor than Olaparib, primarily due to its superior ability to trap PARP1 on DNA, leading to more effective prevention of DNA repair and greater accumulation of DNA damage. We found that JMJD5 knockdown sensitised cells to PARP inhibitor treatment at 0.1μM (Figure 3.3C). We have also noted that cells with JMJD5 knockdown have a significantly reduced ability to form colonies when compared to siControl cells, even in the absence of DDR inhibitors, demonstrated by the decreased plating efficiency (Figure 3.3D). Overall, this data suggests that JMJD5 knockdown sensitises A549 cells to ATM, ATR and PARP inhibitors.

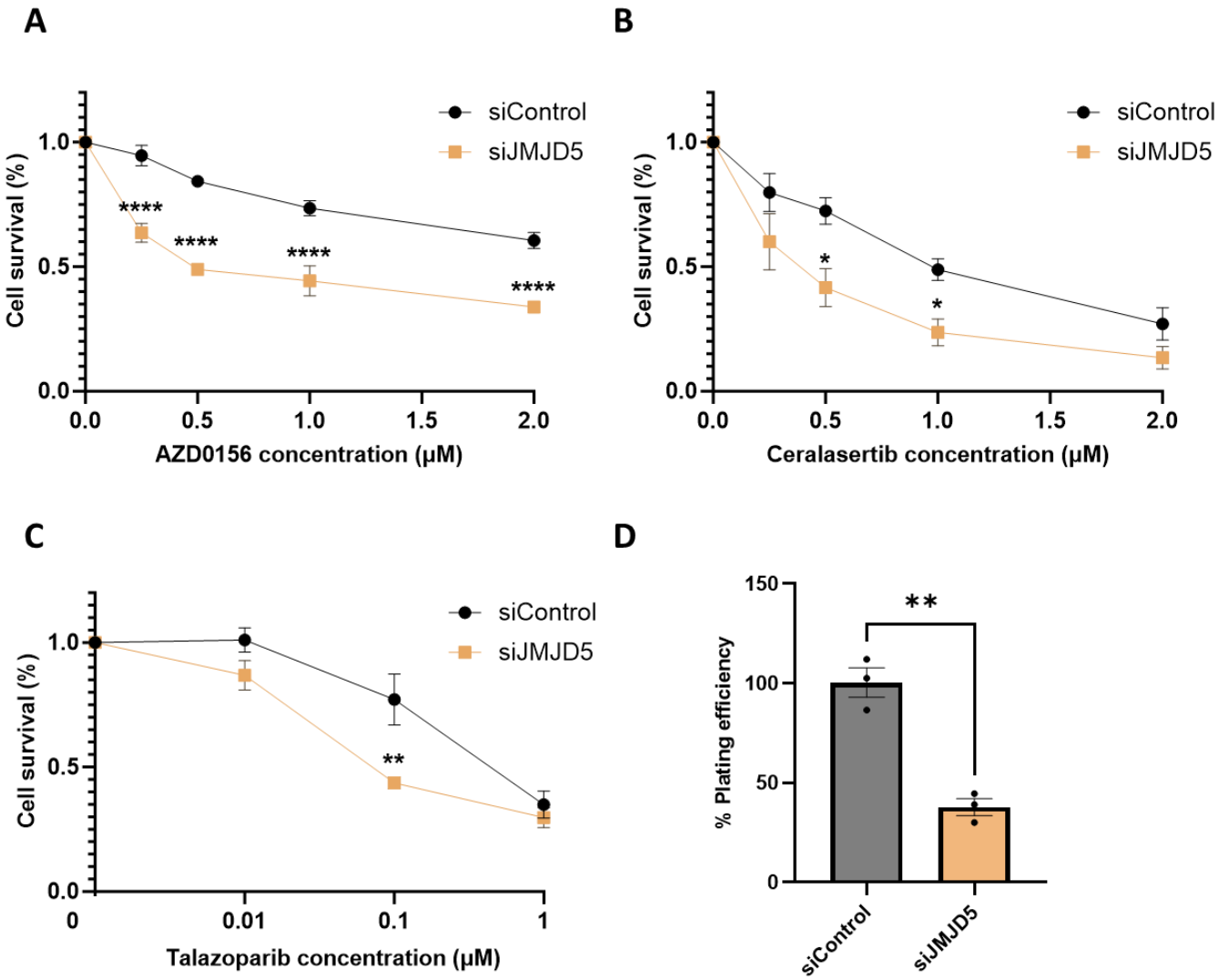

Figure 3.3 JMJD5 knockdown sensitises A549 cells to ATM, ATR and PARP inhibitors.
Colony survival assay of cells treated with inhibitor at indicated concentrations for 24 hours. JMJD5 knockdown sensitises A549 cells to A. ATM inhibitor AZD0156 B. ATR inhibitor Ceralasertib and C. PARP inhibitor Talazoparib. Data presents mean ± SEM of results from three independent biological experiments performed in triplicate. Statistical analyses used unpaired t-test [with p-value ≤ 0.05 (*)]. D. Percentage of plating efficiency from three independent experiments with six replicates represented by mean ± SEM.

3.2.2 Both ATM and ATR inhibitors potentiate JMJD5 knockdown-induced replication stress in A549 cells.

In Chapter 2 (Figures 2.8 and 2.11) we demonstrated that JMJD5 knockdown induces RS, as indicated by the increased frequency of cells with micronuclei and 53BP1 bodies, and that this phenotype is dependent on JMJD5 enzymatic activity. In light of the results above, I was interested in exploring this RS phenotype following treatment with ATM and ATR inhibitors. To do so, I transfected A549 cells with siRNA and after 72 hours treated them with 1μM ATM or ATR inhibitor for 24 hours. I then evaluated the JMJD5 knockdown efficiency and JMJD5 protein levels in the cells by Western blot (Figure 3.4A). IF staining was carried out to quantify the previously used RS markers, micronuclei and 53BP1 bodies. Interestingly, treatment with either ATM or ATR inhibitor significantly increased the percentage of cells with micronuclei in both siControl and knockdown cells when compared to untreated cells. However, this increase was significantly higher in the JMJD5 knockdown cells when compared to the treated control for both inhibitors used (Figure 3.4B). Strikingly, there was a large increase in 53BP1 bodies and 53BP1 foci after ATR inhibitor treatment (Figure 3.4C bottom panels), with a statistically significant increase in the number of 53BP1 bodies per cell in the JMJD5 knockdown group (Figure 3.4D). Interestingly, there were no 53BP1 bodies present after ATM inhibitor treatment, which is consistent with previous findings indicating that ATM is necessary for the formation of 53BP1 bodies (Figure 3.4C) (Harrigan et al. 2011; Fernandez-Vidal, Vignard and Mirey, 2017).

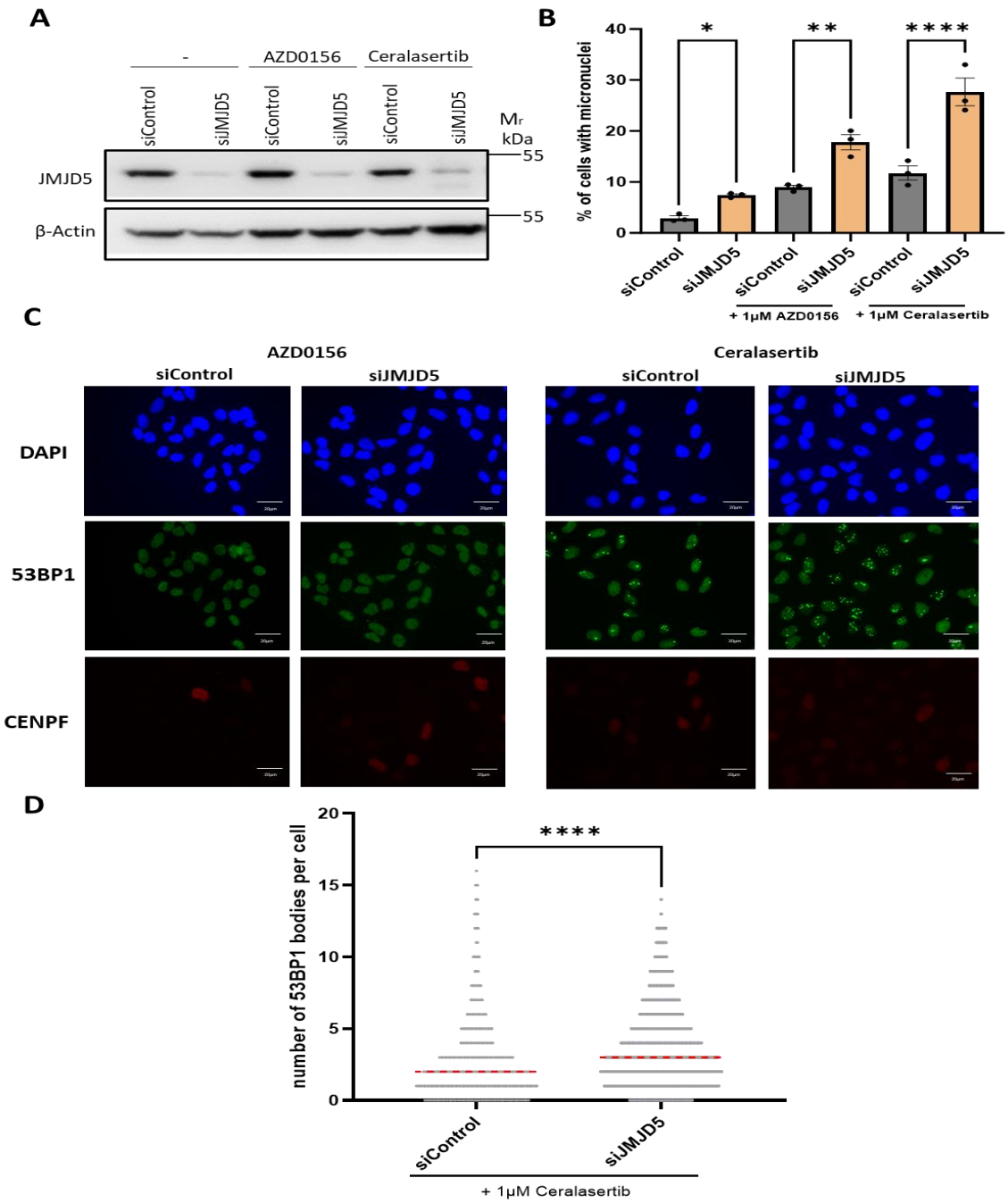

Figure 3.4 The effect of ATM and ATR inhibitors on the replication stress phenotype in A549 cells following JMJD5 knockdown.

A. Representative Western blot to check JMJD5 knockdown efficiency. N=3 B. Percentage of cells that contained any micronuclei. Data represent mean ± SEM from three independent biological replicates. Statistical analyses used one-way ANOVA with Tukey's post hoc test [with p-value ≤ 0.05 (*)]. C. Immunofluorescence images of A549 cells. Cells were transfected and after 72 hours treated with 1μM of either ATM or ATR inhibitor for 24 hours. Afterwards, the cells were harvested, fixed and stained for DAPI (blue), 53BP1 (green) and CENPF (red). Scale bars = 20μm. D. The number of 53BP1 bodies per cell in cells treated with Ceralaserib. The red line indicates the median siControl=2 and siJMJD5=3. Data represent three independent replicates. Statistical analyses used a non-parametric Kruskal–Wallis rank sum test with Dunn's correction (with p-value ≤0.0001 (****)).

3.2.3. The effect of ATM inhibitor AZD0156 on cell cycle and apoptosis in A549 cells with JMJD5 knockdown.

In the section above we presented that JMJD5 knockdown increases the sensitivity and RS phenotypes induced by ATM or ATR inhibition in A549 cells. We next wanted to explore this synergy further by characterising the effect of the treatments on cell cycle and apoptosis.

To determine the cell cycle phase we used the well-established propidium iodide (PI) assay. Because propidium iodide binds non-specifically to nucleic acid, it can be used to monitor the DNA content of cells (Shen, Vignali and Wang, 2017). Cell cycle analysis using PI also detects cells in sub-G1, which indicates DNA content below the normal diploid amount and can be a marker of cell death. However, sub-G1 analysis alone is limited because it only detects dead cells without providing information on the mechanisms of cell death. Therefore, specific methods are needed to detect different types of cell death. Since we were interested in whether JMJD5 inhibition combined with DDR inhibitors causes apoptosis, we used an Annexin V assay. This method is based on the changes in plasma membrane asymmetry that occur during apoptosis, where the loss of plasma membrane integrity is one of the earliest signs (Banfalvi, 2017). Specifically, phosphatidylserine (PS), a membrane phospholipid, becomes exposed to the extracellular environment as it relocates from the inner to the outer layer of the plasma membrane (Banfalvi, 2017). This exposure facilitates the binding of Annexin V, a Ca2+-dependent phospholipid-binding protein, which has a strong affinity for PS. Therefore, cells that exhibit positive annexin V staining can be classified as early apoptotic. To visualise and quantify apoptotic cells, Annexin V is combined with a fluorescent dye such as phycoerythrin (PE). To differentiate between apoptotic and dead cells, staining is combined with other dyes such as 7-Amino-Actinomycin (7-AAD). 7-AAD selectively binds to the DNA of dead cells with permeable membranes, while it is excluded from viable cells (Banfalvi, 2017). Subsequently, the relevant signals can be analysed by flow cytometry.

To investigate the effect of ATM inhibitor on cell cycle and cell death, A549 cells were treated with 10μM of ATM inhibitor for 72 hours and cells were stained with either PI for cell cycle analysis or PE Annexin V and 7-AAD to detect apoptosis. The treatment with ATM inhibitor increased the sub-G1 population of both siControl and JMJD5 knockdown cells with a corresponding decrease in G1 cells (Figure 3.5A). However, there was no significant difference between the effect on the siControl versus JMJD5 knockdown cells at any stage of the cell cycle (Figure 3.5A). Moreover, ATM inhibitor caused A549 cell death indicated by a decrease in double negative (alive) cells and an increase in dead cells (double positive), for both treated samples (Figure 3.5B). However, there was no significant difference between the siControl and JMJD5 knockdown cells.

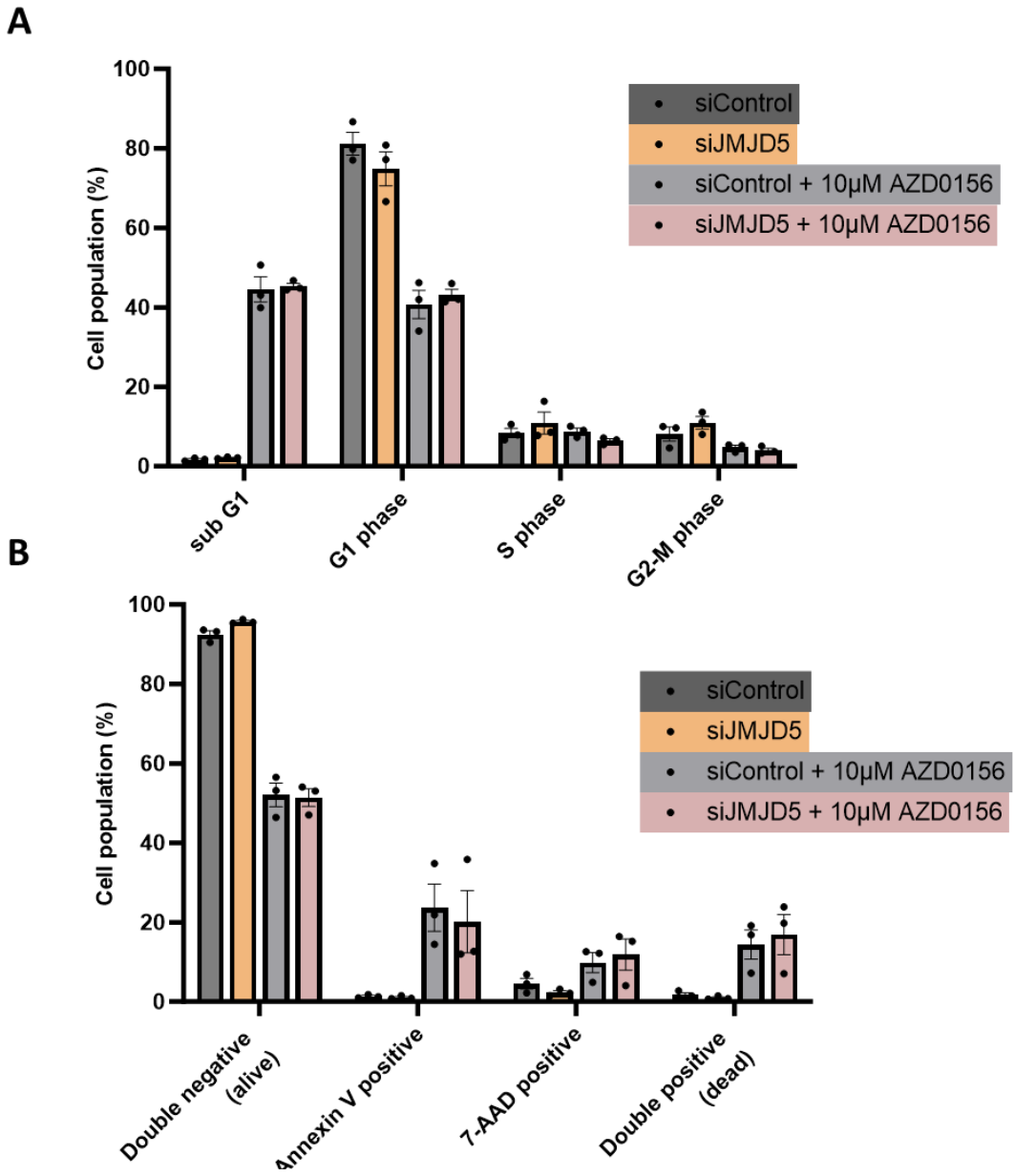

Figure 3.5 The effect of ATM inhibitor AZD0156 on JMJD5 knockdown A549 cells.
The A549 cells were transfected with siRNA control or targeting JMJD5 and after 72 hours treated with 10uM of AZD0156 for 72 hours. The cells were stained with PI for cell cycle analysis (A) or with PE Annexin V and 7-AAD to measure apoptosis (B). Data presents mean ± SEM of results from three independent biological experiments performed in triplicate. Statistical analyses used one-way ANOVA with Tukey's post hoc test [with p-value ≤ 0.05 (*)].

3.2.4 The effect of ATR inhibitor Ceralasertib on cell cycle and apoptosis in A549 cells with JMJD5 knockdown.

As treatment with ATR inhibitor leads to increased cell sensitivity and increased RS in JMJD5 knockdown cells, we also wanted to investigate the effects on cell cycle and apoptosis. Similarly to the effect of ATM inhibitor, the ATR inhibitor caused an increase in the sub-G1 population and a corresponding decrease in the G1 population of both siControl and JMJD5 knockdown cells. However, there was no significant difference between the effect on the siControl versus JMJD5 knockdown cells (Figure 3.6A). The apoptosis analysis showed a decrease in double negative population with an increase in Annexin V positive (indication of early apoptosis) and double positive (dead cells) of both siControl and JMJD5 knockdown cells (Figure 3.6B). However, there was no significant difference between the effect on the siControl versus JMJD5 knockdown cells.

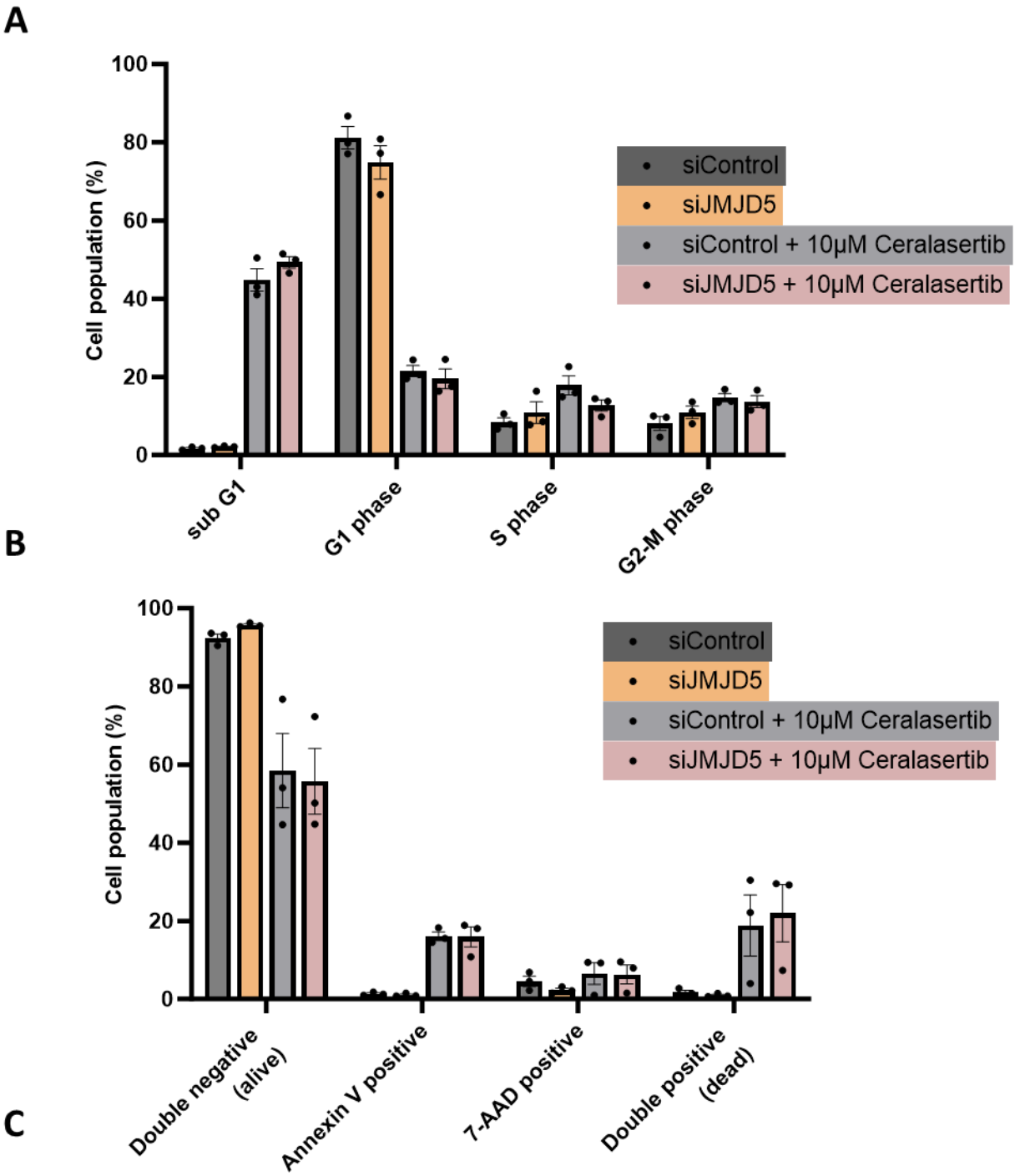

Figure 3.6 The effect of ATR inhibitor Ceralasertib on JMJD5 knockdown A549 cells.
The A549 cells were transfected with siRNA control or targeting JMJD5 and after 72 hours treated with 10uM of Ceralasertib for 72 hours. The cells were stained with PI for cell cycle analysis (A) or with PE Annexin V and 7AAD to measure apoptosis (B). Data presents mean ± SEM of results from three independent biological experiments performed in triplicate. Statistical analyses used one-way ANOVA with Tukey's post hoc test [with p-value ≤ 0.05 (*)].

3.2.5 The effect of ATM and ATR inhibitors on JMJD5 knockdown-induced replication stress in U2OS cells.

We next wanted to evaluate if the effects observed above are limited to a specific cancer cell line or can extend to other tumour cells. This would give a more comprehensive insight into the potential role of JMJD5 in cancer and its potential as a therapeutic target. It was previously shown in the Coleman group that JMJD5 knockdown leads to increased RS markers in U2OS cells (personal communication), making the cell line a suitable model to study for the validation of our hypothesis.

First, we investigated the effect of ATM or ATR inhibitor treatment in JMJD5 knockdown U2OS cells. We transfected U2OS cells with siRNA and after 72 hours treated them with 1μM of either ATM or ATR inhibitor for 24 hours, then evaluated JMJD5 knockdown efficiency by Western blot (Figure 3.7A). Treatment with 1μM ATM inhibitor did not cause an additional increase in the number of micronuclei in siControl or JMJD5 knockdown cells (Figure 3.7B). Treatment with ATR inhibitor resulted in a substantial increase in the percentage of cells with micronuclei in both siControl and knockdown cells when compared to untreated cells. This increase was significantly higher in the JMJD5 knockdown cells when compared to the treated siControl (Figure 3.7B). Similar to the data in A549 cells, there were no 53BP1 bodies present after ATM inhibitor treatment of both control and JMJD5 knockdown cells (Figure 3.7C). In contrast, there was a large increase in 53BP1 bodies and 53BP1 foci after ATR inhibitor treatment (Figure 3.7C).

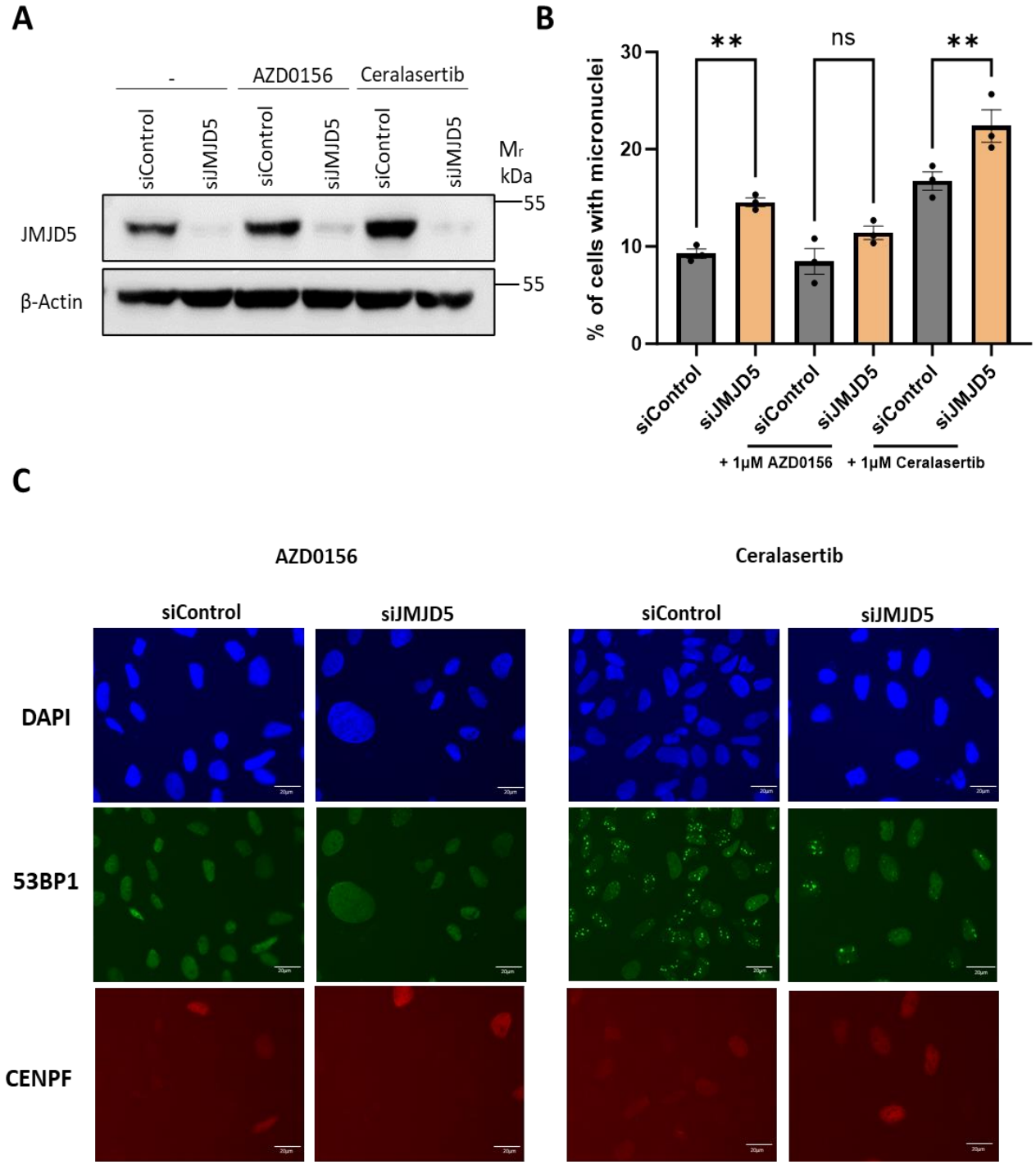

Figure 3.7 The effect of ATM and ATR inhibitors on replication stress in U2OS cells following JMJD5 knockdown.

Cells were transfected with siRNA and after 72 hours treated with 1μM of either ATM or ATR inhibitor for 24 hours. Afterwards, the cells were harvested, fixed and stained for DAPI (blue), 53BP1 (green) and CENPF (red). A. Representative Western blot to assess JMJD5 knockdown efficiency with actin used as a loading control. N=3 B. Percentage of cells that contained any micronuclei. Data represent mean ± SEM from three independent biological replicates. Statistical analyses used one-way ANOVA with Tukey's post hoc test [with p-value ≤ 0.05 (*)]. C. Immunofluorescence images of U2OS cells. Scale bars = 20μm

3.2.6 Treatment with ATM inhibitor AZD0156 causes cell cycle perturbances and increased cell death in JMJD5 knockdown U2OS cells.

After our RS markers analysis, we wanted to investigate the effect of ATM inhibitor on cell cycle and apoptosis in U2OS cells using the flow cytometry methods introduced above. The ATM inhibitor affected the cell cycle of both siControl and JMJD5 knockdown U2OS cells. Interestingly, there was a significantly higher increase in the sub-G1 population of the ATM inhibitor-treated JMJD5 knockdown cells compared to the treated siControl, with a corresponding significant decrease in the G1 population (Figure 3.8A). Moreover, treatment with ATM inhibitor caused a significant decrease in viable JMJD5 knockdown versus siControl cells and a corresponding increase in dead cells (Figure 3.8B). Overall, this data indicates that treatment with ATM inhibitor leads to cell cycle perturbances and increases cell death in JMJD5 knockdown cells.

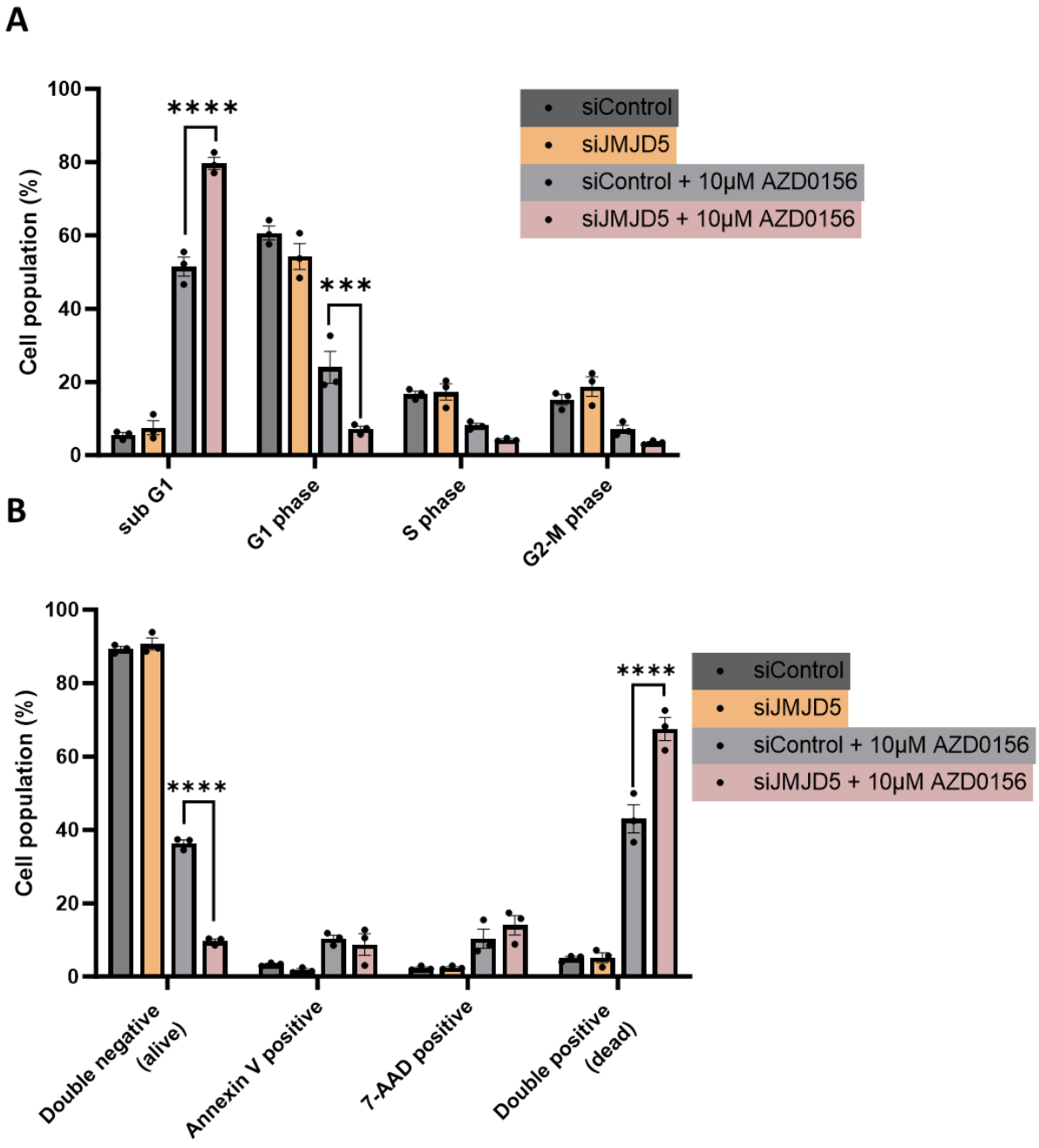

Figure 3.8 The effect of ATM inhibitor AZD0156 on cell cycle and apoptosis in JMJD5 knockdown U2OS cells.

The U2OS cells were transfected with siRNA control or targeting JMJD5 and after 72 hours treated with 10uM of AZD0156 for 72 hours. The cells were stained with PI for cell cycle analysis (A) or with PE Annexin V and 7AAD for apoptosis (B). Data presents mean ± SEM of results from three independent biological experiments. Statistical analyses used one-way ANOVA with Tukey's post hoc test [with p-value ≤ 0.05 (*)].

3.2.7 Treatment with ATR inhibitor Ceralasertib causes cell cycle perturbances and increased cell death in JMJD5 knockdown U2OS cells.

Having demonstrated the effect of ATM inhibitor in our U2OS JMJD5 knockdown model, we were next interested in whether these cells also show sensitivity to ATR inhibitor Ceralasertib. Therefore, we carried out cell cycle and apoptosis analyses, as above. Interestingly, and similarly to ATM inhibitor, treatment with ATR inhibitor caused a statistically significant increase in the sub-G1 population in JMJD5 knockdown cells compared to the treated siControl U2OS cells, with a corresponding decrease in the G1 population (Figure 3.9A). Moreover, the treatment caused a significant decrease in viable JMJD5 knockdown cells compared to the controls. Cells with JMJD5 loss also had a corresponding increase in dead cells (7-AAD positive and double positive) (Figure 3.9B).

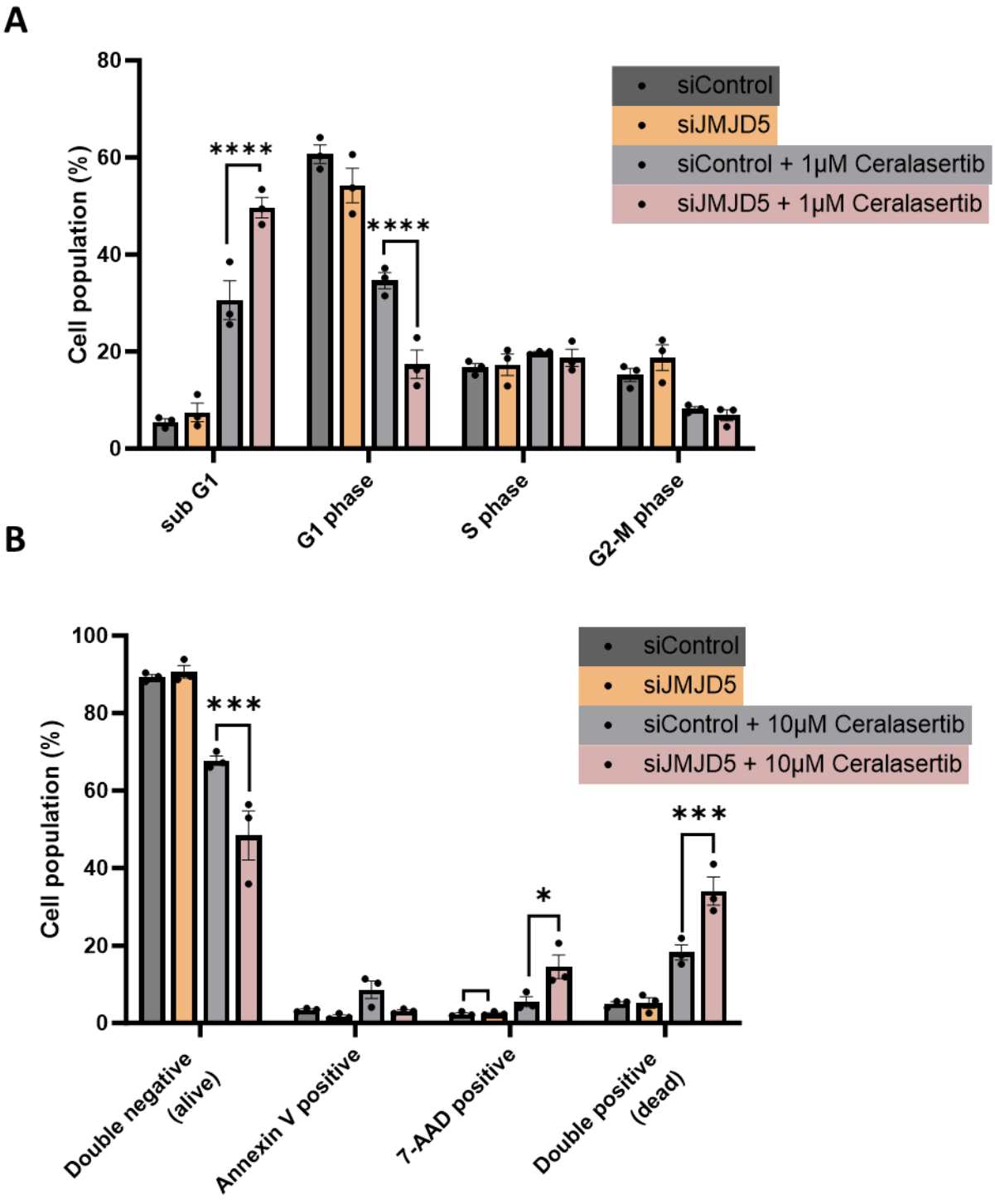

Figure 3.9 The effect of ATR inhibitor Ceralasertib on cell cycle and apoptosis in JMJD5 knockdown U2OS cells.

The U2OS cells were transfected with siRNA control or targeting JMJD5 and after 72 hours treated with 10uM of Ceralasertib for 72 hours. The cells were stained with PI for cell cycle analysis (A) or with PE Annexin V and 7-AAD for apoptosis (B). Data presents mean ± SEM of results from three independent biological experiments. Statistical analyses used one-way ANOVA with Tukey's post hoc test [with p-value ≤ 0.05 (*)].

3.2.8 PARP inhibitor Talazoparib potentiates JMJD5 knockdown-induced replication stress in A549 cells.

In Figure 3.3C we showed that JMJD5 knockdown sensitised A549 cells to PARP inhibitor treatment demonstrated by an increase in cell death. We next decided to explore this phenotype further by analysing RS in both A549 and U2OS cells.

We first looked at the previously used RS markers following the inhibitor treatment in JMJD5 knockdown A549 cells. We transfected A549 cells with siRNA and after 72 hours treated them with 1μM of the PARP inhibitor Talazoparib for 24 hours. Interestingly, treatment with this inhibitor increased the percentage of cells with micronuclei and 53BP1 bodies in both control and knockdown cells when compared to untreated cells (Figure 3.10A and 3.10B). Moreover, this increase was significantly higher in the JMJD5 knockdown cells when compared to the treated siControl for both markers.

To understand the molecular mechanisms underlying this enhanced RS, we wanted to analyse the levels and activation of key DDR pathway proteins. Therefore, we Western blotted protein extracts from cells and observed that JMJD5 knockdown in combination with 0.1μM of Talazoparib leads to a marked increase in p53 levels (Figure 3.10C). Moreover, our results demonstrate an increase in the levels of Chk2 and phospho-Chk2 protein under the same conditions. Interestingly, Mre11 appears to be increased in JMJD5 knockdown cells independent of PARP inhibitor treatment. Lastly, there is a marked increase in yH2AX levels in JMJD5 knockdown cells treated with PARP inhibitor. There was no effect on the levels of PARP, RCCD1 or RAD51. Given the marked increase in p53 expression in the JMJD5 knockdown cells treated with 0.1μM of Talazoparib, and the known roles of p53 in regulating cell cycle arrest, DNA repair and apoptosis, we next decided to analyse cell cycle progression and apoptosis in these cells.

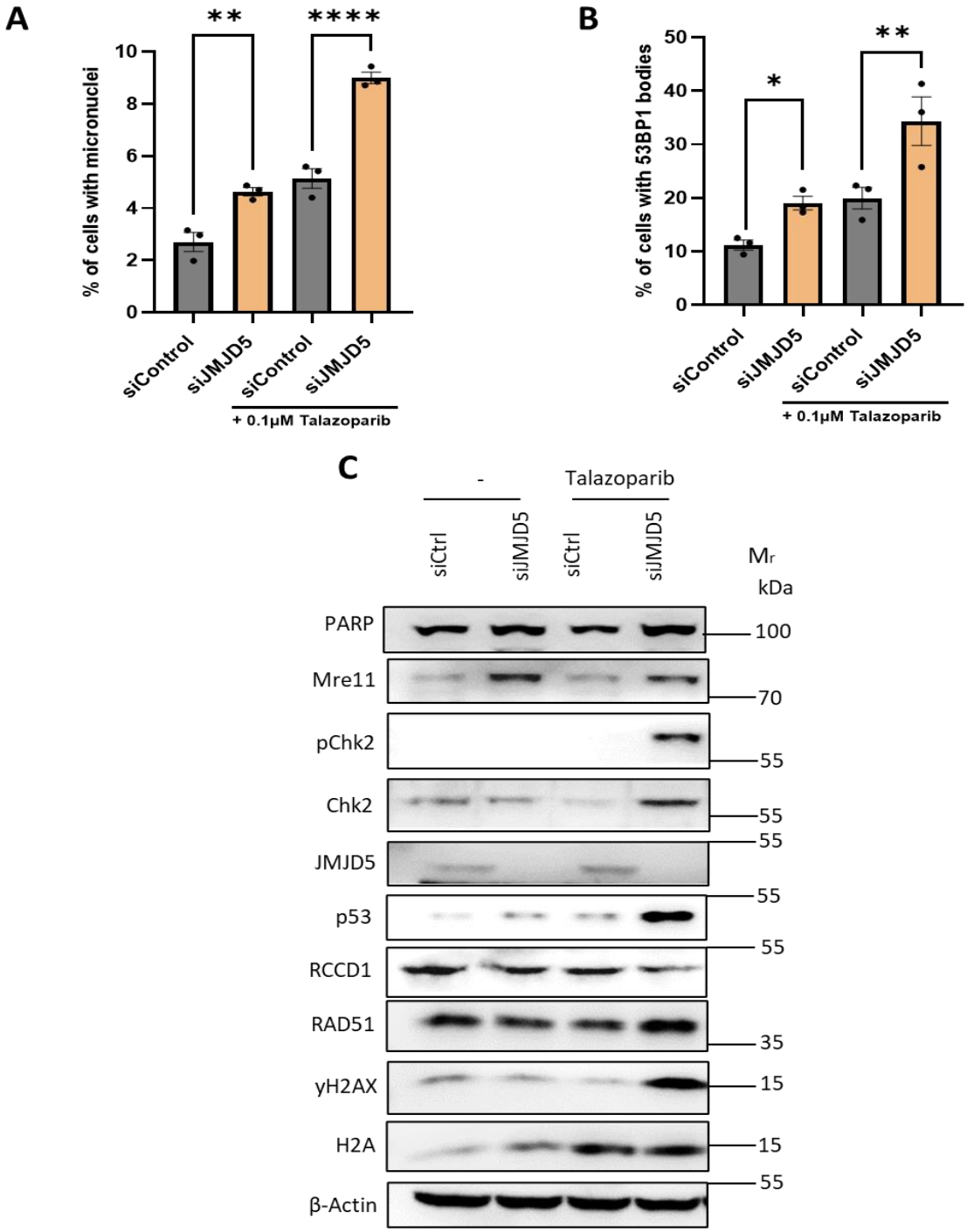

Figure 3.10 The effect of PARP inhibitor Talazoparib on the replication stress markers and protein levels in A549 cells following JMJD5 knockdown.

The effect of Talazoparib on A. micronuclei and B. 53BP1 bodies. The A549 cells were transfected with siRNA targeting JMJD5 and after 72 hours the cells were treated with 0.1μM of Talazoparib for 24 hours. The cells were fixed and stained for DAPI to measure micronuclei (A) or 53BP1 to measure the bodies (B). Data represent mean ± SEM from three independent replicates. Statistical analyses used one-way ANOVA with Tukey's post hoc test [with p-value ≤ 0.05 (*)]. The remaining cells were lysed and protein extracts were prepared to blot for RS and DDR markers with actin used as a loading control, N=3 (C).

3.2.9 Treatment with PARP inhibitor Talazoparib causes cell cycle perturbances and increased cell death in JMJD5 knockdown A549 cells.

To investigate the cellular effects of JMJD5 loss and PARP inhibition, we performed a cell cycle analysis. Interestingly, Talazoparib treatment caused a significantly increased sub-G1 population in JMJD5 knockdown cells relative to siControl cells (Figure 3.11A). In addition, we observed a decrease in the G1 population of both siControl and JMJD5 knockdown cells with a significant decrease in JMJD5 knockdown cells (Figure 3.11A). Interestingly, inhibitor treatment also led to a significant accumulation of cells in the G2-M phase in JMJD5 knockdown cells, consistent with an increase in DNA damage as shown by increased yH2AX expression.

The apoptosis analysis showed that treatment with PARP inhibitor leads to a decrease in the double negative population, with an increase in early apoptotic cells and dead cells of both siControl and JMJD5 knockdown cells (Figure 3.11B). Notably, there was a significantly lower percentage of viable cells in the JMJD5 knockdown population compared to the siControl sample, as well as a significantly higher percentage of dead cells.

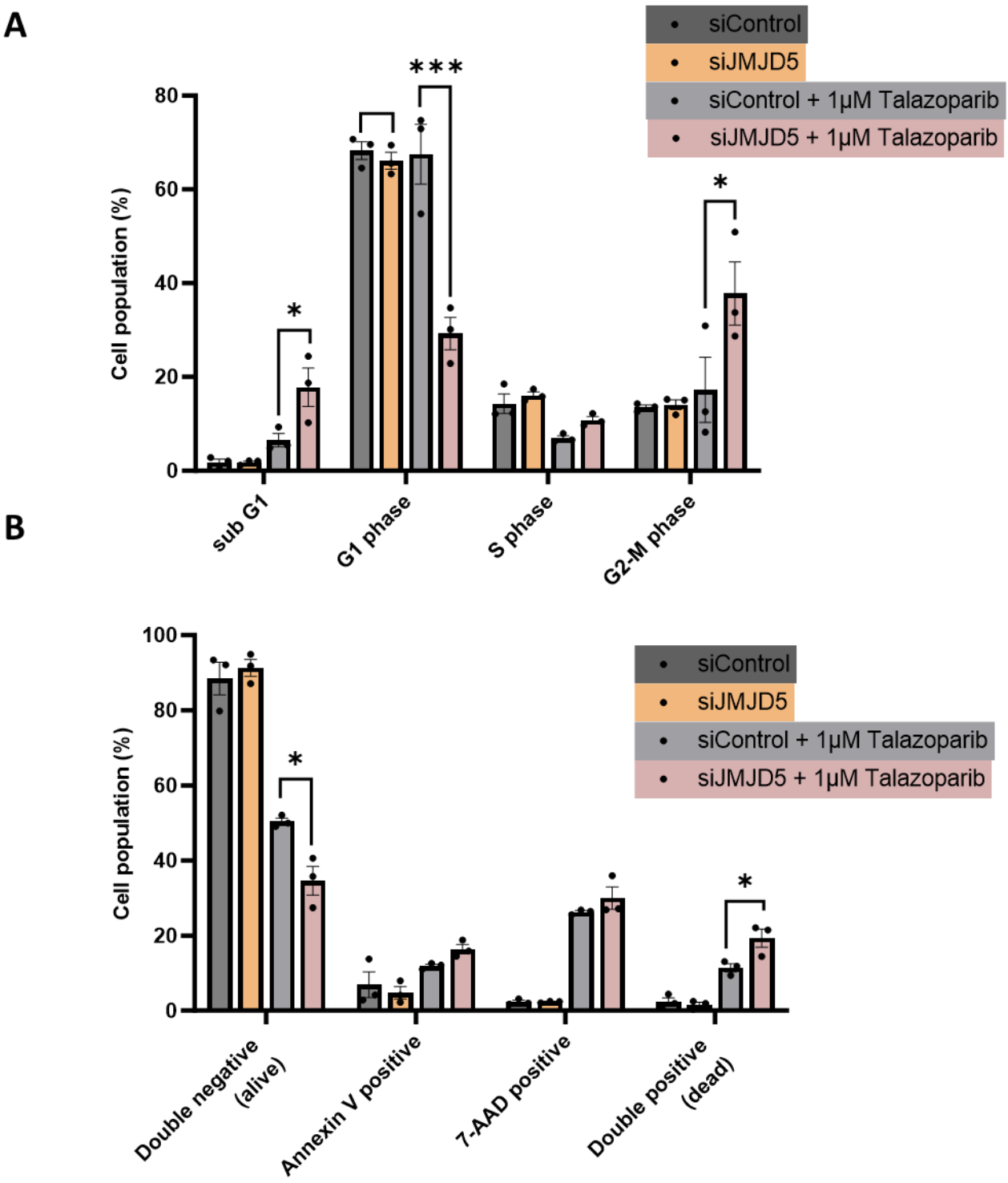

Figure 3.11 The effect of PARP inhibitor Talazoparib on JMJD5 knockdown A549 cells.
The A549 cells were transfected with siRNA control or targeting JMJD5 and after 72 hours treated with 1uM of Talazoparib for 72 hours. The cells were stained with PI for cell cycle analysis (A) or with PE Annexin V and 7-AAD to measure apoptosis (B). Data presents mean ± SEM of results from three independent experiments performed in triplicate. Statistical analyses used one-way ANOVA with Tukey's post hoc test [with p-value ≤ 0.05 (*)].

3.2.10 PARP inhibitor Talazoparib potentiates JMJD5 knockdown-induced replication stress in U2OS cells.

In order to evaluate if the observed effects extend to other cancer cells, we also performed the same set of experiments in U2OS cells. We first analysed the previously used RS markers following inhibitor treatment in JMJD5 knockdown cells. We transfected U2OS cells with siRNA and after 72 hours treated them with 1μM of PARP inhibitor Talazoparib for 24 hours. Treatment with PARP inhibitor increased the percentage of cells with micronuclei and 53BP1 bodies in both siControl and knockdown cells when compared to untreated cells (Figure 3.12A and 3.12B). Moreover, the increase in the number of micronuclei was significantly higher in the JMJD5 knockdown cells when compared to the treated siControl. However, there was no statistical difference between the number of 53BP1 bodies per cell in JMJD5 knockdown and siControl cells.

Similar to our investigation in A549 cells, we wanted to study the molecular mechanisms underlying the effect of JMJD5 knockdown combined with PARP inhibition. Therefore, we analysed the levels of key proteins involved in DDR pathways (Figure 3.12C). Our Western blot results suggest that JMJD5 knockdown combined with PARP inhibition leads to an increase in phospho-Chk2 protein, as also observed in A549 cells. In contrast to A549, there were no significant differences in p53 levels after JMJD5 knockdown. We also did not observe any effect on the levels of PARP, RCCD1, Mre11 or yH2AX. Interestingly, we noted a marked increase in RAD51 levels in JMJD5 knockdown U2OS cells, independent of PARP inhibition (Figure 3.12C), which we did not observe in A549 cells.

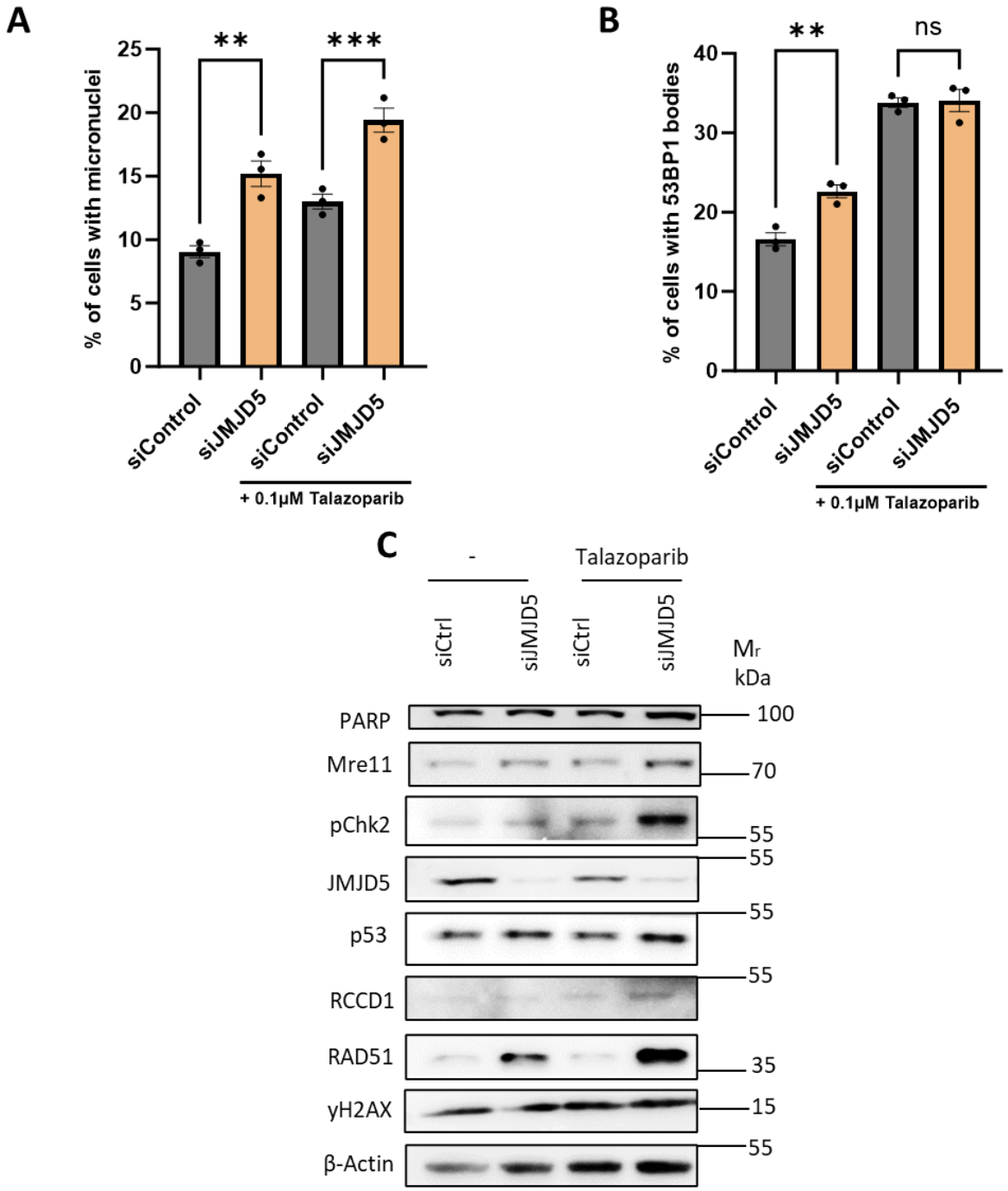

Figure 3.12 The effect of PARP inhibitor Talazoparib on the replication stress markers and protein levels in U2OS cells following JMJD5 knockdown.

The effect of Talazoparib on A. micronuclei and B. 53BP1 bodies. The U2OS cells were transfected with siRNA targeting JMJD5 and after 72 hours the cells were treated with 0.1μM of Talazoparib for 24 hours. The cells were fixed and stained for DAPI to measure micronuclei (A) or 53BP1 to measure the bodies (B). Data represent mean ± SEM from three independent replicates. Statistical analyses used one-way ANOVA with Tukey's post hoc test [with p-value ≤ 0.05 (*)]. The remaining cells were lysed and protein extracts were prepared to blot for RS and DDR markers, N=3 (C).

3.2.11 JMJD5 knockdown causes increase in RAD51 expression in U2OS cells.

In the previous section, we demonstrated that JMJD5 knockdown in U2OS cells leads to an increase in RAD51 protein level. An increase in protein levels observed via Western blot may result from increased transcription or other post-transcriptional regulation such as enhanced translation or reduced degradation. To explore this in more detail, we wanted to determine whether the observed increase in RAD51 protein is due to an upregulation at the mRNA level, suggesting transcriptional regulation. To do so, we have performed quantitative PCR (qPCR) analysis. Interestingly, the qPCR result showed that RAD51 mRNA levels increased more than 2 fold after JMJD5 knockdown (Figure 3.13A). Moreover, treatment with 0.1μM of PARP inhibitor did not alter the RAD51 expression caused by JMJD5 knockdown (Figure 3.13C). We also measured the RAD51 mRNA levels after JMJD5 knockdown in A549 cells: Consistent with the Western blot results indicating no change in RAD51 protein levels (Figure 3.10 above), there was no significant difference in RAD51 expression in JMJD5 knockdown U2OS cells when compared to the siControl (Figure 3.13B). Therefore, the increase in RAD51 expression after JMJD5 knockdown appears to be a cancer cell type-specific event.

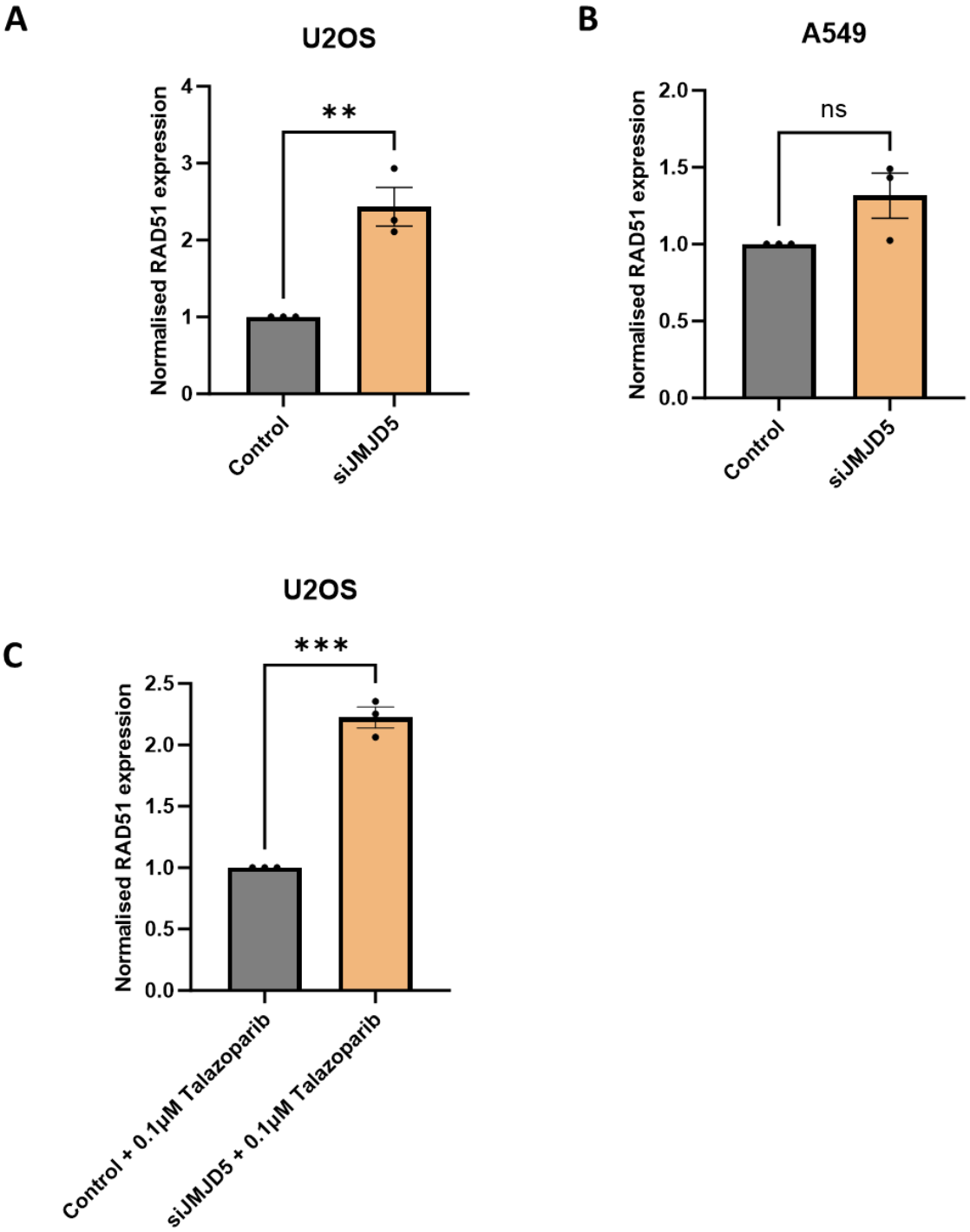

Figure 3.13 mRNA RAD51 expression in JMJD5 knockdown U2OS (A) and A549 cells (B). *A. and B. The cells were transfected with siRNA targeting JMJD5 and collected after 72 hours for RNA extraction and cDNA preparation. C. The U2OS cells were transfected with siRNA targeting JMJD5 for 72 hours, treated with 0.1μM of Talazoparib for 24 hours and collected for RNA extraction and cDNA preparation. was quantified by qPCR relative to GAPDH as a house-keeping gene. Data represent mean ± SEM from three independent replicates. Statistical analyses used unpaired t-test with p-value ≤ 0.01 (**).*

3.2.12 The effect of PARP inhibitor Talazoparib on cell cycle and apoptosis in U2OS cells with JMJD5 knockdown.

In Figure 3.12 we showed an increase in micronuclei in JMJD5 knockdown U2OS cells treated with a PARP inhibitor. To investigate the potential consequences of this enhanced replication stress we examined cell cycle progression and apoptosis as previously for A549 cells. Treatment with Talazoparib led to an increase in the sub-G1 population (and a corresponding decrease in the G1 population) of siControl and JMJD5 knockdown cells (Figure 3.14A). However, there was no significant difference between the two knockdown groups, suggesting no additive effect of JMJD5 siRNA under these conditions. The apoptosis analysis showed a decrease in the double negative population, and an increase in annexin V positive (indication of early apoptosis) and double positive (dead cells) populations of both siControl and JMJD5 knockdown cells following Talazoparib treatment (Figure 3.14B). However, as for the cell cycle analysis, there was no significant difference between the two knockdown groups. Although the cell cycle analysis with PI indicates that Talazoparib treatment may be associated with cell death (due to an increase in sub-G1 population), this was not observed with the Annexin V analysis. Although this requires further investigation, it might indicate that U2OS cells have escape mechanisms preventing cell death since the live cell numbers are comparable between all four populations.

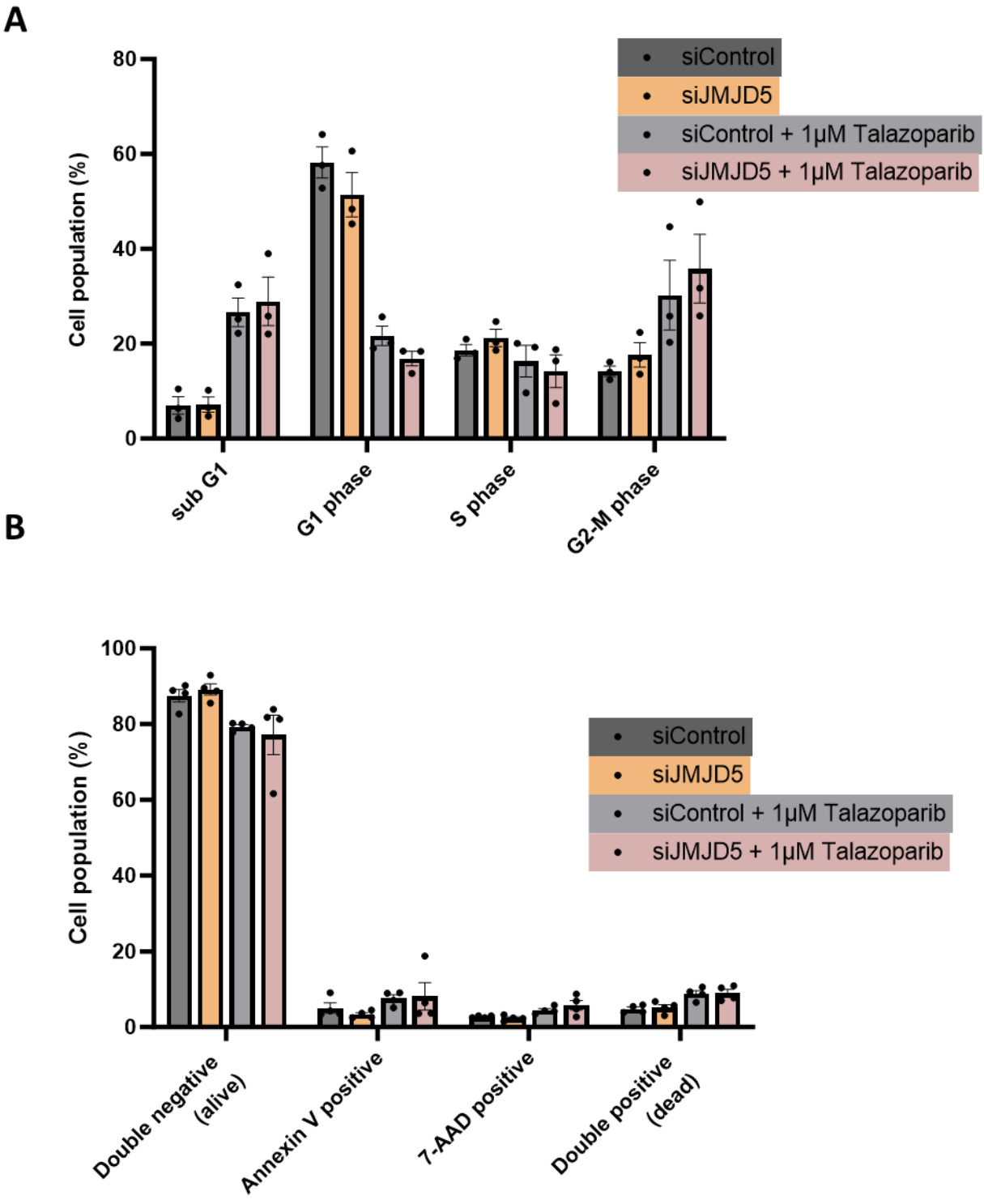

Figure 3.14 The effect of PARP inhibitor Talazoparib on cell cycle and apoptosis in U2OS cells with JMJD5 knockdown.

The U2OS cells were transfected with siRNA control or targeting JMJD5 and after 72 hours treated with 1uM of Talazoparib for 72 hours. The cells were stained with PI for cell cycle analysis (A) or with PE Annexin V and 7-AAD to measure apoptosis (B). Data presents mean ±

SEM of results from three independent experiments performed in triplicate. Statistical analyses used one-way ANOVA with Tukey's post hoc test [with p-value ≤ 0.05 (*)].

3.2.13 Generation of shRNA induced JMJD5 knockdown cell lines

The work thus far was carried out using a single siRNA sequence to model JMJD5 loss. To address this limitation and to take an orthogonal approach, we decided to generate stable A549 and U2OS cell lines expressing doxycycline-inducible short hairpin RNA (shRNA). Therefore, we obtained vectors containing two different shRNA sequences targeting JMJD5 (sh#1 and sh#3) and a non-targeting control shRNA sequence from TransOMIC. As the lentiviral vectors constitutively express puromycin resistance we were able to select the transduced cells. Additionally, doxycycline-inducible expression of green fluorescent protein (GFP) allows to visualise the cells that are expressing shRNA.

Firstly, we wanted to investigate the efficiency of JMJD5 knockdown in these models. Therefore, following puromycin selection, A549 cells were incubated with 1 μg/mL doxycycline for up to 72 hours before first visualising green fluorescent protein (GFP) expression (Figure 3.15A). We found that the majority of cells expressed GFP (with the highest expression at 72 hours), although the level of expression was not completely homogenous across the population. Subsequently, we evaluated JMJD5 mRNA expression levels by quantitative PCR (qPCR). To calculate the knockdown efficiency, we normalised the values to a GAPDH control and calculated JMJD5 mRNA levels relative to a control shRNA sequence. We found that both sequences had a similar knockdown efficiency of around 40% (Figure 3.15B). We also checked the JMJD5 protein knockdown efficiency with each shRNA by western blot and confirmed that both sequences sh#1 and sh#3 showed a strong reduction in JMJD5 protein levels in A549 cells (Figure 3.15C).

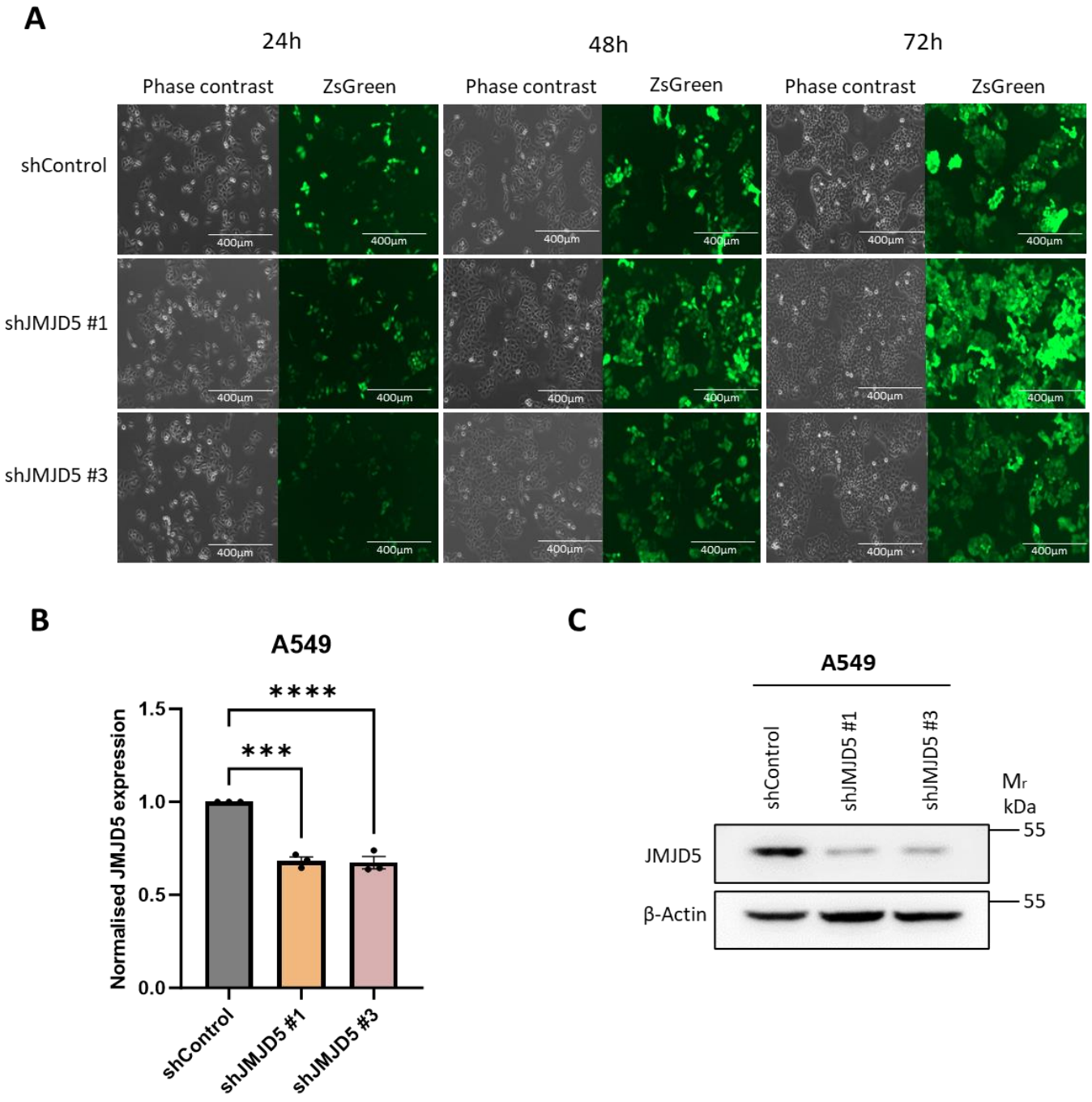

Figure 3.15 Validation of shRNA A549 model.

A. Expression of green fluorescent protein (GFP) was analysed 72 hours after induction with 1 µg/mL doxycycline. Images were acquired using an EVOS inverted microscope equipped with a 10x objective. Scale bars = 400µm B. Evaluation of JMJD5 mRNA levels after 72 hours of doxycycline-induced JMJD5 knockdown by qPCR. Data represent mean ± SEM from three independent replicates. Statistical significance was determined using one-way ANOVA with Tukey's post hoc test [with p-value ≤ 0.001 (****)] C. Representative immunoblot validating knockdown of JMJD5 in stable A549 cell lines expressing doxycycline-inducible control (shControl) or JMJD5-targeting (shJMJD5 #1/#2) shRNAs. Cells were treated with 1 µg/mL doxycycline for 72 hours prior to immunoblotting. β-actin was used as a loading control. N=3

As we wanted to have two independent cell models to study the phenotypic effects of JMJD5 loss we also generated the corresponding U2OS stable cell lines. Similarly to the A549 cell lines, we also evaluated the GFP expression (Figure 3.16A) as well as JMJD5 mRNA and protein levels. The knockdown efficiency of JMJD5 mRNA levels was around 50% for both sequences (Figure 3.16B). Western blot analysis indicated high efficiency of JMJD5 protein loss with sh3 showing the most significant loss of expression (Figure 3.16C).

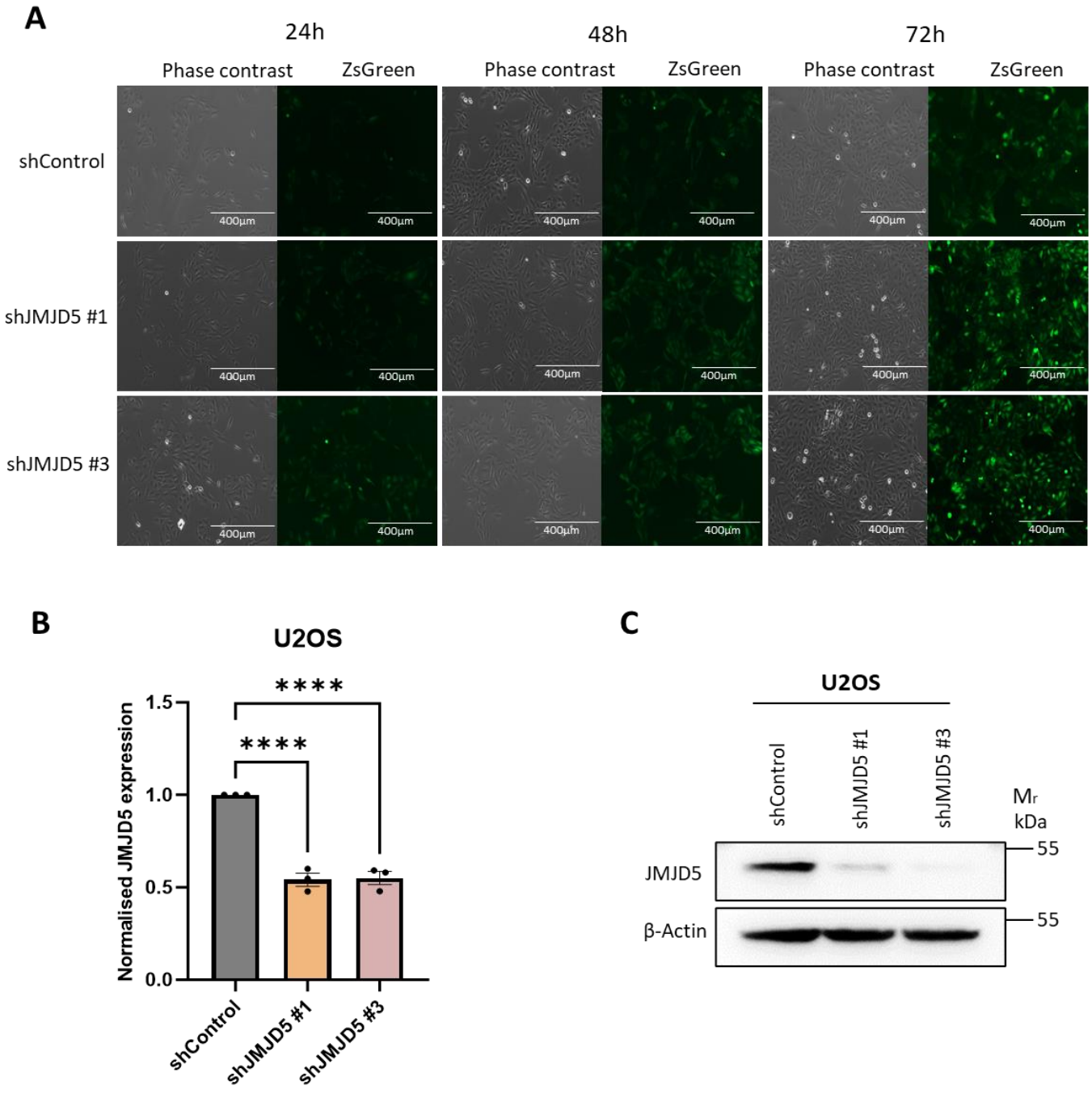

Figure 3.16 Validation of shRNA U2OS model.

A. Expression of green fluorescent protein (GFP) was analysed 72 hours after induction with 1 µg/mL doxycycline. Images were acquired using an EVOS inverted microscope equipped with a 10x objective. Scale bars = 400µm B. Evaluation of JMJD5 mRNA levels following 72 hours by qPCR. Data represent mean ± SEM from three independent replicates. Statistical significance was determined using one-way ANOVA with Tukey's post hoc test [with p-value ≤ 0.001 (****)].C. Representative immunoblot validating knockdown of JMJD5 in stable A549 cell lines expressing doxycycline-inducible control (shControl) or JMJD5-targeting (shJMJD5 #1/#3) shRNAs. Cells were treated with 1 µg/mL doxycycline for 72 hours prior to immunoblotting (C) β-actin was used as a loading control. N=3

3.2.14 ShRNA-mediated JMJD5 knockdown increases replication stress in A549 and U2OS models

To further validate our JMJD5 loss-of-function shRNA models, I investigated 53BP1 bodies and micronuclei following knockdown. Consistent with the siRNA models, depletion of JMJD5 using either shRNA sequence led to a statistically significant increase in cells positive for micronuclei and G1 cells containing 53BP1 bodies for both U2OS (Figure 3.17A and 3.17B) and A549 (Figure 3.17C and 3.17D). Confirming the anticipated replication stress phenotype in these models validated them as useful models for investigating the impact of JMJD5 loss on sensitivity to anticancer agents.

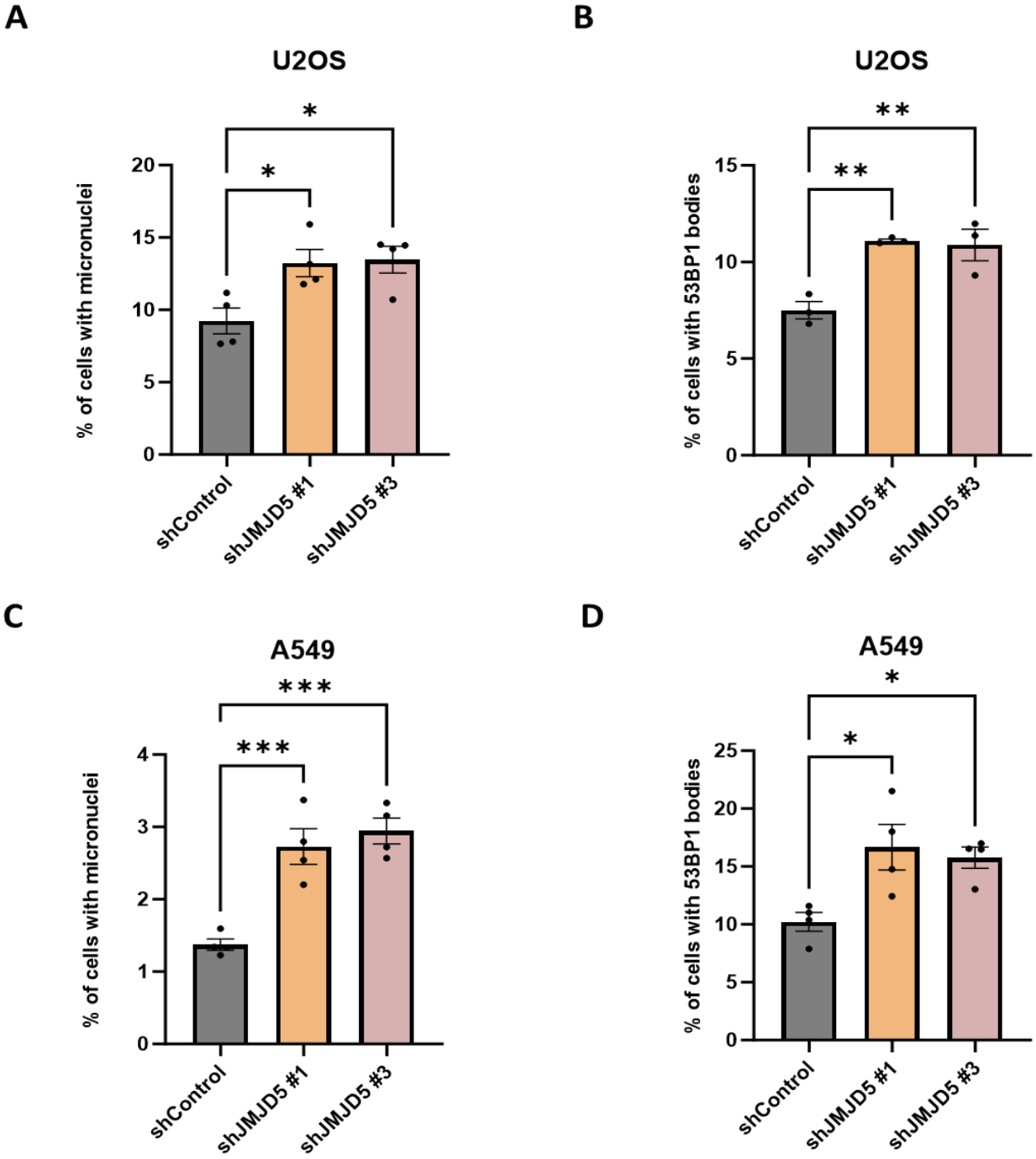

Figure 3.17 JMJD5 knockdown increases replication stress in shRNA A549 and U2OS cells. *Cells were treated with 1µg/ml of doxycycline to induce expression of control shRNA control or shRNA sequences targeting JMJD5 for 72 hours. Loss of JMJD5 increases micronuclei formation in U2OS (C) and A549 (D) cell lines. B and D. Knockdown of JMJD5 in U2OS (B) and A549 (D) cell lines increases 53BP1 bodies. Data represent mean ± SEM from four independent replicates. Statistical analysis was performed using the one-way ANOVA with Tukey's post hoc test where (p-value ≤ 0.05=*, ≤0.01 =**, ≤0.001=***). All experiments represent n=4 biological repeats.*

3.2.15 JMJD5 knockdown sensitises shRNA U2OS and A549 cells to ATM, ATR and PARP inhibitors

Earlier in this chapter we presented data indicating that siRNA-mediated JMJD5 knockdown leads to increased sensitivity to ATM, ATR and PARP inhibitors (Figure 3.3). We next aimed to determine whether these sensitivities were replicated in our new loss-of-function models. As an orthogonal assay to colony survival, we used 96-well cell viability assays, which enable more immediate and automated measurements. Combining these methodologies would allow us to validate and extend the siRNA-based findings, ensuring that the observed effects are not artifacts of off-target gene silencing and are reproducible across different experimental methods and cell lines.

To this end, U2OS and A549 cells were incubated with 1µg/mL doxycycline for 72 hours to induce JMJD5 knockdown. Subsequently, they were treated with either ATM, ATR or PARP inhibitors in the presence of 1µg/mL doxycycline for 5 days. Cell viability was assessed using an MTS assay which utilises the detection of a coloured formazan product as a readout for the presence of viable cells. Consistent with results in the siRNA model (Figure 3.3), JMJD5 shRNA knockdown with sh#3 led to statistically significant differences in cell survival compared to the control at 0.01µM and 0.1µM ATM inhibitor (Figure 3.18B, D). Knockdown with sh#1 only led to a significant difference at the higher dose of 0.1 µM. In the U2OS shRNA cell lines, knockdown using both JMJD5 targeting sequences led to statistically significant decreases in cell viability in response to ATM inhibitor at all doses tested (Figure 3.18A, C).

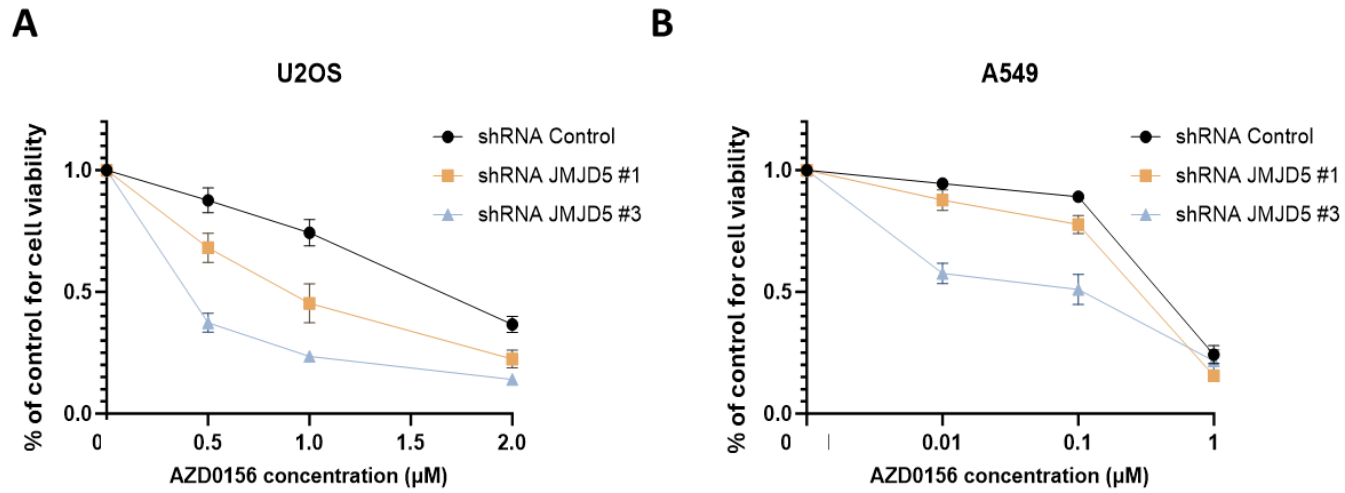

C

Comparison: shControl vs.....	Concentration	Adjusted P Value	Significance
shJMJD5 #1	0.5μM	0.0049	**
shJMJD5 #1	1μM	<0.0001	****
shJMJD5 #1	2μM	0.0401	*
shJMJD5 #3	0.5μM	<0.0001	****
shJMJD5 #3	1μM	<0.0001	****
shJMJD5 #3	2μM	0.0013	**

D

Comparison: shControl vs.....	Concentration	Adjusted P Value	Significance
shJMJD5 #1	0.01μM	0.256	ns
shJMJD5 #1	0.1μM	0.0401	*
shJMJD5 #1	1μM	0.1298	ns
shJMJD5 #3	0.01μM	<0.0001	****
shJMJD5 #3	0.1μM	<0.0001	****
shJMJD5 #3	1μM	0.8054	ns

Figure 3.18 JMJD5 knockdown sensitises shRNA U2OS and A549 cells to ATM inhibitor AZD0156.

U2OS (A) and A549 (B) cells were treated with 1μg/mL of doxycycline to induce shRNA expression resulting in JMJD5 knockdown and subsequently treated with 1μg/mL of doxycycline plus ATM inhibitors for 5 days. Cell viability was measured by MTS assay. Data represent mean ± SEM from three independent replicates with quadruplicate technical repeats. C and D. Statistical analysis was performed using the two-way ANOVA with Dunnett's multiple comparisons test (p-value ≤ 0.05=, ≤0.01 =**, ≤0.001=***).*

Similar to our results for ATM inhibitor, JMJD5 knockdown with either shRNA sequence in U2OS cells led to statistically significant increases in sensitivity to the ATR inhibitor Ceralasertib (Figure 3.19A, C). Similarly, the knockdown of JMJD5 with sh#3 led to a statistically significant increase in sensitivity to Ceralasertib in A549 cells (Figure 3.19B, D).

However, the results for sh#1 are less clear in A549 cells, with statistical significance only achieved at 1µM.

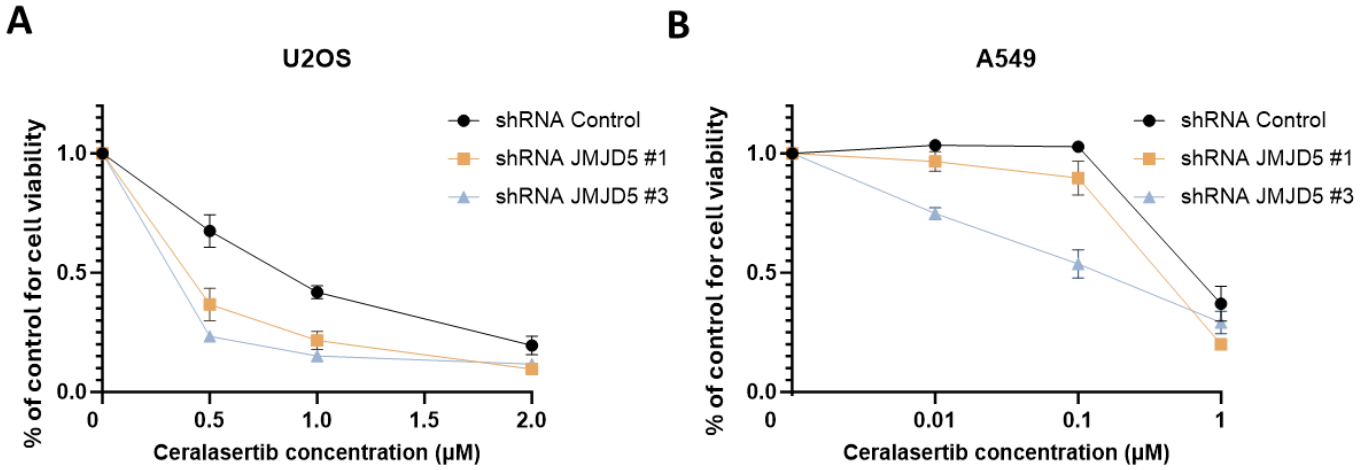

C

Comparison: shControl vs.....	Concentration	Adjusted P Value	Significance
shJMJD5 #1	0.5µM	<0.0001	****
shJMJD5 #1	1µM	0.0005	***
shJMJD5 #1	2µM	0.0831	ns
shJMJD5 #3	0.5µM	<0.0001	****
shJMJD5 #3	1µM	<0.0001	****
shJMJD5 #3	2µM	0.1916	ns

D

Comparison: shControl vs.....	Concentration	Adjusted P Value	Significance
shJMJD5 #1	0.01µM	0.4007	ns
shJMJD5 #1	0.1µM	0.0578	ns
shJMJD5 #1	1µM	0.0127	*
shJMJD5 #3	0.01µM	<0.0001	****
shJMJD5 #3	0.1µM	<0.0001	****
shJMJD5 #3	1µM	0.3037	ns

Figure 3.19 JMJD5 knockdown sensitises shRNA U2OS and A549 cells to ATR inhibitor Ceralasertib.

U2OS and A549 cells were treated with 1µg/mL of doxycycline to induce shRNA expression resulting in JMJD5 knockdown and subsequently treated with 1µg/mL doxycycline plus inhibitors for 5 days. Cell viability was measured by MTS assay. Data represent mean ± SEM from three independent replicates with quadruplicate technical repeats. C and D. Statistical analysis was performed using the two-way ANOVA with Dunnett's multiple comparisons test (p-value ≤ 0.05=, ≤0.01 =**, ≤0.001=***).*

Interestingly, JMJD5 knockdown in U2OS cells also led to statistically significant increases in cell sensitivity across the dose range tested for the PARP inhibitor Talazoparib (Figure 3.20A,

C.). In A549 cells, JMJD5 knockdown only led to a statistically significant decrease in cell survival at 0.1µM Talazoparib (Figure 3.20B, D).

Overall, our data from across two cell models and knockdown approaches confirms that loss of JMJD5 sensitises cancer cells to ATM, ATR and PARP inhibitors.

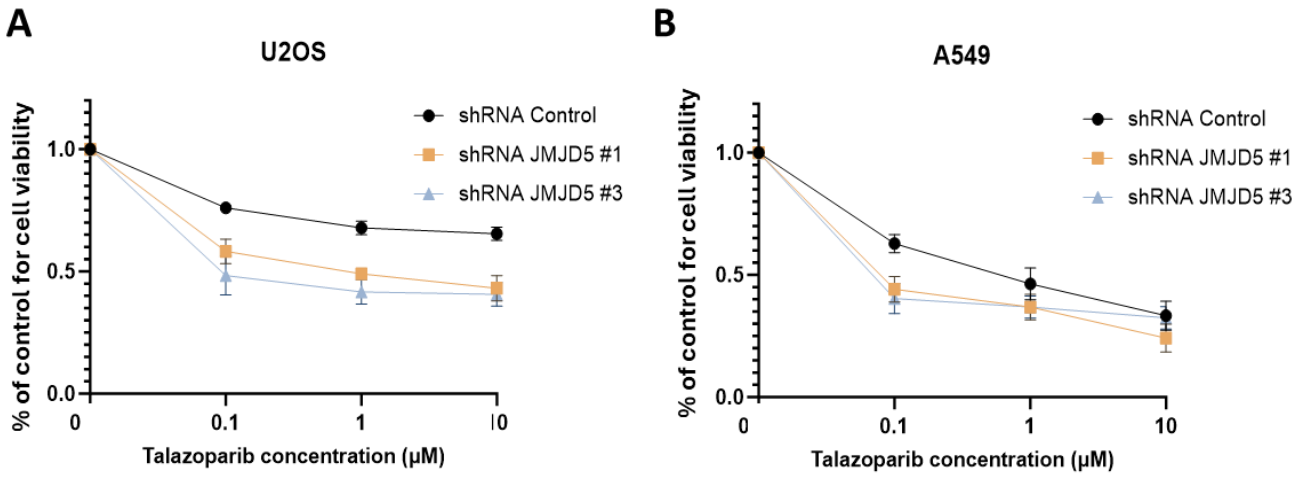

C

Comparison: shControl vs.....	Concentration	Adjusted P Value	Significance
shJMJD5 #1	0.1µM	0.0074	**
shJMJD5 #1	1µM	0.0049	**
shJMJD5 #1	10µM	0.001	**
shJMJD5 #3	0.1µM	<0.0001	****
shJMJD5 #3	1µM	0.0002	***
shJMJD5 #3	10µM	0.0003	***

D

Comparison: shControl vs.....	Concentration	Adjusted P Value	Significance
shJMJD5 #1	0.1µM	0.0174	*
shJMJD5 #1	1µM	0.2738	ns
shJMJD5 #1	10µM	0.2925	ns
shJMJD5 #3	0.1µM	0.0043	*
shJMJD5 #3	1µM	0.2724	ns
shJMJD5 #3	10µM	0.9871	ns

Figure 3.20 JMJD5 knockdown sensitises shRNA U2OS and A549 cells to PARP inhibitor Talazoparib.

U2OS and A549 cells were treated with 1µg/mL of doxycycline to induce shRNA expression resulting in JMJD5 knockdown and subsequently treated with 1µg/mL doxycycline plus inhibitors for 5 days. Cell viability was measured by MTS assay. Data represent mean ± SEM from three independent replicates with quadruplicate technical repeats. C. and D. Statistical analysis was performed using the two-way ANOVA with Dunnett's multiple comparisons test (p-value ≤ 0.05=, ≤0.01 =**, ≤0.001=***).*

3.2.16 Knockdown of JMJD5 can sensitise the U2OS cells to a wide range of different anticancer drugs.

While we were conducting the drug sensitivity experiments in JMJD5 knockdown models, an interesting report was published describing a set of CRISPR screens to discover genes involved in DNA damage responses (Olivieri et al., 2020). The authors performed their screens in an immortalised human retinal pigment epithelial RPE-1 cell line treated with a wide range of genotoxic agents (Olivieri et al., 2020). Their data indicated that JMJD5 knockdown can have both synergistic and resistance interactions with a variety of anticancer drugs (Figure 3.21). Interestingly, their CRISPR screen results showed that JMJD5 loss sensitises cells to a number of agents including ATR inhibitor AZD6738 (Ceralasertib), thus validating our results presented above.

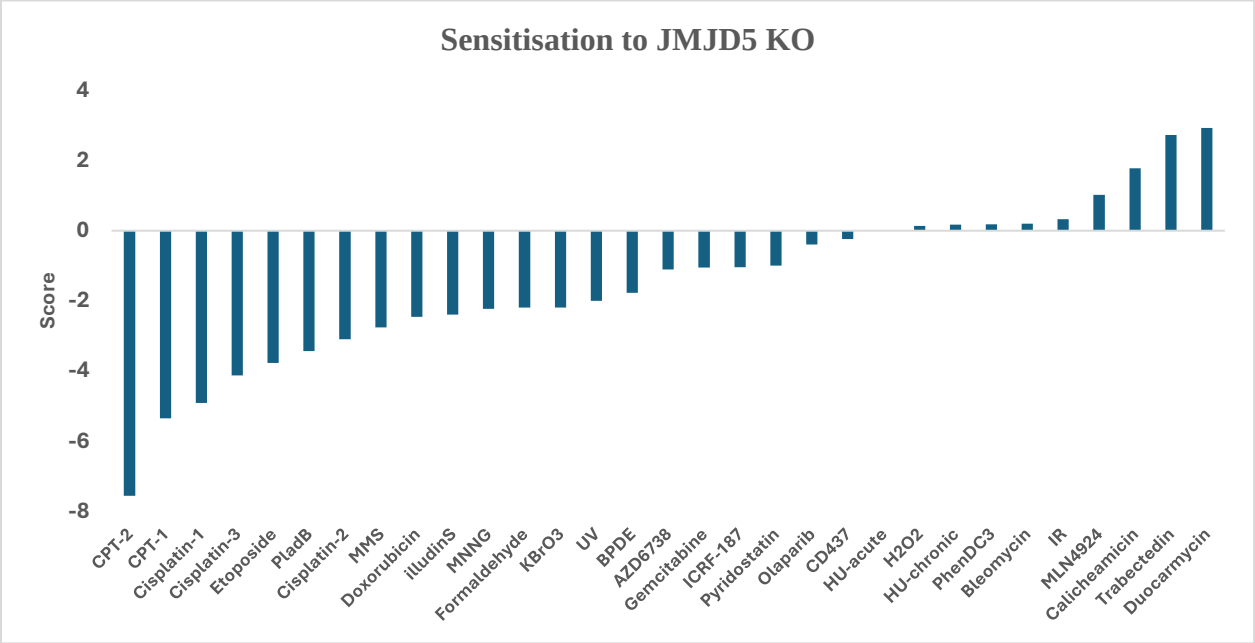

Figure 3.21 CRISPR screen data representing sensitisation/resistance to JMJD5 knockout complied from Olivieri et al., 2020.

Score- gene-level normalised Z-score (negative score indicates sensitivity and positive score indicates resistance) where CTP (Camptothecin), MMS (methyl methanesulfonate), MMNG (Methylnitronitrosoguanidine), BPDE (Benzo(a)pyrene diol epoxide), HU (Hydroxyurea) and IR (Ionising radiation).

Given that our findings align with the ATR inhibitor results of Olivieri et al., we wanted to investigate other compounds from their study. To do that, we selected two drugs that JMJD5 knockdown is reported to sensitise cells to (Doxorubicin and methyl methanesulfonate - MMS) and two that JMJD5 knockdown is reported to cause resistance to (Calicheamicin and Trabectedin). We chose doxorubicin as it is a commonly used chemotherapeutic agent for the treatment of various cancers including breast cancer, leukaemia and lymphoma (Sritharan and Sivalingam, 2021). MMS is a DNA alkylating agent that introduces methyl groups into DNA, causing damage to cancer cells deficient in DNA repair pathways like HR. Calicheamicin is a potent antitumor antibiotic derived from the bacterium *Micromonospora echinospora* that is used in antibody-drug conjugates (ADCs) for targeted anticancer therapy. Trabectedin is a chemotherapeutic agent used in the treatment of soft tissue sarcoma. It binds to the minor groove of DNA, bending the DNA helix towards the major groove which interferes with various DNA repair pathways including HR.

We induced knockdown of JMJD5 in our U2OS shRNA model and after 3 days treated with the chosen drugs at a variety of concentrations for a further 5 days. Surprisingly, we found that JMJD5 knockdown causes cells to be significantly more sensitive to all of the drugs tested (Figure 3.22). Consistent with the results presented above for the PARP, ATM and ATR inhibitors in U2OS cells, sh#3 had a stronger effect on drug sensitivity than sh#1.

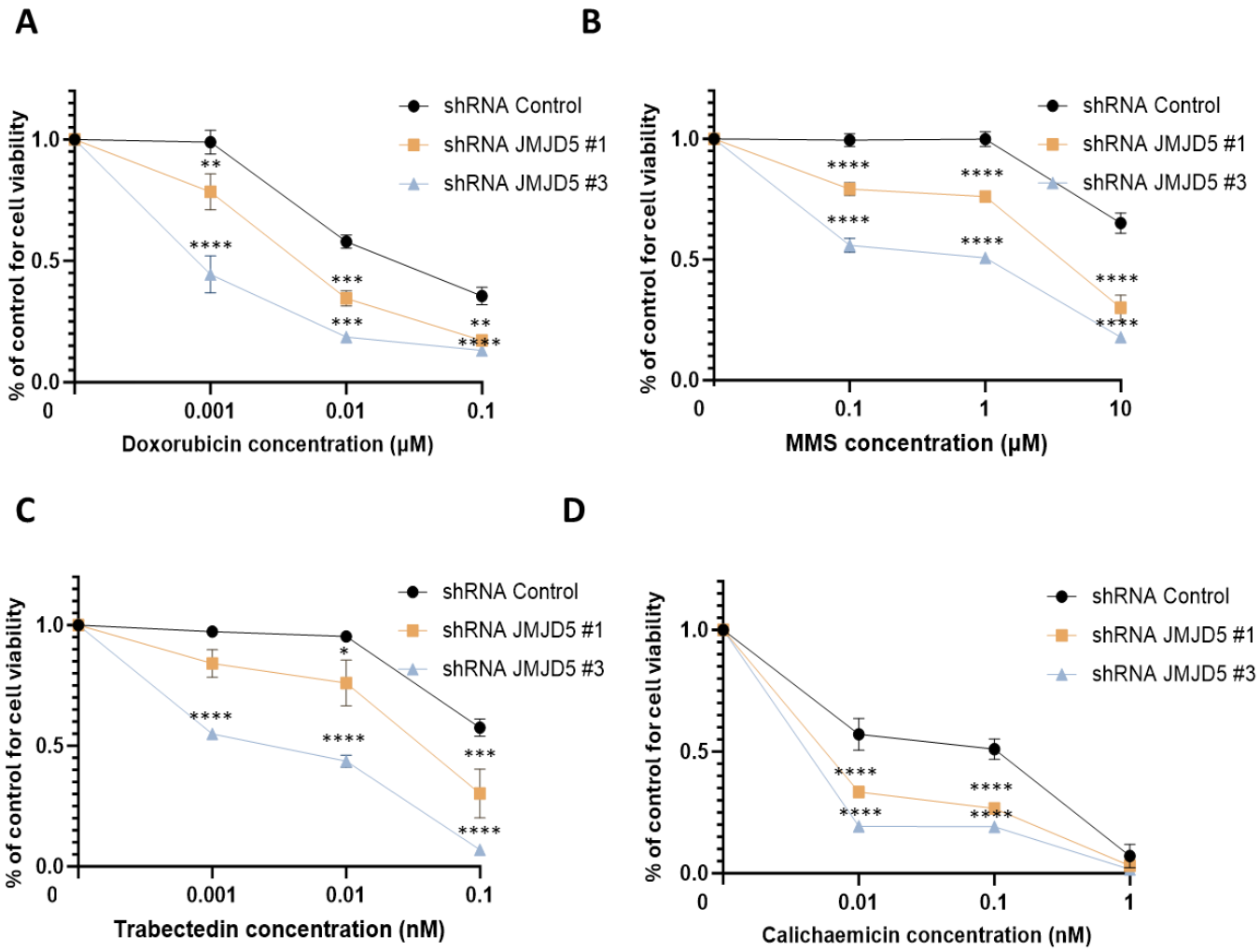

Figure 3.22 JMJD5 knockdown sensitises shRNA U2OS cells to various anticancer drugs: Doxorubicin (A), MMS (B), Calicheamicin (C), and Trabectedin (D).

U2OS cells were treated with 1μg/ml of doxycycline to induce shRNA expression resulting in JMJD5 knockdown and subsequently treated with doxycycline plus indicated drug for 5 days. Cell viability was measured by MTS assay. Data represent mean ± SEM from three independent biological replicates with quadruplicate technical repeats. Statistical analysis was performed using the two-way ANOVA with Dunnett's multiple comparisons test (p-value ≤ 0.05=, ≤0.01 =**, ≤0.001=***).*

3.2.17 Investigating if drug sensitivity is dependent on the enzymatic activity of JMJD5

We have presented data demonstrating that JMJD5 knockdown enhances the sensitivity of cancer cells to DDR inhibitors, suggesting that targeting JMJD5 could synergise with these existing therapies to potentiate their efficacy. Investigating whether this drug sensitisation is

dependent on JMJD5 enzymatic activity will be important for understanding the therapeutic potential of JMJD5 as a drug target in cancer treatment. Elucidating the relationship between JMJD5 enzymatic activity and drug sensitivity will deepen our understanding of JMJD5 function in cancer biology and facilitate the development of novel JMJD5 inhibitors as potential cancer therapeutics.

3.2.17.1 Generation of the reconstitution model

To assess if the sensitisation to chemotherapeutic compounds upon JMJD5 loss is driven by its enzymatic activity we wanted to re-expressed catalytically inactive and WT JMJD5 in cells stably expressing shRNA targeting JMJD5. We decided to use U2OS shRNA cells as we observed a greater sensitisation to all the drugs tested by JMJD5 knockdown in this model. For JMJD5 reconstitution in knockdown cells, we considered using a lentiviral expression vector called 'pIHZ', which is a derivative of pGIPZ that lacks the GFP cDNA and substitutes a puromycin for a hygromycin resistance cassette. This exogenously expressed JMJD5 is not going to be knocked down by the shRNA due to the lack of a 3' untranslated region (UTR) which is only present in the endogenous JMJD5.

Therefore, full-length WT JMJD5 or H321A JMJD5 was PCR cloned with 3XFLAG-tag into the lentiviral expression vector pIHZ for constitutive expression. After successfully verifying the cloned sequences, we transduced U2OS cells with lentiviral particles that would express control EV or 3XFLAG JMJD5 WT or JMJD5 H321A inactive mutant. We performed this as a 'transient' expression experiment in the first instance, so did not select the cells with antibiotics to establish a stable cell line.

First, we assessed JMJD5 expression in our system via Western blot. Figure 3.23A shows a representative Western blot demonstrating successful expression of both JMJD5 WT and JMJD5 H321A in U2OS cells. We note that only overexpressed FLAG-JMJD5, and not endogenous JMJD5, is visible on the blot, likely due to high exogenous expression. We also

wanted to check the transduction efficiency in cells via IF staining prior to any reconstitution drug sensitivity experiments. As shown in Figure 3.23B, the majority of cells showed FLAG-JMJD5 expression. After confirming the successful expression of JMJD5 we progressed to drug sensitivity rescue experiments in this model.

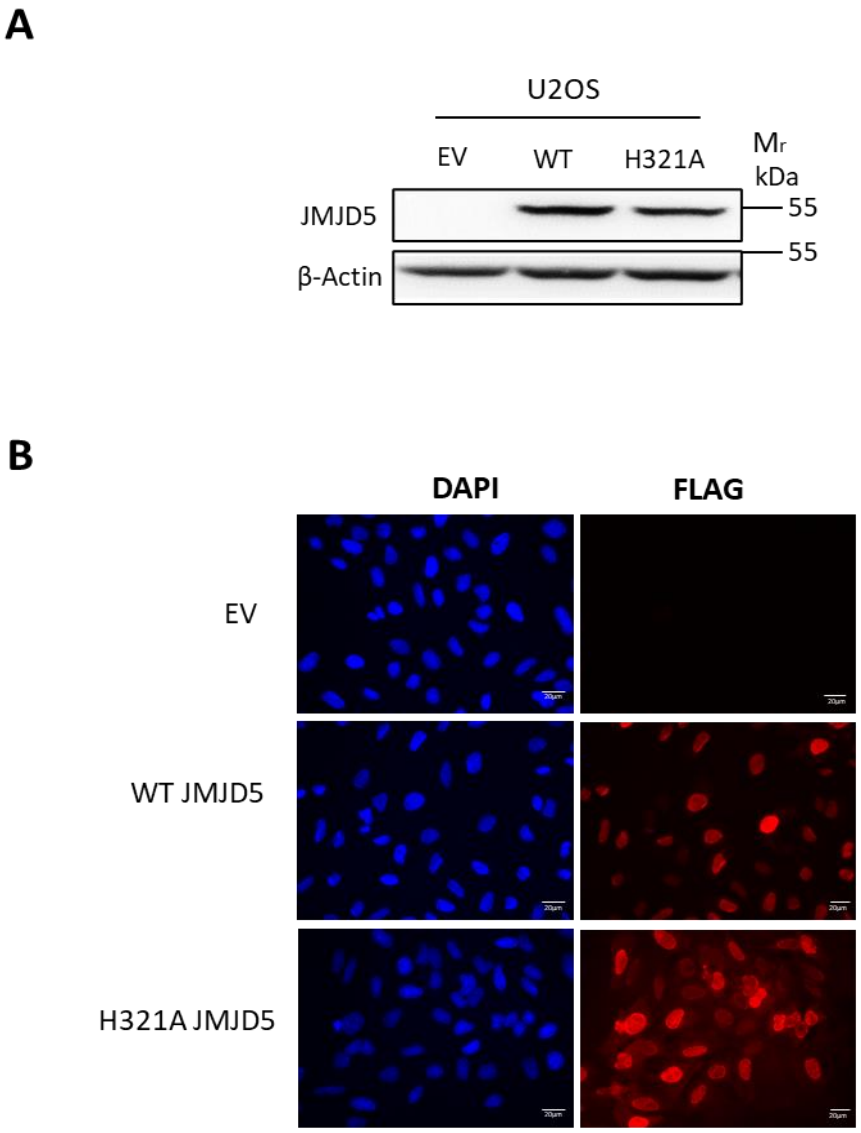

Figure 3.23 Generation of the pIHZ FLAG-JMJD5 model in U2OS cells.
shRNA Control U2OS cells were transduced with lentivirus encoding an empty vector (EV) or 3XFLAG JMJD5 WT or JMJD5 H321A constructs. Twenty-four hours after transduction, the cells were seeded and grown for 3 days before JMJD5 expression was analysed by immunoblot (A), and immunofluorescence (B) A. Western blot evaluating the FLAG-JMJD5 expression with β-Actin as a loading control. N=1 B. Representative immunofluorescence images showing expression of JMJD5. Cells were fixed and stained with an anti-FLAG antibody, and nuclei were stained with DAPI. Scale bars = 20μm

3.2.17.2 Evaluation of drug sensitivity in U2OS cells expressing exogenous JMJD5

Next, we progressed to drug sensitivity rescue experiments following JMJD5 knockdown. The following experiments were carried out using JMJD5 shRNA #3 due to its potency in JMJD5 knockdown and greater sensitisation to drugs. Therefore, shControl or shJMJD5#3 (referred hereafter as shJMJD5) U2OS cells were transduced with lentivirus encoding EV, 3XFLAG JMJD5 WT or 3XFLAG JMJD5 H321A constructs. After 24 hours the cells were seeded into a medium containing 1 μg/mL of doxycycline for 72 hours to induce knockdown. Simultaneously, additional cells were seeded on extra plates for expression analysis four days post-transduction. Following the knockdown period, cells for viability assay were treated with the indicated doses of the PARP inhibitor Talazoparib with 1 μg/mL of doxycycline for 5 days, with cell survival measured using the MTS assay.

First, we evaluated the expression of FLAG-JMJD5 and endogenous JMJD5 knockdown by Western blot 4 days post-transduction. Figure 3.24A shows a high expression of exogenous JMJD5 in both control and JMJD5 knockdown cells, as expected. However, due to high overexpression of FLAG-JMJD5, the signal for endogenous JMJD5 is not visible. Therefore, confirmation of endogenous JMJD5 knockdown by Western was not possible in this model. We also checked the transduction efficiency in cells via IF staining and showed a high level of transduction in assessed cells (Figure 3.24B).

Next, we wanted to confirm whether JMJD5 knockdown leads to increased sensitivity to PARP inhibitor Talazoparib in this system. Consistent with previously shown data, JMJD5 knockdown led to increased sensitivity to Talazoparib (Figure 3.24C), consistent with our previous results (Figure 3.17A). Due to concerns about the magnitude of JMJD5 overexpression in this model, we next evaluated whether overexpression of JMJD5 alone is sufficient to affect sensitivity to Talazoparib. Unfortunately, we found that overexpression of either WT or H321A JMJD5 led to slightly increased sensitivity to PARP inhibitor Talazoparib in shControl cells (Figure 3.24D).

Critically, there was no difference between the sensitivity of shJMJD5 cells expressing either WT or H321A JMJD5 and shJMJD5 cells expressing the control EV (Figure 3.24E). Therefore, we concluded that the reconstitution of JMJD5 function in these knockdown cells was unsuccessful.


A
shControl
shJMJD5
+ 1µg/mL doxycycline
EV
WT
H321A
EV
WT
H321A
Mr
kDa
JMJD5
55
β-Actin
55

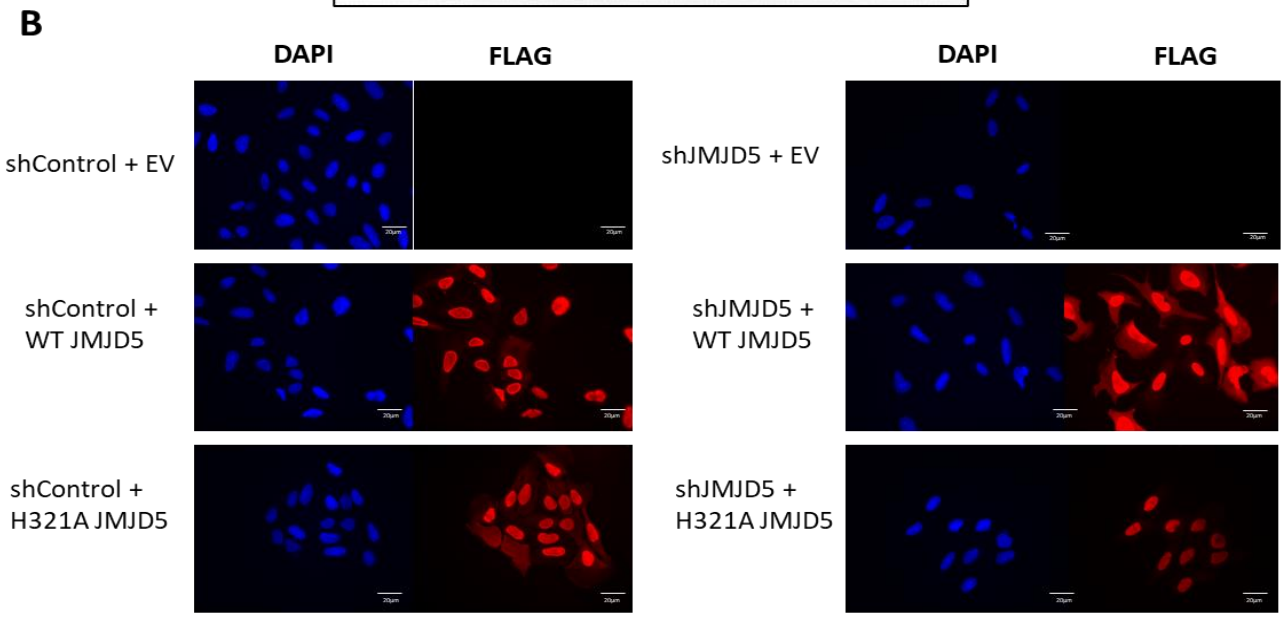
B
DAPI
FLAG
DAPI
FLAG
shControl + EV
shJMJD5 + EV
shControl +
WT JMJD5
shJMJD5 +
WT JMJD5
shControl +
H321A JMJD5
shJMJD5 +
H321A JMJD5

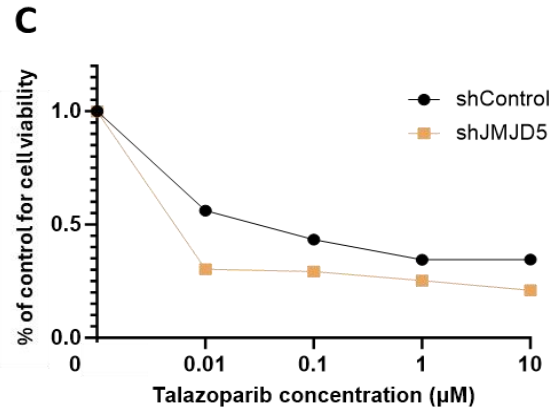
C
% of control for cell viability
1.0
0.5
0.0
0
0.01
0.1
1
10
Talazoparib concentration (µM)
shControl + EV
shJMJD5 + EV

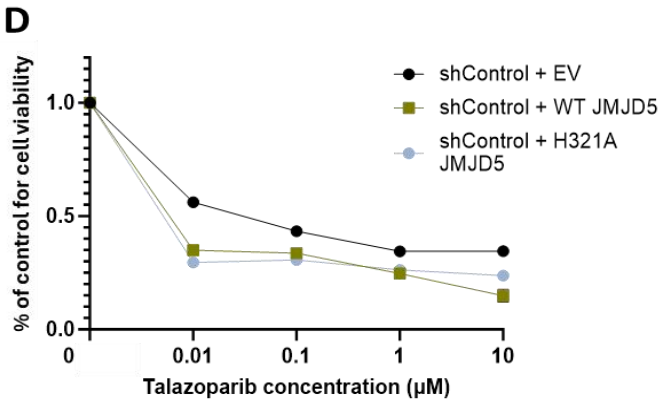
D
% of control for cell viability
1.0
0.5
0.0
0
0.01
0.1
1
10
Talazoparib concentration (µM)
shControl + EV
shControl + WT JMJD5
shControl + H321A
JMJD5

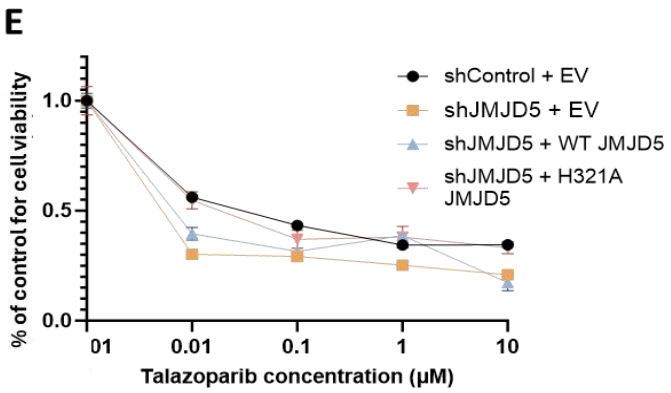
E
% of control for cell viability
1.0
0.5
0.0
01
0.01
0.1
1
10
Talazoparib concentration (µM)
shControl + EV
shJMJD5 + EV
shJMJD5 + WT JMJD5
shJMJD5 + H321A
JMJD5

Figure 3.24 Characterisation of sensitivity to Talazoparib following exogenous expression of FLAG-JMJD5 in endogenous JMJD5 knockdown in U2OS cell model.

The U2OS cells were transduced with lentivirus encoding an empty vector (EV) or 3XFLAG JMJD5 WT or JMJD5 H321A constructs and after 24 hours seeded with media containing 1 µg/mL doxycycline for 72 hours to induce endogenous JMJD5 knockdown. Afterwards, the cells were treated with indicated doses of PARP inhibitor Talazoparib containing 1 µg/mL doxycycline for 5 days and the cell survival was measured using MTS assay. A. Western blot evaluating the JMJD5 expression in control and JMJD5 knockdown 4 days post-transduction in U2OS cells with β-Actin used as loading control. N=1 B. Representative immunofluorescence images showing expression of JMJD5 4 days post-transduction. Cells were fixed and stained with an anti-FLAG antibody, and nuclei were stained with DAPI. Scale bars = 20µm C. Endogenous JMJD5 knockdown causes increased cell sensitivity to Talazoparib. D. Exogenous overexpression of FLAG-JMJD5 WT or H321A increases sensitivity to Talazoparib. F. The effect of re-expression of EV or FLAG-JMJD5 WT/H321A on the sensitivity to Talazoparib in JMJD5 knockdown U2OS cells. Data presents mean ± SEM of results from one independent biological experiment performed in triplicate.

The current model of using transiently transduced U2OS cells was associated with constitutive uncontrolled JMJD5 expression levels that we were not able to titrate. This was potentially problematic because it was associated with increased sensitivity to Talazoparib. Moreover, the high level of JMJD5 overexpression in this system meant that we were not able to visualize the endogenous JMJD5 expression by Western blot to confirm the knockdown. Another problem that we noted was very low raw absorbance values in the viability assays, indicating that the JMJD5 knockdown cells re-expressing either EV or JMJD5 were not proliferating or potentially dying (data not shown). Due to these difficulties, we decided to test an alternative reconstitution system: a doxycycline-inducible 3xFLAG-JMJD5 A549 stable cell lines with transient siRNA-mediated JMJD5 knockdown that has proven a reliable model to study the effect of exogenously expressed variants of JMJD5 (Chapter 2).

3.2.17.3 Evaluation of drug sensitivity in doxycycline inducible JMJD5 A549 cells with transient JMJD5 knockdown

In order to evaluate this system for reconstitution experiments, we used a similar experimental set up as in Chapter 2 (Figure 2.11). A549 cells stably expressing EV, WT or H321A JMJD5 were incubated with 25 ng/mL of doxycycline for 7 days followed by JMJD5 siRNA. The

expression of JMJD5 was evaluated by Western blot 3 days after transfection (Figure 3.25A). Three days post JMJD5 knockdown, the cells were treated with the indicated doses of PARP inhibitor Talazoparib for a further 5 days before measuring cell survival by MTS assay.

Firstly, we note that in this model we were able to simultaneously detect endogenous and exogenous JMJD5 expression and confirm successful knockdown (Figure 3.25A). Next, we confirmed that endogenous JMJD5 knockdown leads to increased sensitivity to PARP inhibitor Talazoparib in this system (Figure 3.25B). Due to our concerns that JMJD5 overexpression can itself lead to increased Talazoparib sensitivity, we were interested in evaluating whether expression of JMJD5 in this inducible pTIPZ system would also affect the sensitivity of A549 cells to PARP inhibitor. Although 25 ng/mL of doxycycline induces only moderate levels of JMJD5 expression (Figure 3.25A), this appears sufficient to modestly increase sensitivity to PARP inhibitor (Figure 3.25C). Moreover, there was no difference between the PARP inhibitor sensitivity of JMJD5 knockdown cells expressing either WT or H321A JMJD5 or the control EV. Therefore, we concluded that we had not achieved successful functional reconstitution of JMJD5 (Figure 3.25D).

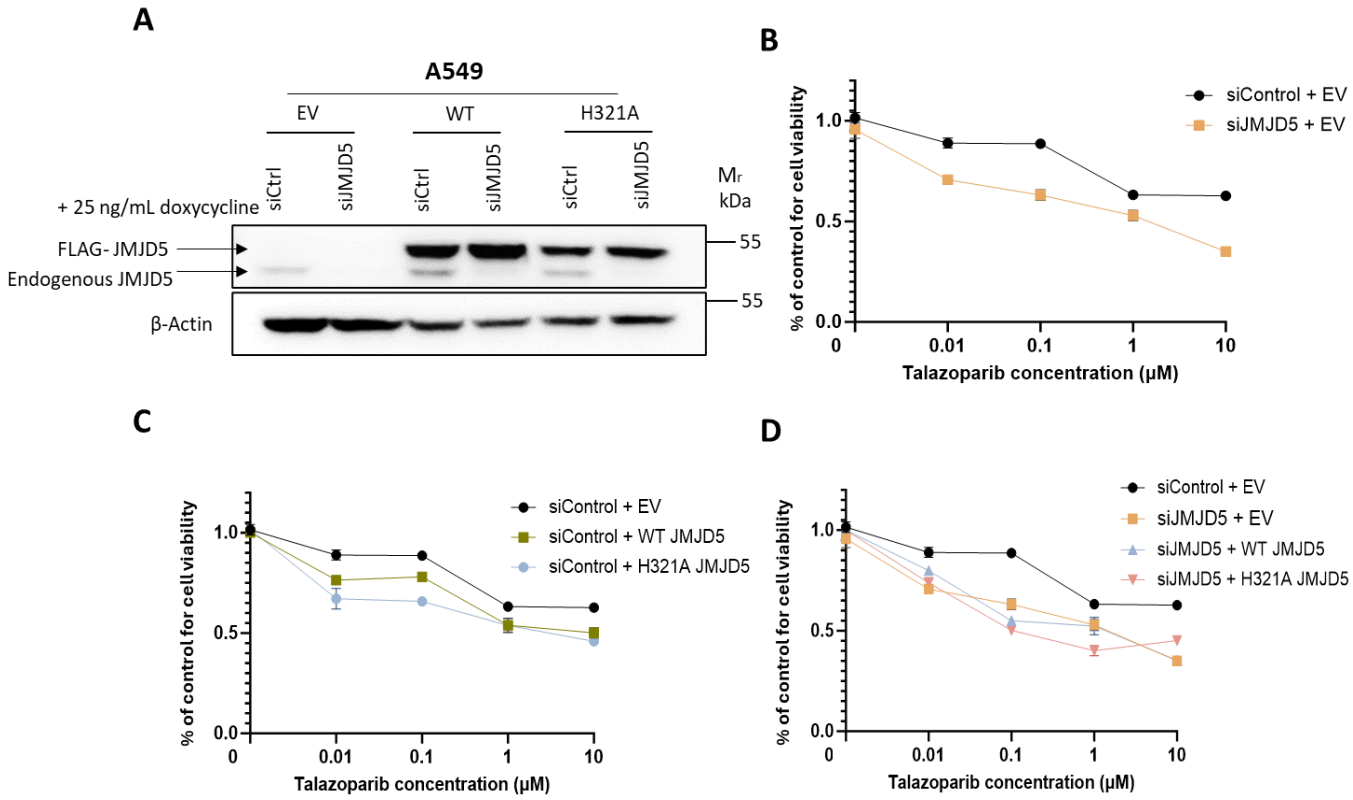

Figure 3.25 Characterisation of sensitivity to Talazoparib following exogenous expression of FLAG-JMJD5 in endogenous JMJD5 knockdown in A549 cell model.

A549 cells were incubated with 25 ng/mL doxycycline for 7 days to induce exogenous expression of empty vector (EV) or 3XFLAG JMJD5 WT or H321A constructs. Afterwards, cells were transfected with the indicated siRNA for 72 hours to knockdown endogenous JMJD5 and treated with indicated doses of PARP inhibitor Talazoparib with 25 ng/mL doxycycline for 5 days. The cell survival was measured using an MTS assay. A. Western blot evaluating the exogenous (top band) and endogenous (bottom band) JMJD5 expression in control and JMJD5 knockdown 3 days post-transfection in A549 cells with β-Actin used as loading control. N=1 B. Endogenous JMJD5 knockdown causes increased cell sensitivity to Talazoparib in A549 cells. C. Exogenous overexpression of FLAG-JMJD5 WT or H321A increases sensitivity to Talazoparib. D. The effect of re-expression of EV or FLAG-JMJD5 WT/H321A on the sensitivity to Talazoparib in JMJD5 knockdown A549 cells. Data represent mean ± SEM from one independent experiment with quadruplicate technical repeats.

3.2.17.3 Evaluation of drug sensitivity reconstitution in stable JMJD5 doxycycline inducible A549 cells with transient JMJD5 knockdown using colony formation assay

For our next attempt to rescue the drug sensitivity, we decided to use the current pTIPZ A549 system but with a few modifications. Firstly, we decided to test a different drug, specifically an

ATR inhibitor because there is a considerably wider sensitivity window based on our previous data (Figure 3.16B). Secondly, we decided to decrease the dose of doxycycline to 10 ng/mL to try and reduce the overexpression of FLAG-JMJD5 from that achieved with 25 ng/mL. Therefore, cells were seeded in 10 ng/mL of doxycycline and the following day transfected with JMJD5 siRNA in the presence of 10 ng/mL doxycycline for 72 hours. Subsequently, cells were treated with the indicated doses of ATR inhibitor plus 10 ng/mL doxycycline for a further 24 hours. Subsequently, the media was changed to 10ng/mL doxycycline and the colonies were left to grow for 10 days. Consistent with the previous data, we observed that endogenous JMJD5 knockdown leads to increased sensitivity to ATR inhibitor Ceralasertib (Figure 3.26B). Interestingly, we did not observe an impact of exogenous JMJD5 expression with 10 ng/mL doxycycline on the sensitivity of cells to the lower doses of ATR inhibitor used (0.5 and 1.0 mM; Figure 3.26C). Nonetheless, the re-expression of either WT or H31A JMJD5 did not rescue JMJD5 knockdown-induced sensitivity to ATR inhibitor (Figure 3.26D).

We also evaluated the endogenous and exogenous expression of JMJD5 by Western blot 3 days after siRNA transfection (Figure 3.26A). Interestingly, we observed that JMJD5 knockdown cells exhibit higher expression of exogenous JMJD5 despite being incubated in the same doxycycline concentration as control cells. This phenomenon could potentially be driving cell sensitivity to ATR inhibitor in the knockdown cells and preventing the rescue. Therefore, we next attempted to further reduce the level of FLAG-JMJD5 overexpression in JMJD5 knockdown cells.

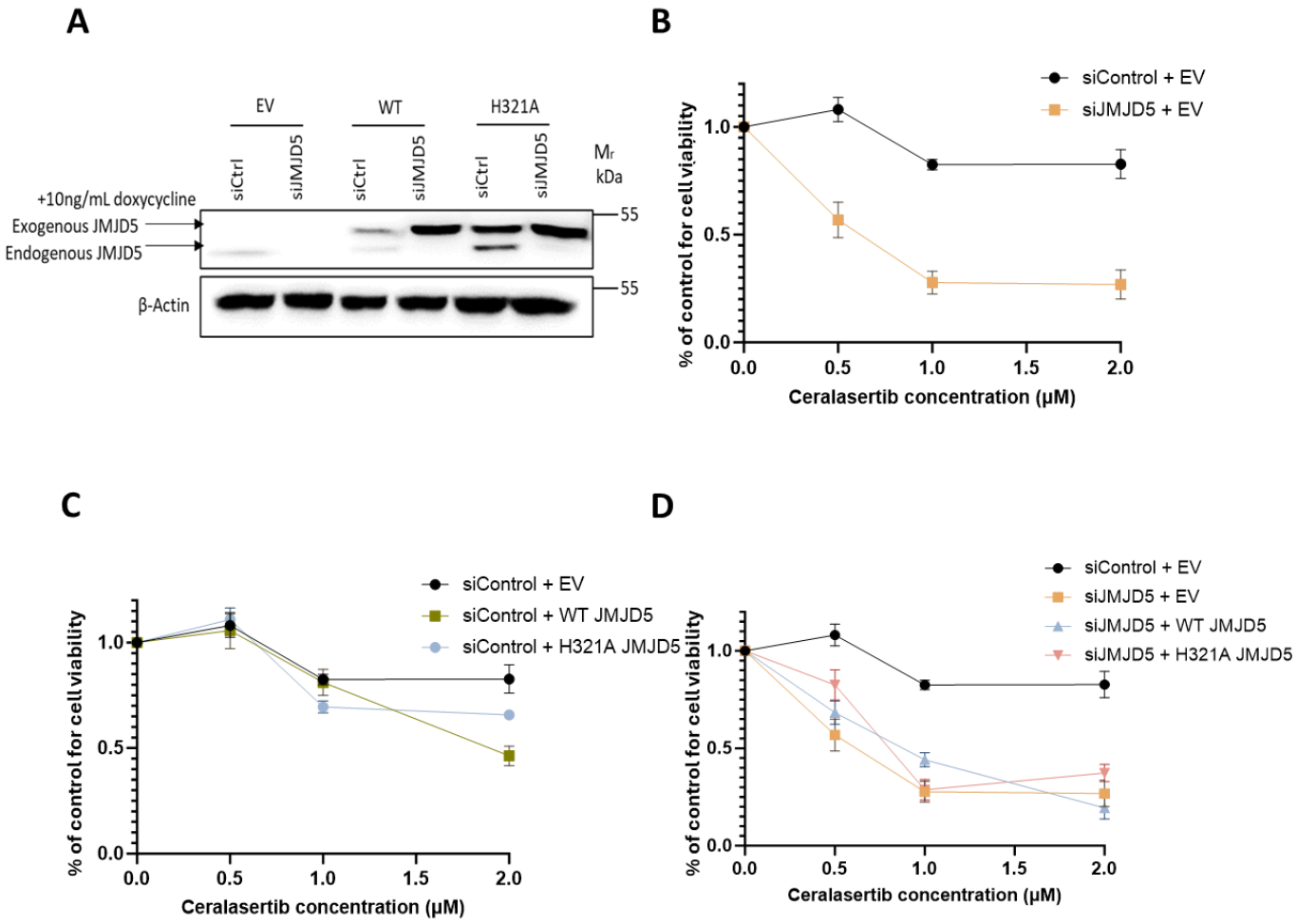

Figure 3.26 Characterisation of sensitivity to ATR inhibitor Ceralasertib following exogenous expression of FLAG-JMJD5 in endogenous JMJD5 knockdown in A549 cell model.

The A549 cells were seeded in 10 ng/mL of doxycycline to induce exogenous expression of empty vector (EV) or 3XFLAG JMJD5 WT or H321A constructs. The cells were transfected with siRNA targeting JMJD5 in the presence of 10 ng/mL of doxycycline. Subsequently, the cells were treated with indicated doses of ATR inhibitor with 10 ng/mL doxycycline for 24 hours. Afterwards, the media was changed to 10 ng/mL of doxycycline and the colonies were left to grow for 10 days. A. Western blot evaluating the exogenous (top band) and endogenous (bottom band) JMJD5 expression in control and JMJD5 knockdown 3 days post-transfection in A549 cells with β-Actin used as loading control. N=1 B. Endogenous JMJD5 knockdown causes increased cell sensitivity to Ceralasertib in A549 cells. C. Evaluation of the effect of exogenous overexpression of FLAG-JMJD5 WT or H321A on sensitivity to Ceralasertib. D. The effect of re-expression of EV or FLAG-JMJD5 WT/H321A on the sensitivity to Ceralasertib in JMJD5 knockdown A549 cells. Data represent mean ± SEM from one independent experiment with quadruplicate technical repeats.

3.2.17.4 Evaluation of drug sensitivity reconstitution in stable A549 cells with transient JMJD5 knockdown using colony formation assay in the absence of doxycycline

As we were aware that our doxycycline-inducible system is 'leaky' (Figure 2.9), which results in JMJD5 expression in the absence of doxycycline, we next wanted to evaluate drug sensitivity reconstitution in that context. We determined the expression of endogenous and exogenous JMJD5 by Western blot 3 days after transfection (Figure 3.27A). Interestingly, even in the absence of doxycycline, JMJD5 knockdown cells still exhibit higher exogenous JMJD5 expression when compared to the control cells.

We confirmed that endogenous JMJD5 knockdown leads to an increase in sensitivity to ATR inhibitor Ceralasertib under these conditions (Figure 3.27B). However, we still observed an impact of exogenous WT JMJD5 expression alone on sensitivity (Figure 3.27C). Furthermore, there was no difference between the sensitivity of siJMJD5 cells expressing either WT or H321A JMJD5 and siJMJD5 cells expressing EV. Therefore, we again concluded that successful reconstitution was not achieved (Figure 3.25D).

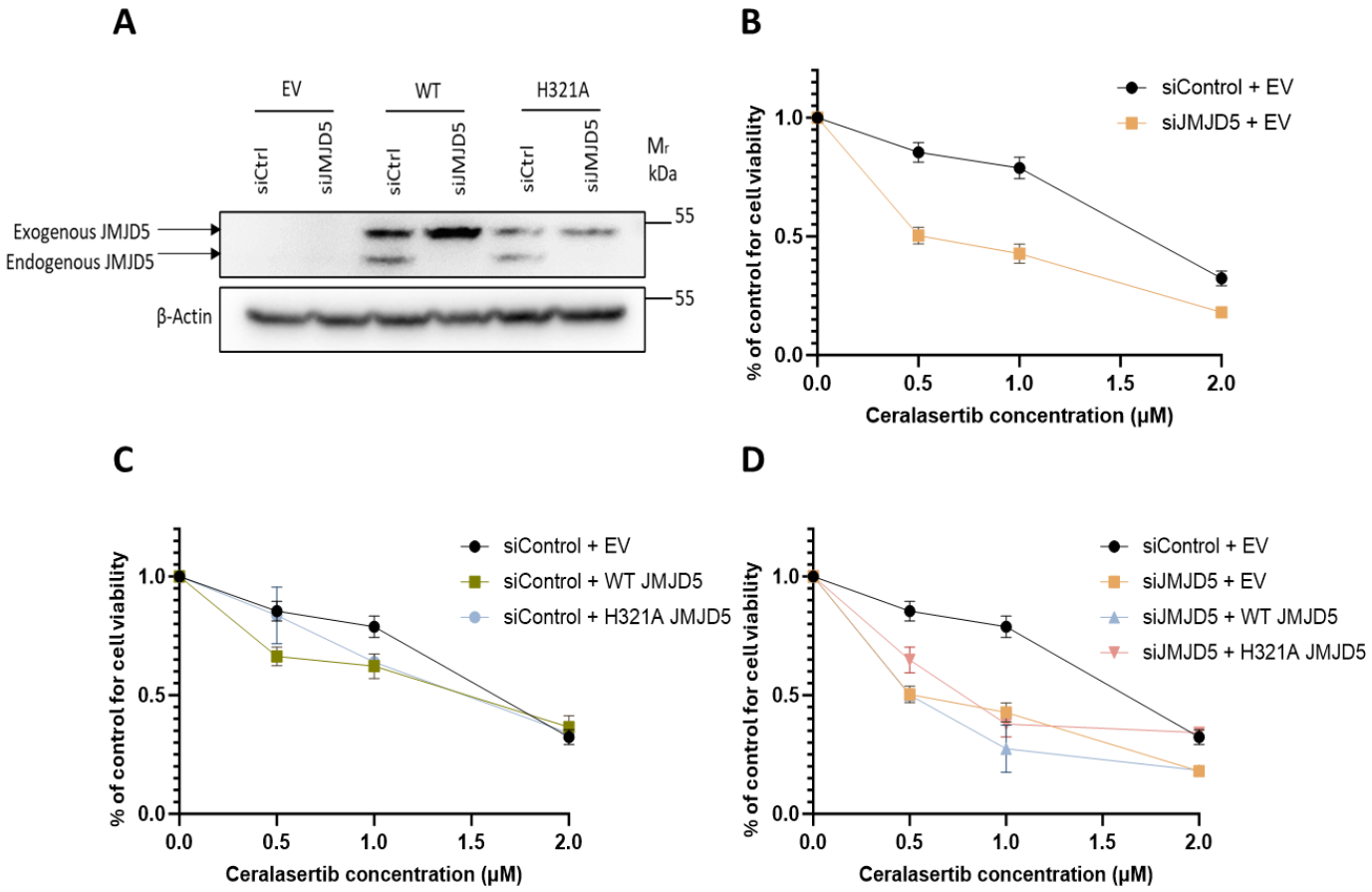

Figure 3.27 Characterisation of sensitivity to ATR inhibitor Ceralasertib following exogenous expression of FLAG-JMJD5 in endogenous JMJD5 knockdown in A549 cell model in the absence of doxycycline.

The A549 cells were transfected with siRNA targeting JMJD5 for 72 hours and treated with indicated doses of ATR inhibitor for 24 hours. Afterwards, the media was changed and the colonies were left to grow for 10 days. A. Western blot evaluating the exogenous (top band) and endogenous (bottom band) JMJD5 expression in control and JMJD5 knockdown 3 days post-transfection in A549 cells with β-Actin used as loading control. N=1 B. Endogenous JMJD5 knockdown causes increased cell sensitivity to Ceralasertib in A549 cells. C. Evaluation of the effect of exogenous overexpression of FLAG-JMJD5 WT or H321A on sensitivity to Ceralasertib. D. The effect of re-expression of EV or FLAG-JMJD5 WT/H321A on the sensitivity to Ceralasertib in JMJD5 knockdown A549 cells. Data represent mean ± SEM from one independent experiment with quadruplicate technical repeats.

Overall, in all the models and conditions tested, we were not able to successfully reconstitute JMJD5 function in JMJD5 knockdown cells to prevent the sensitisation to sensitivity to DDR inhibitors. Unfortunately, therefore, we were unable to determine whether the sensitisation phenotype was dependent on JMJD5 hydroxylase activity.

3.2.17.5 JMJD5 knockdown leads to decreased RCCD1 expression which is not rescued by exogenous FLAG-JMJD5 expression

Thus far, our reconstitution experiments had all been focused on successful re-expression of JMJD5, but the effect on other components of the pathway was not tested. Work by Dr Tristan Kennedy within the Coleman group has focused on exploring the interaction of JMJD5 with RCCD1 (introduced in Chapter 1 section 1.2). Dr Kennedy has discovered that RCCD1, and its interaction with JMJD5, is critical for the role of JMJD5 in replication fidelity and genome stability. Furthermore, Dr Kennedy has shown that JMJD5 and RCCD1 depend on each other for their normal expression. Therefore, we next considered the possibility that RCCD1 expression might be altered in our reconstitution experiments. Interestingly, we reproducibly observe that endogenous JMJD5 knockdown in our A549 model leads to a noticeable reduction in RCCD1 expression levels (Figure 3.28). Importantly, the exogenous re-expression of 3xFLAG-JMJD5 is not able to rescue the RCCD1 expression to physiological levels (Figure 3.28). Considering the recently discovered importance of RCCD1 for JMJD5 function, this may be a potential explanation for the lack of drug sensitivity rescue in our models. Unfortunately, due to time constraints, we were unable to explore this further.

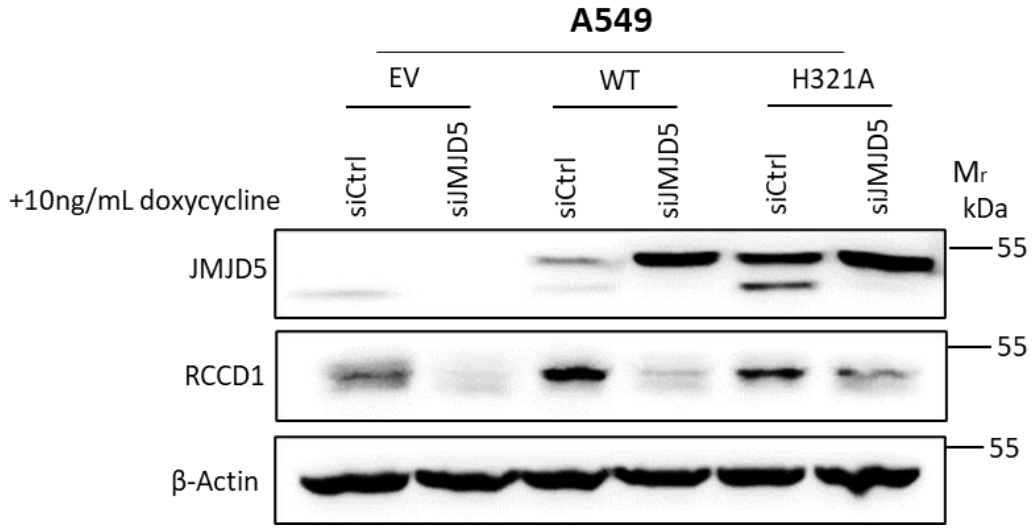

Figure 3.28 Representative Western blot of A549 pTIPZ 3XFLAG-JMJD5 reconstitution system.

A549 cells were treated with the indicated amount of doxycycline (ng/mL) for 7 days. Cells were then transfected with the indicated siRNA for 72 hours before being harvested. Samples were then Western blotted for JMJD5, RCCD1 and β-Actin as loading control. N=3

3.3 Discussion

In this chapter, we evaluated the cellular phenotypes associated with JMJD5 loss in combination with DNA-damaging agents. Using different JMJD5 knockdown models in different cancer cell lines, we showed that the loss of JMJD5 can sensitise cancer cells to DNA-damaging agents, although the downstream consequences may vary between different cancer cell types. We also evaluated the importance of JMJD5 enzymatic activity in the observed sensitivity phenotypes. Overall, these findings are consistent with the role of JMJD5 in DDR and suggest its potential as a therapeutic target for cancer.

3.3.1 JMD5 loss sensitises both A549 and U2OS cells to ATM inhibitors

In line with what was observed in a CRISPR screen where JMJD5 was identified to have a possible lethal interaction with ATM inhibition (Dr Nicholas Davies and Professor Tanja Stankovic, personal communication), our results showed that JMJD5 siRNA knockdown significantly increased the sensitivity of A549 cells to ATM inhibitor (Figure 3.3A). Consistent with these results, our cell viability assays in JMJD5 shRNA knockdown models also led to

increased sensitivity of A549 and U2OS cells to ATM inhibitor (Figures 3.18). The increased sensitivity to ATM inhibitor suggests that JMJD5 may play a role in the DDR, consistent with previous reports (Chapter 1, section 1.2.2). However, the underlying mechanisms remain unclear. One possibility is that JMJD5 may act in parallel or downstream of ATM signalling to help repair DNA damage or sustain cell survival under RS conditions. Further studies are needed to determine the nature of this sensitivity, including monitoring of the type of DNA damage by performing comet assays, which can determine the presence of SSBs and DSBs.

To further characterise the increased sensitivity phenotype, we investigated RS markers. We found that JMJD5 knockdown in A549 cells significantly increased micronuclei after treatment with an ATM inhibitor (Figure 3.4B), which indicates chromosomal instability and the presence of unresolved DNA damage. Unlike A549 cells, the treatment of U2OS cells with an ATM inhibitor did not cause an additional increase in the number of micronuclei (Figure 3.7B). Although the reason for this difference is not yet clear, it could be related to the high basal levels of micronuclei in U2OS cells (Figure 3.7B), or differences in ATM function between the two cell types.

We also investigated the effect of JMJD5 knockdown in combination with kinase inhibitors on cell cycle and apoptosis. Interestingly, Huang et al. reported that the downregulation of JMJD5 causes cell cycle arrest in the G2/M phase in A549 cells. Our data did not show any effect of JMJD5 loss on the G2/M phase of the cell cycle. However, we observed a modest decrease in G1 phase cells and an increase in S phase cells. The differential phenotypes observed after JMJD5 knockdown in our model when compared to Huang et al. may be due to the use of different siRNA sequences targeting JMJD5, as well as the possibility that cells have accumulated different mutations due to the age of the cells. In addition, despite increased RS and sensitivity to ATM inhibition, the cell cycle profiles of JMJD5 knockdown A549 cells treated with the ATM inhibitor were similar to those of inhibitor-treated control cells (Figures

3.5A). Overall, the lack of significant cell cycle changes in response to JMJD5 knockdown might indicate that A549 cells proceed through the cell cycle under these conditions, despite the presence of DNA damage, possibly leading to an increase in mitotic errors.

The Annexin V assay also indicated no significant difference in apoptosis between JMJD5 knockdown and control A549 cells treated with or without ATM inhibitor (Figure 3.5B). Whether JMJD5 knockdown and inhibitor-treated A549 cells might experience other forms of cell death, such as senescence or mitotic catastrophe, which are not captured by the Annexin V/7AAD assay, is not clear. Further investigation is required to determine whether the cells are undergoing any of these processes. For example, in the future, senescence could be investigated using assays such as the senescence-associated β-galactosidase (SA-β-Gal) staining assay. Indeed, JMJD5 was shown to mediate histone H3 N-tail proteolytic cleavage, which is associated with senescence (Shen et al., 2017).

We observed slightly different results in U2OS cells, where JMJD5 knockdown combined with ATM inhibition significantly decreased the G1 population without significantly altering the S or G2/M phases (Figures 3.8A). The reduction in G1 cells was associated with a significant increase in the sub-G1 peak (Figures 3.8B), which is indicative of reduced DNA content, likely due to DNA fragmentation, a hallmark of apoptosis (Peitsch, Muller and Tschopp, 1993). This indicates that DDR inhibitors induce cell death in U2OS cells which is exacerbated by JMJD5 loss.

The differential response between A549 and U2OS cells implies that the role of JMJD5 and phenotypes associated with its loss may be context-dependent and influenced by the specific genetic or epigenetic landscape of each cell line. For example, A549 cells have a point mutation in the KRAS gene (G12S) which leads to constitutive activation of AKT (Young-Kwon et al., 2010), which can promote cell cycle progression and proliferation, and inhibit apoptosis (He et al., 2021). Such differences could have contributed to the observed differential responses.

3.3.2 JMD5 loss sensitises both A549 and U2OS cells to ATR inhibitors

We also demonstrated that JMJD5 knockdown in both siRNA and shRNA models significantly increased the sensitivity of both cell lines to the ATR inhibitor Ceralasertib (Figures 3.3B, 3.19). Our results are in line with those observed in a CRISPR screen conducted by Olivieri et al., who also reported that JMJD5 loss confers sensitivity to the same ATR inhibitor. Our subsequent RS analysis showed that treatment with ATR inhibitor significantly increased the number of micronuclei in both cancer cell lines (Figures 3.4 and 3.7), as expected. Furthermore, treatment with the ATR inhibitor led to a statistically significant increase in the number of 53BP1 bodies in JMJD5 knockdown A549 cells (Figure 3.4D).

Since ATR normally plays a role in stabilising replication forks, the ability of cells to manage RS is compromised upon ATR inhibition (Yano and Shiotani, 2023). The fact that JMJD5 loss exacerbates RS in ATR inhibitor-treated cells may therefore suggest that JMJD5 is crucial for the RS response, possibly by playing a role in the stability of replication forks (also discussed further in 3.3.4). Further research should investigate the effect of JMJD5 loss on replication fork dynamics, particularly under RS conditions, including those induced by DDR inhibitors. To do so, techniques such as the DNA fibre assay can be used.

Similar to our results for the ATM inhibitor, cell cycle profiles and apoptosis assay results were markedly different in A549 and U2OS cells treated with the ATR inhibitor. JMJD5 knockdown in A549 cells did not affect cell cycle progression or apoptosis when compared to the control cells (Figures 3.6A, B). In contrast, in U2OS cells JMJD5 knockdown combined with ATR inhibition significantly affected the cell cycle (Figure 3.9A) and cell death (Figure 3.9B). As mentioned above, these differences are likely due to the different genetic landscapes of these cell lines.

3.3.3 JMJD5 loss confers sensitivity to PARP inhibitor

Our data indicated that JMJD5 loss sensitised A549 and U2OS cells to the PARP inhibitor Talazoparib with both knockdown approaches (Figures 3.3C and 3.20A, B). This is consistent with the results of the CRISPR screening conducted by Zimmermann et al., indicating that JMJD5 loss may have a synthetic lethal interaction with PARP inhibition.

This suggests that PARP inhibitors, similar to ATM and ATR inhibitors, may be therapeutically useful in cancers with altered JMJD5 pathway function. Furthermore, our data suggest that the combination of PARP and JMJD5 inhibition may be a novel therapeutic strategy. PARP inhibitors are currently approved for BRCA-mutated breast, ovarian, prostate, and pancreatic cancer (Zheng et al., 2020). Ongoing studies are investigating the use of PARP inhibitors in endometrial (Musacchio et al., 2020) and lung (Olivares-Hernandez et al., 2023) cancers, particularly in combination with other therapies. Most current combination strategies with PARP inhibitors involve chemotherapeutic agents and other DDR inhibitors, such as ATM and ATR inhibitors, as well as inhibitors of Chk1 and Chk2 kinases, DNA protein kinase, and WEE1 (Bhamidipati et al., 2023). Since, to our knowledge, the combination of inhibitors that target PARP with those that target 2OG oxygenases has not yet been evaluated, our findings represent an exciting new avenue for future studies.

The molecular basis of the synergies described remains unclear. However, our analyses of the RS response showed a significant increase in both RS markers (Figure 3.10A, B), in JMJD5 knockdown cells treated with Talazoparib. This suggests that JMJD5 may play a role in resolving RS that accumulates when PARP is inhibited, possibly by facilitating the restart of stalled replication forks or by aiding in the repair of collapsed forks. PARP inhibitors trap PARP on DNA, forming a physical obstruction on the DNA strand and blocking the replication machinery, leading to replication fork stalling (Liao et al., 2018). Stalled forks can undergo fork reversal, a protective process where the fork structure regresses and forms a four-stranded DNA

structure in an attempt to provide time for repair mechanisms to resolve the damage (Liao et al., 2018). If a stalled replication fork cannot be repaired, it may collapse and generate DSBs. Interestingly, we found that JMJD5 knockdown cells treated with the PARP inhibitor had a significant increase in phosphorylated Chk2 (Figures 3.10C), which is activated in response to DSBs by ATM (discussed in section 3.1.2). This suggests that the combination of JMJD5 knockdown and PARP inhibition may lead to significant DNA damage in the form of DSBs (consistent with the marked increase in yH2AX expression) as a result of collapsed forks, which activate ATM and subsequently Chk2 in the process of HR. Indeed, JMJD5 has been implicated in HR (Amendola et al., 2017). Moreover, Chk2 phosphorylation is a signal that stops cell cycle progression and activates DDR pathways or induces apoptosis. Interestingly, in A549 cells, this correlated with the observed cell cycle arrest (increased G2-M population) (Figure 3.11A) and apoptosis (increased sub-G1 population and decreased live cells) (Figure 3.11B). In addition, our data showed that JMJD5 knockdown in A549 cells treated with a PARP inhibitor led to a significant increase in p53 protein levels (Figure 3.10C) which can also indicate cell cycle arrest and apoptosis. This correlates with our findings, showing a significant decrease in live cells and an increase in dead cells upon JMJD5 knockdown and PARP inhibitor treatment.

In U2OS cells, JMJD5 knockdown in combination with a PARP inhibitor significantly increased the number of micronuclei (Figure 3.12A) which is consistent with the phenotypes observed in A549 cells. However, we did not observe an increase in 53BP1 bodies (Figure 3.12B) which suggests differences in DDR pathways or the presence of compensatory mechanisms in different cancer types. Indeed, cell response to DNA damage is a complex process that varies in different cancer types (Wang, Hen and Ao, 2021)

Moreover, in contrast to our A549 results, U2OS cells did not show a significant difference in p53 expression, cell cycle progression, or apoptosis following JMJD5 knockdown or PARP inhibitor treatment. Instead, these cells exhibited a significant increase in RAD51 expression

(Figure 3.12C and Figure 3.13A, C), both with and without PARP inhibitor treatment. As RAD51 is a key protein involved in HR, the upregulation of RAD51 in U2OS cells might suggest that the loss of JMJD5 in these cells activates HR to repair the DNA damage induced by PARP inhibition. Indeed, the activation of ATM/ATR pathways in response to DNA damage can lead to the induction of RAD51 expression (Pauklin et al., 2005). In addition, increased RAD51 levels were shown to correlate with the induction of the DNA damage response (Pauklin et al., 2005).

Overall, the data in this chapter demonstrate that JMJD5 loss can sensitise cancer cells to PARP inhibitors which supports further investigation regarding combination therapy with JMJD5 and PARP inhibitors.

3.3.4 JMJD5 loss causes sensitivity to a wide range of anticancer agents

Since Olivieri et al. published a CRISPR screen indicating that JMJD5 knockdown can have both synergistic and resistance interactions with a variety of anticancer drugs (Figure 3.21), we further investigated the role of JMJD5 in modulating these responses. This would help us to understand whether combining these agents with JMJD5 inhibitors would be a feasible therapeutic strategy. Indeed, a number of preclinical studies have evaluated the effects of combining DDR inhibitors, such as PARP inhibitors, with other anticancer agents, such as trabectedin, and reported synergistic interactions in cancer cells (Ordonez et al., 2015; Laroche et al., 2017; Pignochino et al., 2017).

The results from Olivieri et al. suggest that JMJD5 loss can also confer sensitivity to Doxorubicin and MMS, which we investigated here and confirmed their findings (Figure 3.22A and B). In addition, Olivieri et al. reported that JMJD5 loss can lead to resistance to other compounds, such as Trabectedin and Calicheamicin. Interestingly, our data disagree with these findings, as we show that JMJD5 knockdown also leads to increased sensitivity to these drugs (Figure 3.22C, D). The difference in results may be due to various factors, including choice of

cells, loss-of-function approaches, and experimental set-up. For example, in the CRISPR screen conducted by Olivieri et al. immortalised human retinal pigment epithelial RPE-1 cells were used. As RPE-1 cells are non-cancerous they will have a different genetic and epigenetic profile from cancer cells, which could affect the cellular response to JMJD5 loss as well as drug treatments. Importantly, p53 was knocked out in the RPE-1 model used, which could also be a key factor contributing to the differential responses observed. The lack of p53 alters key regulatory pathways involved in the DNA damage response, apoptosis, and cell cycle regulation, which can significantly modify how cells respond to DNA-damaging agents. In particular, the cytotoxic effects of trabectedin (Bozkurt et al., 2013) have been shown to be dependent on p53; therefore, in p53-deficient cells the mechanism of drug action is likely to be compromised, leading to resistance. As both U2OS and A549 cells express WT p53, this may explain the different results. Nonetheless, the toxic effect of calicheamicin is independent of the p53 status (Prokop et al., 2003). Therefore, the differences in the responses may be attributed to differences in the loss-of-function models, doses, and duration of treatment. Olivieri et al. utilised the CRISP-Cas9 technique to generate gene knockouts, whereas we used shRNA-mediated gene knockdown; therefore, the degree of gene disruption was different. In addition, a complete gene knockout could lead to the activation of compensatory mechanisms, whereas an incomplete reduction of the protein level may not be sufficient to activate alternative pathways. Additionally, Olivieri et al used sublethal doses of each drug (0.075nM – 1nM for Trabectedin and 0.05nM – 0.5nM for Calicheamicin) for approximately 10 population doublings. In our experimental set up we used doses of 0.001nM – 0.1nM for Trabectedin and 0.01nM – 1nM for Calicheamicin, with treatment for only 5 days. The differences in the duration of drug treatments, especially prolonged exposures used by Olivieri et al., can affect cellular responses owing to the development of adaptive responses, chronic DDR activation,

and changes in gene expression. In the absence of p53, where apoptosis is not triggered in response to DNA damage, cells may have more opportunity to adapt and survive.

In the future, it would be interesting to investigate the effect of JMJD5 knockdown on driving sensitivity or resistance to other compounds reported in the CRISPR screen. Furthermore, it would be interesting to explore the potential lethality interactions observed through orthogonal approaches, such as JMJD5 inhibitors (discussed in Chapter 4) and ATM/ATR mutations. This is especially relevant as ATM mutations are present in a variety of tumours with the highest prevalence of around 40% in mantle cell lymphoma, ~ 18% in colorectal cancers and ~10% in lung and prostate cancers (Choi, Kipps and Kurzrock, 2016). Although mutations in ATR are much less prevalent, they are still reported in various tumour types, including breast and ovarian cancers. Cells with ATM or ATR mutations often exhibit an altered sensitivity to DDR inhibitors and anticancer agents. Therefore, investigating whether JMJD5 loss/inhibition alone leads to increased death in such cells is warranted. Moreover, it would be interesting to evaluate whether JMJD5 inhibition synergises with PARP or ATR inhibitors in ATM-deficient cancer cells, for example.

3.3.5 Is increased cancer cell sensitivity to DNA-damaging agents dependent on enzymatic activity?

In this chapter, we also investigated whether the observed sensitivities to different anticancer agents and DDR inhibitors were due to JMJD5 knockdown or the loss of its enzymatic activity.

Overall, we developed two different models for reconstitution experiments: a ‘transient’ expression system in U2OS cells (Figure 3.23) and a doxycycline-inducible model in A549 cells. However, owing to the number of limitations in both systems, successful reconstitution was not achieved (Figure 3.27D). During these studies, we observed that overexpression of JMJD5 was sufficient to sensitise to Talazoparib, which complicated the interpretation of the results (Figures 3.24D and 3.25D). If JMJD5 is involved in replication fork stability and/or HR,

its overexpression may lead to excessive DNA damage signalling which could potentiate the effects of DNA-damaging agents. Alternatively, its overexpression could titrate critical regulatory factors away from specific subcellular locations in which they function.

When troubleshooting the reconstitution experiments, we also explored the JMJD5 binding protein RCCD1 and showed that JMJD5 knockdown led to decreased RCCD1 expression (Figure 3.28). This is consistent with the work by Dr Tristan Kennedy within the Coleman group, who showed that the interaction of RCCD1 with JMJD5 is critical for the role of JMJD5 in replication fidelity and GS and that JMJD5 and RCCD1 depend on each other for their normal expression (Tristan Kennedy, personal communication). Therefore, the observation that exogenous re-expression of JMJD5 failed to rescue RCCD1 expression might explain the lack of drug sensitivity rescue observed in these models. This suggests that the drug sensitisation phenotypes observed here may be more complex and involve multiple components of the JMJD5 pathway.

One potential reason why exogenous re-expression of 3xFLAG-JMJD5 failed to rescue RCCD1 expression could be that the presence of the FLAG tag might have affected its interaction with RCCD1. In the future, co-immunoprecipitation experiments could be performed using different JMJD5 constructs (untagged, FLAG-tagged, and other tagged versions) to determine the correct conditions under which the JMJD5:RCCD1 interaction is maintained.

Another potential problem could be localisation issues caused by the FLAG tag which might affect the interaction with critical binding proteins. Involved in subcellular targeting. Although our IF images showed that 3xFLAG JMJD5 is present in the nucleus, its specific subnuclear localisation may differ from that of endogenous JMJD5. Future reconstitution experiments could address these issues by testing the function of untagged JMJD5.

3.3.6 Chapter conclusions

The increased sensitivity of JMJD5 knockdown cells to various DDR inhibitors and anticancer agents highlights the potential therapeutic value of targeting JMJD5. This suggests that JMJD5 inhibition could be a strategy to enhance the efficacy of existing treatments. Therefore, the development of specific JMJD5 inhibitors and exploration of their combination with other anticancer agents is of interest, which we explore in the next chapter.

Chapter 4: The effect of JMJD5 inhibitors on cancer cells

4.1 Introduction

In the preceding chapter, we showed that the knockdown of JMJD5 sensitises cancer cells to a variety of anticancer drugs. Therefore, JMJD5 has potential as a therapeutic target and the development of JMJD5 inhibitors is warranted.

4.1.1 Competitive inhibitors of 2OG-oxygenases

Due to the proposed role of 2OG-oxygenases in a wide range of cellular processes, such as epigenetic regulation, hypoxic responses, and diseases, including cancer, there is increasing interest in targeting this class of enzymes. This appears feasible because they have a relatively accessible and chemically distinct active site, which allows for the design of competitive inhibitors that mimic their cofactor, 2OG (Rose et al., 2011).

Competitive inhibitors of prolyl hydroxylase enzymes have been developed and are currently being evaluated in clinical trials, including FG-4592 (Roxadustat) (Provenzano et al., 2016), pan-hydroxylase inhibitor dimethyloxalylglycine (DMOG), AKB-6548 (Vadadustat) (Pergola et al., 2016), and BAY 85-3934 (Molidustat) (Beck et al., 2018). Roxadustat has recently been approved for the treatment of anaemia associated with chronic kidney disease (Barratt et al., 2021). Several other compounds have shown promising anticancer effects in preclinical studies. For example, GSK-J1 and its cell-permeable derivative GSK-J4 target JMJD3/UTX demethylases and have been shown to reduce the proliferation of leukaemia (Chu et al., 2020), glioblastoma (Sui et al., 2017), and breast cancer (Yan et al., 2017) cells by modulating gene expression and inducing apoptosis. In addition, TACH101 is a potent small-molecule inhibitor of KDM4 that showed potent anticancer activity in various cancer cell lines and organoid models, as well as inhibiting tumour growth *in vivo* (Chandhasin et al., 2023).

4.1.2 Inhibitors of JmjC-only family for cancer

Recently, there has been growing interest in developing inhibitors of the JmjC-only family. Inhibitors targeting several members of this family are currently in the early stages of development and are showing promise as potential anticancer agents. For example, first-in-class inhibitors targeting RIOX2 (MINA53) have been shown to engage with this enzyme in tumour cell lines and to enhance their sensitivity to conventional chemotherapy (Nowak et al., 2021). The overexpression of JMJD6 in multiple cancer types and its association with poor patient prognosis has also rationalised the development of inhibitors (Yang et al., 2020). JMJD6 inhibitors suppress cancer cell growth, induce apoptosis, and sensitise renal cell carcinoma cells to the anticancer agent sunitinib (Ran et al., 2019; Xiao et al., 2022; Zheng et al., 2022). These examples highlight the feasibility of targeting JmjC-only hydroxylases and the potential for developing inhibitors of closely related enzymes such as JMJD5.

4.1.3 JMJD5 as a target

The results presented earlier in this thesis suggest that JMJD5 knockdown sensitises different cancer cell lines to clinically available anticancer drugs, such as PARP, ATM, and ATR inhibitors. Collectively, these findings indicate that JMJD5 may be a potential new therapeutic target and the development and use of JMJD5 inhibitors are warranted. Recently, first-in-class small-molecule inhibitors of JMJD5 were developed by the Schofield group at Oxford University and characterised *in vitro*. However, the effect of these inhibitors on tumour cells was not known.

Therefore, one of the key aims of this project and our collaboration with the Schofield group was to evaluate the effect of JMJD5 inhibitors on cancer cells, both in isolation and in combination with established therapeutics and evaluate their potential as anticancer agents.

4.1.4 First-in-class small molecule JMJD5 inhibitors

The Schofield group developed small molecule JMJD5 inhibitors based on pyridine-2,4-dicarboxylic acid (2,4-PDCA), which mimics 2OG and, as such, is a broad-spectrum inhibitor of 2OG oxygenases. By screening an in-house library of 2,4-PDCA analogues using a mass spectrometry (MS) based approach they identified 5-aminoalkyl-substituted derivatives as novel JMJD5 inhibitors (Figure 4.1A-B). Figure 4.1C shows the binding of one of the 2, 4-PDCA derivatives to the JMJD5 active site.

A

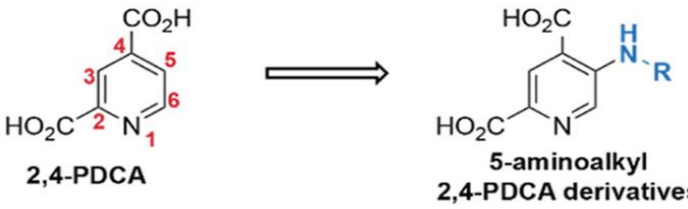

B

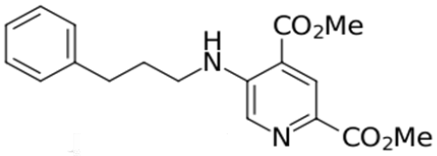

Inhibitor 88

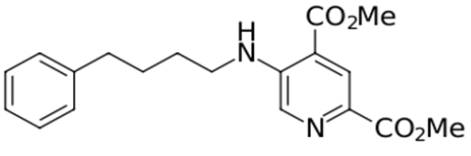

Inhibitor 90

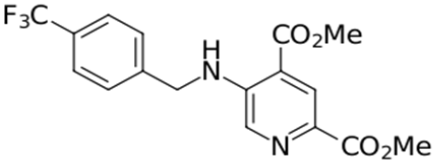

Inhibitor 92

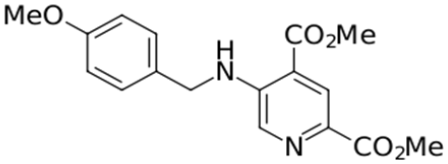

Inhibitor 93

C

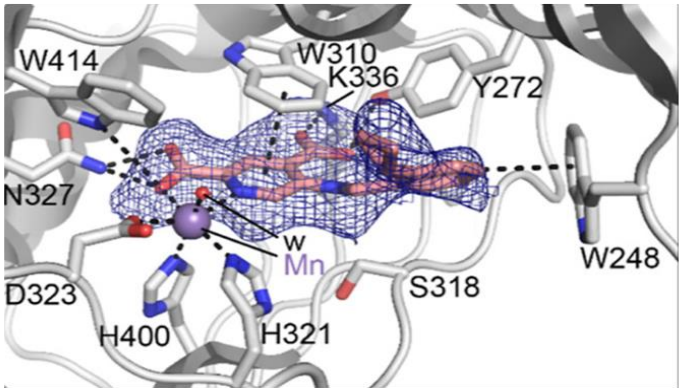

D

Inhibitor	IC50 JMJD5 (μM)	IC50 PHD2 (μM)	IC50 FIH (μM)	IC50 AspH (μM)	IC50 KDM4A (μM)	IC50 RIOX2 (μM)
Inhibitor 88	0.3 ± 0.1	>50	29.7 ± 6.2	2.8 ± 0.4	28.2 ± 4.1	27.3 ± 6.7
Inhibitor 90	0.4 ± 0.2	20.4 ± 0.8	25.6 ± 4.5	1.9 ± 0.2	3.6 ± 0.7	26.1 ± 1.9
Inhibitor 92	0.5 ± 0.1	>50	28.8 ± 6.4	1.2 ± 0.1	6.2 ± 1.1	27.5 ± 7.1
Inhibitor 93	0.4 ± 0.1	>50	31.7 ± 3.0	2.0 ± 0.4	15.5 ± 1.9	27.6 ± 7.1

Figure 4.1 First-in-class inhibitors of JMJD5.

A. Chemical structures of 2,4-PDCA- and 5-aminoalkyl-substituted derivatives. B. Chemical structures of JMJD5 inhibitors 88-93.C. Binding of the 5-Aminoalkyl-substituted 2,4-PDCA derivative to the JMJD5 active site (grey: JMJD5) (pink: carbon backbone of the JMJD5 inhibitor). D. IC50 values of JMJD5 inhibitors for recombinant JMJD5 and selected 2OG oxygenases. Adapted from Brewitz et al. 2023.

The Schofield group initially provided four inhibitors named 88, 90, 92, and 93 for testing in our cellular models (Figure 4.1B). The Schofield group had previously characterised the inhibitory activity of the compounds against recombinant JMJD5 and a variety of other 2OG oxygenases including PHD2, FIH, aspartate/asparagine–β-hydroxylase (AspH), KDM4A, and RIOX2, using solid-phase extraction mass spectrometry (SPE-MS) inhibition assays. The half-maximal *in vitro* inhibitory concentration (IC50) values for each compound are presented in Figure 4.1D.

Following the development of the initial set of JMJD5 inhibitors, two additional inhibitors (referred to as 37 and 38) were identified with increased selectivity towards JMJD5 *in vitro* (personal communication from Dr. Lennart Brewitz). Figure 4.2 presents the chemical structures of inhibitors 37 and 38 together with their IC50 values for recombinant JMJD5 and several other 2OG oxygenases (data provided by Dr Brewitz).

A

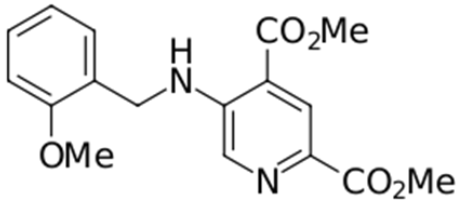

Inhibitor 37

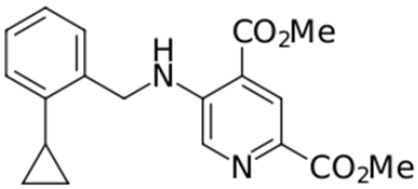

Inhibitor 38

B

Inhibitor	IC50 JMJD5 (μM)	IC50 PHD2 (μM)	IC50 FIH (μM)	IC50 AspH (μM)	IC50 KDM4A (μM)	IC50 RIOX2 (μM)
Inhibitor 37	0.7 ± 0.2	>50	36.3 ± 8.0	0.9 ± 0.2	11.3 ± 2.9	>50
Inhibitor 38	0.7 ± 0.1	>50	>50	8.9 ± 5.0	>50	>50

Figure 4.2 Chemical structures of the newer JMJD5 inhibitors 37 and 38 (A), together with their IC50 values for recombinant JMJD5 and selected 2OG oxygenase members (B).
Adapted from Brewitz et al., 2023

4.2 Results

4.2.1 JMJD5 inhibitors are toxic to cancer cell lines

Next, we tested the four JMJD5 inhibitors on a panel of cancer cell lines: A549, PC3-prostate cancer cells, and HeLa cervical carcinoma cells. Initially, we investigated their effects on cell proliferation using an MTS cell viability assay. The data indicated that all JMJD5 inhibitors decreased cell viability in A549 cells (Figure 4.3A) with half-maximum cytotoxicity concentration (CC50) values between 6.45μM and 30.74μM (Figure 4.3D). Preliminary assessment in PC3 and HeLa cells showed variable effects (Figure 4.3B, C). For example, only compound 90 affected the viability of HeLa cells, with a CC50 value of 38.086 μM. Accurate calculation of the CC50 values for the other inhibitors was impossible because of their low

potency. Overall, the effect of these JMJD5 inhibitors on cell viability depends on the particular inhibitor used and the cancer cell type.

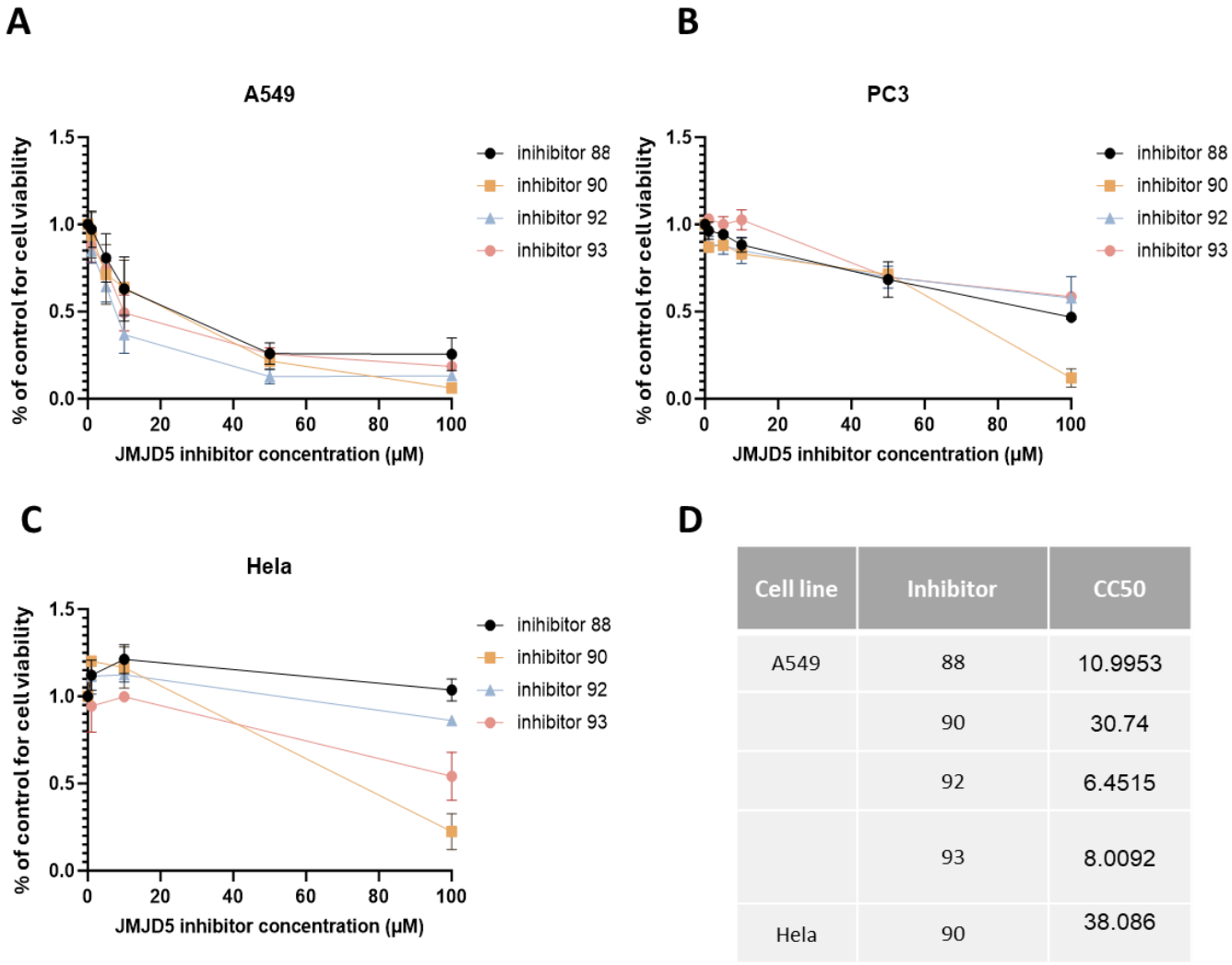

Cell line	Inhibitor	CC50
A549	88	10.9953
	90	30.74
	92	6.4515
	93	8.0092
Hela	90	38.086

Figure 4.3 JMJD5 inhibitors are toxic to cancer cell lines.
Cells were treated with the indicated JMJD5 inhibitors: 88, 90, 92 and 93 for 72 hours and cell viability was measured using the MTS cell viability assay. Effect of the four initial JMJD5 inhibitors on A. A549, B. PC3 and C. Hela cells. D. CC50 values for the JMJD5 inhibitors. The data represents the mean ± SEM of three independent replicates with quadruplicate technical repeats.

4.2.2 Inhibitors 37 and 38 are toxic to cancer cell lines.

We investigated the effect of 37 and 38 on cancer cell viability using MTS cell viability assays as above. Consistent with the previous inhibitors, we did not observe significant toxicity in HeLa cells (data not shown), possibly because they express only trace amounts of JMJD5 (Wang et al., 2013). Therefore, HeLa cells may not be a good model for studying JMJD5 inhibitors and were excluded from subsequent assays.

Treatment with inhibitor 37 had no effect on the viability of PC3 cells, whereas inhibitor 38 reduced viability at the highest doses tested (Figure 4.4A). Similarly, inhibitor 37 did not have a significant effect on the viability of U2OS cells, whereas inhibitor 38 caused significant toxicity, even at the lower doses tested (Figure 4.4B). In contrast, 37 and 38 markedly reduced the viability of A549 cells, with CC50 values of 10 μM and 2.41μM, respectively (Figure 4.4B, C).

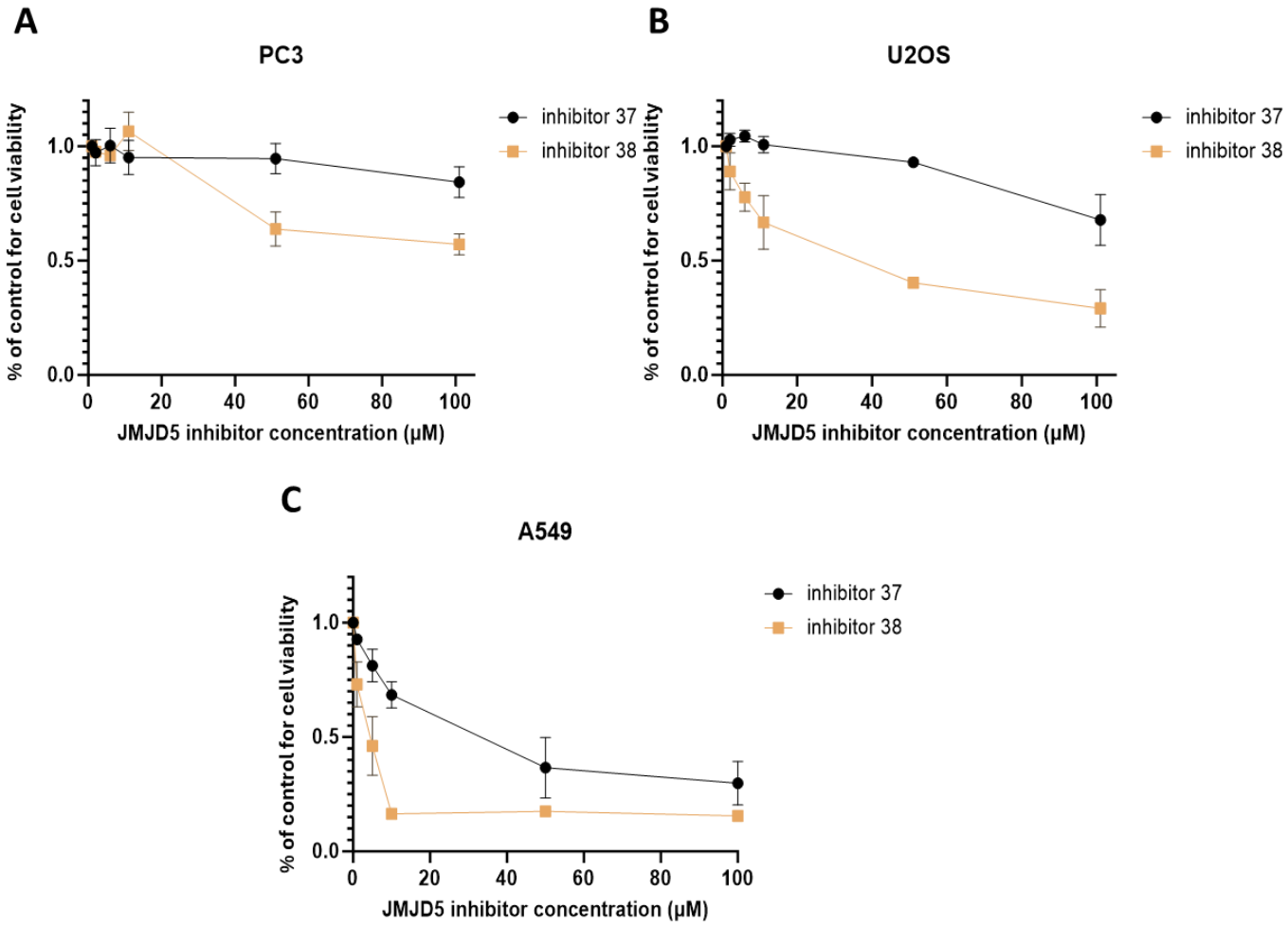

Figure 4.4 JMJD5 inhibitors 37 and 38 are toxic to cancer cell lines.

Cells were treated with the JMJD5 inhibitors 37 or 38 for 72 hours, and cell viability was measured using the MTS cell viability assay. Effects of JMJD5 inhibitors on A. A549, B. U2OS and C. PC3 cells. Data represent the mean ± SEM of three independent experiments with quadruplicate technical repeats.

To have an orthogonal approach to evaluate the effect of JMJD5 inhibitors on cell viability, we used the cyQUANT assay. This assay uses a fluorescent dye that binds to nucleic acids, which supports direct and highly sensitive measurement of cell number. As shown in Figure 4.5A, the cyQUANT assay results for A549 cells were similar to the MTS results (Figure 4.4A), with CC50 values of 10.04μM for 37 and 0.65 μM for 38. In addition, the cyQUANT profile for U2OS closely overlapped with the corresponding MTS assays (Figure 4.4B), with a CC50 value of 5.91μM for inhibitor 38 (Figure 4.5 B).

Overall, our data suggest that inhibitor 38 has a markedly more toxic effect on cancer cell viability than inhibitor 37.

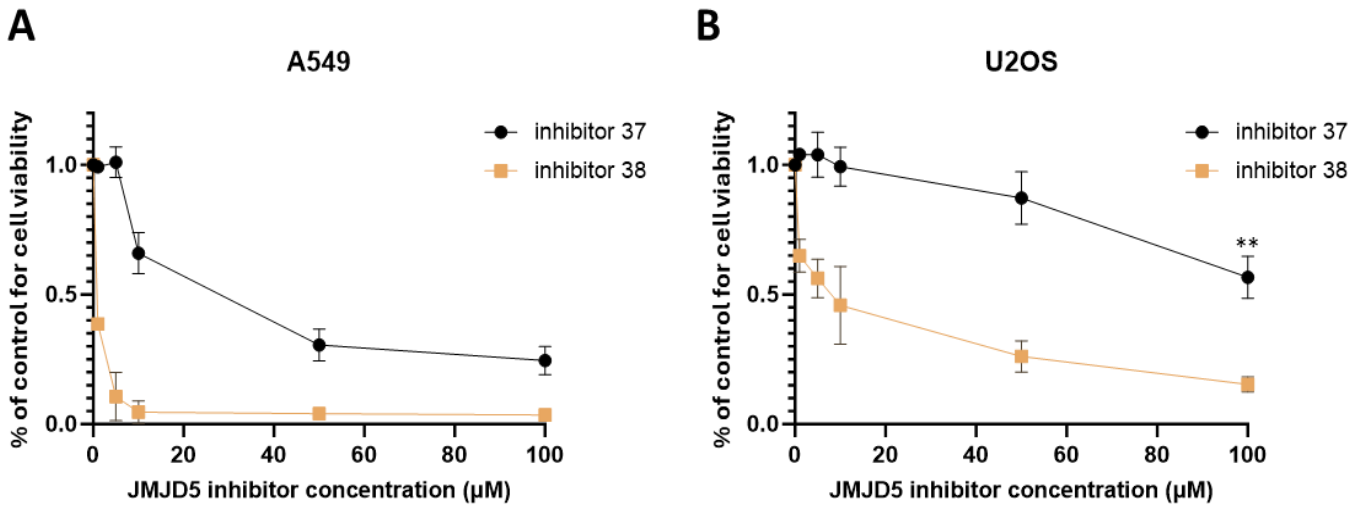

Figure 4.5 JMJD5 inhibitors 37 and 38 show toxicity in cancer cell lines.
Cells were treated with the indicated JMJD5 inhibitors 37 or 38 for 72 hours, and cell viability was measured using the cyQUANT viability assay. Effect of JMJD5 inhibitors on A549 (A) and U2OS cells (B). Data represent mean ± SEM from three independent replicates with quadruplicate technical repeats.

4.2.3 Treatment with JMJD5 inhibitors increases replication stress

In previous chapters, we demonstrated that loss of JMJD5 increases basal RS in A549 and U2OS cells (Figure 3.17). We also showed that this increase in RS is dependent on JMJD5 enzymatic activity (Figure 2.11). Therefore, we rationalised that JMJD5 inhibitors should also cause RS in these models. Consistent with the hypothesis, treating A549 and U2OS cells with either 1μM of inhibitor 37 or 38 for 24 h led to a significant increase in micronuclei (Figure 4.6A and 4.6B). Both JMJD5 inhibitors also caused a significant increase in the percentage of A549 cells with 53BP1 bodies (Figure 4.6C). Similar results were obtained in U2OS cells, although statistical significance was only achieved for inhibitor 38 (Figure 4.6D). Overall, these results indicate that JMJD5 inhibitors cause RS.

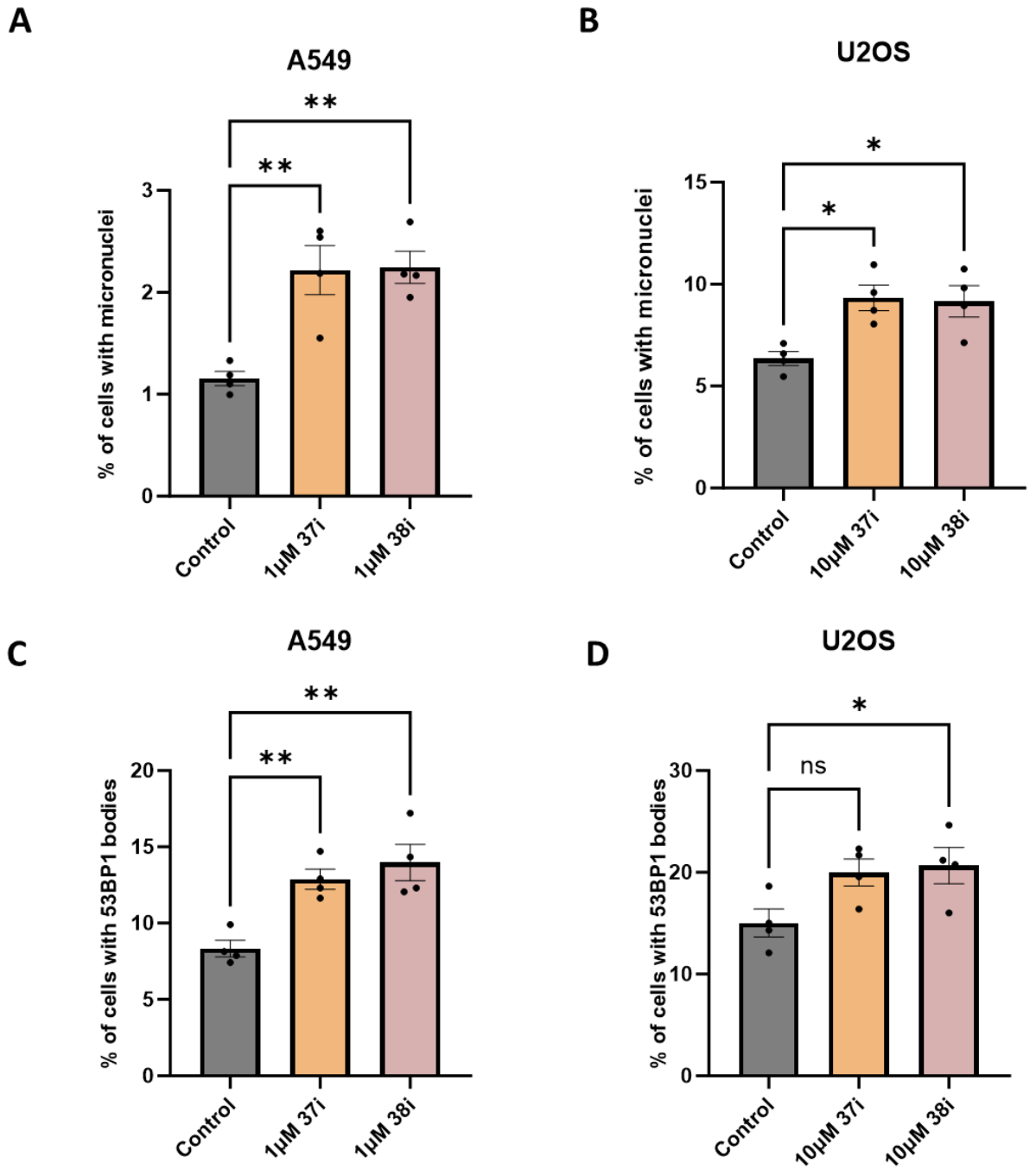

Figure 4.6 Treatment with JMJD5 inhibitors increases replication stress (micronuclei and 53BP1 bodies) in A549 and U2OS cells.

Cells were treated with 1μM of either inhibitor 37 or inhibitor 38 for 24 hours which resulted in increased formation of micronuclei as well as increased 53BP1 bodies in A549 (A. and C.) and U2OS (B. and D.). Data represent mean ± SEM from four independent replicates. Statistical analysis was performed using the one-way ANOVA with Tukey's post hoc test where (p-value ≤ 0.05=, ≤0.01 =**, ≤0.001=***).*

4.2.4 JMJD5 inhibitors lead to cell cycle perturbations in cancer cell lines

Previously we characterised the effect of JMJD5 knockdown and drug treatments on cell cycle and apoptosis. Therefore, we next evaluated the effect of JMJD5 inhibitors on these phenotypes.

To this end, we treated cells with 1μM (A549) or 10μM (U2OS) inhibitor 37 or 38 for 24 hours. Subsequently, the cells were fixed and stained with PI, and cell cycle progression was measured using flow cytometry. Treatment of A549 cells with either inhibitor led to a statistically significant reduction in G1 phase cells when compared to the DMSO control (Figure 4.7A). Moreover, we observed a corresponding increase in S and G2/M phase cells. The number of sub-G1 phase cells also increased slightly, although this was not statistically significant. Similar phenotypes were observed in U2OS cells, as follows. Treatment with 37 and 38 caused a statistically significant reduction in G1 phase U2OS cells, together with an increase in S-phase cells (Figure 4.7B).

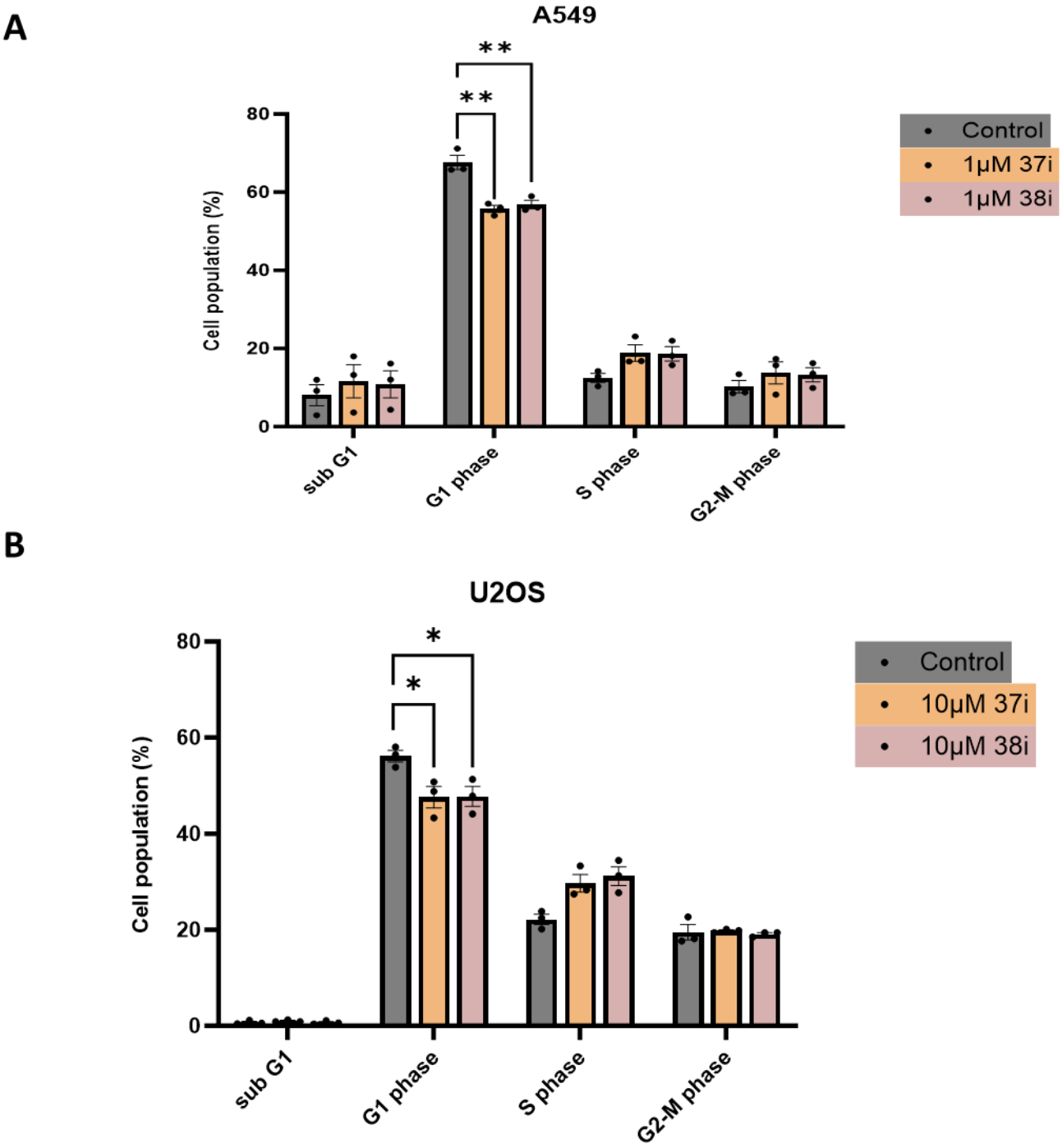

Figure 4.7 Cell cycle analysis of cancer cells treated with JMJD5 inhibitors.
A549 (A) and U2OS cells (B) were treated with 1μM or 10μM of either inhibitor 37 or 38 for 24 hours, collected and stained with PI for cell cycle analysis. Data are presented as the mean ± SEM of three independent experiments performed in triplicates. Statistical analyses used one-way ANOVA with Tukey's post hoc test [with p-value ≤ 0.05 (*)].

4.2.5 Apoptosis analysis in cancer cells treated with JMJD5 inhibitors.

In the previous section, we observed a slight increase in the sub-G1 population of A549 cells in response to JMJD5 inhibitors. Therefore, we next explored this further by analysing apoptosis using an Annexin V assay.

A549 and U2OS cells were treated with the indicated doses of JMJD5 inhibitors for 72 h, and the cells were stained with PE, Annexin V, and 7-AAD. Interestingly, treatment of A549 cells with 10 μM inhibitor 37 or 38 led to a statistically significant decrease in the live cell population compared to the DMSO control (Figure 4.8A), consistent with the cell cycle data. Moreover, both inhibitors increased the percentage of early apoptotic A549 cells, with a statistically significant increase observed with inhibitor 38. In contrast, neither JMJD5 inhibitor caused apoptosis in U2OS cells at the concentrations used (Figure 4.8B), which is consistent with the lack of sub G1 population in the cell cycle analyses.

Overall, the data indicates that JMJD5 inhibitors have cytostatic and -toxic effects in A549 cells, whereas in U2OS cells, they have a predominantly cytostatic effect.

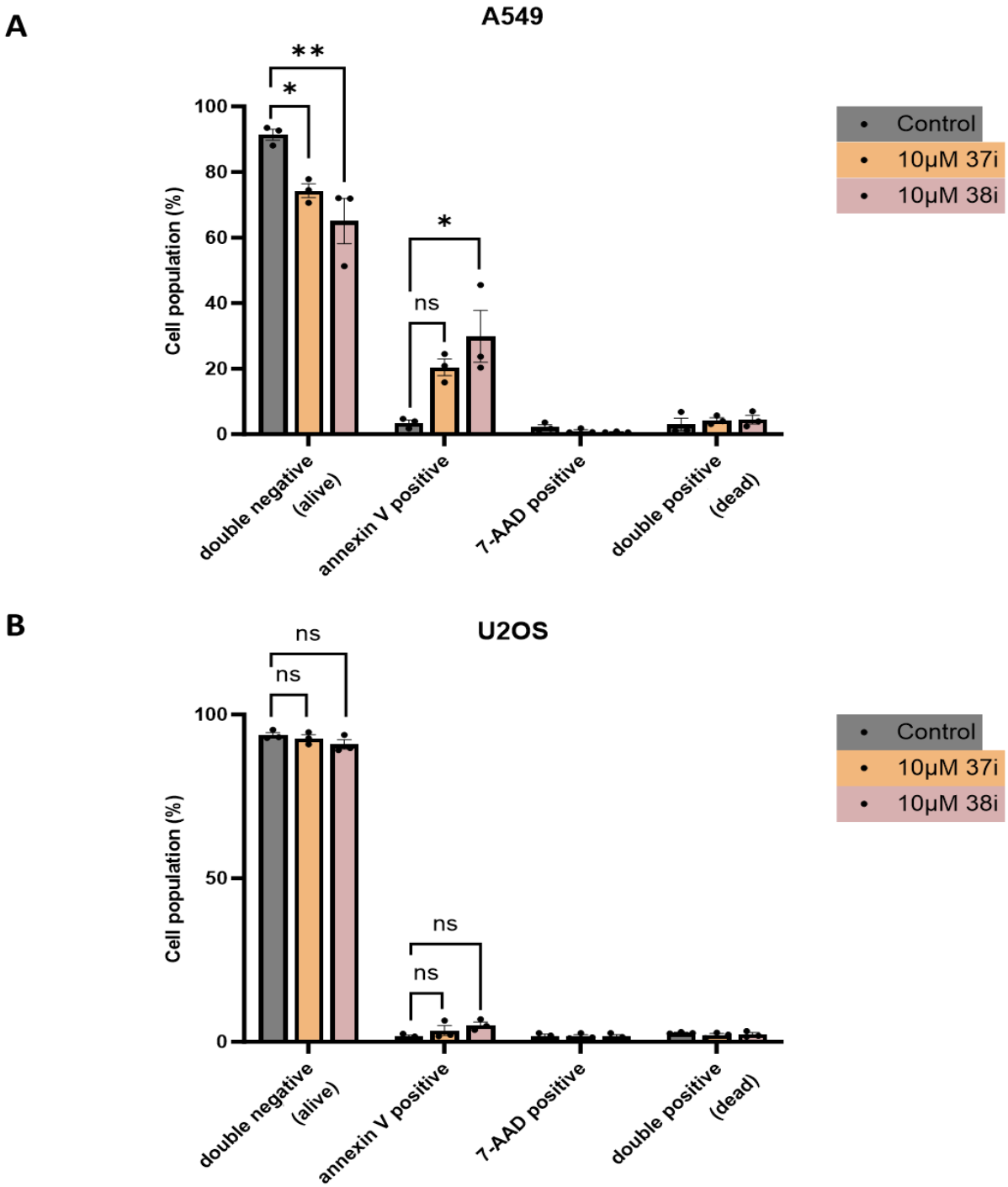

Figure 4.8 Analysis of apoptosis in A549 and U2OS cells treated with JMJD5 inhibitors.
A549 (A) and U2OS cells (B) were treated with 10μM of either inhibitor 37 or 38 for 72 hours. The cells were detached by trypsinisation, counted, and stained with PE Annexin V and 7AAD to measure apoptosis. Data presents mean ± SEM of results from three independent experiments performed in triplicate. Statistical analyses used one-way ANOVA with Tukey's post hoc test [with p-value ≤ 0.05 (*)].

4.2.6 The effect of JMJD5 inhibitors on cancer cell sensitivity to PARP, ATM and ATR inhibitors

In Chapter 3, we showed that JMJD5 knockdown sensitises cells to a variety of anticancer agents. Therefore, we next evaluated whether JMJD5 inhibitors behave in a similar manner. To this end, we treated A549 and U2OS cells with a fixed dose of JMJD5 inhibitor 37 or 38 together with a range of concentrations of doxorubicin or PARP, ATM, or ATR inhibitors for 72 hours. Our data suggest that 2 μM 37 did not increase the sensitivity of A549 cells to doxorubicin (Figure 4.9A, C). In contrast, 2 μM inhibitor 38 showed a trend towards increasing sensitivity, although this was not statistically significant. In U2OS cells, 10μM of inhibitor 38 did not increase sensitivity to doxorubicin at any of the concentrations tested (Figure 4.9B, D). However, treatment with 10μM 37 led to statistically significant sensitisation to 0.001μM doxorubicin.

A

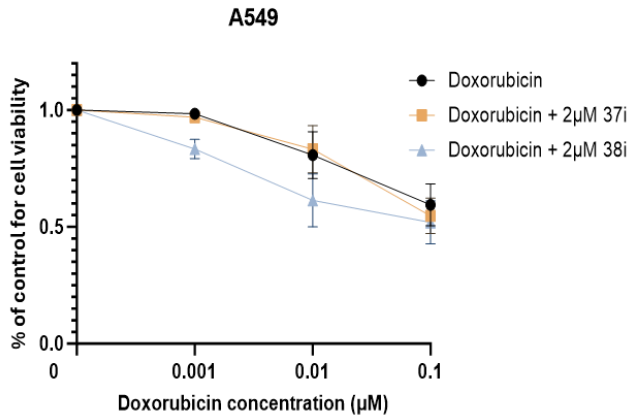

B

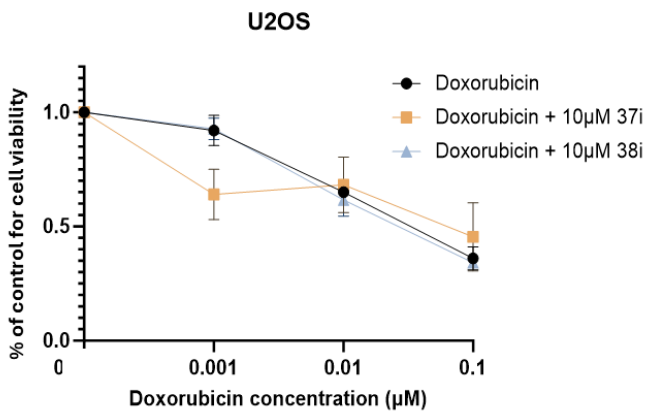

C

Comparison: Doxorubicin vs Doxorubicin +	Concentration	Adjusted P Value	Significance
2μM 37i	0.001μM	0.9822	ns
2μM 37i	0.01μM	0.9548	ns
2μM 37i	0.1μM	0.8521	ns
2μM 38i	0.001μM	0.2303	ns
2μM 38i	0.01μM	0.1042	ns
2μM 38i	0.1μM	0.6671	ns

D

Comparison: Doxorubicin vs Doxorubicin +	Concentration	Adjusted P Value	Significance
10μM 37i	0.001μM	0.0154	*
10μM 37i	0.01μM	0.9172	ns
10μM 37i	0.1μM	0.5023	ns
10μM 38i	0.001μM	0.9953	ns
10μM 38i	0.01μM	0.9071	ns
10μM 38i	0.1μM	0.9719	ns

Figure 4.9 Effect of JMJD5 inhibitors on A549 and U2OS cell sensitivity to Doxorubicin. *Cells were treated with either 2μM for A549 cells (panels A and C) or 10μM for U2OS cells (panels B and D) of JMJD5 inhibitor and a range of doxorubicin concentrations simultaneously for 72 hours and cell viability was measured by MTS assay. Data represent mean ± SEM from three independent replicates with quadruplicate technical repeats. Statistical analysis was performed using two-way ANOVA with Dunnett's multiple comparisons where (p-value ≤ 0.05=*, ≤0.01 =**, ≤0.001=***).*

We next investigated the effect of the JMJD5 inhibitors on the sensitivity to Talazoparib. Although 1μM 37 did not affect the sensitivity of A549 cells to this PARP inhibitor, 1μM 38 did significantly increase sensitivity to 0.1μM and 1μM Talazoparib (Figure 4.10A, C). However, combining 10μM of either 37 or 38 with Talazoparib did not increase the sensitivity of U2OS cells to any of the concentrations of Talazoparib tested (Figure 4.10B, D).

A

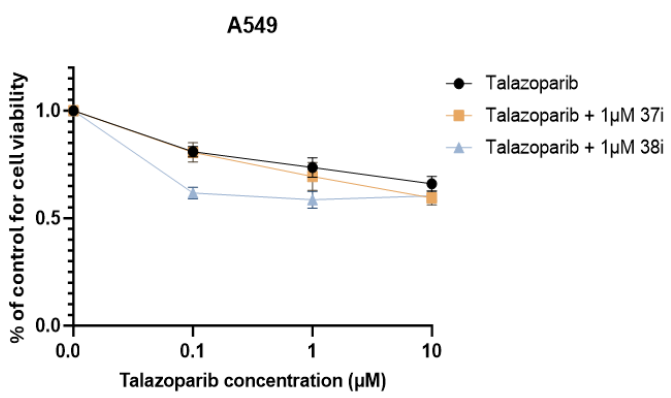

B

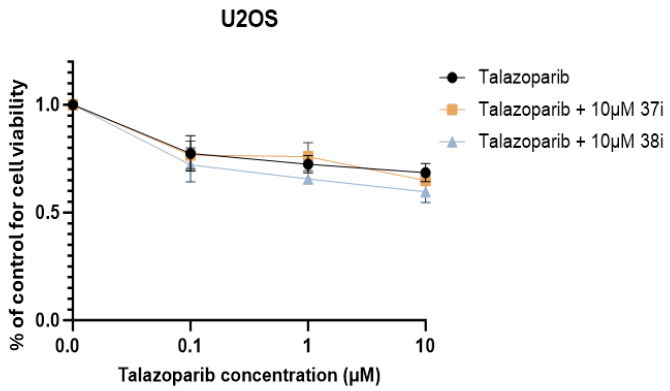

C

Comparison: Talazoparib vs Talazoparib +	Concentration	Adjusted P Value	Significance
1μM 37i	0.1μM	0.9976	ns
1μM 37i	1μM	0.586	ns
1μM 37i	10μM	0.2983	ns
1μM 38i	0.1μM	0.001	***
1μM 38i	1μM	0.008	**
1μM 38i	10μM	0.4051	ns

D

Comparison: Talazoparib vs Talazoparib +	Concentration	Adjusted P Value	Significance
10μM 37i	0.1μM	0.9936	ns
10μM 37i	1μM	0.8213	ns
10μM 37i	10μM	0.8112	ns
10μM 38i	0.1μM	0.6662	ns
10μM 38i	1μM	0.5112	ns
10μM 38i	10μM	0.3364	ns

Figure 4.10. Effect of JMJD5 inhibitors on A549 and U2OS cell sensitivity to the PARP inhibitor Talazoparib.

Cells were treated with either 1μM for A549 cells (panels A and C) or 10μM for U2OS cells (panels B and D) of JMJD5 inhibitor and a range of Talazoparib concentrations simultaneously for 72 hours and cell viability was measured by MTS assay. Data represent mean ± SEM from three independent replicates with quadruplicate technical repeats. Statistical analysis was performed using the two-way ANOVA with Dunnett's multiple comparisons where (p-value ≤ 0.05=, ≤0.01 =**, ≤0.001=***).*

Next, we investigated the effect on sensitivity to ATR inhibitors. Treatment with 1μM 37 did not affect sensitivity to ATR inhibitor in A549 cells (Figure 4.11A, C). Although inhibitor 38 may have had a subtle effect, the difference was not statistically significant. However, in U2OS cells 10μM 38 led to significantly increased sensitivity to 0.5μM and 1μM Ceralasertib (Figure 4.11B, D). In contrast, inhibitor 37 did not affect the sensitivity to Ceralasertib at any of the doses tested.

A

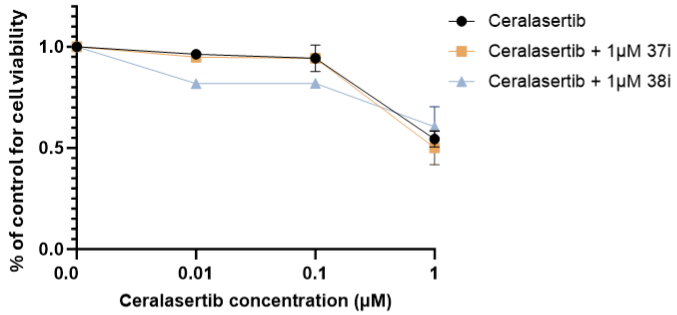

B

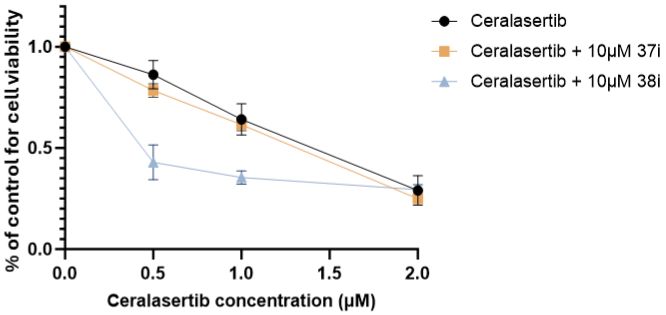

C

Comparison: Ceralasertib vs Ceralasertib +	Concentration	Adjusted P Value	Significance
1μM 37i	0.01μM	0.9621	ns
1μM 37i	0.1μM	>0.9999	ns
1μM 37i	1μM	0.7207	ns
1μM 38i	0.01μM	0.0549	ns
1μM 38i	0.1μM	0.1102	ns
1μM 38i	1μM	0.5365	ns

D

Comparison: Ceralasertib vs Ceralasertib +	Concentration	Adjusted P Value	Significance
10μM 37i	0.5μM	0.4197	ns
10μM 37i	1μM	0.9035	ns
10μM 37i	2μM	0.772	ns
10μM 38i	0.5μM	<0.0001	****
10μM 38i	1μM	0.0006	***
10μM 38i	2μM	0.9963	ns

Figure 4.11 Effect of JMJD5 inhibitors on A549 and U2OS cell sensitivity to the ATR inhibitor Ceralasertib.

Cells were treated with either 1μM for A549 cells (panels A and C) or 10μM for U2OS cells (panels B and D) of JMJD5 inhibitor and a range of ATR inhibitor concentrations simultaneously for 72 hours and cell viability was measured by MTS assay. Data represent mean ± SEM from three independent replicates with quadruplicate technical repeats. Statistical analysis was performed using the two-way ANOVA with Dunnett's multiple comparisons where (p-value ≤ 0.05=, ≤0.01 =**, ≤0.001=***).*

Finally, we investigated the effects of combining JMJD5 inhibitors with the ATM inhibitor AZD0156. Interestingly, treatment with 1μM 37 or 38 significantly increased A549 cell sensitivity to 0.01μM and 0.1μM AZD0156 (Figure 4.12A, C). Only treatment with inhibitor 38 increased sensitivity to AZD0156 in U2OS cells, (Figure 4.12B, D).

A

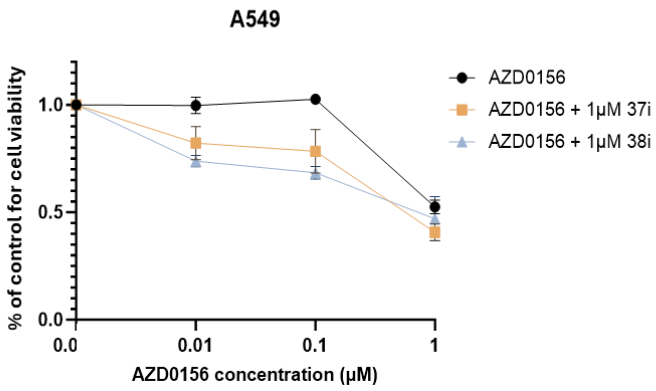

B

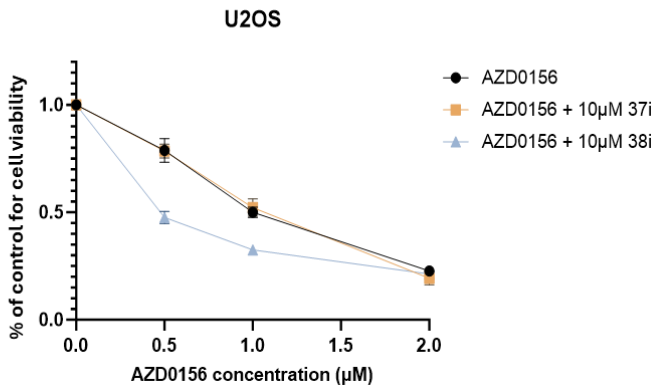

C

Comparison: AZD0156 vs AZD0156+	Concentration	Adjusted P Value	Significance
1μM 37i	0.01μM	0.0471	*
1μM 37i	0.1μM	0.0061	**
1μM 37i	1μM	0.2146	ns
1μM 38i	0.01μM	0.0035	**
1μM 38i	0.1μM	0.0002	***
1μM 38i	1μM	0.6791	ns

D

Comparison: AZD0156 vs AZD0156+	Concentration	Adjusted P Value	Significance
10μM 37i	0.5μM	0.9953	ns
10μM 37i	1μM	0.7827	ns
10μM 37i	2μM	0.5734	ns
10μM 38i	0.5μM	<0.0001	***
10μM 38i	1μM	0.0002	**
10μM 38i	2μM	0.9098	ns

Figure 4.12 Effect of JMJD5 inhibitors on the sensitivity of A549 and U2OS cells to the ATM inhibitor AZD0156.

Cells were treated with either 1μM for A549 cells (panels A and C) or 10μM for U2OS cells (panels B and D) of JMJD5 inhibitor and a range of AZD0156 concentrations simultaneously for 72 hours and cell viability was measured by MTS assay. Data represent mean ± SEM from three independent replicates with quadruplicate technical repeats. Statistical analysis was performed using the two-way ANOVA with Dunnett's multiple comparisons where (p-value ≤ 0.05=, ≤0.01 =**, ≤0.001=***).*

Overall, our data suggest that JMJD5 inhibitors can sensitise cancer cell lines to a variety of anticancer drugs. However, the level of sensitisation varies depending on the cell line and drug used.

4.2.7 Investigating if JMJD5 inhibitors engage with their target in cells

Next, we investigated whether JMJD5 inhibitors demonstrate evidence of target engagement in cells. A typical approach to investigate this for a protein-modifying enzyme would be to measure substrate modification after treating cells. Another approach, specific to 2OG

oxygenases, is to test the ability of the inhibitor to 'trap' the substrate on the hydroxylase using immunoprecipitation experiments. This approach has been widely used as a substrate discovery approach using DMOG (Rose et al., 2011), and more recently has been applied to demonstrate target engagement of MINA53 inhibitors in tumour cells (Nowak et al., 2021). However, both approaches require knowledge of the physiological substrate which has probably not yet been identified for JMJD5. That being said, the Coleman group has identified candidates with a substrate-like binding profile (but without confirmed hydroxylation sites) that we reasoned could be used to test for engagement of JMJD5 inhibitors in cells. A member of the Coleman group observed that DMOG increased the binding of endogenous MCM3 and MCM5 to wild-type JMJD5, but not the catalytically inactive H321A mutant (Figure 4.13). MCM3 and MCM5 are essential components of the minichromosome maintenance (MCM) complex, which plays a critical role in the initiation and regulation of DNA replication by forming part of the helicase that unwinds DNA at replication forks (Ibarra et al., 2008).

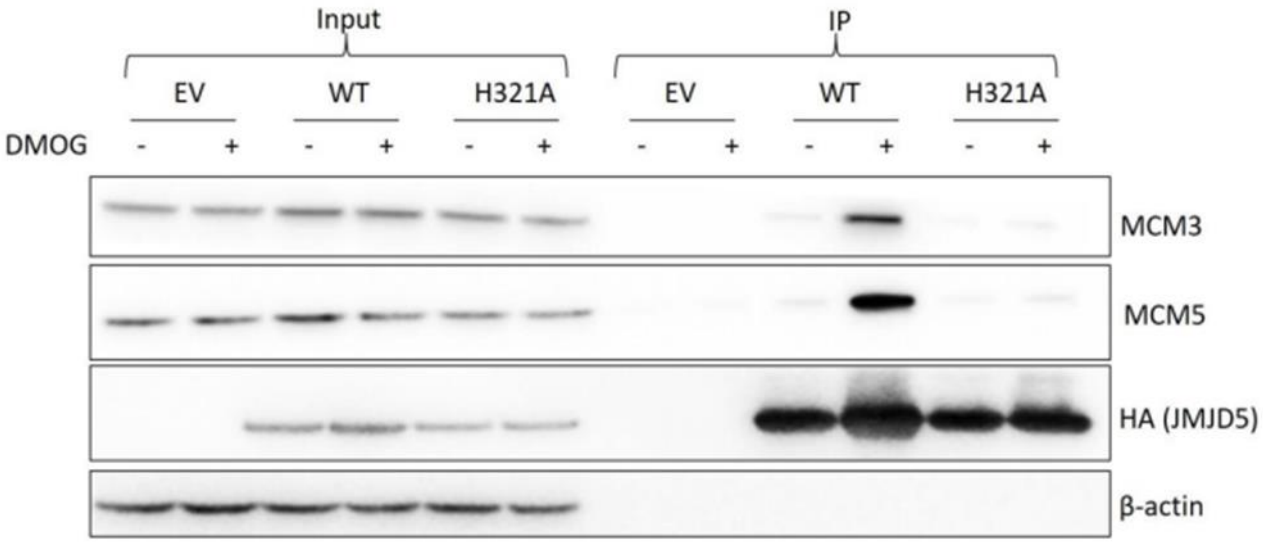

Figure 4.13 MCM3 and MCM5 interactions with wild-type JMJD5 increased in the presence of DMOG.

HEK293T cells transiently expressing an EV or HA-JMJD5 WT or H321A vector were incubated with 1mM of DMOG for 16 hours prior to anti-HA immunoprecipitation (IP). NOG (1mM) was added if the cells were treated with DMOG before IP. B-Actin was used as a loading control. N=3 biological repeats, performed by Dr Sally Fletcher.

Although these results suggest that MCM3 and MCM5 show substrate-like binding patterns, we have yet to identify any JMJD5-dependent hydroxylation sites. However, for the purposes of our initial JMJD5 inhibitor investigation, we thought it could be worthwhile to evaluate the effect of JMJD5 inhibitors on the interaction between MCM3 and MCM5.

We chose to focus on inhibitor 38, as it showed a more significant effect on cell viability in our cancer cell models. HEK293T cells were transfected with either empty vector or WT HA-tagged JMJD5 for 24 h and treated with DMSO control, 1mM DMOG or 10μM of inhibitor 38 for 16 h. We performed anti-HA IP and immunoblotted the extracts for MCM3 and MCM5. Consistent with previous findings, treatment with DMOG increased the interaction between JMJD5 and both MCM3 and MCM5 (Figure 4.14). However, treatment with the JMJD5 inhibitor 38 did not affect binding to either MCM3 or MCM5.

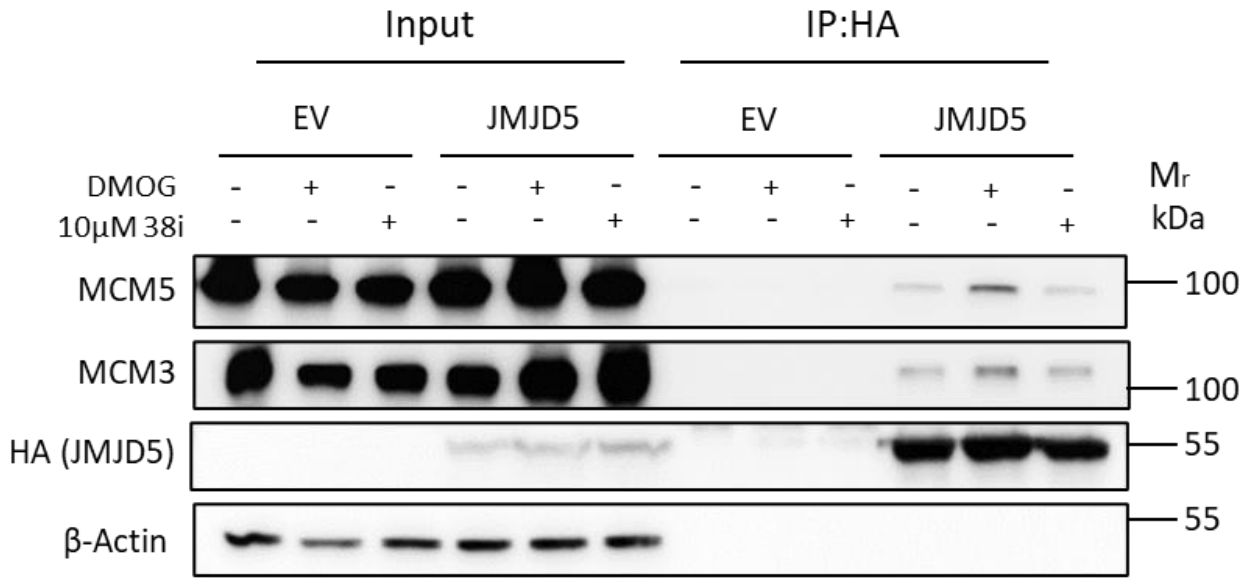

Figure 4.14 Immunoprecipitation analysis was performed to investigate whether JMJD5 inhibitor 38 demonstrated JMJD5 target engagement.

HEK293T cells transiently expressing an EV or HA-JMJD5 vector were incubated with 10μM of inhibitor 38 or 1 mM of DMOG for 16 hours prior to anti-HA immunoprecipitation (IP). β-Actin was used as a loading control. N=3

4.3 Discussion

In this chapter, we evaluated the effect of first-in-class inhibitors (5-aminoalkyl-substituted derivatives of 2,4-PDCA) of JMJD5 on cancer cell lines. We initially tested first-generation inhibitors and observed promising effects on cell viability. Following this, second-generation JMJD5 inhibitors were developed with greater *in vitro* specificity (inhibitors 37 and 38) and their effects on cancer cell lines were also evaluated. We showed that these novel JMJD5 inhibitors decreased the viability of cancer cell lines, which was associated with increased RS and cell cycle perturbations. We also evaluated their ability to sensitise cells to DDR inhibitors and obtained promising results. Overall, the findings presented in this chapter support the role of JMJD5 inhibitors as potential anticancer agents.

4.3.1 JMJD5 inhibitors are toxic to cancer cell lines

The results in this chapter indicate that JMJD5 inhibitors decrease the viability of cancer cell lines (Figures 4.2 and 4.4). This contrasts with our previous data with JMJD5 knockdown where we did not observe such striking effects on cell viability. This could be due to a higher level of JMJD5 loss of function with the inhibitors than the knockdown efficiency obtained in our models, or a variety of other experimental differences. For example, the consequences of loss of expression (knockdown) could be different to those of expression without activity (inhibitors). However, our inhibitor results are consistent with other studies that have demonstrated impaired cancer cell proliferation and viability in response to loss of JMJD5 (Ishimura et al., 2012) (Zhang et al., 2015). Notably, the cell models used in these two studies were not the same as those we used, which could explain the different results obtained.

Another potential limitation of our results is that we observed toxicity at concentrations at which the tested JMJD5 inhibitors are known to inhibit other 2OG oxygenases *in vitro*. Based on the *in vitro* IC50 values for the first initial set of inhibitors (88-93) and inhibitor 37, doses above 1μM could be inhibiting other members of the family (Figure 4.1C). This concern should be

caveated by the fact that we do not yet know what level of JMJD5 inhibitors we achieved inside cells. Nonetheless, it is possible that JMJD5 inhibitors could impact the function of other members of the family with similar loss of function phenotypes. For example, loss/inhibition of KDM4A reduces cell proliferation in a variety of cancer cell lines, including breast (Pei et al., 2023), prostate (Cui et al., 2020), and liver (Cao et al., 2024). Therefore, it is currently not possible to conclude whether the decrease in cell viability we observe is specifically due to JMJD5 inhibition. Further work is required to assess specificity in cells, ideally through quantitative measurements of hydroxylation/demethylation events catalysed by a variety of 2OG oxygenases.

It is important to note that we only tested JMJD5 inhibitors in a limited number of tumour cell lines. Future research should incorporate a wider variety of cancer types and models. Future work should also aim to understand why some cells are less sensitive to JMJD5 inhibitors than others. A number of reasons could explain these variations, such as genetic differences or levels of endogenous JMJD5 expression. For example, it is possible that the expression levels of JMJD5 in HeLa and PC3 cells (less sensitive) might be lower than those in A549 cells (more sensitive). Indeed, it has been shown that HeLa cells express low levels of JMJD5 (Wang et al., 2013). Other considerations could include differences in the mechanism of inhibitor uptake and potential efflux by membrane transporters in cancer cells. HeLa cells express various multidrug resistance (MDR) proteins that can actively remove chemotherapeutic agents from cells, contributing to poor responses (Takara et al., 2006). Nonetheless, further studies are needed to understand the factors that determine the sensitivity of JMJD5 inhibitors. Comparing the results of such studies in both normal and cancer cells will also be important in determining the potential therapeutic potential of JMJD5 inhibitors.

A major limitation of the work in this chapter is that we could not determine how selective the JMJD5 inhibitors are in cells. Selectivity studies are important because, like most inhibitors that

target 2OG oxygenases, the inhibitors characterised here are competitive inhibitors of the shared cofactor 2OG. In addition, we were unable to determine the efficacy of the inhibitors because we could not test whether JMJD5 activity was impaired in cells due to the lack of a known substrate. Further studies are needed to test the efficacy and selectivity of these compounds once a bona fide JMJD5 substrate has been discovered.

4.3.2 Phenotypes associated with JMJD5 loss vs JMJD5 inhibition

Limited in our ability to directly test inhibitor efficacy and specificity, we decided to investigate whether inhibitors cause phenotypes that would be consistent with JMJD5 loss of function. Based on our earlier work using JMJD5 knockdown models we focussed on RS. Interestingly, we found that treatment of both A549 and U2OS cells with inhibitor 37 or 38 increased the levels of RS markers (Figure 4.6). In particular, inhibitor 38 showed a significant difference compared to the control. Although these data could be consistent with target engagement and JMJD5 inhibition, we cannot rule out the possibility of off-target inhibition of other 2OG oxygenases with roles in replication fidelity such as KDM4A (Van Rechem et al., 2020).

Our initial experiments showed that JMJD5 inhibitors decreased the viability of cancer cells. However, we did not know whether the observed effect was due to a decrease in proliferation or an increase in cell death. To address this question, we carried out flow cytometry analysis of cell cycle and apoptosis. Our results showed that treatment of both A549 and U2OS with either inhibitor led to a statistically significant reduction in the population of cells in the G1 phase and an increase in S phase cells (Figure 4.7). This is consistent with our results in Chapter 3, where we reproducibly observed that JMJD5 knockdown led to a modest decrease in G1 cells and an increase in S-phase cells.

Our apoptosis analysis showed that treatment of A549 cells with 10 μM 37 or 38 led to a significant decrease in live cells (Figure 4.10A), which is also consistent with our cell cycle sub-G1 data. Moreover, both inhibitors increased the percentage of early apoptotic A549 cells,

with a significant increase observed with inhibitor 38. Conversely, inhibitor 38 did not appear to cause apoptosis in U2OS cells (Figure 4.10B), despite its ability to reduce cell viability. This suggests that inhibitor 38 may have a cytostatic effect on U2OS cells by reducing cell proliferation rather than directly killing the cells. Another possibility is that inhibitor-treated U2OS cells undergo death via other mechanisms that are not detected by the annexin V/7AAD assay, such as mitotic catastrophe. One of the characteristics of mitotic catastrophe is the presence of micronuclei, which are increased in cells treated with JMJD5 inhibitors.

The data presented here are at odds with those in Chapter 3, where JMJD5 knockdown did not affect the percentage of live, apoptotic, or dead cells. These results again suggest that the observed effects of JMJD5 inhibitor treatment, especially inhibitor 38 at the concentration used, may not be specific to JMJD5 inhibition. That being said, other studies have reported that JMJD5 affects apoptosis. For example, Yao et al. reported that JMJD5 inhibition induced apoptosis in oral squamous cell carcinoma (Yao et al., 2019). Further work is required to determine the contribution of JMJD5 inhibition to the cellular phenotypes described in this chapter.

To further investigate the specificity of JMJD5 inhibitors, we propose an epistasis experiment combining JMJD5 knockdown and treatment with inhibitors 37 or 38. If the inhibitors act specifically through JMJD5, we would expect the combined treatment to not induce the additional phenotype beyond that observed with knockdown alone, as the pathway would already be maximally perturbed. However, if an additional or exacerbated phenotype emerges in cells subjected to both knockdown and inhibitor treatment, this would suggest either off-target effects of the inhibitors or incomplete JMJD5 depletion via knockdown. This approach would allow for a deeper mechanistic understanding of the inhibitors' effects and can help determine JMJD5-specific phenotypes from those arising from off-target or dose-dependent toxicity.

4.3.3 Combining JMJD5 inhibitors with anticancer agents

Based on our data indicating that JMJD5 knockdown enhances the sensitivity of cancer cells to various anticancer agents, we aimed to explore the feasibility of combining JMJD5 and DDR inhibitors. Overall, we observed variable responses to JMJD5 inhibitors between cell lines and anticancer compounds. This contrasts with our JMJD5 knockdown models, where we consistently observed increased sensitisation to DDR inhibitors. The differences in cellular responses to JMJD5 knockdown and inhibition could be due to various reasons, such as the extent and specificity of JMJD5 activity modulation, the potential for off-target effects, compensatory cellular mechanisms, temporal dynamics of target engagement, and context-dependent roles of JMJD5 in DNA repair and cell cycle regulation.

Nonetheless, from a therapeutic perspective, the ability of JMJD5 inhibition to sensitise cancer cells to DNA-damaging agents and DDR inhibitors suggests a potential role for these compounds in combination therapies. Further studies are warranted to investigate the molecular mechanisms involved in facilitating the observed sensitivities. Moreover, the identification of biomarkers, including JMJD5 expression levels or mutations in DDR genes, such as ATM, will be crucial for selecting patients who are most likely to benefit from JMJD5-targeted treatments.

The tumour microenvironment plays a critical role in cancer progression and treatment response. Therefore, another important consideration is the response to JMJD5 inhibition under hypoxic conditions (further discussed in Chapter 5). Given that 2OG oxygenases, including JMJD5, may be sensitive to oxygen levels, investigating the effects of JMJD5 inhibitors in hypoxic tumours is highly relevant. Furthermore, exploring the combined effects of JMJD5 inhibition and chemotherapy under hypoxic conditions may reveal novel therapeutic strategies.

4.3.4 Chapter conclusions

In conclusion, despite the limitations in the analysis of JMJD5 inhibitor selectivity, our data are supportive of targeting JMJD5 in cancer cells. Our results indicated that JMJD5 inhibitors could

be beneficial in cancer therapy alone or in combination with other anticancer agents. Considering the ongoing work to develop JMJD5 inhibitors with even greater efficacy and specificity, further cellular research will be required to evaluate their effects on normal and cancer cells. From a long-term perspective, the translational development of JMJD5 inhibitors will require more studies to evaluate the cancer types responsive to JMJD5 inhibitors, together with a clear evaluation of JMJD5's role in cancer biology and identification of its biological substrate.

Chapter 5. Final discussion

The work presented in this thesis contributed to the investigation of JMJD5 loss-of-function in the context of genome stability and synergistic drug interactions, as well as to the initial analysis of JMJD5 inhibitors as potential anticancer agents. We demonstrated that JMJD5 cancer mutations affecting the JmjC catalytic domain led to loss of enzymatic activity and increased RS and GI. We also showed that loss of JMJD5 sensitises different cancer cell lines to a wide range of anticancer agents, including DDR inhibitors and conventional chemotherapy drugs. Furthermore, our work demonstrating that JMJD5 inhibitors are toxic to selected cancer cells suggests that further preclinical evaluations are warranted. In this section, we explore the broader significance of the discoveries and discuss potential future paths.

5.1 Therapeutic potential of targeting JMJD5

Despite the success of PARP inhibitors in anticancer therapy, drug resistance is a major issue that leads to disease relapse and poor patient prognosis (Giudice et al., 2022). Therefore, current approaches to overcome resistance are focused on combinational therapies that combine PARP inhibition with other inhibitors of DDR or immune-checkpoint inhibition (Fu et al., 2024). Nonetheless, additional targets are needed to overcome the complex and evolving mechanisms of resistance. In light of our data indicating that loss of JMJD5 can sensitise cancer cells to PARP inhibitors, JMJD5 has emerged as a potential new therapeutic target.

Targeting a tumour suppressor gene in cancer therapy may seem counterintuitive, as they are typically involved in maintaining GS and preventing cancer growth. Nonetheless, in the case of proteins involved in DDR, targeting tumour suppressors involved in genome maintenance can have a unique therapeutic rationale, as cells harbouring mutations in genes such as p53, BRCA1/2, or ATM often exhibit high RS and rely on remaining DDR mechanisms to survive

(Li et al., 2023). In these cells, further inhibiting other DDR proteins can push them into a state of catastrophic GI and death (Topatana et al., 2020).

Importantly, in addition to addressing resistance mechanisms in tumours already sensitive to PARP inhibitors, JMJD5 inhibitors could open new therapeutic possibilities by sensitising BRCA-wild-type tumours to PARP inhibition. Typically, PARP inhibitors are the most effective in BRCA-mutant or HR-deficient cancers which usually include breast, prostate, or ovarian tumours (Zheng et al., 2020). Nonetheless, many cancers have wild-type BRCA genes and functional HR, which limits the use of PARP inhibitors in these cases. Our data indicates that loss of JMJD5 sensitises some cancer cells to PARP inhibitors, which could perhaps create a 'BRCAness' like state, suggesting that targeting JMJD5 could be a strategy to expand the use of PARP inhibitors to a new population of patients. Currently, treatment options for patients harbouring wild-type BRCA tumours are limited in terms of targeted therapies that exploit DDR vulnerabilities. Therefore, utilising JMJD5 inhibition in this context could be an attractive option for expanding treatment options. Further research is needed to evaluate whether JMJD5 inhibition induces similar sensitivity phenotypes in other preclinical cancer models such as organoids and *in vivo* experiments.

Another possible therapeutic strategy is to use PARP, ATM, and ATR inhibitors in cancer cells harbouring JMJD5 mutations. Although mutations in JMJD5 in tumours are relatively rare (approximately 2% according to cBioPortal and COSMIC), it is possible that JMJD5 is functionally inactivated in wild-type tumours. For example, inactivation by the tumour microenvironment (discussed more below) or post-transcriptional deregulation could contribute to the frequency of JMJD5 loss of function in cancer. Furthermore, it is possible that the broader regulatory network of JMJD5 could also be deregulated in cancer, which could also create BRCAness like states that could be targeted. For example, the JMJD5 interactor RCCD1 has been implicated in cancer, with reports indicating a role as an oncogene (Cheng et al., 2019)

and tumour suppressor gene (Cai et al., 2014). Interestingly, RCCD1 is affected in many of the same tumour types as JMJD5 including breast (Ferreira et al., 2019), lung (Cheng et al., 2019), prostate (Gusev et al., 2019), and pancreatic cancers (Zhong et al., 2020). Recent work within the Coleman group by Dr. Tristan Kennedy showed that RCCD1 knockdown causes an increase in RS in cancer cells, and that these phenotypes are epistatic with JMJD5 loss, suggesting they act in the same pathway. If true, this would suggest that RCCD1 inactivation would also sensitise tumour cells to DDR inhibitors, which could be investigated in the future using approaches and models similar to those presented here. Such work could support targeting of RCCD1 as another therapeutic opportunity.

Future work should also aim to discover other proteins involved in the JMJD5 pathway that could be exploited for developing novel cancer therapies. If these components are deregulated in cancer, they could act as potential drug targets. Because JMJD5 is an enzyme, and the role of JMJD5 in GS is activity-dependent, its substrate(s) likely also play a role in GS and potentially replication fidelity. The identification of the biological substrate of JMJD5 would not only enhance the understanding of its role in cancer biology but could also provide an additional potential drug target.

The increased sensitivity to PARP, ATM, and ATR inhibitors upon JMJD5 loss is associated with cell cycle arrest, increased apoptosis, and elevated levels of RS markers, although the precise effects depend on the cancer cell line. Although preliminary, and based on a small number of models, this might indicate that the role of JMJD5 is dependent on the tissue or the genetic context of cells in which it is expressed. This possibility might also explain the debate between the role of JMJD5 as a tumour suppressor vs an oncogene. The apparent context-dependent roles of JMJD5 may be unsurprising, considering that many DDR proteins exhibit tissue-specific functions and responses depending on the genetic landscape and cellular environment. Indeed, mutations of DNA repair genes in different DDR pathways tend to have

tissue-specific effects on patients, leading to tissue-specific phenotypes (Sun, Osterman and Li, 2019). For example, although BRCA1 plays a well-established and crucial role in DDR, the impact of mutations in this gene varies considerably depending on the tissue type. BRCA1 mutations in breast tissue are associated with a risk of malignancy of 55-72% by the age of 70 years. Whereas in pancreatic tissue, BRCA1 mutations are associated with a risk of 1-3% (Petrucelli et al., 1998). Overall, further research is needed to explore the factors modifying JMJD5's role in cancer. Such studies could include a large panel of different cancer cell lines from different tissues, and with known genetic status such as wild-type and mutant p53 and BRCA1/2.

In addition to the candidate and hypothesis-driven studies discussed above, unbiased genetic screens could also have significant value. For example, CRISPR-based screens in JMJD5 loss of function models could help identify novel genetic interactions and new potential synthetic lethality partners. This would allow for the discovery and validation of new therapeutic targets that can be exploited in combination with JMJD5 inhibition. Such screens could be performed in JMJD5 knockout tumour cell models, which should be feasible to generate (He et al., 2016). Any hits generated from the screens could be validated using the approaches presented in this thesis. Due to the context-dependent role of JMJD5 in different tumour types and phenotypes associated with its loss, the cancer cell types to be screened should be carefully considered, including the expression level of JMJD5.

The identification of synthetic lethal interactions with JMJD5 could be used to stratify patients based on their genetic profiles. For example, tumours harbouring mutations in genes that are synthetically lethal with JMJD5 could be particularly susceptible to combination therapies involving JMJD5 inhibitors, allowing for more personalised and effective treatment. Indeed, there are several synthetic lethal combinations that have led to the stratification of patients for

targeted therapies with the most well-known example being patients' stratification based on their BRCA mutation status in PARP inhibitors treatment (Lord and Ashworth, 2017).

5.2 JMJD5 loss/inhibition in the context of hypoxia and oncometabolites

Another avenue for future research should focus on exploring JMJD5 loss/inhibition in the context of hypoxia, given the potential sensitivity of 2OG oxygenases to oxygen levels. Importantly, data from cellular experiments indicate different oxygen affinities and sensitivities among members of the 2OG oxygenase family (Fletcher and Coleman, 2020). For example, protein hydroxylases JMJD4 (Feng et al., 2015), MINA53, and NO66 (Ge et al., 2012) have been shown to retain significant catalytic activity, even under severe hypoxic conditions (≤ 0.1% oxygen levels). Currently, there is limited knowledge about the activity of JMJD5 under hypoxic conditions. A report by Wang et al. showed that JMJD5 is upregulated by hypoxia and is crucial for hypoxia-induced cell proliferation (Wang et al., 2013). Therefore, further investigation regarding JMJD5 in the context of hypoxia is needed, especially because hypoxia has been shown to contribute to RS. Studies have demonstrated that severe hypoxic conditions impair DNA replication (Pires et al., 2010; Foskolou et al., 2016). Chronic periods of hypoxia for more than 12 h can prevent fork restart (Pires et al., 2010). This may be particularly relevant here considering the role of JMJD5 in replication fork dynamics, which requires further investigation.

If JMJD5 activity is compromised by tumoural hypoxia, this could create an environment in which tumour cells are critically dependent on the remaining JMJD5 function. Such cells could display enhanced sensitivity to JMJD5 and DDR inhibitors. Since hypoxia is a major contributor to resistance to conventional chemotherapy and radiotherapy (Boulefour et al., 2021), JMJD5 inhibition, combined with DDR inhibitors, could represent a novel therapeutic strategy for targeting hypoxic tumour regions.

Another important consideration is the function of the JMJD5 in the context of oncometabolites. As discussed in Chapter 1, oncometabolites have been shown to inhibit 2OG oxygenases which can contribute to tumourigenesis via several different mechanisms, including the dysregulation of DDR pathways (Inoue et al.,2016; Sulkowski et al., 2020). Whether JMJD5 is sensitive to oncometabolites is not yet clear, although preliminary data is supportive (Schofield group, personal communication). Based on our knockdown data, inhibition of JMJD5 by oncometabolites could sensitise to PARP, ATM, and ATR inhibitors. Furthermore, oncometabolites could enhance the effects of JMJD5 inhibitors by further reducing JMJD5 activity through combined 2OG competitive inhibition. Tumours with high levels of oncometabolites, such as those with IDH mutations (Fletcher and Coleman, 2020), may be particularly susceptible to such combination therapies.

5.3 Final conclusions

In this thesis, we have expanded the understanding of the role of JMJD5 in cancer. We have shown that JMJD5 loss is associated with increased RS and that this sensitises cancer cells to DDR inhibitors, as well as other anticancer agents. Our initial evaluation of first-in-class JMJD5 inhibitors provides a basis for future investigations into the effects of JMJD5 inhibitors as anticancer agents. Overall, this study provides a solid foundation for further characterisation of JMJD5 as a novel anticancer target in the context of combinational therapies using JMJD5 inhibitors. In Figure 5.1 we provide a working model for JMJD5 in replication fork restart and HR.

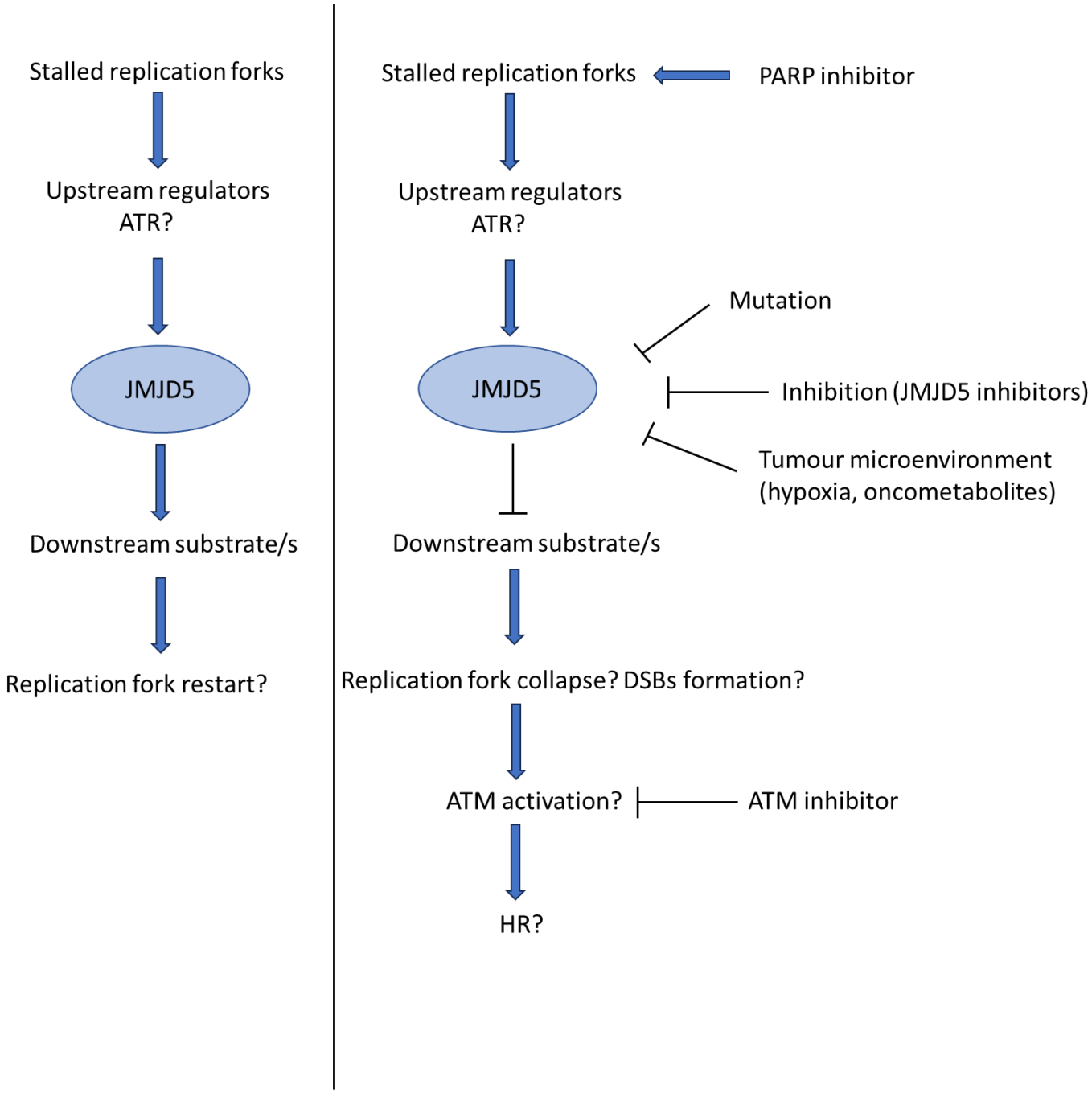

Figure 5.1 The working model for JMJD5 in replication fork restart and HR.

The activity of the JMJD5 may be regulated by upstream proteins in response to RS. JMJD5 in turn may hydroxylate downstream substrate/s to promote replication fork restart. Additionally, JMJD5 may be inhibited through mutation, inhibition or the tumour microenvironment which may lead to replication for collapse and formation of DSBs leading to the activation of HR.

Chapter 6. Materials and methods

6.1 Molecular biology techniques

6.1.1 Vectors and plasmids

In this study, JMJD5 constructs were derived from pEF6 vectors, which had been previously developed by the Coleman group. These vectors were utilised to generate FLAG-tagged pTIPZ and FLAG-tagged pIHZ constructs, including JMJD5 WT and mutant variants. The pTIPZ vector represents a modified version of the commercial pTRIPZ vector (Figure 6.1A), with the red fluorescent protein (RFP) cDNA excised (Dhamarcon). The pIHZ,vector is a derivative of pGIPZ (Figure 6.1B) that lacks the green fluorescent protein (GFP) cDNA and substitutes a puromycin for a hygromycin resistance cassette.

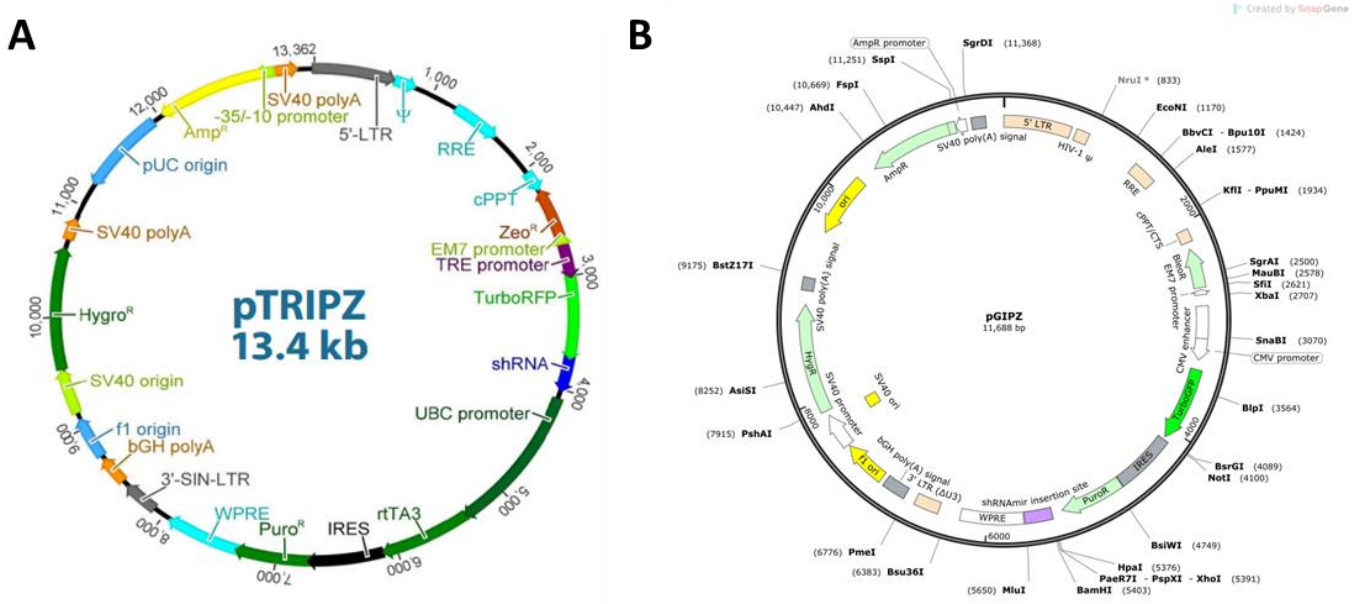

Figure 6.1 Vector maps. A. pTRIPZ lentiviral vector. Figure from Horizondiscovery B. pGIPZ vector. Figure from SnapGene.

6.1.2 Polymerase chain reactions

Polymerase chain reactions (PCRs) used to make pTIPZ vectors were set up using Phusion® High-fidelity DNA polymerase (NEB) according to the manufacturer's instructions. PCR products were separated by DNA gel electrophoresis with 1% (w/v) agarose gel. DNA bands

were subsequently isolated and solubilised using the Gen-Elute™ Gel Extraction kit (Sigma-Aldrich). The PCR products and vectors of interest were digested using relevant restriction enzymes for 1 hour at 37°C. The digested vectors were additionally treated with calf intestinal alkaline phosphatase (CIP, NEB, 0290S). Digestion products were run on 2% (w/v) agarose gel and bands cut out were solubilised through the Gen-Elute™ Gel Extraction kit. The constructs were ligated with plasmid at the appropriate ratios using T4 DNA ligase (NEB) at 25°C for 10 minutes and heat inactivated at 65°C for 10 minutes. Ligated plasmids were transformed into NEB 5-alpha electrocompetent *E.coli* and plated onto LB-Agar Ampicillin resistant plates followed by overnight incubation at 37°C. Single colonies were picked and inoculated into 5 mL of LB and incubated overnight at 37°C and 200 rpm. Plasmid DNA was purified using the Gen-Elute Plasmid Miniprep kit (Sigma-Aldrich) and plasmids were sequenced by SourceBioscience to verify the correct incorporation of the insert.

Table 6.1 List of primers used for PCR cloning.

Construct	Primers 5' to3'
pTIPZ 3x-FLAG JMJD5	Forward: TATGAGGGGCCATGGGAGACTACAAAGACCATGAGGGATTATAAAGATCATGACATCGACTACAAGGATGAGATGATAAGGGGAGACACCCACT
	Reverse: AATATACCTCAGGCTACGACCACCAGAAGCT

6.1.3 RNA extraction and cDNA synthesis

RNA was extracted from cell pellets using the Sigma GeneElute Mammalian Total RNA extraction kit. cDNA was generated from RNA (1 µg in a 10 µl reaction) using the High

Capacity cDNA reverse transcription kit (Applied Biosystems) according to the manufacturer's protocol.

6.1.4 Quantitative PCR

qPCR was performed using the Fast Sybr Green Master Mix (Thermo, 4385612) according to the manufacturer's protocol. Biological repeats were done with technical triplicates and GAPDH was used as normalisation control. qPCR was performed on QuantStudio™ 5 PCR machine and the comparative ΔΔCt method was used for quantification of gene expression.

Table 6.2 Primers used for qPCR.

qPCR primer	Sequence (5' to 3')
KDM8	Forward: CACAGATGAGGAATGGTCCCAG Reverse: GCTGATGTCCTGCTTCAACTCC
RAD51	Forward: TATCCAGGACATCACTGCCA Reverse: GGTGAAGGAAAGGCCATGTA
GAPDH	Forward: AGCCACATCGCTCAGACAC Reverse: GCCCAATACGACCAAATCC

6.2 Cell biology techniques

6.2.1 Cell culture

A549, U2OS, HCA-7 and HEK293T cells were cultured in Dulbecco's Modified Eagle Medium (DMEM) with 1% (v/v) penicillin/streptomycin (P/S) and 10% (v/v) Fetal Bovine Serum (FBS) and maintained at 37°C in a humidified 5% CO_2 incubator. All the cell lines were directly bought from ATCC or gifted from other research groups within the Birmingham institute that bought them from ATCC. Upon 70-80% confluency, cells were removed from culture flasks

using TripLE express trypsin (ThermoFisher Scientific). Trypsin was inactivated using culture media before re-seeding cells into culture flasks. Alternatively, cells to be plated for experiments were first counted using an automated counter (Invitrogen™ Countess II™). Stable cell lines were cultured as above with the addition of 1 μg/mL puromycin. All cell lines were routinely tested for mycoplasma contamination.

6.2.2 Drug treatments

The stock concentration of ATM inhibitor AZD0156 was prepared by dissolving in 70% (v/v) ethanol to 3mM stock concentration and aliquots were stored at -80ºC. ATR inhibitor Ceralasrtib (AZD6738),PARP inhibitor Talazoparib and MMS were prepared at the stock concentration of 10mM in DMSO. Doxorubicin, Calicheamicin and Trabectedin powder were dissolved in DMSO to a stock concentration of 10mM. All JMJD5 inhibitors were dissolved in DMSO to a stock concentration of 100mM. All the drugs aliquots were stored at - 80ºC.

Table 6.3 List of reagents used to treat cells.

Reagent	Source
Doxycycline	Sigma, D9891
DMSO	Sigma, D2650
Talazoparib	Selleckchem, S7048
AZD0156	Selleckchem, S8375
Ceralaserib	Selleckchem, S7693
Doxorubicin	Sigma, 44583
MMS	Sigma, 129925
Calicheamicin	Cambridge Bioscience, HY-19609
Trabectedin	Sigma, TA9H9876DC6F
JMJD5 inhibitors	Christopher Schofield group

6.2.3 Plasmid transfection

HEK293T cells were seeded in 6 well plates at a density $5x10^5$ and transfected after 24 hours using FuGENE® HD (Promega) according to the manufacturer's instructions. Briefly, plasmid DNA was added to Opti-MEM® reduced serum medium and vortexed. FuGENE was added to the mixture at a ratio of 3 µL per 1 µg of plasmid DNA, vortexed and incubated for 30 minutes at room temperature (RT). Transfection mixtures were added to the cells in droplets and cells were harvested after 48 hours.

6.2.4 RNA transfection

Small interfering RNA (siRNA) transfection using the Lipofectamine™ RNAiMAX (Thermofisher) was performed as per the manufacturer's instructions. Briefly, 24 hours before

transection recipient cells were seeded in 10 cm dishes at a density of $5x10^5$ cell/ml. 8 µL siRNA (Sigma) at 50 µM concentration (final concentration of 30nM) was added to 500 µL of Opti-MEM. Pre-mix was prepared by mixing 10 µL of RNAiMAX with 500 µL of Opti-MEM per transfection and the volume of 500 µL was subsequently added to each tube containing siRNA and left to incubate for 15 minutes at RT. While incubating, the media on cells was changed then 1 mL of transfection mixture was added in dropwise motion to each plate. Cells were harvested after 72 hours.

Table 6.4 List of siRNAs.

siRNA target	Sigma siRNA ID	Referred to in text as:
SIC001 MISSION siRNA Universal Negative Control	SIC001	siCtrl
JMJD5	SASI_Hs0100082891	siJMJD5

6.2.5 Lentiviral transduction

HEK293T cells were transfected with 500 ng of lentiviral vector and packaging vectors pMD2.G (150 ng) and psPAX2 (350 ng) using FuGENE® HD transfection reagent according to the procedure described above. After 48 hours, a medium containing the virus was collected, filtered using 0.45 µm PES filters and added to recipient A549 or U2OS cells. Cells were then incubated with the virus for 24 hours and transduced cells were selected using 1 µg/mL of Puromycin (Gibco).

6.2.6 shRNA knockdown

Stable expression short hairpin RNA (shRNA) cell lines were generated using lentiviral transduction as detailed above. Doxycycline (1 µg/mL) was used to induce the expression of shRNA plasmids.

Table 6.5 List of shRNAs.

Target	Sequence (5' to 3')	Referred to in text as:
JMJD5	UUUUUCUAACUUCACAUCUGGA	shRNA JMJD5 #1
JMJD5	CCCAAGUGAAGAAACCACC	shRNA JMJD5 #3

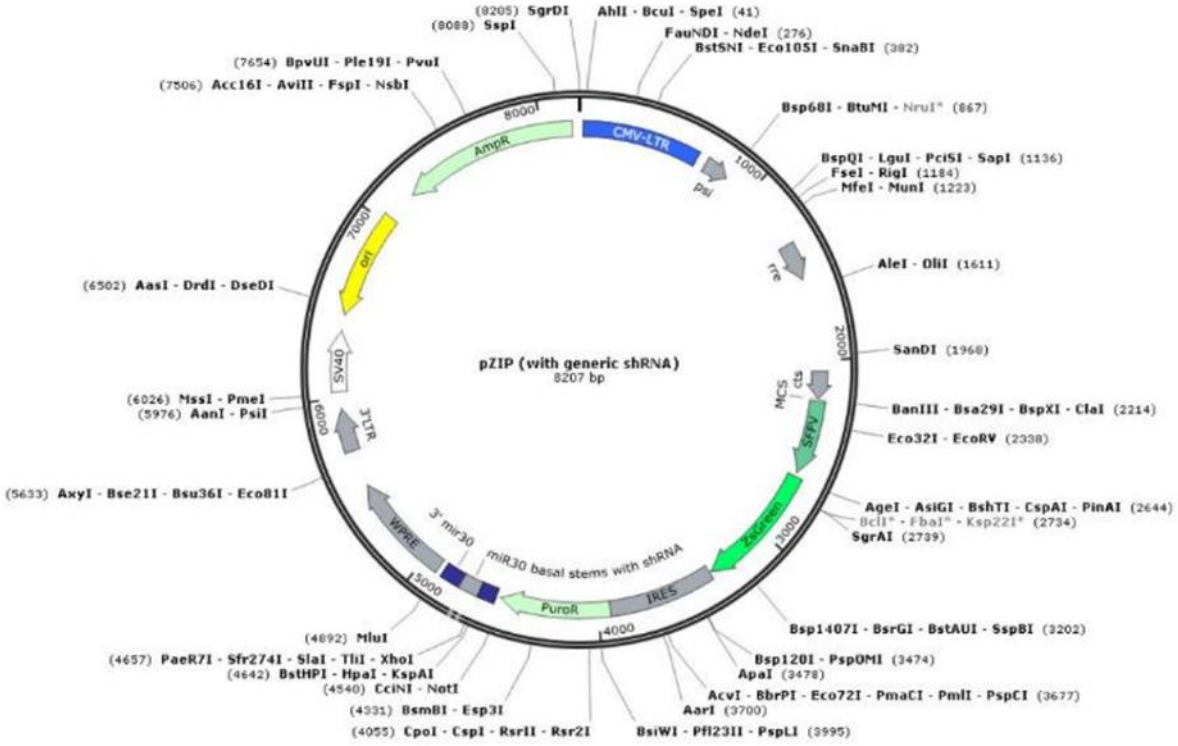

Figure 6.2 Vector map used for doxycycline-inducible JMJD5 shRNA.

Figure from SanpGene,.

6.2.7 Cell viability assays

Cell proliferation/viability was measured using both MTS assay (CellTiter 96 Aqueous One 667 Solution Cell Proliferation Assay, Promega), Resazurin (Abcam) and cyQUANT assay (CyQUANT™ NF Cell Proliferation Assay, ThermoFisher).

For MTS assays, CellTiter 96 Aqueous MTS reagent (Promega) and Phenazine methosulfate (PMS, Sigma-Aldrich®) were dissolved in 1X PBS according to the manufacturer's protocol. MTS working reagent was made by combining 1 mL MTS with 50 µL of PMS and added into each well. The cells were incubated for 1 hour at 37˚C 5% CO_2, protected from light, then absorbance was measured at 490 nm using an EnSpire™ Multimode plate reader (Perkin Elmer).

For cyQUANT assays, the reagents were prepared according to the manufacturer's protocol and added to the cells. The cells were incubated for 1 hour at 37˚C 5% CO_2, protected from light, then fluorescent was measured with excitation at ~485 nm and emission detection at ~530 nm using an EnSpire™ Multimode plate reader (Perkin Elmer).

For the Resazurin assay, the stock stain reagent was diluted in 1X PBS according to the manufacturer's protocol and 20 µL added into each well. The cells were incubated for 2 hours at 37˚C 5% CO_2, protected from light, then fluorescence was measured at Ex/Em 560/590 nm using an EnSpire™ Multimode plate reader (Perkin Elmer).

6.2.8 Colony formation assay

A549 cells were seeded at a density of $5x10^5$ in 10 cm dishes and after 24 hours transfected with siRNA to knockdown JMJD5, as described above. The cells were then reseeded on 6 well plates 48 hours after transfection at a density of 200 cells/plate (for controls and lower drug concentrations) or 500 cells/plate (for higher drug concentrations), in triplicate. The next day, the cells were treated with indicated drugs at specific concentrations for 24 hours and afterwards incubated in drug-free medium for additional 7 days to form colonies. Subsequently, colonies were stained with 0.01% (w/v) crystal violet for 30 minutes, washed and counted the next day.

Plating efficiency and % survival calculation:

(PE) =(Number of cells plated / Number of colonies formed)×100

% Survival=(Colonies in control group / Colonies in treated group)×100

6.2.9 Immunofluorescent staining and image acquisition

Cells on coverslips were pre-extracted on ice for 5 minutes using a buffer containing 20 mM NaCl, 3 mM $MgCl_2$, 300 mM sucrose, 10 mM PIPES, 0.5% (v/v) Triton X-100 followed by fixation using 4% (w/v) paraformaldehyde (PFA) in PBS for 15 minutes at RT. Afterwards, the cells were permeabilised in 0.1% (v/v) Triton X-100 in PBS at RT for 10 minutes and blocked in 1% Bovine serum albumin (BSA) in PBS for one hour at RT. The coverslips were incubated in primary antibodies made up in 1% (w/v) BSA in PBS at RT for one hour in a humidified dark plate. The full list of antibodies used and dilutions can be found in Table 6.6 The coverslips were then washed three times in cold 1% (w/v) BSA in PBS followed by one-hour incubation with secondary antibodies (Table 6.6) The coverslips were washed three times with cold PBS and incubated for 10 min with 4',6 diamidino-2-phenylindole (DAPI) (Invitrogen™) to stain nuclei. Prolong® Gold Antifade Reagent (Cell Signalling Technology) was used to mount the coverslips onto microscope slides. Images were taken using 40X objective on a Leica DM6000 fluorescent microscope and processed with ImageJ v1.54.

Table 6.6 The full list of antibodies used for immunofluorescent staining and dilutions.

Antibody	Source and catalogue number	Dilution
Anti-53BP1	Bio-Techne, NB100-904V	1:500
CENPF	BD Biosciences, 610768	1:500
FLAG	Sigma-Aldrich, F1804-1MG	1:1000
Rabbit 488nm	Life technologies, A11070	1:1000
Mouse 555nm	Life technologies, A31570	1:1000

6.2.10 Cell cycle analysis

Cell cycle analysis was performed on A549 and U2OS cells fixed in ice-cold 70% ethanol. Cells were harvested by trypsinisation and incubated with 100 µg/mL RNase A (Thermo Fisher Scientific) and stained with 20 µg/mL propidium iodide (Sigma), then analysed using Beckman Coulter CytoFLEX S. Representative FACS profiles were generated using Beckman CytExpert software v2.5.0.77.

6.2.11 Apoptosis analysis

Apoptosis was analysed using flow cytometry with staining for PE-conjugated Annexin V and 7-AAD according to the manufacturer's directions for the apoptosis detection kit (BD Pharmingen™). Briefly, cells were detached from the plates using trypsin, spun down and resuspended in PBS. Subsequently, cells were counted and $1x10^6$ cells were re-suspended in 1ml of 1X binding buffer. Next, cells were stained with 5 µL of annexin-PE and 5 µL of 7-AAD

according to the kit protocol and incubated for 15 minutes at RT in the dark. The samples were analysed using Beckman Coulter CytoFLEX S and Beckman CytExpert software v2.5.0.77.

6.3 Biochemical techniques

6.3.1 Whole cell extracts

The cells were harvested and lysed in radioimmunoprecipitation assay (RIPA) buffer (150 mM NaCl, 25 mM Tris pH 8, 1% v/v NP40, 0.5% v/v sodium deoxycholate, 0.1% v/v SDS) or JIES buffer (100 mM NaCl, 20 mM TrisHCl pH 7.4, 5 mM MgCl2, 0.5% v/v NP-40) containing 1X protease inhibitors (Sigma) and when appropriate 1X phosphatase inhibitors (Sigma) at a ratio to the volume of the cell pellets of 1:2, incubated on ice for 10 minutes and samples in RIPA were sonicated for 10 seconds. Subsequently, cells were pelleted for 10 minutes at 14,000 rpm and 4°C, and protein concentration was measured using the Pierce 660 nm assay (Thermofisher) as per manufacturer instruction for microplate procedure. Protein concentration was estimated using the BSA standard curve and normalised with RIPA or JIES buffer. Subsequently, the samples were resuspended in 6x Laemmli Loading Buffer (6x: 125 mM Tris-HCl [pH 6.8], 6% (w/v) SDS, 50% (v/v) glycerol, 225 mM dithiotheitol (DTT), 0.1% (w/v) bromophenol blue) to a final concentration of 1X, vortexed and boiled for 5 minutes.

6.3.2 Immunoprecipitation

For immunoprecipitation, cells were harvested on ice and lysed by rotation for 1 h at 4°C in JIES buffer containing 1x SIGMAFAST™ protease inhibitor cocktail (Sigma-Aldrich, S8830). Subsequently, lysates were clarified (10 minutes at 21,910 x g at 4°C) and input fractions were collected. Then, anti-hemagglutinin (HA) agarose beads (Sigma-Aldrich, A2095) were added to the supernatants, and samples were rotated for 4 hours at 4°C. Afterwards, beads were washed 6 times with JIES buffer followed by peptide elution (100 µg/mL HA or 100 µg/mL FLAG peptide in 20 mM Tris pH8 and 100 mM NaCl) at 2000 rpm for 15 minutes in a

thermomixer. The supernatant was removed from the beads and an appropriate volume of 6x Laemmli buffer was added, and the samples boiled at 95°C for 5 minutes.

6.3.3 SDS-PAGE and Western blot analysis

Samples were loaded onto 12% (v/v) polyacrylamide gel and proteins were separated using Sodium dodecyl sulphate-polyacrylamide gel electrophoresis (SDS-PAGE) with the Mini PROTEAN Tetra apparatus (Bio-Rad), at 160 V for 1 hour in running buffer (25 mM Tris-HCl pH 8.3, 192 mM glycine, 0.1% (w/v) SDS). Proteins were transferred onto a (methanol activated) polyvinylidene difluoride membrane (GE Healthcare) at 320 mA for 30 minutes in transfer buffer (25 mM Tris pH 8.3, 192 mM glycine, 20% (v/v) methanol) and blocked in 5% (w/v) milk or 5% (w/v) BSA in PBS-T (Phosphate-Buffered Saline with 0.1% (v/v) Tween) for 1 hour. The membranes were incubated in primary antibody overnight at 4ºC (or 1 hour at RT for HRP-tagged antibodies) followed by HRP-tagged secondary antibody incubation for 1 hour. All the antibodies were made up in 5% (w/v) milk in PBS-T or 5% (w/v) BSA in PBS-T. The full list of dilutions used can be found in Table 6.7 below. Proteins were detected using Clarity Max ECL Western Blotting Substrates (Bio-Rad) or SuperSignal™ West Femto Maximum Sensitivity Substrate (Thermo) and imaged using a Vilber Lourmat FusionFX imager.

Table 6.7 The full list of antibodies used for Western blot and dilutions.

Antibody	Source and catalogue number	Dilution
JMJD5	Collaborators Matsuura Yoshiharu Lab, Japan	1:250
HRP- β-Actin	Abcam Ab49900	1:25000
HRP-HA	Roche 12CA5	1:2000
HRP-FLAG	Sigma A8592	1:10000
RCCD1	Abcam, Ab122570	1:500
P53	Calbiochem, OP43	1:500
RAD51	Abcam, ab63801	1:1000
H2A	Merc, 07-146	1:1000
yH2AX	Merck, 05-636	1:1000
PARP	Cell Signaling Technology, 9542S	1:1000
Chk2	Merck, 05-649	1:1000
pChk2	Cell Signaling Technology, 2661	1:1000
Anti-rabbit HRP	NEB, 7074	1:2000
Anti-mouse HRP	NEB,7076	1:2000

6.3.4 *In vitro* hydroxylation assays

Reactions were prepared for 20 µg of GST-tagged recombinant wild-type JMJD5 and P395Q, T354M and H321A mutants with 100 µM Fe (II), 200 µM 2OG, 500 µM ascorbate, and 50 mM HEPES pH 7.5. Reactions were initiated by the addition of RPS6 peptide (^{129}VPRRLGPKRASRIRKL^{144}) in buffer (50 mM Tris-HCl pH 7.5, 150 mM NaCl and 1 mM DTT) to a final concentration of 100µM and incubation at 37°C for 1 hour. Samples with substrate buffer only served as a negative control. The reactions were stopped by quenching with 1% (v/v) formic acid. To detect hydroxylation activity, the Succinate-Glo™ JmjC Demethylase/Hydroxylase Assay (Promega) was used. Briefly, quenched samples were diluted 1:10 in water and 5 µL of the diluted reaction was mixed with an equal volume of Succinate-Glo™ detection reagent 1 and incubated at RT for 1 hour. Afterwards, 10 µL of Succinate-Glo™ detection reagent 2 was added, mixed and incubated for 10 minutes at RT. Luminescence was measured by PerkinElmer Enspire plate reader.

6.3.5 Recombinant protein expression in bacteria

BL21 competent E. coli were transformed with each pGEX-4T-1 JMJD5 WT, P395Q, T354M and H321A were used to start a culture of 10 ml in 2X Luria Broth (LB) with ampicillin and grown in a shaking incubator at 37°C and 200 rpm overnight. On the second day, the starter cultures were diluted 1:100 in 2X LB with 50 µg/mL ampicillin and grown at 37°C 200 rpm shaking until the culture reached an optical density (OD) of 0.6 at 600 nm which was measured using a Nanodrop spectrophotometer. Once at the correct OD the cultures were incubated for 1 hour at 18°C to equilibrate then protein expression was induced with 0.5 mM of Isopropyl β-d-1- thiogalactopyranoside (IPTG) and cultures grown overnight at 18°C shaking at 200 rpm. The next day, cultures were harvested by pelleting at 4000 rpm for 20 minutes at 4°C using

Beckman ultracentrifuge JLA-9.1000 rotor and bacteria were lysed with lysis buffer (50mM Tris pH 8; 300mM NaCl; 0.5mM Tris(2-carboxyethyl) phosphine (TCEP); Protease Inhibitor Cocktail (1 Tablet per 100ml); Turbonuclease 1:10000; Lysozyme 0.5mg/ml, Triton X-100 0.1% v/v). Samples were rotated for 1 hour at 4°C then stored overnight at -70°C. The following day, lysates were thawed and pelleted for 15 minutes at 18,000 rpm at 4°C using Beckman high-speed centrifuge with JA25.50 rotor. Supernatants were transferred to 50 mL tubes and glutathione beads were added (500 µl per 50ml of JMJD5 WT/T354M and 150 µl for JMJD5 P395Q) and incubated rotating overnight at 4°C. The next day, the glutathione beads were washed 6x with wash buffer (50mM Tris pH 8; 300mM NaCl; 0.5mM TCEP; Triton X-100 0.10% v/v) and the supernatant was removed by spinning for 1 minute at 1000 rpm at 4°C. Protein was eluted in three sequential elutions with elution buffer (10mM glutathione in wash buffer) by rotating the samples for 10 minutes at RT and pelleting the beads for 2 minutes at 1000 rpm. The appropriate fractions were combined, pelleted for 2 minutes, 14000 rpm at 4°C to remove the remaining glutathione beads and dialysed overnight using GeBAFlex MaxiTubes (Generon) in dialysis buffer containing 50mM Tris pH 8; 300mM NaCl; 0.5mM TCEP. On day 6 the protein samples were concentrated for 2.5 hours using Vivaspin 6 3000 MWCO PES spin columns at 4°C and 4020 rpm. Protein concentration was measured using a Nanodrop2000. Relative protein concentrations were checked by running a commercial gel Novex™ WedgeWell™ 8-16% gels (cat. no. XP08165BOX, Invitrogen) including known concentration samples that was stained with Coomassie stain.

6.4 Bioinformatics analysis

6.4.1 Structural analysis

Structural analysis was done using the protein modelling software ChimeraX v1.7 (Pettersen et al., 2021).

6.5 Statistical analysis

Statistical analyses were performed in GraphPad Prism v10.1.1 using an unpaired t-test or a one-way ANOVA with either Bonferroni's or Tukey's post hoc test. Additionally, two-way ANOVA with Dunnett's multiple comparisons test or the non-parametric Kruskal–Wallis rank sum test was used when appropriate. All the experiments were done with at least three independent biological repeats. Differences were considered significant at $p < 0.05$. The error bars represent the standard error of the mean.

Bibliography

Adzhubei, I. A., Schmidt, S., Peshkin, L., Ramensky, V. E., Gerasimova, A., Bork, P., Kondrashov, A. S., & Sunyaev, S. R. (2010). A method and server for predicting damaging missense mutations. Nature Methods, 7(4), 248-249. doi:10.1038/nmeth0410-248.

Amendola, P. G., Zaghet, N., Ramalho, J. J., Vilstrup Johansen, J., Boxem, M., & Salcini, A. E. (2017). JMJD-5/KDM8 regulates H3K36me2 and is required for late steps of homologous recombination and genome integrity. PLoS Genetics, 13(2), e1006632. doi:10.1371/journal.pgen.1006632.

Anglana, M., Apiou, F., Bensimon, A., et al. (2003). Dynamics of DNA replication in mammalian somatic cells: Nucleotide pool modulates origin choice and interorigin spacing. Cell, 114(3), 385-394. doi:10.1016/S0092-8674(03)00569-5.

Ball, H. L., Ehrhardt, M. R., Mordes, D. A., et al. (2007). Function of a conserved checkpoint recruitment domain in ATRIP proteins. Molecular and Cellular Biology, 27(9), 3367-3377. doi:10.1128/mcb.02238-06.

Banfalvi, G. (2017). Methods to detect apoptotic cell death. Apoptosis, 22, 306-323. doi:10.1007/s10495-016-1333-3.

Barratt, J., Andric, B., Tataradze, A., Schömig, M., Reusch, M., Valluri, U., et al. (2021). Roxadustat for the treatment of anaemia in chronic kidney disease patients not on dialysis: A phase 3, randomised, open-label, active-controlled study (DOLOMITES). Nephrology Dialysis Transplantation, 36(9), 1616-1628. doi:10.1093/ndt/gfab080.

Beck, H., Jeske, M., Thede, K., Stoll, F., Flamme, I., Akbaba, M., et al. (2018). Discovery of Molidustat (BAY 85-3934): A small-molecule oral HIF-prolyl hydroxylase (HIF-PH) inhibitor for the treatment of renal anemia. ChemMedChem, 13(10), 988-1003. doi:10.1002/cmdc.201700783.

Bell, S.P. and Dutta, A. (2002) DNA Replication in Eukaryotic Cells. Annual Review of Biochemistry, 71 (1): 333–374. doi:10.1146/annurev.biochem.71.110601.135425.

Bhamidipati, D., Haro-Silerio, J. I., Yap, T. A., et al. (2023). PARP inhibitors: enhancing efficacy through rational combinations. *British Journal of Cancer*, 129, 904–916. doi:10.1038/s41416-023-02326-7.

Bicknell, L. S., Bongers, E. M. H. F., Leitch, A., Brown, S., Schoots, J., Harley, M. E., et al. (2011a). Mutations in the pre-replication complex cause Meier-Gorlin syndrome. Nature Genetics, 43(4), 356-359. doi:10.1038/ng.775.

Bozkurt, E., Atmaca, H., Uzunoglu, S., Uslu, R., & Karaca, B. (2013). P53 modulates trabectedin mediated cytotoxicity in glioblastoma multiforme cells (U-87MG and T98G). Annals of Oncology, 24(Suppl 6), i30. doi:10.1093/annonc/mdt047.3.

Bryant, H., Schultz, N., Thomas, H. *et al.* Specific killing of BRCA2-deficient tumours with inhibitors of poly(ADP-ribose) polymerase. *Nature* 434, 913–917 (2005). https://doi.org/10.1038/nature03443

Bueno, M. T. D., Baldascini, M., Richard, S., & Lowndes, N. F. (2018). Recruitment of lysine demethylase 2A to DNA double strand breaks and its interaction with 53BP1 ensures genome stability. Oncotarget, 9(22), 15915-15930. doi:10.18632/oncotarget.24482.

Byun, T. S., Pacek, M., Yee, M. C., et al. (2005). Functional uncoupling of MCM helicase and DNA polymerase activities activates the ATR-dependent checkpoint. Genes & Development, 19(9), 1040-1052. doi:10.1101/gad.1301205.

Cao, W., Ren, Y., Liu, Y., Cao, G., Chen, Z., & Wang, F. (2024). KDM4A-AS1 promotes cell proliferation, migration, and invasion via the miR-4306/STX6 axis in hepatocellular carcinoma. Critical Reviews in Eukaryotic Gene Expression, 34(4), 55–68. https://doi.org/10.1615/CritRevEukaryotGeneExpr.2024051414

Chang, W. H., Forde, D., & Lai, A. G. (2019). Dual prognostic role of 2-oxoglutarate-dependent oxygenases in ten cancer types: implications for cell cycle regulation and cell adhesion maintenance. Cancer Communications, 39(1), 23. doi:10.1186/s40880-019-0378-x.

Choi, M., Kipps, T., & Kurzrock, R. (2016). ATM mutations in cancer: therapeutic implications. Molecular Cancer Therapeutics, 15(8), 1781-1791. doi:10.1158/1535-7163.MCT-15-0945.

Chu, X., Zhong, L., Yu, L., Xiong, L., Li, J., Dan, W., et al. (2020). GSK-J4 induces cell cycle arrest and apoptosis via ER stress and the synergism between GSK-J4 and decitabine in acute myeloid leukemia KG-1a cells. Cancer Cell International, 20, 209. doi:10.1186/s12935-020-01297-6. PMID: 32514253; PMCID: PMC7268296

Cimprich, K. A., & Cortez, D. (2008). ATR: An essential regulator of genome integrity. Nature Reviews Molecular Cell Biology, 9(8), 616-627. doi:10.1038/nrm2450.

Cockman, M. E., Lancaster, D. E., Stolze, I. P., et al. (2006). Posttranslational hydroxylation of ankyrin repeats in IκB proteins by the hypoxia-inducible factor (HIF) asparaginyl hydroxylase,

factor inhibiting HIF (FIH). Proceedings of the National Academy of Sciences of the United States of America, 103(40), 14767-14772. doi:10.1073/pnas.0606877103.

Coleman, M. L., McDonough, M. A., Hewitson, K. S., et al. (2007). Asparaginyl hydroxylation of the notch ankyrin repeat domain by factor inhibiting hypoxia-inducible factor. Journal of Biological Chemistry, 282(33), 24027-24038. doi:10.1074/jbc.M704102200.

Cortez, D., Glick, G., & Elledge, S. J. (2004). Minichromosome maintenance proteins are direct targets of the ATM and ATR checkpoint kinases. Proceedings of the National Academy of Sciences of the United States of America, 101(27), 10078-10083. doi:10.1073/pnas.0403410101.

Cortez, D. (2015). Preventing replication fork collapse to maintain genome integrity. DNA Repair, 32, 149-157. doi:10.1016/j.dnarep.2015.04.026.

Cui, S. Z., Lei, Z. Y., Guan, T. P., Fan, L. L., Li, Y. Q., Geng, X. Y., Fu, D. X., Jiang, H. W., & Xu, S. H. (2020). Targeting the USP1 dependent KDM4A protein stability as a potential prostate cancer therapy. Cancer Science, 111(12), 4398–4407. https://doi.org/10.1111/cas.14375

Das, M., Singh, S., Pradhan, S., et al. (2014). MCM paradox: Abundance of eukaryotic replicative helicases and genomic integrity. Molecular Biology International, 2014, 1-11. doi:10.1155/2014/574850.

Del Rizzo, P. A., Krishnan, S., & Trievel, R. C. (2012). Crystal structure and functional analysis of JMJD5 indicate an alternate specificity and function. Molecular and Cellular Biology, 32(19), 4044-4052. doi:10.1128/MCB.00705-12.

Dillon, M. T., Guevara, J., Mohammed, K., Patin, E. C., Smith, S. A., Dean, E., et al. (2024). Durable responses to ATR inhibition with ceralasertib in tumors with genomic defects and high inflammation. Journal of Clinical Investigation, 134(2), e175369. doi:10.1172/JCI175369. PMID: 37934611; PMCID: PMC10786692.

Fanning, E., Klimovich, V., & Nager, A. R. (2006). A dynamic model for replication protein A (RPA) function in DNA processing pathways. Nucleic Acids Research, 34(15), 4126-4137. doi:10.1093/nar/gkl550.

Fenech, M., Kirsch-Volders, M., Natarajan, A. T., et al. (2011). Molecular mechanisms of micronucleus, nucleoplasmic bridge and nuclear bud formation in mammalian and human cells. Mutagenesis, 26(1), 125-132. doi:10.1093/mutage/geq052.

Fernandez-Vidal, A., Vignard, J., & Mirey, G. (2017). Around and beyond 53BP1 nuclear bodies. International Journal of Molecular Sciences, 18(12), 2611. doi:10.3390/ijms18122611.

Fletcher, S. C., & Coleman, M. L. (2020). Human 2-oxoglutarate-dependent oxygenases: Nutrient sensors, stress responders, and disease mediators. Biochemical Society Transactions, 48(5), 1843-1858. https://doi.org/10.1042/BST20200116

Fletcher, S. C., Hall, C. L., Kennedy, T. J., et al. (2023). Impaired protein hydroxylase activity causes replication stress and developmental abnormalities in humans. Journal of Clinical Investigation, 133(7). doi:10.1172/jci152784.

Foskolou, I. P., Biasoli, D., Olcina, M. M., & Hammond, E. M. (2016). Measuring DNA replication in hypoxic conditions. Advances in Experimental Medicine and Biology, 899, 11-25. doi:10.1007/978-3-319-26666-4_2

Garribba, L., Wu, W., Özer, Ö., et al. (2018). Inducing and detecting mitotic DNA synthesis at difficult-to-replicate loci. Methods in Enzymology, 601, 45-58. doi:10.1016/bs.mie.2017.11.025.

Ge, X. Q., Jackson, D. A., & Blow, J. J. (2007). Dormant origins licensed by excess Mcm2-7 are required for human cells to survive replicative stress. Genes & Development, 21(24), 3331-3341. doi:10.1101/gad.457807.

Ge, X. Q., & Blow, J. J. (2010). Chk1 inhibits replication factory activation but allows dormant origin firing in existing factories. Journal of Cell Biology, 191(7), 1285-1297. doi:10.1083/jcb.201007074.

Ge, W., Wolf, A., Feng, T., Ho, C.-H., Sekirnik, R., Zayer, A., et al. (2012). Oxygenase-catalyzed ribosome hydroxylation occurs in prokaryotes and humans. Nature Chemical Biology, 8(11), 960-962. doi:10.1038/nchembio.1078.

Gelot, C., Magdalou, I., & Lopez, B. S. (2015). Replication stress in mammalian cells and its consequences for mitosis. Genes, 6(2), 267-298. doi:10.3390/genes6020267.

Gu, Y. Z., Moran, S. M., Hogenesch, J. B., et al. (1998). Molecular characterization and chromosomal localization of a third α-class hypoxia inducible factor subunit, HIF3α. Gene Expression, 7(3), 205-213.

Gu, L., Hickey, R. J., & Malkas, L. H. (2023). Therapeutic targeting of DNA replication stress in cancer. Genes, 14(7), 1346. doi:10.3390/genes14071346.

Harley, M. E., Murina, O., Leitch, A., Higgs, M. R., Bicknell, L. S., Yigit, G., et al. (2016). TRAIP promotes DNA damage response during genome replication and is mutated in primordial dwarfism. Nature Genetics, 48(1), 36-43. doi:10.1038/ng.3471.

Harrigan, J. A., Belotserkovskaya, R., Coates, J., Dimitrova, D. S., Polo, S. E., Bradshaw, C. R., et al. (2011). Replication stress induces 53BP1-containing OPT domains in G1 cells. Journal of Cell Biology, 193(1), 97-108. doi:10.1083/jcb.201009110.

He, Z., Wu, J., Su, X., Zhang, Y., Pan, L., Wei, H., et al. (2016). JMJD5 (Jumonji Domain-containing 5) associates with spindle microtubules and is required for proper mitosis. Journal of Biological Chemistry, 291(9), 4684-4697. doi:10.1074/jbc.M115.699637.

He, Y., Sun, M. M., Zhang, G. G., et al. (2021). Targeting PI3K/Akt signal transduction for cancer therapy. Signal Transduction and Targeted Therapy, 6, 425. doi:10.1038/s41392-021-00828-5.

Helmrich, A., Ballarino, M., & Tora, L. (2011). Collisions between replication and transcription complexes cause common fragile site instability at the longest human genes. Molecular Cell, 44(6), 966-977. doi:10.1016/j.molcel.2011.10.013.

Herlihy, A. E., & de Bruin, R. A. (2017). The role of the transcriptional response to DNA replication stress. Genes (Basel), 8(3), 92. doi:10.3390/genes8030092. PMID: 28257104; PMCID: PMC5368696.

Hewitson, K. S., Holmes, S. L., Ehrismann, D., et al. (2008). Evidence that two enzyme-derived histidine ligands are sufficient for iron binding and catalysis by factor inhibiting HIF (FIH). Journal of Biological Chemistry, 283(38), 25971-25978. doi:10.1074/jbc.M804999200.

Hopkins, T. A., Ainsworth, W. B., Ellis, P. A., Donawho, C. K., DiGiammarino, E. L., Panchal, S. C., et al. (2019). PARP1 trapping by PARP inhibitors drives cytotoxicity in both cancer cells and healthy bone marrow. Molecular Cancer Research, 17(2), 409-419. doi:10.1158/1541-7786.MCR-18-0138.

Hsia, D. A., Tepper, C. G., Pochampalli, M. R., Hsia, E. Y., Izumiya, C., Huerta, S. B., et al. (2010). KDM8, a H3K36me2 histone demethylase that acts in the cyclin A1 coding region to regulate cancer cell proliferation. Proceedings of the National Academy of Sciences of the United States of America, 107(21), 9671-9676. doi:10.1073/pnas.0913435107.

Huang, X., Zhang, L., Qi, H., Shao, J., & Shen, J. (2013). Identification and functional implication of nuclear localization signals in the N-terminal domain of JMJD5. Biochimie, 95(11), 2114-2122. doi:10.1016/j.biochi.2013.07.016.

Huang, X., Zhang, S., Qi, H., Wang, Z., Chen, H. W., Shao, J., et al. (2015). JMJD5 interacts with p53 and negatively regulates p53 function in control of cell cycle and proliferation. Biochimica et Biophysica Acta, 1853(10 Pt A), 2286-2295. doi:10.1016/j.bbamcr.2015.05.016.

Huo, D., Chen, H., Cheng, Y., Song, X., Zhang, K., Li, M. J., et al. (2020). JMJD6 modulates DNA damage response through downregulating H4K16ac independently of its enzymatic activity. Cell Death & Differentiation, 27(3), 1052-1066. doi:10.1038/s41418-019-0437-5.

Ibarra, A., Schwob, E., & Mendez, J. (2008). Excess MCM proteins protect human cells from replicative stress by licensing backup origins of replication. Proceedings of the National Academy of Sciences of the United States of America, 105(26), 8956–8961. https://doi.org/10.1073/pnas.0803976105

Inoue, S., Li, W. Y., Tseng, A., Beerman, I., Elia, A. J., Bendall, S. C., et al. (2016). Mutant IDH1 downregulates ATM and alters DNA repair and sensitivity to DNA damage independent of TET2. Cancer Cell, 30(2), 337-348. doi:10.1016/j.ccell.2016.06.014.

Ishimura, A., Minehata, K., Terashima, M., Kondoh, G., Hara, T., & Suzuki, T. (2012). Jmjd5, an H3K36me2 histone demethylase, modulates embryonic cell proliferation through the regulation of Cdkn1a expression. Development, 139(4), 749-759. doi:10.1242/dev.074567.

Jaakkola, P., Mole, D. R., Tian, Y. M., et al. (2001). Targeting of HIF-α to the von Hippel-Lindau ubiquitylation complex by O2-regulated prolyl hydroxylation. Science, 292(5516), 468-472. doi:10.1126/science.1059796.

Jette, N. R., Radhamani, S., Arthur, G., Ye, R., Goutam, S., Bolyos, A., et al. (2019). Combined poly-ADP ribose polymerase and ataxia-telangiectasia mutated/Rad3-related inhibition targets

ataxia-telangiectasia mutated-deficient lung cancer cells. British Journal of Cancer, 121(7), 600-610. doi:10.1038/s41416-019-0528-7.

Johansson, C., Tumber, A., Che, K., Cain, P., Nowak, R., Gileadi, C., & Oppermann, U. (2014). The roles of Jumonji-type oxygenases in human disease. Epigenomics, 6(1), 89-120. doi:10.2217/epi.13.79. PMID: 24579949; PMCID: PMC4233403.

Jones, M. A., Covington, M. F., DiTacchio, L., Vollmers, C., Panda, S., & Harmer, S. L. (2010). Jumonji domain protein JMJD5 functions in both the plant and human circadian systems. Proceedings of the National Academy of Sciences of the United States of America, 107(50), 21623-21628. doi:10.1073/pnas.1014204107.

Jones, M. A., & Harmer, S. (2011). JMJD5 functions in concert with TOC1 in the Arabidopsis circadian system. Plant Signaling & Behavior, 6(3), 445-448. doi:10.4161/psb.6.3.14517.

Kaelin, W. G., Jr., & Ratcliffe, P. J. (2008). Oxygen sensing by metazoans: The central role of the HIF hydroxylase pathway. Molecular Cell, 30(4), 393-402. https://doi.org/10.1016/j.molcel.2008.04.009

Kafer, G. R., Li, X., Horii, T., Suetake, I., Tajima, S., Hatada, I., et al. (2016). 5-Hydroxymethylcytosine marks sites of DNA damage and promotes genome stability. Cell Reports, 14(6), 1283-1292. doi:10.1016/j.celrep.2016.01.027.

Kemiha, S., Poli, J., Lin, Y. L., Lengronne, A., & Pasero, P. (2021). Toxic R-loops: Cause or consequence of replication stress? DNA Repair, 107, 103199. doi:10.1016/j.dnarep.2021.103199.

Khoueiry, R., Sohni, A., Thienpont, B., et al. (2017). Lineage-specific functions of TET1 in the postimplantation mouse embryo. Nature Genetics, 49(7), 1061-1072. doi:10.1038/ng.3868.

Khoury-Haddad, H., Guttmann-Raviv, N., Ipenberg, I., Huggins, D., Jeyasekharan, A. D., & Ayoub, N. (2014). PARP1-dependent recruitment of KDM4D histone demethylase to DNA damage sites promotes double-strand break repair. Proceedings of the National Academy of Sciences of the United States of America, 111(7), E728-E737. doi:10.1073/pnas.1315890111.

Klose, R. J., Kallin, E. M., & Zhang, Y. (2006). JmjC-domain-containing proteins and histone demethylation. Nature Reviews Genetics, 7(9), 715-727. doi:10.1038/nrg1945.

Knapp, K. M., Sullivan, R., Murray, J., Gimenez, G., Arn, P., D'Souza, P., et al. (2020). Linked-read genome sequencing identifies biallelic pathogenic variants in DONSON as a novel cause of Meier-Gorlin syndrome. Journal of Medical Genetics, 57(3), 195-202. doi:10.1136/jmedgenet-2019-106396.

Krasilnikova, M. M., & Mirkin, S. M. (2004). Replication stalling at Friedreich's Ataxia (GAA)n repeats in vivo. Molecular and Cellular Biology, 24(6), 2286-2295. doi:10.1128/mcb.24.6.2286-2295.2004.

Kubota, E., Williamson, C. T., Ye, R., Elegbede, A., Peterson, L., Lees-Miller, S. P., et al. (2014). Low ATM protein expression and depletion of p53 correlates with olaparib sensitivity in gastric cancer cell lines. Cell Cycle, 13(13), 2129-2137. doi:10.4161/cc.29315.

Laroche, A., Chaire, V., Le Loarer, F., Algéo, M. P., Rey, C., Tran, K., et al. (2017). Activity of trabectedin and the PARP inhibitor rucaparib in soft-tissue sarcomas. Journal of Hematology & Oncology, 10(1), 84. doi:10.1186/s13045-017-0451-x. PMID: 28399901; PMCID: PMC5387279.

Lee, J., Kumagai, A., & Dunphy, W. G. (2007). The Rad9-Hus1-Rad1 checkpoint clamp regulates interaction of TopBP1 with ATR. Journal of Biological Chemistry, 282(39), 28036-28044. doi:10.1074/jbc.M702611200.

Li, J., Mahajan, A., & Tsai, M. D. (2006). Ankyrin repeat: A unique motif mediating protein-protein interactions. Biochemistry, 45(51), 15168-15178. doi:10.1021/bi062188q.

Li, H., Li, Q., Jing, H., Zhao, J., Zhang, H., Ma, X., et al. (2021). Expression and prognosis analysis of JMJD5 in human cancers. Frontiers in Bioscience (Landmark Edition), 26(10), 707-716. doi:10.52586/4981.

Li, N., Gao, N., & Zhai, Y. (2023). DDK promotes DNA replication initiation: Mechanistic and structural insights. Current Opinion in Structural Biology, 78, 102504. doi:10.1016/j.sbi.2023.102504.

Liao, H., Winkfein, R. J., Mack, G., Rattner, J. B., & Yen, T. J. (1995). CENP-F is a protein of the nuclear matrix that assembles onto kinetochores at late G2 and is rapidly degraded after mitosis. Journal of Cell Biology, 130(3), 507-518. doi:10.1083/jcb.130.3.507.

Liao, H., Ji, F., Helleday, T., & Ying, S. (2018). Mechanisms for stalled replication fork stabilization: new targets for synthetic lethality strategies in cancer treatments. EMBO Reports, 19(9), e46263. doi:10.15252/embr.201846263.

Lima, M., Bouzid, H., Soares, D. G., Selle, F., Morel, C., Galmarini, C. M., et al. (2016). Dual inhibition of ATR and ATM potentiates the activity of trabectedin and lurbinectedin by perturbing the DNA damage response and homologous recombination repair. Oncotarget, 7(18), 25885-25901. doi:10.18632/oncotarget.8292. PMID: 27029031; PMCID: PMC5041952.

Liu, C., Gilmont, R. R., Benndorf, R., et al. (2000). Identification and characterization of a novel protein from Sertoli cells, PASS1, that associates with mammalian small stress protein hsp27. Journal of Biological Chemistry, 275(25), 18724-18731. doi:10.1074/jbc.M001981200.

Liu, Y., & Bodmer, W. F. (2006). Analysis of P53 mutations and their expression in 56 colorectal cancer cell lines. Proceedings of the National Academy of Sciences, 103(4), 976-981. https://doi.org/10.1073/pnas.0510146103

Liu, H., Wang, C., Lee, S., Deng, Y., Wither, M., Oh, S., et al. (2017). Clipping of arginine-methylated histone tails by JMJD5 and JMJD7. Proceedings of the National Academy of Sciences of the United States of America, 114(37), E7717-E7726. doi:10.1073/pnas.1705303114.

Liu, G., Qi, H., & Shen, J. (2023). JMJD5 inhibits lung cancer progression by regulating glucose metabolism through the p53/TIGAR pathway. Medical Oncology, 40, 145. doi:10.1007/s12032-023-02016-7.

Livraghi, L., & Garber, J. E. (2015). PARP inhibitors in the management of breast cancer: current data and future prospects. BMC Medicine, 13, 188. doi:10.1186/s12916-015-0425-1.

Loenarz, C., & Schofield, C. J. (2008). Expanding chemical biology of 2-oxoglutarate oxygenases. Nature Chemical Biology, 4(3), 152-156. https://doi.org/10.1038/nchembio0308-152

Loenarz, C., & Schofield, C. J. (2011). Physiological and biochemical aspects of hydroxylations and demethylations catalyzed by human 2-oxoglutarate oxygenases. Trends in Biochemical Sciences, 36(1), 7-18. https://doi.org/10.1016/j.tibs.2010.07.002

Lopez-Girona, A., Tanaka, K., Chen, X. B., et al. (2001). Serine-345 is required for Rad3-dependent phosphorylation and function of checkpoint kinase Chk1 in fission yeast. Proceedings of the National Academy of Sciences of the United States of America, 98(20), 11289-11294. doi:10.1073/pnas.191557598.

Lord, C. J., & Ashworth, A. (2017). PARP inhibitors: Synthetic lethality in the clinic. Science, 355(6330), 1152-1158. doi:10.1126/science.aam7344.

Luzhna, L., Kathiria, P., & Kovalchuk, O. (2013). Micronuclei in genotoxicity assessment: from genetics to epigenetics and beyond. Frontiers in Genetics, 4, 131. doi:10.3389/fgene.2013.00131.

Macheret, M., & Halazonetis, T. D. (2015). DNA replication stress as a hallmark of cancer. Annual Review of Pathology: Mechanisms of Disease, 10, 425-448. doi:10.1146/annurev-pathol-012414-040424.

Majka, J., Binz, S. K., Wold, M. S., et al. (2006). Replication protein A directs loading of the DNA damage checkpoint clamp to 5′-DNA junctions. Journal of Biological Chemistry, 281(38), 27855-27861. doi:10.1074/jbc.M605176200.

Masson, N., Willam, C., Maxwell, P. H., et al. (2001). Independent function of two destruction domains in hypoxia-inducible factor-α chains activated by prolyl hydroxylation. EMBO Journal, 20(18), 5197-5206. doi:10.1093/emboj/20.18.5197.

Marcon, E., Ni, Z., Pu, S., Turinsky, A. L., Trimble, S. S., Olsen, J. B., et al. (2014). Human-chromatin-related protein interactions identify a demethylase complex required for chromosome segregation. Cell Reports, 8(1), 297-310. doi:10.1016/j.celrep.2014.05.055.

Maréchal, A., & Zou, L. (2013). DNA damage sensing by the ATM and ATR kinases. Cold Spring Harbor Perspectives in Biology, 5(9), a012716. doi:10.1101/cshperspect.a012716.

McDonough, M. A., Loenarz, C., Chowdhury, R., Clifton, I. J., & Schofield, C. J. (2010). Structural studies on human 2-oxoglutarate dependent oxygenases. Current Opinion in Structural Biology, 20(6), 659-672. https://doi.org/10.1016/j.sbi.2010.08.006

McKinnon, P. J. (2004). ATM and ataxia telangiectasia. EMBO Reports, 5(8), 772-776. doi:10.1038/sj.embor.7400205.

Mejlvang, J., Feng, Y., Alabert, C., et al. (2014). New histone supply regulates replication fork speed and PCNA unloading. Journal of Cell Biology, 204(1), 29-43. doi:10.1083/jcb.201305017.

Min, A., Im, S. A., Jang, H., Kim, S., Lee, M., Kim, D. K., et al. (2017). AZD6738, a novel oral inhibitor of ATR, induces synthetic lethality with ATM deficiency in gastric cancer cells. Molecular Cancer Therapeutics, 16(4), 566-577. doi:10.1158/1535-7163.MCT-16-0378. PMID: 28138034.

Minocherhomji, S., Ying, S., Bjerregaard, V. A., et al. (2015). Replication stress activates DNA repair synthesis in mitosis. Nature, 528(7581), 286-290. doi:10.1038/nature16139

Mirza-Aghazadeh-Attari, M., Mohammadzadeh, A., Yousefi, B., Mihanfar, A., Karimian, A., & Majidinia, M. (2019). 53BP1: A key player of DNA damage response with critical functions in cancer. DNA Repair (Amst), 73, 110-119. doi:10.1016/j.dnarep.2018.11.005.

Mizushima, T., Takahashi, N., & Stillman, B. (2000). Cdc6p modulates the structure and DNA binding activity of the origin recognition complex in vitro. Genes & Development, 14(13), 1631-1641. doi:10.1101/gad.14.13.1631.

Mordes, D. A., Glick, G. G., Zhao, R., & Cortez, D. (2008). TopBP1 activates ATR through ATRIP and a PIKK regulatory domain. Genes & Development, 22(11), 1478-1489. doi:10.1101/gad.1666208.

Musacchio, L., Caruso, G., Pisano, C., Cecere, S. C., et al. (2020). PARP inhibitors in endometrial cancer: Current status and perspectives. Cancer Management and Research, 12, 6123-6135. doi:10.2147/CMAR.S221001.

Nagaoka, K., Bai, X., Ogawa, K., Dong, X., Zhang, S., Zhou, Y., et al. (2019). Anti-tumor activity of antibody drug conjugate targeting aspartate-β-hydroxylase in pancreatic ductal adenocarcinoma. Cancer Letters, 449, 87–98. doi:10.1016/j.canlet.2019.02.006

Nishizawa, Y., Nishida, N., Konno, M., Kawamoto, K., Asai, A., Koseki, J., et al. (2017). Clinical significance of histone demethylase NO66 in invasive colorectal cancer. Annals of Surgical Oncology, 24(3), 841-849. doi:10.1245/s10434-016-5395-9.

Nowak, R. P., Tumber, A., Hendrix, E., Ansari, M. S. Z., Sabatino, M., Antonini, L., et al. (2021). First-in-class inhibitors of the ribosomal oxygenase MINA53. Journal of Medicinal Chemistry, 64(23), 17031-17050. doi:10.1021/acs.jmedchem.1c00605.

O'Driscoll, M., Ruiz-Perez, V. L., Woods, C. G., et al. (2003). A splicing mutation affecting expression of ataxia-telangiectasia and Rad3-related protein (ATR) results in Seckel syndrome. Nature Genetics, 33(4), 497-501. doi:10.1038/ng1129.

Oh, S., & Janknecht, R. (2012). Histone demethylase JMJD5 is essential for embryonic development. Biochemical and Biophysical Research Communications, 420(1), 61-65. doi:10.1016/j.bbrc.2012.02.125.

Olivares-Hernández, A., Roldán-Ruiz, J., Miramontes-González, J. P., Toribio-García, I., García-Hernández, et al. (2023). Efficacy and safety of PARP inhibitor in non-small cell lung cancer: A systematic review with meta-analysis. Chinese Clinical Oncology, 12(6), 62. https://doi.org/10.21037/cco-23-58.

Olivieri, M., Cho, T., Álvarez-Quilón, A., Li, K., Schellenberg, M. J., Zimmermann, M., et al. (2020). A genetic map of the response to DNA damage in human cells. Cell, 182(2), 481-496.e21. doi:10.1016/j.cell.2020.05.040.

Ordonez, J., Amaral, A., Carcaboso, A., Herrero-Martín, D., Del, M., García-Macías, C., et al. (2015). The PARP inhibitor olaparib enhances the sensitivity of Ewing sarcoma to trabectedin. Oncotarget, 6(13), 11959-11973. doi:10.18632/oncotarget.4303.

Patel, J., Landers, K., Mortimer, R. H., et al. (2010). Regulation of Hypoxia Inducible Factors (HIF) in hypoxia and normoxia during placental development. Placenta, 31(11), 951-957. doi:10.1016/j.placenta.2010.08.008.

Pauklin, S., Kristjuhan, A., Maimets, T., & Jaks, V. (2005). ARF and ATM/ATR cooperate in p53-mediated apoptosis upon oncogenic stress. Biochemical and Biophysical Research Communications, 334(3), 679-688. doi:10.1016/j.bbrc.2005.06.097

Pei, J., Zhang, S., Yang, X., Han, C., Pan, Y., Li, J., Wang, Z., Sun, C., & Zhang, J. (2023). Epigenetic regulator KDM4A activates Notch1-NICD-dependent signaling to drive tumorigenesis and metastasis in breast cancer. Translational Oncology, 28, 101615. https://doi.org/10.1016/j.tranon.2022.101615

Peitsch, M. C., Müller, C., & Tschopp, J. (1993). DNA fragmentation during apoptosis is caused by frequent single-strand cuts. Nucleic Acids Research, 21(18), 4206-4209. doi:10.1093/nar/21.18.4206.

Pergola, P. E., Spinowitz, B. S., Hartman, C. S., Maroni, B. J., & Haase, V. H. (2016). Vadadustat, a novel oral HIF stabilizer, provides effective anemia treatment in nondialysis-dependent chronic kidney disease. Kidney International, 90(5), 1115-1122. doi:10.1016/j.kint.2016.07.019

Perkhofer, L., Schmitt, A., Romero Carrasco, M. C., Ihle, M., Hampp, S., Ruess, D. A., et al. (2017). ATM deficiency generating genomic instability sensitizes pancreatic ductal adenocarcinoma cells to therapy-induced DNA damage. Cancer Research, 77(20), 5576-5590. doi:10.1158/0008-5472.CAN-17-0747.

Pignochino, Y., Capozzi, F., D'Ambrosio, L., Dell'Aglio, C., Basiricò, M., Canta, M., et al. (2017). PARP1 expression drives the synergistic antitumor activity of trabectedin and PARP1 inhibitors in sarcoma preclinical models. Molecular Cancer, 16(1), 86. doi:10.1186/s12943-017-0652-5. PMID: 28454547; PMCID: PMC5410089.

Pires, I. M., Bencokova, Z., Milani, M., Folkes, L. K., Li, J. L., Stratford, M. R., et al. (2010). Effects of acute versus chronic hypoxia on DNA damage responses and genomic instability. Cancer Research, 70(3), 925-935. doi:10.1158/0008-5472.CAN-09-2715.

Ploumakis, A., & Coleman, M. L. (2015). OH, the places you'll go! Hydroxylation, gene expression, and cancer. Molecular Cell, 58(5), 729-741. https://doi.org/10.1016/j.molcel.2015.04.031

Pothof, J., van Haaften, G., Thijssen, K., Kamath, R. S., Fraser, A. G., Ahringer, J., et al. (2003). Identification of genes that protect the C. elegans genome against mutations by genome-wide RNAi. Genes & Development, 17(4), 443-448. doi:10.1101/gad.1060703.

Prokop, A., Wrasidlo, W., Lode, H., et al. (2003). Induction of apoptosis by enediyne antibiotic calicheamicin θII proceeds through a caspase-mediated mitochondrial amplification loop in an entirely Bax-dependent manner. Oncogene, 22(56), 9107-9120. doi:10.1038/sj.onc.1207196.

Provenzano, R., Besarab, A., Sun, C. H., Diamond, S. A., Durham, J. H., Cangiano, J. L., et al. (2016). Oral hypoxia-inducible factor prolyl hydroxylase inhibitor Roxadustat (FG-4592) for the treatment of anemia in patients with CKD. Clinical Journal of the American Society of Nephrology, 11(6), 982-991. doi:10.2215/CJN.06890615.

Ramazi, S., & Zahiri, J. (2021). Post-translational modifications in proteins: Resources, tools, and prediction methods. Database, 2021, baab012. https://doi.org/10.1093/database/baab012

Ran, T., Xiao, R., Huang, Q., Yuan, H., Lu, T., & Liu, W. (2019). In silico discovery of JMJD6 inhibitors for cancer treatment. ACS Medicinal Chemistry Letters, 10(12), 1609-1613. doi:10.1021/acsmedchemlett.9b00264.

Reynolds, J. J., Bicknell, L. S., Carroll, P., Higgs, M. R., Shaheen, R., Murray, J. E., et al. (2017). Mutations in DONSON disrupt replication fork stability and cause microcephalic dwarfism. Nature Genetics, 49(4), 537-549. doi:10.1038/ng.3801.

Riches, L. C., Trinidad, A. G., Hughes, G., Jones, G. N., Hughes, A. M., Thomason, A. G., et al. (2020). Pharmacology of the ATM inhibitor AZD0156: potentiation of irradiation and olaparib responses preclinically. Molecular Cancer Therapeutics, 19(1), 13-25. doi:10.1158/1535-7163.MCT-19-0434.

Riera, A., Fernández-Cid, A., & Speck, C. (2013). The ORC/Cdc6/MCM2–7 complex, a new power player for regulated helicase loading. Cell Cycle, 12(14), 2155-2156. doi:10.4161/cc.25336.

Rose, N. R., McDonough, M. A., King, O. N., Kawamura, A., & Schofield, C. J. (2011). Inhibition of 2-oxoglutarate dependent oxygenases. Chemical Society Reviews, 40(8), 4364-4397. https://doi.org/10.1039/c0cs00203h.

Rose, M., Burgess, J. T., O'Byrne, K., Richard, D. J., & Bolderson, E. (2020). PARP inhibitors: clinical relevance, mechanisms of action and tumor resistance. Frontiers in Cell and Developmental Biology, 8, 879. doi:10.3389/fcell.2020.00879.

Saldivar, J. C., Cortez, D., & Cimprich, K. A. (2017). The essential kinase ATR: ensuring faithful duplication of a challenging genome. Nature Reviews Molecular Cell Biology, 18(10), 622-636. doi:10.1038/nrm.2017.67.

Saran, A. R., Kalinowska, D., Oh, S., Janknecht, R., & DiTacchio, L. (2018). JMJD5 links CRY1 function and proteasomal degradation. PLoS Biology, 16(11), e2006145. doi:10.1371/journal.pbio.2006145.

Saxena, S., & Zou, L. (2022). Hallmarks of DNA replication stress. *Molecular Cell*, *82*(12), 2298-2314. doi:10.1016/j.molcel.2022.05.004.

Shen, J., Xiang, X., Chen, L., Wang, H., Wu, L., Sun, Y., et al. (2017). JMJD5 cleaves monomethylated histone H3 N-tail under DNA damaging stress. EMBO Reports, 18(12), 2131-2143. doi:10.15252/embr.201744577.

Shen, Y., Vignali, P., & Wang, R. (2017). Rapid profiling cell cycle by flow cytometry using concurrent staining of DNA and mitotic markers. Bio Protoc, 7(16), e2517. doi:10.21769/BioProtoc.2517. PMID: 28868333; PMCID: PMC5580980.

Shen, J., Liu, G., & Qi, H. et al. (2023). JMJD5 inhibits lung cancer progression by facilitating EGFR proteasomal degradation. Cell Death & Disease, 14, 657. doi:10.1038/s41419-023-06194-0.

Sim, N.-L., Kumar, P., Hu, J., Henikoff, S., Schneider, G., & Ng, P. C. (2012). SIFT web server: predicting effects of amino acid substitutions on proteins. Nucleic Acids Research, 40(W1), W452-W457. doi:10.1093/nar/gks539.

Smits, V. A. J., Reaper, P. M., & Jackson, S. P. (2006). Rapid PIKK-dependent release of Chk1 from chromatin promotes the DNA-damage checkpoint response. Current Biology, 16(2), 150-159. doi:10.1016/j.cub.2005.11.066.

Song, J., Zheng, J., Liu, X., et al. (2022). A novel protein encoded by ZCRB1-induced circHEATR5B suppresses aerobic glycolysis of GBM through phosphorylation of JMJD5. Journal of Experimental & Clinical Cancer Research, 41(1), 1-20. doi:10.1186/s13046-022-02374-6.

Sritharan, S., & Sivalingam, N. (2021). A comprehensive review on time-tested anticancer drug doxorubicin. Life Sciences, 278, 119527. doi:10.1016/j.lfs.2021.119527. PMID: 33887349.

Strowitzki, M. J., Cummins, E. P., & Taylor, C. T. (2019). Protein hydroxylation by hypoxia-inducible factor (HIF) hydroxylases: unique or ubiquitous? Cells, 8(5), 384. doi:10.3390/cells8050384. PMID: 31035491; PMCID: PMC6562979.

Sui, A., Xu, Y., Li, Y., Hu, Q., Wang, Z., Zhang, H., et al. (2017). The pharmacological role of histone demethylase JMJD3 inhibitor GSK-J4 on glioma cells. Oncotarget, 8(40), 68591-68598. doi:10.18632/oncotarget.19793. PMID: 28978140; PMCID: PMC5620280.

Sulkowski, P. L., Corso, C. D., Robinson, N. D., Scanlon, S. E., Purshouse, K. R., Bai, H., et al. (2017). 2-Hydroxyglutarate produced by neomorphic IDH mutations suppresses homologous recombination and induces PARP inhibitor sensitivity. Science Translational Medicine, 9(375). doi:10.1126/scitranslmed.aal2463.

Sulkowski, P. L., Sundaram, R. K., Oeck, S., Corso, C. D., Liu, Y., Noorbakhsh, S., et al. (2018). Krebs-cycle-deficient hereditary cancer syndromes are defined by defects in homologous-recombination DNA repair. Nature Genetics, 50(8), 1086-1092. doi:10.1038/s41588-018-0156-0.

Suzuki, T., Minehata, K.-i., Akagi, K., Jenkins, N. A., & Copeland, N. G. (2006). Tumor suppressor gene identification using retroviral insertional mutagenesis in Blm-deficient mice. The EMBO Journal, 25(14), 3422-3431. doi:10.1038/sj.emboj.7601213.

Takara, K., Obata, Y., Yoshikawa, E. et al. Molecular changes to HeLa cells on continuous exposure to cisplatin or paclitaxel. Cancer Chemother Pharmacol 58, 785–793 (2006). https://doi.org/10.1007/s00280-006-0226-5

Tasaki, E., Mitaka, Y., Nozaki, T., Kobayashi, K., Matsuura, K., & Iuchi, Y. (2018). High expression of the breast cancer susceptibility gene BRCA1 in long-lived termite kings. Aging (Albany NY), 10(10), 2668-2683. doi:10.18632/aging.101578. PMID: 30312170; PMCID: PMC6224230.

Teye, K., Tsuneoka, M., Arima, N., Koda, Y., Nakamura, Y., Ueta, Y., et al. (2004). Increased expression of a Myc target gene Mina53 in human colon cancer. American Journal of Pathology, 164(1), 205-216. doi:10.1016/S0002-9440(10)63111-2.

Thakur, C., Lu, Y., Sun, J., Yu, M., Chen, B., & Chen, F. (2014). Increased expression of mdig predicts poorer survival of the breast cancer patients. Gene, 533(1), 70-76. doi:10.1016/j.gene.2013.09.043.

Thys, R. G., & Wang, Y. H. (2015). DNA replication dynamics of the GGGGCC repeat of the C9orf72 gene. Journal of Biological Chemistry, 290(48), 28953-28962. doi:10.1074/jbc.M115.660324.

Toledo, L. I., Altmeyer, M., Rask, M. B., et al. (2013). ATR prohibits replication catastrophe by preventing global exhaustion of RPA. Cell, 155(5), 1088-1101. doi:10.1016/j.cell.2013.10.043.

Topatana, W., Juengpanich, S., Li, S., Cao, J., Hu, J., Lee, J., et al. (2020). Advances in synthetic lethality for cancer therapy: cellular mechanism and clinical translation. Journal of Hematology & Oncology, 13(1), 118. doi:10.1186/s13045-020-00941-y.

Tsuneoka, M., Fujita, H., Arima, N., Teye, K., Okamura, T., Inutsuka, H., et al. (2004). Mina53 as a potential prognostic factor for esophageal squamous cell carcinoma. Clinical Cancer Research, 10(21), 7347-7356. doi:10.1158/1078-0432.CCR-03-0543.

Van Rechem, C., Ji, F., Mishra, S., Chakraborty, D., Murphy, S. E., Dillingham, M. E., et al. (2020). The lysine demethylase KDM4A controls the cell-cycle expression of replicative canonical histone genes. *Biochimica et Biophysica Acta. Gene Regulatory Mechanisms, 1863*(10), 194624. https://doi.org/10.1016/j.bbagrm.2020.194624

Vendetti, F. P., Lau, A., Schamus, S., Conrads, T. P., O'Connor, M. J., & Bakkenist, C. J. (2015). The orally active and bioavailable ATR kinase inhibitor AZD6738 potentiates the anti-tumor effects of cisplatin to resolve ATM-deficient non-small cell lung cancer in vivo. Oncotarget, 6(42), 44289-44305. doi:10.18632/oncotarget.6297.

Vesela, E., Chroma, K., Turi, Z., et al. (2017). Common chemical inductors of replication stress: Focus on cell-based studies. Biomolecules, 7(1), 1-18. doi:10.3390/biom7010019.

Wallez, Y., Dunlop, C. R., Johnson, T. I., Koh, S.-B., Fornari, C., Yates, J. W. T., et al. (2018). The ATR inhibitor AZD6738 synergizes with gemcitabine in vitro and in vivo to induce pancreatic

ductal adenocarcinoma regression. Molecular Cancer Therapeutics, 17(8), 1670-1682. doi:10.1158/1535-7163.MCT-18-0143.

Wang, H., Zhou, X., Wu, M., Wang, C., Zhang, X., Tao, Y., et al. (2013). Structure of the JmjC-domain-containing protein JMJD5. Acta Crystallographica Section D: Biological Crystallography, 69(Pt 10), 1911-1920. doi:10.1107/S0907444913016748.

Wang, H. J., Hsieh, Y. J., Cheng, W. C., Lin, C. P., Lin, Y. S., Yang, S. F., et al. (2014). JMJD5 regulates PKM2 nuclear translocation and reprograms HIF-1α-mediated glucose metabolism. Proceedings of the National Academy of Sciences of the United States of America, 111(1), 279-284. doi:10.1073/pnas.1311249111.

Wang, C., Jette, N., Moussienko, D., Bebb, D. G., & Lees-Miller, S. P. (2017). ATM-deficient colorectal cancer cells are sensitive to the PARP inhibitor olaparib. Translational Oncology, 10(2), 190-196. doi:10.1016/j.tranon.2017.01.001

Wang, Q., Liu, P. Y., Liu, T., & Lan, Q. (2019). The histone demethylase NO66 induces glioma cell proliferation. Anticancer Research, 39(11), 6007-6014. doi:10.21873/anticanres.13806.

Wang, H. J., Pochampalli, M., Wang, L. Y., Zou, J. X., Li, P. S., Hsu, S. C., et al. (2019). KDM8/JMJD5 as a dual coactivator of AR and PKM2 integrates AR/EZH2 network and tumor metabolism in CRPC. Oncogene, 38(1), 17-32. doi:10.1038/s41388-018-0410-6.

Wang, M., Chen, S., & Ao, D. (2021). Targeting DNA repair pathway in cancer: Mechanisms and clinical application. Molecular Carcinogenesis, 60(1), 95-104. https://doi.org/10.1002/mco2.103.

Wang, H., Wang, J., Liu, J., et al. (2022). Jumonji-C domain-containing protein 5 suppresses proliferation and aerobic glycolysis in pancreatic cancer cells in a c-Myc-dependent manner. Cellular Signalling, 93(February), 110282. doi:10.1016/j.cellsig.2022.110282.

Ward, I. M., & Chen, J. (2001). Histone H2AX is phosphorylated in an ATR-dependent manner in response to replicational stress. Journal of Biological Chemistry, 276(51), 47759-47762. doi:10.1074/jbc.C100569200.

Webb, J. D., Murányi, A., Pugh, C. W., et al. (2009). MYPT1, the targeting subunit of smooth-muscle myosin phosphatase, is a substrate for the asparaginyl hydroxylase factor inhibiting hypoxia. Journal of Biological Chemistry, 284(8), 4943-4952. doi:10.1074/jbc.M806477200.

Williamson, C. T., Muzik, H., Turhan, A. G., Zamò, A., O'Connor, M. J., Bebb, D. G., et al. (2010). ATM deficiency sensitizes mantle cell lymphoma cells to poly(ADP-ribose) polymerase-1 inhibitors. Molecular Cancer Therapeutics, 9(2), 347-357. doi:10.1158/1535-7163.MCT-09-0732.

Williamson, C. T., Kubota, E., Hamill, J. D., Klimowicz, A., Ye, R., Muzik, H., et al. (2012). Enhanced cytotoxicity of PARP inhibition in mantle cell lymphoma harbouring mutations in both ATM and p53. EMBO Molecular Medicine, 4(6), 515-527. doi:10.1002/emmm.201200232.

Willaume, S., Rass, E., Fontanilla-Ramirez, P., Moussa, A., Wanschoor, P., & Bertrand, P. (2021). A link between replicative stress, lamin proteins, and inflammation. Genes, 12(4), 552. doi:10.3390/genes12040552.

Wilkins, S. E., Islam, M. S., Gannon, J. M., Markolovic, S., Hopkinson, R. J., Ge, W., et al. (2018). JMJD5 is a human arginyl C-3 hydroxylase. Nature Communications, 9(1), 1180. doi:10.1038/s41467-018-03498-0.

Woodward, A. M., Göhler, T., Luciani, M. G., et al. (2006). Excess Mcm2-7 license dormant origins of replication that can be used under conditions of replicative stress. Journal of Cell Biology, 173(5), 673-683. doi:10.1083/jcb.200602108.

Wu, J., He, Z., Wang, D.-L., & Sun, F.-L. (2016). Depletion of JMJD5 sensitizes tumor cells to microtubule destabilizing agents by altering microtubule stability. Cell Cycle, 15(21), 2980-2989. doi:10.1080/15384101.2016.1220402.

Wu, B. H., Chen, H., Cai, C. M., Fang, J. Z., Wu, C. C., Huang, L. Y., et al. (2016). Epigenetic silencing of JMJD5 promotes the proliferation of hepatocellular carcinoma cells by down-regulating the transcription of CDKN1A. Oncotarget, 7(6), 6847-6863. doi:10.18632/oncotarget.6847.

Xiao, R., Ran, T., Huang, Q., & Liu, W. (2022). A specific JMJD6 inhibitor potently suppresses multiple types of cancers both in vitro and in vivo. Proceedings of the National Academy of Sciences of the United States of America, 119(34), e2200753119. doi:10.1073/pnas.2200753119.

Xiang, X., Ma, X., Fang, M., Zhong, L., Liu, H., Liu, H., et al. (2019). Jumonji domain containing 5 is a potential prognostic indicator in non-small cell lung cancer patients who received platinum-based chemotherapy. Translational Cancer Research, 8(7), 2535-2542. doi:10.21037/tcr.2019.10.03.

Xu, W., Yang, H., Liu, Y., Yang, Y., Wang, P., Kim, S. H., et al. (2011). Oncometabolite 2-hydroxyglutarate is a competitive inhibitor of α-ketoglutarate-dependent dioxygenases. Cancer Cell, 19(1), 17-30. doi:10.1016/j.ccr.2010.12.014.

Xuan, F., Huang, M., Zhao, E., & Cui, H. (2018). MINA53 deficiency leads to glioblastoma cell apoptosis via inducing DNA replication stress and diminishing DNA damage response. Cell Death & Disease, 9(11), 1062. https://doi.org/10.1038/s41419-018-1084-x.

Yan, N., Xu, L., Wu, X., Zhang, L., Fei, X., Cao, Y., & Zhang, F. (2017). GSKJ4, an H3K27me3 demethylase inhibitor, effectively suppresses the breast cancer stem cells. Experimental Cell Research, 359(2), 405-414. doi:10.1016/j.yexcr.2017.08.024. PMID: 28823831.

Yang, M., Chowdhury, R., Ge, W., et al. (2011). Factor-inhibiting hypoxia-inducible factor (FIH) catalyses the post-translational hydroxylation of histidinyl residues within ankyrin repeat domains. FEBS Journal, 278(7), 1086-1097. doi:10.1111/j.1742-4658.2011.08022.x.

Yang, M., Ge, W., Chowdhury, R., et al. (2011). Asparagine and aspartate hydroxylation of the cytoskeletal ankyrin family is catalyzed by factor-inhibiting hypoxia-inducible factor. Journal of Biological Chemistry, 286(9), 7648-7660. doi:10.1074/jbc.M110.193540.

Yang, Z., Zhuang, L., Szatmary, P., Wen, L., Sun, H., Lu, Y., et al. (2015). Upregulation of heat shock proteins (HSPA12A, HSP90B1, HSPA4, HSPA5 and HSPA6) in tumour tissues is associated with poor outcomes from HBV-related early-stage hepatocellular carcinoma. International Journal of Medical Sciences, 12(3), 256-263. doi:10.7150/ijms.10712.

Yang, J., Chen, S., Yang, Y., Ma, X., Shao, B., Yang, S., et al. (2020). Jumonji domain-containing protein 6 and its role in cancer. Cell Proliferation, 53(2), e12747. https://doi.org/10.1111/cpr.12747.

Yano, K., Shiotani, B. (2023). Emerging strategies for cancer therapy by ATR inhibitors. *Cancer Science*, 114(7), 2709-2721. doi:10.1111/cas.15845.

Yao, Y., Zhou, W. Y., & He, R. X. (2019). Down-regulation of JMJD5 suppresses metastasis and induces apoptosis in oral squamous cell carcinoma by regulating p53/NF-κB pathway. Biomedicine & Pharmacotherapy, 109, 1994-2004. doi:10.1016/j.biopha.2018.11.104.

Yeh, T.-L., Leissing, T. M., Abboud, M. I., Thinnes, C. C., Atasoylu, O., Holt-Martyn, J. P., et al. (2017). Molecular and cellular mechanisms of HIF prolyl hydroxylase inhibitors in clinical trials. Chemical Science, 8(11), 7651-7668. doi:10.1039/c7sc02582a.

Yeo, K. S., Tan, M. C., Lim, Y. Y., et al. (2017). JMJD8 is a novel endoplasmic reticulum protein with a JmjC domain. Scientific Reports, 7(1), 1-10. doi:10.1038/s41598-017-15676-z.

Yoon, Y.-K., Kim, H.-P., Han, S.-W., Oh, D. Y., et al. (2010). KRAS mutant lung cancer cells are differentially responsive to MEK inhibitor due to AKT or STAT3 activation: Implication for combinatorial approach. Molecular Carcinogenesis, 49(10), 910-921. https://doi.org/10.1002/mc.20607.

Youn, M. Y., Yokoyama, A., Fujiyama-Nakamura, S., Ohtake, F., Minehata, K., Yasuda, H., et al. (2012). JMJD5, a Jumonji C (JmjC) domain-containing protein, negatively regulates osteoclastogenesis by facilitating NFATc1 protein degradation. The Journal of Biological Chemistry, 287(16), 12994-13004. doi:10.1074/jbc.M111.337238.

Young, L. C., McDonald, D. W., & Hendzel, M. J. (2013). Kdm4b histone demethylase is a DNA damage response protein and confers a survival advantage following γ-irradiation. Journal of Biological Chemistry, 288(29), 21376-21388. doi:10.1074/jbc.M113.486290.

Yu, J., Wang, Z., & Wang, Y. (2022). BrdU Incorporation Assay to Analyze the Entry into S Phase. *Methods in molecular biology (Clifton, N.J.)*, *2579*, 209–226. https://doi.org/10.1007/978-1-0716-2736-5_16

Zeman, M. K., & Cimprich, K. A. (2014). Causes and consequences of replication stress. Nature Cell Biology, 16(1), 2-9. doi:10.1038/ncb2897.

Zhao, Z., Sun, C., Li, F., Han, J., Li, X., & Song, Z. (2015). Overexpression of histone demethylase JMJD5 promotes metastasis and indicates a poor prognosis in breast cancer. International Journal of Clinical and Experimental Pathology, 8(9), 10325-10334.

Zhang, R., Huang, Q., Li, Y., Song, Y., & Li, Y. (2015). JMJD5 is a potential oncogene for colon carcinogenesis. International Journal of Clinical and Experimental Pathology, 8(6), 6482-6489.

Zhang, W., Li, K., Wang, T., Wu, M., & Li, L. (2021). Discovery of JMJD7 inhibitors with the aid of virtual screening and bioactivity evaluation. Bioorganic & Medicinal Chemistry Letters, 45, 128139. doi:10.1016/j.bmcl.2021.128139.

Zheng, H., Tie, Y., Fang, Z., et al. (2019). Jumonji domain-containing 6 (JMJD6) identified as a potential therapeutic target in ovarian cancer. Signal Transduction and Targeted Therapy, 4, 24. doi:10.1038/s41392-019-0055-8.

Zheng, F., Zhang, Y., Chen, S., Weng, X., Rao, Y., & Fang, H. (2020). Mechanism and current progress of poly ADP-ribose polymerase (PARP) inhibitors in the treatment of ovarian cancer. Biomedicine & Pharmacotherapy, 123, 109661. doi:10.1016/j.biopha.2019.109661.

Zhu, H., Hu, S., & Baker, J. (2014). JMJD5 regulates cell cycle and pluripotency in human embryonic stem cells. Stem Cells, 32(8), 2098-2110. doi:10.1002/stem.1693.

Zimmermann, M., Murina, O., Reijns, M. A. M., Agathanggelou, A., Challis, R., Tarnauskaitė, Ž., et al. (2018). CRISPR screens identify genomic ribonucleotides as a source of PARP-trapping lesions. Nature, 559(7713), 285-289. doi:10.1038/s41586-018-0291-z.

Zou, Y., Liu, Y., Wu, X., et al. (2006). Functions of human replication protein A (RPA): From DNA replication to DNA damage and stress responses. Journal of Cellular Physiology, 208(2), 267-273. doi:10.1002/jcp.20622.